

## Journal of Polymer Science

## Part A-1: Polymer Chemistry

## Contents

HIROSHI NARITA, TOMOYUKI OKIMOTO, and SEISHI MACHIDA: Polymerization of Acrylamide Initiated with Pinacol-Ceric Ion Redox System.....	2725
M. R. GRANCIO and D. J. WILLIAMS: Molecular Weight Development in Constant-Rate Styrene Emulsion Polymerization.....	2733
THEODORE SULZBERG and ROBERT J. COTTER: Charge-Transfer Complexing in Polymer Mixtures. IV. Acceptor Polymers from Nitrophthalic Acids and Their Mixtures with Donor Polymers from Aryliminodiethanols.....	2747
J. E. HERWEH and W. Y. WHITMORE: Poly-2-oxazolidones: Preparation and Characterization.....	2759
YASUSHI JOH, HEIMEI YUKI, and SHUNSUKE MURAHASHI: Stereospecific Polymerization of Isobutyl Vinyl Ether by $AlR_2-VCl_n$ Catalysts. I. Influence of Preparative Conditions of the Catalysts.....	2775
HIDEKI SHIOZAKI and YOSHIO TANAKA: Salt-Catalyzed Reaction between Styrene Oxide and Silk Fibroin.....	2791
N. BEREDJICK and W. J. BURLANT: Polymerization of Monolayers of Vinyl and Divinyl Monomers.....	2807
KATSUKIYO ITO: Treatments of Cross-Termination Rate Constants in Radical Copolymerization.....	2819
TAKUJI HIRAHARA, TAKAAKI SUGIMURA, and YUJI MINOURA: Polymerization of Vinyl Monomers by Diphenylsulfone-Potassium Complexes.....	2827
KAZUYUKI HORIE, ITARU MITA, and HIROTARO KAMBE: Calorimetric Investigation of Polymerization Reactions. IV. Curing Reaction of Polyester Fumarate with Styrene.....	2839
TOYOKI KUNITAKE, TOSHIHIDE NAKASHIMA, and CHUJI ASO: Syntheses and Reactions of Ferrocene-Containing Polymers. III. Cyclopolymerization of 1,1'-Divinylferrocene.....	2853
I. VANCsÓ-SZMERCSÁNYI, E. MAKAY-BÖDY, E. SZABÓ-RÉTHY, and P. HIRSCHBERG: Studies on Polyesterification Reactions: Calculation of the Rates of Reverse Reactions.....	2861
ERNEST MARÉCHAL: Polymérisation et Copolymérisation Cationiques des Methylindenes.....	2867
S. L. REEGEN and K. C. FRISCH: Isocyanate-Catalyst and Hydroxyl-Catalyst Complex Formation.....	2883
PHAM-QUANG-THO et JEAN GUILLOT: Étude de la Cotacticité des Copolymères Acrylonitrile-Méthacrylate de Méthyle par Résonance Magnétique Nucleaire—haute Résolution.....	2893
DONALD F. ANDERSON and D. A. MCKENZIE: Mechanism of the Thermal Stabilization of Poly(vinyl chloride) with Metal Carboxylates and Epoxy Plasticizers.....	2905
W. K. BUSFIELD and R. W. HUMPHREY: Mechanism of the Polymerization of Trifluoroacetaldehyde Initiated by Azobisisobutyronitrile.....	2923

(continued inside)

# Journal of Polymer Science: Part A-1: Polymer Chemistry

**Board of Editors:** H. Mark • C. G. Overberger • T. G. Fox

## **Advisory Editors:**

R. M. Fuoss • J. J. Hermans • H. W. Melville • G. Smets

**Editor:** C. G. Overberger      **Associate Editor:** E. M. Pearce

## **Advisory Board:**

T. Alfrey, Jr.	E. M. Fettes	C. S. Marvel	W. H. Sharkey
W. J. Bailey	N. D. Field	F. R. Mayo	W. R. Sorenson
D. S. Ballantine	F. C. Foster	R. B. Mesrobian	V. T. Stannett
M. B. Birenbaum	H. N. Friedlander	H. Morawetz	J. K. Stille
F. A. Bovey	K. C. Frisch	M. Morton	M. Szwarc
J. W. Breitenbach	N. G. Gaylord	S. Murahashi	A. V. Tobolsky
W. J. Burlant	W. E. Gibbs	G. Natta	E. J. Vandenberg
G. B. Butler	A. R. Gilbert	K. F. O'Driscoll	L. A. Wall
S. Bywater	J. E. Guillet	S. Okamura	F. X. Werber
T. W. Campbell	H. C. Haas	P. Pino	O. Wichterle
W. L. Carrick	J. P. Kennedy	C. C. Price	F. H. Winslow
H. W. Coover, Jr.	W. Kern	B. Rånby	M. Wismer
F. Danusso	J. Lal	J. H. Saunders	
F. R. Eirich	R. W. Lenz	C. Schuerch	

## *Contents (continued), Vol. 8*

L. J. TANGHE, W. J. REBEL, and R. J. BREWER: Prehump in the Gel-Permeation Chromatography Fractionation of Pulp Cellulose Acetate. . . . .	2935
N. LAKSHMINARAYANAIHAH and FASIH A. SIDDIQI: Relationship Between Membrane Potential and Electrolyte Uptake by Ion-Exchange Membranes. . . . .	2949
ZENJIRO OSAWA, TETSUAKI SHIBAMIYA, and TOSHIO KAWAMATA: Catalytic Action of Metallic Salts in Autoxidation and Polymerization. IV. Polymerization of Methyl Methacrylate by Cobalt(II) or (III) Acetylacetonate- <i>tert</i> -Butyl Hydroperoxide or Dioxane Hydroperoxide. . . . .	2957
R. S. BAUER and W. W. SPOONER: Radiation-Induced Polymerization of Isobutylene Oxide. . . . .	2971
YOSHIKI KOBUKE, TAKAYUKI FUENO, and JUNJI FURUKAWA: Polymerization of <i>cis</i> - and <i>trans</i> -Cinnamitriles by Anionic Catalysts. . . . .	2979

(continued on inside back cover)

The Journal of Polymer Science is published in four sections as follows: Part A-1, Polymer Chemistry, monthly; Part A-2, Polymer Physics, monthly; Part B, Polymer Letters, monthly; Part C, Polymer Symposia, irregular.

Published monthly by Interscience Publishers, a Division of John Wiley & Sons, Inc., covering one volume annually. Publication Office at 20th and Northampton Sts., Easton, Pa. 18042. Executive, Editorial, and Circulation Offices at 605 Third Avenue, New York, N. Y. 10016. Second-class postage paid at Easton, Pa. Subscription price, \$325.00 per volume (including Parts A-2, B, and C). Foreign postage \$15.00 per volume (including Parts A-2, B, and C).

Copyright © 1970 by John Wiley & Sons, Inc. All rights reserved. No part of this publication may be reproduced by any means, nor transmitted, or translated into a machine language without the written permission of the publisher.

## Polymerization of Acrylamide Initiated with Pinacol-Ceric Ion Redox System

HIROSHI NARITA, TOMOYUKI OKIMOTO, and  
SEISHI MACHIDA, *Chemical Laboratory of Textile Fibers,  
Kyoto University of Industrial Arts and Textile Fibers,  
Matsugasaki, Sakyo-ku, Kyoto, Japan*

### Synopsis

Polymerization of acrylamide initiated with a pinacol-ceric ion redox system was investigated. The polymer obtained was found to contain one cerium atom in a polymer molecule. It was considered that the cerium atom was introduced into the polymer molecule by the termination reaction as there is no cerium atom in the initiating radical in the present system. A similar termination reaction was attained by ferric ion but not by cerous ion. The metal ion was considered to terminate the polymerization to form a stable polymer. Some considerations on the structure of the reaction product relating to the polymerization mechanism were discussed.

### INTRODUCTION

It has been reported<sup>1</sup> that a polyacrylamide containing cerium atom was produced in polymerization of acrylamide initiated with ceric salt, and the polymer contained iron when a ferric salt was added in the same system.<sup>2</sup> On the basis of studies by electrophoresis, polarography, and infrared spectrometry, it was proposed that the polymer combines with the metal and that only one cerium atom is present per polymer chain. The metal was considered to be introduced in the termination of the polymerization. The initiation mechanism for the acrylamide-ceric ion system is not yet clear. It has not been confirmed whether or not cerium atom is present in the primary radical.

The present communication deals with the polymerization of acrylamide initiated with the pinacol-ceric ion redox system. As the primary radical which initiates the polymerization,  $(\text{CH}_3)_2\dot{\text{C}}\text{OH}$ , contains no cerium atom, no cerium atom is introduced into the polymer by the initiation reaction. However in the present experimental results, the polymer was found to contain one cerium atom per molecular chain, and the metal was found to combine with the end of the polymer chain in the termination. Some termination mechanisms are discussed.

## EXPERIMENTAL

### Materials

Acrylamide was purified by recrystallization from acetone, mp 84°C. Pinacol was recrystallized from water, mp 46°C. Ammonium cerium(IV) nitrate, cerous nitrate, ferric nitrate and nitric acid were obtained commercially.

### Polymerization

Polymerizations were carried out in the reaction vessel shown in Figure 1. Acrylamide and pinacol solution were placed in one side, ammonium cerium(IV) nitrate solution and nitric acid were placed in the other; cerous nitrate or ferric nitrate solution, if used, was placed in this side. Polymerization tubes were sealed under nitrogen. After heating the vessel to 15°C in a thermostat, the two solutions were mixed. After a certain reaction time, the solution mixture was poured into acetone. The polymer was separated on a glass filter and dried under reduced pressure at room temperature.

To obtain a polymer sample for analysis, a 200 ml four-necked flask was used as a reaction vessel. The polymer obtained was purified with Sephadex G-25 to eliminate metal salt present as contaminant.

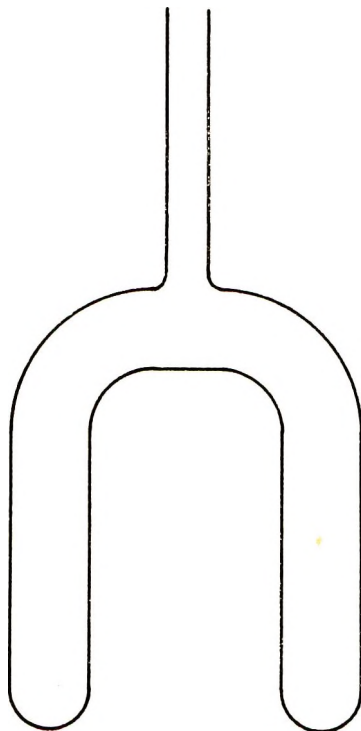


Fig. 1. Polymerization apparatus.

### Analysis of Polymer

A quantity of polymer was subjected to combustion in a crucible. The residue was dissolved in dilute sulfuric acid solution and ammonium persulfate added to oxidize the cerous ion to ceric ion. The ceric ion thus formed was determined spectrophotometrically.<sup>3</sup>

The molecular weight of polymer was determined by means of vapor-pressure osmometry in aqueous solution.

Infrared spectra of polymers were measured as KBr disks (4000–650  $\text{cm}^{-1}$ ) and as Nujol mulls (700–100  $\text{cm}^{-1}$ ).

Polarographic analysis was carried out with 1.0*M* tetramethylamine bromide solution as an electrolyte.

### RESULTS AND DISCUSSION

The relation between ceric ion concentration and conversion obtained in the polymerization is shown in Figure 2. Even at a relatively low reaction temperature (15°C), appreciably high conversion are obtained. In the previous report,<sup>1</sup> the maximum conversion was only a few per cent in the absence of pinacol in the reaction system; in that case, the initiation probably involves the reaction of acrylamide with ceric ion. It was previously known that such an initiation of polymerization is rather unusual in that system. To the contrary, in the present system containing pinacol the polymerization is initiated as follows:



where P and R· are pinacol and the primary radical,  $(\text{CH}_3)_2\dot{\text{C}}\text{OH}$ , respectively. As the pinacol–ceric ion redox system is highly reactive, initiation by the reaction of acrylamide with ceric ion is negligible.<sup>4</sup>

In Figure 2, maxima are observed, the peak shifting to higher ceric ion concentration with increasing pinacol concentration. First, when the

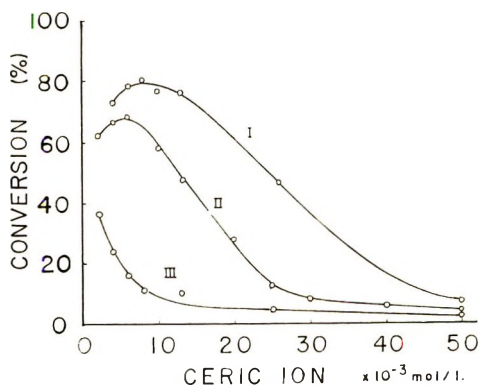


Fig. 2. Plots of conversion vs. ceric ion concentration: (I)  $[\text{P}] = 0.016$  mole/l.; (II)  $[\text{P}] = 0.008$  mole/l.; (III)  $[\text{P}] = 0.002$  mole/l.  $[\text{Acrylamide}] = 1.59$  mole/l.,  $[\text{HNO}_3] = 0.05$  mole/l., 15°C, 60 min.

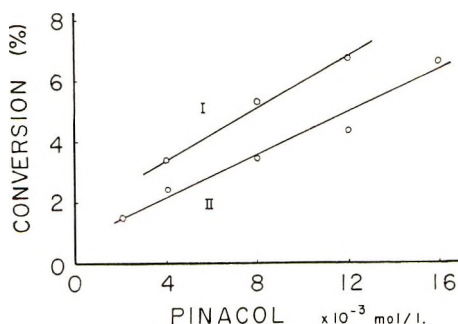


Fig. 3. Plots of conversion vs. pinacol concentration: (I)  $[Ce^{IV}] = 4.0 \times 10^{-2}$  mole/l.; (II)  $[Ce^{IV}] = 5.0 \times 10^{-2}$  mole/l. [Acrylamide] = 1.59 mole/l.,  $[HNO_3] = 0.05$  mole/l.,  $15^\circ C$ , 60 min.

pinacol concentration is in excess relative to ceric ion, a primary radical is generated, depending on the concentration of ceric ion, as shown by eq. (1), and conversion increases with concentration of ceric ion. Next, when the concentration of ceric ion becomes higher and exceeds that of pinacol, the primary radical is consumed by ceric ion, as shown in eq. (2):



The conversion decreases with further increasing concentration of ceric ion. Thus a maximum appears relative to the two reactions (1) and (2). The peak on the curve shifts towards higher ceric ion concentration with increasing pinacol concentration.

The relation between conversion and concentration of pinacol is shown in Figure 3. As large amount of primary radical is supplied according to the concentration of pinacol added, the conversion increases with the concentration of pinacol. The slope of two curves must be essentially parallel, as indicated by eq. (3) developed in the previous report.<sup>4</sup>

$$R_p = k([M]^2/[Ce^{IV}])[P] \quad (3)$$

On curve I at the lower concentration of ceric ion, a large proportion of ceric ion is consumed in the formation of the complex with pinacol [eq. (1)], and the excess of ceric ion which reacts with the primary radical is decreased [eq. (2)]. So the conversion is increased with increasing concentration of pinacol. Thus the slope became slightly more steep than that at the higher concentration of ceric ion.

After the maximum conversion of polymerization, the excess of ceric ion reacts with polymer radical as well as primary radical. The polymerization reaction is terminated as shown in eq. (4):



where  $M_n \cdot$  denotes a polymer radical. It was previously made clear that reaction (4) proceeds preferentially to the reaction (5) at the higher concentrations of ceric ion:



Polymerization conditions, and molecular weight and cerium content of polymer are summarized in Table I. It was found that both conversion and molecular weight decrease with the concentration of ceric ion and that reciprocal of the molecular weight is proportional to the concentration of ceric ion, as shown in Figure 4. From those results, it is clear that the termination scheme (4) actually occurs.

The cerium content of polymer increases with the concentration of ceric ion. The number of cerium atoms per polymer chain is almost unity, but in experiments 1 and 7 small values (0.14 and 0.08, respectively) are found, shown in Table I. In experiments 1, 6, and 7 the polymerization was carried out at a low concentration of ceric ion, so reactions (4) and (5) occur simultaneously. The polymer obtained is a mixture of polymer

TABLE I  
Polymerization of Acrylamide in Aqueous Solution at 15°C During 60 Minutes

Expt. no.	[Acrylamide], mole/l.	[Ceric ion], $\times 10^{-3}$ , mole/l.	[Pinnacol], mole/l.	[HNO <sub>3</sub> ], mole/l.	Yield, % <sup>a</sup>	$\bar{M}$	Cerium content, %	Number of cerium atoms per polymer chain $N^b$
1	1.59	10.4	0.004	0.05	20.9	3190	0.57	0.14
2	1.59	20.8	0.004	0.05	7.29	1320	11.1	1.05
3	1.59	30.2	0.004	0.05	4.99	1240	14.1	1.25
4	1.59	41.6	0.004	0.05	4.75	1030	15.1	1.11
5	1.59	48.7	0.004	0.05	4.87	804	22.4	1.29
6	1.59	10.4	0.010	0.05	—	2780	Trace	—
7	1.59	20.8	0.010	0.05	29.1	2710	0.40	0.08
8	1.59	31.2	0.010	0.05	8.94	2350	6.75	1.13
9	1.59	41.6	0.010	0.05	7.05	2140	7.02	1.07
10	1.59	51.9	0.010	0.05	6.92	1660	10.8	1.28

<sup>a</sup> Crude polymer, not purified by Sephadex G-25.

<sup>b</sup>  $N = \bar{M} \times \text{cerium content} \div 140.10$ .

having no cerium atom in the chain and that having one cerium atom at the end of the chain. The small values of cerium content in the polymer are obtained in this way. Above that concentration of ceric ion, the polymerization is terminated only with ceric ion, and the number of cerium atoms combined with the polymer chain is unity. Thus the cerium atom must be combined by the mechanism of termination of the scheme (4).

Similar polymerizations at a concentration of ceric ion of  $1 \times 10^{-2}$  mole/l. in the presence of cerous nitrate or ferric nitrate were carried out; the conversion curves are shown in Figure 5. It is considered from Table I that the amount of ceric ion is enough to initiate the polymerization reaction but insufficient for the termination reaction. The conversion decreases on addition of ferric ion, which is involved only in the termination reaction.<sup>2</sup> In the polymerization in the presence of cerous ion, however,

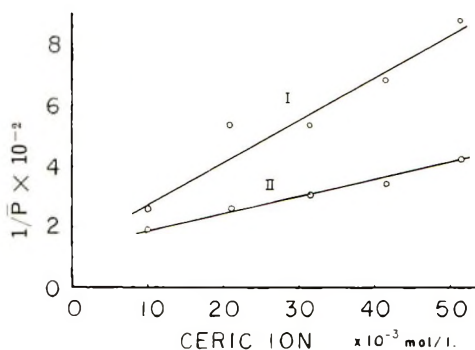


Fig. 4. Plots of  $1/\bar{P}$  vs. ceric ion concentration: (I)  $[P] = 0.004$  mole/l.; (II)  $[P] = 0.010$  mole/l.  $[\text{Acrylamide}] = 1.59$  mole/l.,  $[\text{HNO}_3] = 0.005$  mole/l.,  $15^\circ\text{C}$ , 60 min.

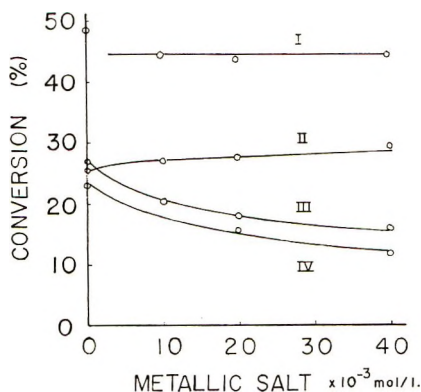


Fig. 5. Plots of conversion vs. concentrations of cerous ion and ferric ion: (I)  $\text{Ce}^{\text{III}}$ ,  $[P] = 0.078$  mole/l.,  $[\text{Ce}^{\text{IV}}] = 1.04 \times 10^{-2}$  mole/l., 40 min; (II)  $\text{Ce}^{\text{III}}$ ,  $[P] = 0.082$  mole/l.,  $[\text{Ce}^{\text{IV}}] = 1.00 \times 10^{-2}$  mole/l., 10 min; (III)  $\text{Fe}^{\text{III}}$ ,  $[P] = 0.081$  mole/l.,  $[\text{Ce}^{\text{IV}}] = 1.03 \times 10^{-2}$  mole/l., 15 min; (IV)  $\text{Fe}^{\text{III}}$ ,  $[P] = 0.077$  mole/l.,  $[\text{Ce}^{\text{IV}}] = 1.00 \times 10^{-2}$  mole/l., 10 min.  $[\text{Acrylamide}] = 1.54$  mole/l.,  $[\text{HNO}_3] = 0.05$  mole/l.,  $15^\circ\text{C}$ .

the conversion is independent of cerous ion concentration; therefore it is obvious that the cerous ion has no bearing on the termination reaction.

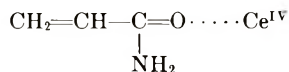
The polymer obtained is pale yellow powder and absorbs light of wavelength of  $252 \text{ m}\mu$  in solution. The wavelength is different from that ( $278 \text{ m}\mu$ ) of ammonium cerium(IV) nitrate solution. On the polarogram of polymer, a halfwave potential of  $-1.6 \text{ V}$  which appears in the ammonium cerium(IV) nitrate solution is not shown. It is not believed that the polymer is contaminated with ceric salt. The halfwave potential of a Ce complex would be shifted more to the negative side.

The difference between the infrared spectra of the present polymer and polyacrylamide obtained with potassium persulfate as an initiator was little.

The viscosity of the polymer solution was increased by heating.



Fujii et al.<sup>5</sup> considered an intermediate compound of vinylcarbazole radical and cerous or ferrous ion in a process of dimerization of vinylcarbazole initiated by ceric ion and ferric ion. Takahashi et al.,<sup>6</sup> on the other hand, proposed a complex compound composed of acrylamide and ceric salt:



In the present system no reaction of polymer radical with cerous ion occurred. The polymer radical would react with ceric ion at a terminal end to give a similar complex as that proposed by Takahashi, and a stable structure would be obtainable.

### References

1. H. Narita and S. Machida, *Makromol. Chem.*, **97**, 209 (1966).
2. H. Narita, S. Okamoto, and S. Machida, *Makromol. Chem.*, **111**, 14 (1968).
3. A. I. Medakia and B. J. Byren, *Anal. Chem.*, **23**, 453 (1951).
4. H. Narita, S. Okamoto, and S. Machida, *Makromol. Chem.*, **125**, 15 (1969).
5. H. Fujii, R. Cellin, and A. Ledwith, paper presented 18th Annual Meeting, Society of Polymer Chemistry of Japan, Kyoto, 1969.
6. T. Takahashi, Y. Hori, and I. Sato, *J. Polym. Sci. A-1*, **6**, 2091 (1968).

Received November 25, 1969

Revised February 24, 1970

## Molecular Weight Development in Constant-Rate Styrene Emulsion Polymerization\*

M. R. GRANCIO<sup>†</sup> and D. J. WILLIAMS, *Chemical Engineering Department, The City College of The City University of New York, New York, New York 10031*

### Synopsis

Continuously uniform latices were applied in an experimental study of molecular weight development in constant-rate styrene emulsion polymerization. The formulation around which this study centered exhibited Smith-Ewart, case II kinetics from zero to about 60% conversion with a constant conversion rate of  $13 \pm 2\%$ /hr and a final particle diameter of 2300 Å. By utilizing an inhibitor perturbation technique, we directly confirmed that free radicals are generated from  $K_2S_2O_8$  by a first-order process with 100% efficiency. We further confirmed that, in contrast to current theories for constant rate polymerization, both the instantaneous values of  $\bar{M}_n$  and  $\bar{M}_v$  may increase 6- to 9-fold. Little or no chain branching is evidenced. We interpret these findings to mean that radicals are not utilized with 100% efficiency in emulsion polymerization.

### INTRODUCTION

Our recent research into the fundamentals of styrene emulsion polymerization reaction kinetics has become channelled along two primary lines of investigation: (a) the morphology of the growing monomer-polymer particle and (b) the development of molecular weight with conversion. Our experimental studies have centered around the use of two formulations which produce continuously uniform latices and which display Smith-Ewart, case II kinetics from zero to about 60% conversion.<sup>1</sup> The constant rates of conversion for these are  $13 \pm 2$  and  $21 \pm 2\%$ /hr, with resulting particle diameters of 2300 and 1950 Å, respectively.

As reported in an earlier paper,<sup>1</sup> the most novel aspect of this investigation is that dealing with the latex particle morphology. Briefly in review, we reported substantial evidence to support a heterogeneous core-shell morphology for the growing monomer-polymer particles during constant rate growth. In this core-shell model, a growing particle consists of an expanding polymer-rich core surrounded by a monomer-rich shell. The outer shell serves as the major locus of polymerization while virtually none

\* Presented in part to The Division of Organic Coatings and Plastics Chemistry, The American Chemical Society, Minneapolis, April, 1969.

<sup>†</sup> Present address: Monsanto Company, Hydrocarbon and Polymer Research Department, Indian Orchard, Massachusetts 01051.

occurs within the central core because of its monomer-starved condition. A Smith-Ewart, on-off, mechanism prevails within the monomer-rich shell. The core is pictured as growing outward somewhat as a ball of string constructed from many single strands.

In this paper we report the results of our recent molecular weight development and radical generation studies. The Smith-Ewart theory<sup>2</sup> as well as its modified forms<sup>3-10</sup> predict the generation of constant molecular weight polymer during periods of constant rate polymerization, while a severalfold increase is generally observed. The earliest work<sup>11</sup> on this problem was based only on viscosity-average molecular weight measurements. Later work<sup>12</sup> presented number-average measurements as well, but these measurements were derived from a 21%/hr formulation in which the number-average molecular weight values approached 10<sup>6</sup>. Since this was very near the upper operating limit of membrane osmometry, a lower reaction rate and lower molecular weights were required to obtain more reliable data. To this end we halved the anionic soap content previously used<sup>12</sup> in the 21%/hr formulation to obtain a 13%/hr formulation, and it is for this formulation that we now report molecular weight development and the rate of radical generation. Molecular weight development is discussed in terms of cumulative and instantaneous number- and viscosity-average molecular weight as well as its distribution as analyzed by gel-permeation chromatography (GPC). The rate of radical generation for an actual emulsion polymerization in progress was established both by initiator decomposition measurements and inhibitor perturbation methods.

### MOLECULAR WEIGHT DEVELOPMENT

Since we are utilizing continuously uniform latices, the overall molecular weight properties are the same as the individual particle properties. This is significant in that it allows one to study particle size-dependent parameters without averaging over a range of particle sizes. In addition, the rate processes per particle, such as rates of initiation, termination and propagation, will all be identical for each and every particle and simply equal to the overall values divided by the total number of particles. Thus, we are able to focus attention on the individual particle as a reactor unit.

Since we have shown that the formulation of interest exhibits case II, Smith-Ewart kinetics,<sup>1</sup> the instantaneous number-average molecular weight  $\bar{M}_{ni}$ , can be predicted from the kinetic chain length equation. For steady state, termination by combination, and 100% radical efficiency, the result is simply

$$\bar{M}_{ni} = [(R_p/k_d[I]_0) \exp \{k_d t\}](M_0) \quad (1)$$

where  $R_p$  is the overall rate of polymerization,  $k_d$  is the initiator decomposition constant,  $[I]_0$  is the initial initiator concentration,  $t$  is time and  $M_0$  is the molecular weight of monomer. The decomposition constant  $k_d$  as measured by Kolthoff et al.<sup>13</sup> was found to be on the order of 10<sup>-4</sup> min.<sup>-1</sup>.

For this low value of  $k_d$  the exponential term in eq. (1) is almost unity throughout the course of reaction. Thus, since  $k_d$  and  $[I]_0$  are constants, eq. (1) predicts a constant instantaneous number average molecular weight during the ideal period when  $R_p$  is constant. As we indicated earlier, all variants of the Smith-Ewart theory<sup>3-10</sup> also predict  $\bar{M}_{ni}$  constant for these same conditions.

Previous investigations<sup>7-11</sup> have utilized the pure aqueous decomposition kinetics of Kolthoff and Miller<sup>13</sup> in predicting molecular weights. This is not a valid approach in view of the fact that other studies have shown that persulfate decomposes as much as eight times faster in the presence of soaps.<sup>14,15</sup> Up to now initiator decomposition has not been followed throughout the course of reaction in the actual polymerization medium. We have introduced an inhibitor perturbation technique to accomplish this and we report such data here. Another important, but unsubstantiated, assumption which investigators are prone to evoke is that free radicals are utilized with 100% efficiency. Our work raises serious question as to the validity of this assumption.

The instantaneous viscosity average molecular weight cannot be predicted as simply as the number average. However, under steady state conditions and in the absence of side reactions which lead to chain branching, one would expect the ratio,  $\bar{M}_{vi}/\bar{M}_{ni}$  to remain constant, independent of conversion.

Cumulative molecular weights are, of course, measured in practice. Instantaneous values were calculated from material balances on the cumulative curves at 10% intervals. For example, if the cumulative number average molecular weights at 20 and 30% conversion were measured as  $A$  and  $B$  then the instantaneous number average molecular weight being generated at 25% conversion  $X$ , was calculated from

$$\frac{0.20}{A} + \frac{0.10}{X} = \frac{0.30}{B}$$

The instantaneous viscosity average molecular weights were calculated from

$$0.20A + 0.10X = 0.30B$$

## EXPERIMENTAL

### Polymerization

The polymerizations were conducted in both a bottle polymerizer and a paddle-mixed, one-liter kettle reactor at  $60 \pm 1^\circ\text{C}$ . The entire formulation, except for the initiator, was charged initially and nitrogen purged for one-half hour to eliminate an induction period. Monomer and water were distilled and nitrogen purged. The formulation for this study is 180 g water, 100 g monomer, 0.15 g sodium lauryl sulfate, 3.0 g Triton X-100 (a nonionic octylphenoxyethyl surfactant, product of Rohm and Haas Co.,

Philadelphia, Pa.), 0.500 g  $K_2S_2O_8$  and 0.085 g KOH. This formulation had a conversion rate of  $13 \pm 2\%/hr$ , up to about 60%, a final particle diameter = 2300 Å, and pH = 9 (constant).

The data of runs marked KI, KII denote kettle runs while those marked BI, BII, BIII denote bottle runs. A single bottle run was comprised of several identically charged bottles, since the contents of an entire bottle were required for molecular weight analysis at low conversion. Conversions were determined primarily by gravimetric means. For further details on the characteristics of this formulation see references (1,12).

### Initiator Kinetics

**Initiator Decomposition.** The rate of persulfate decomposition in alkaline soap solution was determined via an iodine titration technique developed by Kolthoff et al.<sup>13,16</sup> Attempts at direct titration of a latex failed because of endpoint obscurity, so the titrations were carried out in the absence of latex or monomer but in soap solutions corresponding to the requirements of our 13%/hr formulation (180 g water, 3.00 g Triton X-100, 0.15 g sodium lauryl sulfate, 0.075 g KOH, and 0.500 g  $K_2S_2O_8$ ). These solutions were charged in bottles, which were then placed in the bottle polymerizer for 1–4 hr at  $60 \pm 1^\circ C$ , withdrawn, and cooled in ice water. Two kettle runs were also made at 3 hr and  $4\frac{3}{4}$  hr. The reactor samples were acidified with acetic acid. KI (10 g) was added and allowed to react with the residual  $K_2S_2O_8$  for 30 min with agitation. The released iodine was titrated quantitatively with sodium thiosulfate.

This technique was developed for pure aqueous solutions. The fact that the presence of the soaps did not significantly alter the validity of the titrations was substantiated by titrations: three samples of 0.5  $K_2S_2O_8$  in 180 ml water and three other samples with 0.5  $K_2S_2O_8$ , 0.15 g sodium lauryl sulfate, and 3.00 g Triton X-100 in 180 ml water. The first set of samples required 37.0, 36.8, and 36.6 ml of 0.1 *N* sodium thiosulfate while the second set required 37.4, 37.5, and 36.2 ml. Thus, the soaps did not alter the results of the titration.

Some scatter was observed in the data. This could be attributed to two factors: (a) the soap foamed making titration difficult and (b) the presence of surfactant masked the endpoint. The foaming problem could probably be eliminated with an inactive antifoaming agent.

**Radical Generation Rates.** Inhibitor studies were conducted to measure the rate of generation of free radicals in the actual aqueous reaction medium. This was done to verify and amplify the decomposition data. Here an aqueous solution of paraquinone was added to a reaction, 1, 2, or 3 hr in progress, and the radical generation rate was measured by the length of the inhibition period before reaction resumed. Figure 1 shows a sample curve. Polymerization ceased within moments after the addition of paraquinone solution to the reacting latex; a clean inhibition period was observed; and eventually polymerization resumed. Although paraquinone is more water-soluble than styrene-soluble, a sufficient quantity probably entered

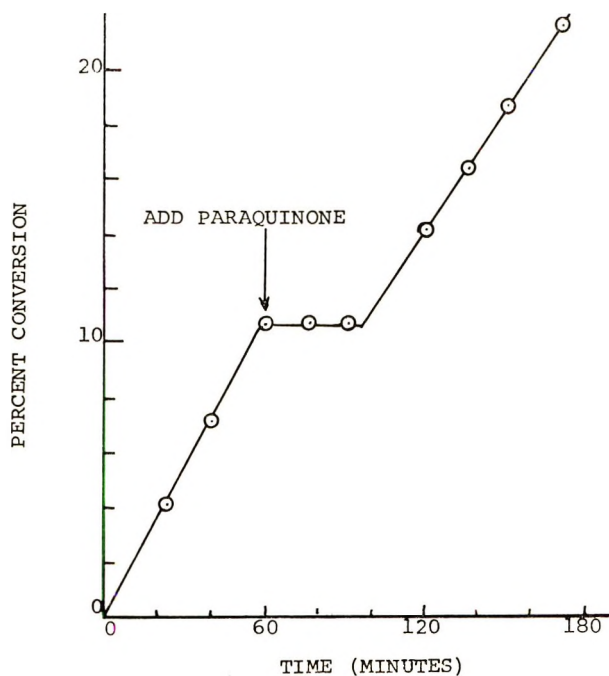


Fig. 1. Sample inhibitor curve.

monomer-polymer particles to stop previously activated chains within minutes.

A reaction mechanism reported by Price and Read,<sup>17</sup> in which two moles of quinone are consumed for each mole of radicals captured, was found to best fit the data.

### Molecular Weight Development

**Sample Preparation.** Polystyrene was precipitated in granular form from the latex in methanol acidified with sulfuric acid. The polymer was recovered by filtration and washed repeatedly with methanol and water. Subsequently, the polystyrene was redissolved in toluene, precipitated as a fine powder with methanol in a Waring Blendor, and methanol-washed several times. GPC measurements showed that this procedure eliminated all polymer of molecular weight less than 6000.

**Viscosity-Average Molecular Weight.** Intrinsic viscosities were determined by the one-point method of Maron<sup>18</sup> from relative viscosities of dilute toluene solutions measured at 30°C in Cannon-Ubbelohde dilution viscometers. In the exponential relationship  $\eta = KM^a$  the constants of Goldberg et al.<sup>19</sup> were used:  $K = 3.7 \times 10^{-4}$  and  $a = 0.62$ .

**Number-Average Molecular Weight.** Osmotic pressures were measured with a Mechrolab 501 high-speed osmometer utilizing an ArRo 300-D gel cellophane membrane (ArRo Laboratories, Inc., Joliet, Illinois 60434).

Toluene solutions were used at 37°C, with concentrations ranging from 1 to 10 g/l.

**Molecular Weight Distribution.** The GPC analysis was performed by Dr. A. E. Hamielec of McMaster University. Calibration was accomplished with the samples sent for analysis by use of the molecular weight values we had determined in our laboratory.

## RESULTS

### Radical Generation

**Initiator Decomposition.** The data in Figure 2 indicate that the decomposition of potassium persulfate in aqueous alkaline (pH = 9) soap solution, corresponding to the 13%/hr formulation, is first-order with  $k_d = 1.30 \times 10^{-3} \text{ min}^{-1}$ . This value is more than three times that determined by Kolthoff and Miller<sup>13</sup> in the absence of soaps. In Figure 2, the two dotted lines represent bounds on the data. The high bound indicates  $k_d = 1.55 \times 10^{-3} \text{ min}^{-1}$ , while the low bound yields  $k_d = 1.05 \times 10^{-3} \text{ min}^{-1}$ . Thus the maximum error in using  $k_d = 1.3 \times 10^{-3} \text{ min}^{-1}$  is  $\pm 20\%$ . These data and their implication in molecular weight development will be discussed after a consideration of rates of generation of free radicals.

**Radical Generation Rates.** The inhibition period studies with water-soluble inhibitors verified the nature of the aqueous phase free-radical generation process. Comparison of columns E and F in Table I show that the measured induction periods are in close agreement with those predicted from decomposition data. Thus, free radicals are formed in the aqueous phase by a 100% efficient first-order decomposition of persulfate, and the presence of dissolved monomer, latex, and the physical location of the soap do not alter the decomposition kinetics derived from the aqueous soap solution studies. The agreement between the two techniques is reassuring, but

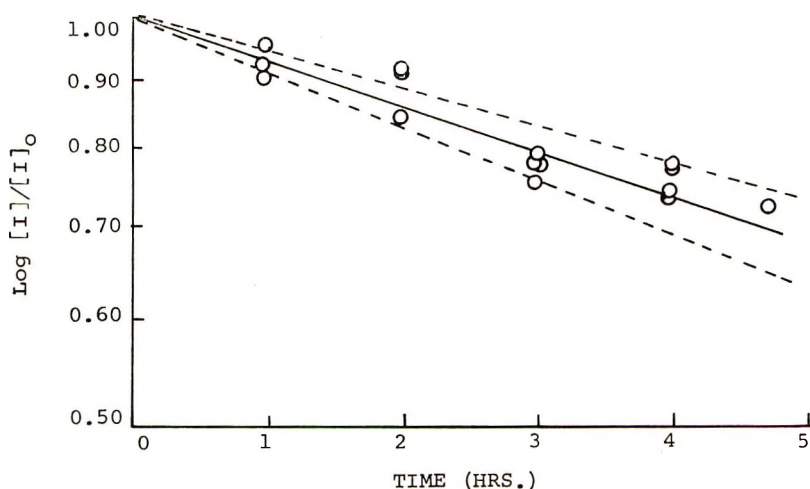


Fig. 2. Decomposition of  $\text{K}_2\text{S}_2\text{O}_8$  in alkaline soap solution.

TABLE I  
Inhibitor Data

	A	B	C	D	E	F
	Reaction time, min <sup>a</sup>	Conversion rate, %/hr <sup>b</sup>	PQ added, g	Induction period, min	Adjusted Induction period, min <sup>c</sup>	Expected induction period, min <sup>d</sup>
1	15	12.0	0.032	32.0	29.6	29
2	60	14.5	0.008	7.0	7.8	7.5
3	60	13.4	0.016	13.0	13.5	15
4	60	10.6	0.032	36.0	29.4	30
5	60	10.3	0.032	36.0	28.6	30
6	120	12.8	0.032	32.0	31.2	33
7	180	15.4	0.032	30.0	35.5	36

<sup>a</sup> Reaction time at which inhibitor was added.

<sup>b</sup> Conversion rate before addition of inhibitor.

<sup>c</sup> Induction period adjusted to an initial conversion rate of 13.0%/hr, obtained by multiplying the measured induction period by the ratio of column B to 13.0.

<sup>d</sup> Expected induction period based on reaction mechanism, decomposition data, and 100% radical generation efficiency.

the inhibitor method is probably the most direct and useful general approach in such studies.

Furthermore, comparison of runs, 1, 4, 6, and 7, (Table I) in which 0.32 g of paraquinone have been added to reactions 15, 60, 120, and 180 min in progress show that there is no unusual variation in the radical generation process throughout the course of a run. To verify the quantitative nature of the study, notice that runs 2, 3, and 4, show that the inhibition period is directly proportional to the quantity of inhibitor added. Further comparison of runs 4 and 5 underscores the reproducibility of the measurements.

In Table I, an adjusted inhibition period was determined by multiplying the observed induction period by the ratio of the observed conversion rate before the addition of paraquinone to 13.0. The reasoning behind the adjustment is as follows. As previously reported,<sup>1</sup> it was not possible to reproduce rate behavior exactly. Hence, the inhibition runs each exhibited slightly different initial conversion rates. We believe that the slight variations in conversion rates should be directly associated with slight variations in the initiator decomposition kinetics, with higher rates reflecting the accelerated decomposition and lower rates decelerated decompositions. So, by adjusting the inhibition period, all of the data were "corrected" to the average decomposition kinetics which yield an average conversion rate of 13%/hr. Although the corrections are small and they do not substantially alter the arguments made, they are in a direction which "smoothes" the data.

### Molecular Weight Development

All the molecular weight data are compiled in Table II. The asterisked data indicate duplicate determinations of the same sample. In such cases the reproducibility between measurements was well within  $\pm 5\%$ .



TABLE II  
 Molecular Weight Data

Run and sample <sup>a</sup>	C, %	Intrinsic viscosity	$M_v \times 10^{-6}$	$M_n \times 10^{-6}$
KI- 1	17.5	1.97	0.822	2.33
2	34.1	2.51, 2.52*	1.12, 1.16*	3.18, 3.03*
3	50.0	1.96, 1.97*	0.776, 0.778*	3.79
4	76.0	2.68	1.10	4.46
5	97.0	2.75, 2.80*	1.25, 1.36*	3.79
KII- 1	8.0	—	—	2.08
2	22.0	2.30, 1.95*	0.852, 0.784*	3.20
3	36.0	2.54	1.20	4.04, 4.04*
4	54.0	2.83	1.30	4.88
5	92.0	3.27	1.60	4.04
BI- 6	42.0	2.89	1.44	
10	100.0	3.49	1.84	
BII- 3	23.0	2.35	1.07	
BIII-1	5.0	1.70	0.632	
2	14.0	1.75	0.735	
3	22.0	2.15	0.920	
4	30.0	2.00	0.880	
6	58.0	2.96	1.448	

<sup>a</sup> KI, KII are kettle runs; BI, BII, BIII are bottle polymerizer runs.

Number-average molecular weight samples were taken from kettle runs KI and KII. The cumulative data are shown in Figure 3. The rate curves for these runs are shown as curves I and II in Figure 1 of reference 1; note the constant rate behavior up to about 60% conversion. In Figure 3, an average molecular weight curve is drawn between the curves for runs KI and KII. Either molecular weight development curve (KI or KII) lies

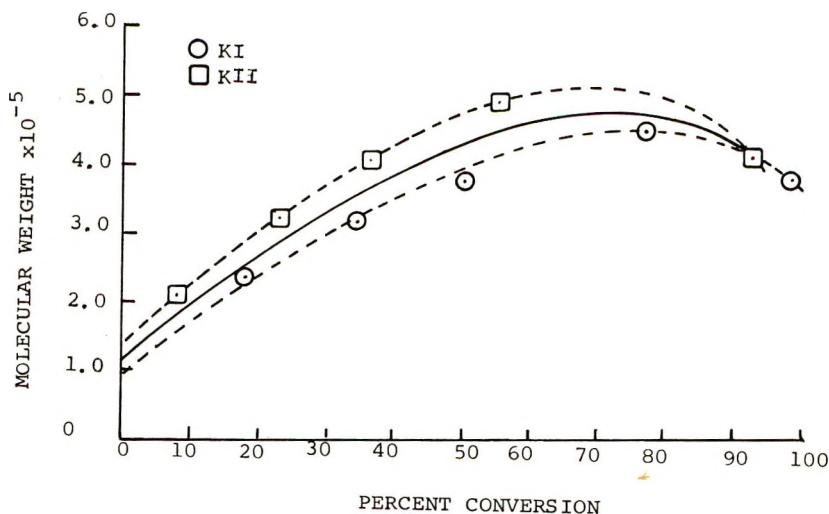


Fig. 3. Number-average molecular weight, cumulative.

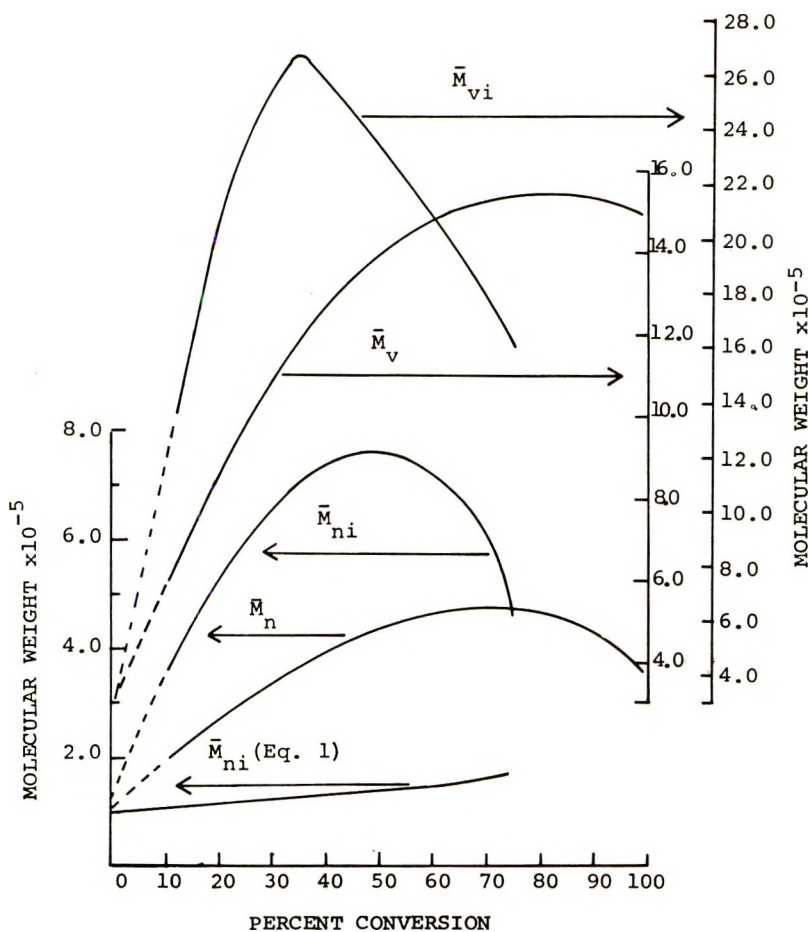


Figure 4.

within  $\pm 10\%$  of the average curve. Instantaneous number-average molecular weights were calculated from the cumulative average curve and are presented in Figure 4 with the average curve for subsequent discussion.

Intrinsic viscosity-conversion behavior is presented in Figure 5. Samples for this curve were obtained from several different reactors, all with conversion rates of  $13 \pm 2\%$ /hr. With the exception of the 50% conversion sample from KII, all the viscosity data points between 0 and 60% conversion lie within  $\pm 15\%$ , computed on the basis of  $\bar{M}_v$ , of the average curve. In fact, half the data points in this range are on the average curve. After 60% the scatter may have been caused by the marginal stability which our formulation exhibited either in the bottle polymerizer at high conversions or in the kettle reactor after considerable material had been removed in earlier sampling. The viscosity data are plotted in Figure 4 as cumulative and instantaneous viscosity average molecular weight for subsequent discussion.

These two curves were derived from computations based on the average curve of Figure 5.

Molecular weight distribution curves for individual samples at 22, 34, and 36 conversion were obtained by means of GPC. There was no marked dif-

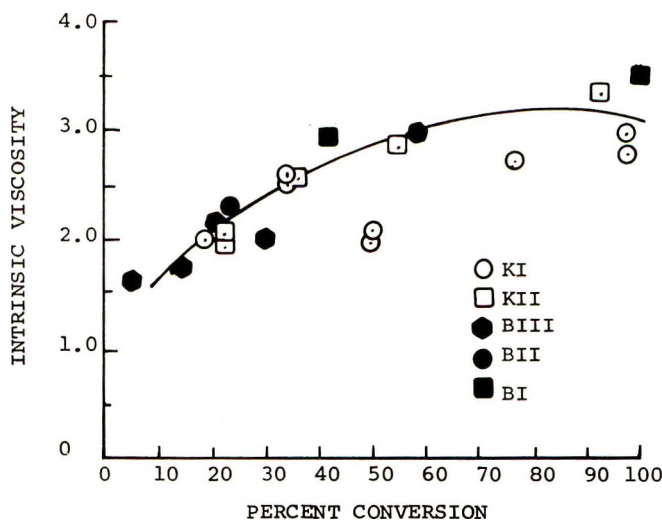


Fig. 5. Intrinsic viscosity vs. conversion.

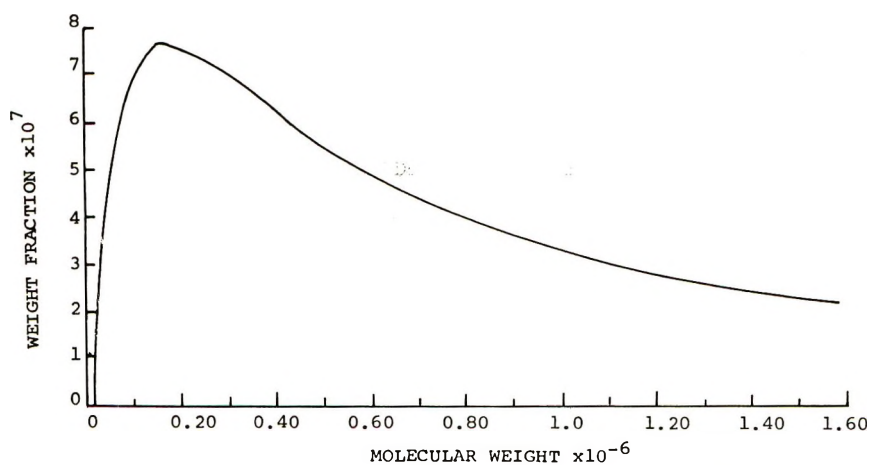


Fig. 6. Molecular weight distribution for sample K-II-3 (36% C).  $\bar{M}_n = 404,000$ ;  $\bar{M}_w = 1,440,000$ ;  $M_v = 1,200,000$ ;  $M_w/M_n = 3.57$ ; highest molecular weight observed =  $1.52 \times 10^7$ .

ference between the samples. Figure 6 shows the 36% conversion sample from run KII. The data cannot be used extensively for interpretation because of inaccuracies in determining weight fractions much beyond 10%. Some useful information can be gleaned from the distribution data however.

First, the distribution curves are very similar to one reported for the GPC analysis of the final product of a similar styrene emulsion polymerization system (Fig. 4 of reference 20) although they are somewhat different from curves obtained by fractional precipitation.<sup>20,21</sup> Second, the molecular weight distribution curves are similar to each other thereby indicating no radical change in polymerization mechanism during the ideal period. Third, the data reveal that all polymer of molecular weight less than 6,000 has been lost in the cleaning process. Finally, for the sake of compactness, the entire distribution curve has not been drawn. Nonetheless, in each instance the highest molecular weight species found was between 13 and 15 million. Further molecular weight distribution analysis will be considered when we consider the composite results of our molecular weight analysis shown in Figure 4.

### DISCUSSION

The results of our molecular weight development studies are summarized in Figure 4. The instantaneous and cumulative number-average and viscosity-average molecular weight curves were all derived from the average curves of Figures 3 and 5. Also shown is the predicted instantaneous number-average molecular weight from eq. (1) for  $R_p = 13\%/hr$  and  $k_d = 1.3 \times 10^{-3} \text{ min.}^{-1}$ .

TABLE III  
Tabulation of Data Derived from Figure 4

Conversion, %	$\bar{M}_v/\bar{M}_n$		Ratio of predicted to measured instantaneous $\bar{M}_n$
	Cumulative	Instantaneous	
0			1.00
10	3.00		0.306
15		3.22	
20	3.09		0.226
25		3.96	
30	3.14		0.193
35		3.78	
40	3.21		0.180
45		3.10	
50	3.26		0.182
55		2.94	
60	3.28		0.212
65		2.94	
70	3.26		0.290
75		3.30	

A number of significant observations can be drawn from Figure 4.

(a) The molecular weight curves are typical and "ordinary." The cumulative viscosity-average molecular weight development curve is similar in shape to those reported by Williams and Bobalek<sup>11</sup> and Smith<sup>22</sup> for similar

systems. Further, the cumulative number-average curve is similar in shape to the cumulative viscosity-average curve. The ratios of cumulative viscosity to number-average and instantaneous viscosity to number-average molecular weight are compiled in Table III. It can be seen that the cumulative viscosity-average to number-average molecular weight ratios increase slightly from 3.00 to 3.28 during the entire constant rate period. This slight increase in the cumulative ratio is expected because of the continuous increase in molecular weight during the reaction. Since the instantaneous values are calculated from average curves, which already involve some experimental error, these and their ratios will be subject to additional uncertainties. Even so, we still observe that the ratios of instantaneous viscosity-average to number-average molecular weight vary only moderately and randomly about an average value of 3.32. The fact that both the cumulative and instantaneous ratios remain essentially constant with conversion is indicative of a normal mode of polymerization with little or no chain branching.

(b) The molecular weight increase during the constant-rate period, between 0 and 60% conversion, is definite and significantly large. The cumulative viscosity-average molecular weight increases about 500% from 300,000 to 1,500,000 while the instantaneous viscosity average molecular weight increases 880% from 300,000 to 2,650,000 during the ideal period. During this same period, the cumulative number-average molecular weight increases 450% from 110,000 to 480,000 while the instantaneous number-average molecular weight increases 680% from 150,000 to 750,000. All these increasing trends are far greater than the indicated scatter in the original molecular weight data.

(c) There is a definite conflict between current steady-state theory and observation. If the measured instantaneous number-average molecular weight is extrapolated to zero time, the molecular weight determined is in complete agreement with that predicted from steady-state theory and the decomposition data. This agreement is indicative of the internal consistency of the molecular weight and decomposition data. As the reaction proceeds, however, the measured instantaneous molecular weight rapidly deviates from that predicted. As Figure 4 shows, the shapes of the experimental and predicted  $\bar{M}_{ni}$  curves are at variance. The measured  $\bar{M}_{ni}$  curve rises steeply, tapers off, and eventually begins to decrease, whereas the predicted curve is a sluggishly increasing exponential. While we have no firm explanation for the behavior just described, we believe that the most straightforward way to interpret these findings is that, although the radicals may be generated with 100% efficiency, they are not utilized with 100% efficiency. The independent study of van den Hull and Vanderhoff<sup>23</sup> supports this. However, their investigation was neither sufficiently extensive nor particularly directed toward this problem, so it does not suggest a concrete mechanism for radical inefficiency. Therefore, further research is required both to verify this postulate and to establish a mechanism by which radicals may be rendered inactive.

## CONCLUSIONS

In this and the previous paper<sup>1</sup> we have presented a comprehensive set of data for a single emulsion polymerization formulation. Analysis of these data has led to advances in our understanding of the fundamental mechanisms in styrene emulsion polymerization. First we have presented<sup>1</sup> substantial evidence for a core-shell morphology. Second, we have provided evidence to substantiate the notion that free radicals are generated by a first order mechanism with 100% efficiency. Third, in contrast to current theories which predict the generation of constant molecular weight during a period of constant rate growth we have shown that molecular weights may actually increase six to nine times their initial values. Finally, these results suggest that radicals may not be utilized with 100% efficiency. We present the pertinent data in detail in a form useful to serve as a basis for additional or alternative interpretation and as a basis for further research.

The major portion of this work was supported by a grant from the National Science Foundation-NSF GK-1375. We acknowledge with thanks the assistance of Professor A. E. Hamielec of McMaster University in obtaining and analyzing our GPC data.

This paper is based on the Ph. D. Thesis of M. R. Grancio, The City College of The City University of New York, 1969.

## References

1. M. R. Grancio and D. J. Williams, *J. Polym. Sci. A-1*, **8**, 2617 (1970).
2. W. V. Smith and R. H. Ewart, *J. Chem. Phys.*, **16**, 592 (1948).
3. W. H. Stockmayer, *J. Polym. Sci.*, **24**, 314 (1957).
4. J. T. O'Toole, *J. Appl. Polym. Sci.*, **9**, 1291 (1965).
5. J. L. Gardon, *J. Polym. Sci. A-1*, **6**, 687 (1968).
6. J. L. Gardon, *J. Polym. Sci. A-1*, **6**, 623 (1968).
7. J. L. Gardon, *J. Polym. Sci. A-1*, **6**, 643 (1968).
8. J. L. Gardon, *J. Polym. Sci. A-1*, **6**, 665 (1968).
9. J. L. Gardon, *J. Polym. Sci. A-1*, **6**, 2853 (1968).
10. J. L. Gardon, *J. Polym. Sci. A-1*, **6**, 2859 (1968).
11. D. J. Williams and E. G. Bobalek, *J. Polym. Sci. A-1*, **4**, 3065 (1966).
12. D. J. Williams and M. R. Grancio, *New Concepts in Emulsion Polymerization* (*J. Polym. Sci. C*, **27**), J. C. H. Hwa and J. W. Vanderhoff, Eds., Interscience, New York, 1969, p. 139.
13. I. M. Kolthoff and I. K. Miller, *J. Amer. Chem. Soc.*, **73**, 3055 (1951).
14. I. M. Kolthoff, E. J. Meehan, and E. M. Carr, *J. Amer. Chem. Soc.*, **75**, 1479 (1953).
15. B. M. E. van der Hoff, *J. Polym. Sci.*, **44**, 241 (1960).
16. I. M. Kolthoff and E. M. Carr, *Anal. Chem.*, **25**, No. 2, 298 (1953).
17. C. C. Price and D. H. Read, *J. Polym. Sci.*, **1**, 44 (1946).
18. S. H. Maron, *J. Appl. Polym. Sci.*, **5**, 282 (1961).
19. A. I. Goldberg, W. P. Hohenstein, and H. Mark, *J. Polym. Sci.*, **2**, 503 (1947).
20. J. J. Krackeler and H. Naidus, paper presented to Division of Polymer Chemistry, American Chemical Society Meeting, 1966; *Polymer Preprints*, **7**, No. 2, 791 (1966).
21. Von S. Jovanovic, J. Romatowski, and G. V. Schulz, *Makromol. Chem.*, **85**, 227 (1965).
22. W. V. Smith, *J. Amer. Chem. Soc.*, **70**, 3695 (1948).
23. H. J. van den Hull and J. W. Vanderhoff, paper presented at American Chemical Society Meeting, 1969; *Polymer Preprints*, **10**, No. 1, 318 (1969).

Received September 30, 1969

Revised April 6, 1970

## Charge-Transfer Complexing in Polymer Mixtures. IV. Acceptor Polymers from Nitrophthalic Acids and Their Mixtures with Donor Polymers from Aryliminodiethanols

THEODORE SULZBERG and ROBERT J. COTTER, *Union Carbide Corporation, Chemicals and Plastics, Bound Brook, New Jersey 08805*

### Synopsis

A series of electron acceptor polyesters was prepared from 5-nitroisophthalic, nitroterephthalic, and 4,6-dinitroisophthalic acids. Those polymers prepared at high molecular weight were tough, soluble, linear materials of well-defined structure. These materials were mixed with electron-donor polymers based on aryliminodiethanols where the aryl group was phenyl, *p*-anisyl, 2,5-dimethoxyphenyl, and 3,4,5-trimethoxyphenyl. The effects of the mixtures on the mechanical, spectral, viscometric, and conductive properties were studied and compared to the component polymers.

A previous paper in this series described the synthesis of a new class of donor polymers derived from aryliminodiethanols.<sup>1</sup> They represented a new advance in studies of charge-transfer complexing in polymer mixtures because they were high molecular weight, tough materials of well defined structure. Their electron-donating ability was demonstrated with various monomeric  $\pi$  acceptors.<sup>1,2</sup>

The present report describes the preparation of acceptor polymers which could be mixed with these donor polymers and a study of the resulting interactions. They meet the same criteria, i.e., high molecular weight, known structures and reasonable toughness.

There appears to be only two other reports of polymers specifically prepared as acceptor polymers. Smets<sup>3</sup> described the nitration of polystyrene to give poly-2,4-dinitrostyrene. The product was characterized by nitrogen analysis. Its complexes with 1-naphthylamine were also reported. In the second case, Yang and Gaoni<sup>4</sup> found that a mixture of 2-vinylpyridine and 2,4,6-trinitrostyrene polymerized exothermically at room temperature, even though the latter monomer does not homopolymerize. Their evidence suggested that donor-acceptor interactions occurred prior to polymerization and remained in the final product.

To determine the type of substituents best suited for preparing aromatic acceptor polymers, we compared the electric moments of benzene derivatives containing electron-withdrawing substituents. The data, as shown in

TABLE I  
Electric Moments of Benzene Derivatives (C<sub>6</sub>H<sub>5</sub>A)  
Substituted with Electron-Withdrawing Groups<sup>a</sup>

A	Electric moment, Debyes <sup>b</sup>
Br	1.5
Cl	1.6
COOCH <sub>2</sub> CH <sub>3</sub>	1.9
CCl <sub>3</sub>	2.1
COCH <sub>3</sub>	2.8
NO	3.1
SO <sub>3</sub> H	3.8
CN	4.0
NO <sub>2</sub>	4.0

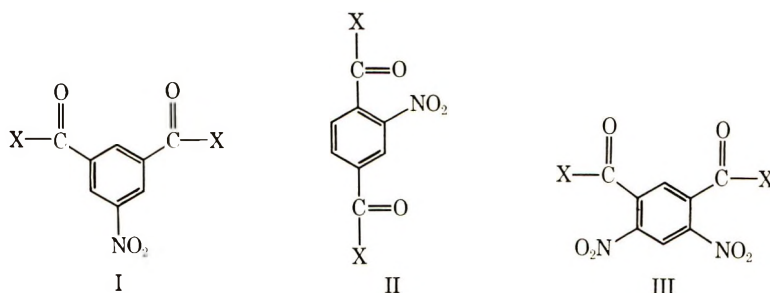
<sup>a</sup> Data of Noller.<sup>5</sup>

<sup>b</sup> The direction of the electric moment is away from the aromatic ring.

Table I, reveals that the nitro and cyano groups are best suited for that purpose.

The use of polystyrenes containing nitro and cyano substituents as acceptor polymers was rejected because of the brittle nature of vinylaromatic polymers. Further, these polymers have an electron-donating methylene group on the aromatic ring which could decrease its acceptor capability.

In order to obtain tough, high molecular weight polymers containing only electron-withdrawing substituents in the aromatic ring, the polyesters of the nitrophthalic acids Ia, IIa and IIIa were prepared.\*



a; X = OH

b; X = Cl

c; X = OCH<sub>3</sub>

## EXPERIMENTAL

### Monomers

Nitroterephthalic and 5-nitroisophthalic acids were obtained from Aldrich Chemical Company and Matheson, Coleman and Bell (MCB), re-

\* When this work was started, polymers derived from these acids had not been reported. Subsequently, low molecular weight polymers of I and II were described.<sup>6</sup>



spectively, and were used as received to prepare the acid chlorides. Bisphenol A (Union Carbide) was recrystallized from benzene and melted at 156°C (reported<sup>7</sup> mp 157°C). 1,6-Hexanediol (MCB) was distilled at 110°C/3 mm prior to use and stored in a sealed tube to prevent moisture contamination. The reported boiling point<sup>8</sup> is 146–149°C/17 mm.

#### *5-Nitroisophthaloyl Chloride*

A mixture of 100 g of 5-nitroisophthalic acid, 700 ml of thionyl chloride, and 5 ml of dimethyl formamide was heated to reflux. After 2 days, the excess thionyl chloride was distilled out and the resulting residue sublimed twice at 80°C/0.05 mm. An 80% yield of 5-nitroisophthaloyl chloride, mp 68°C, resulted (reported<sup>9</sup> mp 67.5–68°C).

#### *Nitroterephthaloyl Chloride*

A mixture of 60 g of nitroterephthalic acid, 400 ml SOCl<sub>2</sub>, and 5 ml of dimethylformamide was heated to reflux for 2 days and then the excess SOCl<sub>2</sub> was removed by distillation. The liquid residue was distilled rapidly through a small Claisen head (bp 140–148°C/0.4 mm). The distillate was put through a Vigreux column to give 41 g (58%) of nitroterephthaloyl chloride, bp 126.5–134.0°C/0.10–0.29 mm (reported<sup>10</sup> bp 174°/8 mm).

#### *4,6-Dinitroisophthaloyl Chloride*

**Methyl 4,6-dinitro-*m*-toluate.** The nitration of *m*-toluic acid to a mixture of 2,6- and 4,6-dinitro-*m*-toluic acids and the separation of methyl 4,6-dinitro-*m*-toluate was done by the procedure of Blatt.<sup>11</sup> From 54 g (0.4 mole) of *m*-toluic acid, 30.0 g (32%) of the ester was obtained.

**Methyl 4,6-dinitroisophthalate.** A mixture of 14.3 g (0.6 mole) of methyl-4,6-dinitro-*m*-toluate and 170 ml of concentrated sulfuric acid was cooled to –7°C, and a solution of 13 g of chromic oxide in 20 ml of water was added dropwise while maintaining the temperature between 10 and 20°C. After addition was complete, the reaction mixture was cooled to 5°C, poured onto ice, and the solid collected. After washing twice with ice-water, the product was air dried. The product (14.2 g, 88%) melted at 210–213°C.

ANAL. Calcd for C<sub>9</sub>H<sub>6</sub>N<sub>2</sub>O<sub>8</sub>: C, 40.01%; H, 2.24%; N, 10.37%. Found: C, 40.65%; H, 2.38%; N, 10.36%.

The infrared spectrum had carbonyl bands at 5.72 μ (ester) and 5.80 μ (acid) and an acid hydroxyl at 3.6–4.0 μ.

The NMR spectrum in perdeuteropyridine showed three-OCH<sub>3</sub> protons at 3.94 ppm, one aromatic proton at 8.53 ppm, and one aromatic proton at 8.84 ppm.

**4,6-Dinitroisophthalic Acid.** Methyl 4,6-dinitroisophthalate (10.2 g, 0.38 mole) was suspended in 300 ml of concentrated HCl and heated to reflux overnight. After cooling, the solution was extracted four times with 100 ml of ether. This was washed twice with 20 ml of ice water. After

drying over  $MgSO_4$ , the ether was filtered and removed to leave 7.2 g (70%) of a pale yellow solid. After one recrystallization from water, it melted at  $237^\circ C$  (reported mp  $246-247^\circ C$  for 4,6-dinitroisophthalic acid).

**4,6-Dinitroisophthaloyl Chloride.** A solution of 4,6-dinitroisophthalic acid (53 g, 0.21 mole), 400 ml of thionyl chloride, and 4 ml of dimethylformamide was refluxed for 2 days. The excess thionyl chloride was distilled out under reduced pressure and the residue recrystallized from chloroform-hexane to give 27.4 g (45%) of 4,6-dinitroisophthaloyl chloride, mp  $96-101^\circ C$ . A vacuum sublimation gave pale yellow crystals, mp  $102-103^\circ C$  [reported mp<sup>12</sup>  $106^\circ C$  (from carbon tetrachloride)].

#### *Bis(2-hydroxyethyl)-5-nitroisophthalate*

After heating a solution of 63 g (0.3 mole) of 5-nitroisophthalic in 450 ml of *N,N*-dimethylformamide to  $100^\circ C$ ,  $\sim 30$  g of ethylene oxide was bubbled in over a 2-hr period. The *N,N*-dimethylformamide was removed under reduced pressure and the crude product (96 g) was dissolved in 450 ml of boiling water. Sodium carbonate was added to bring the pH to 8. The solution was cooled and solid collected. Recrystallization from 1.8 liters of water gave 17 g (18%) of bis(2-hydroxyethyl)-5-nitrosophthalate, mp  $137-138^\circ C$ . Polymer grade material was obtained by recrystallization from ethanol.

ANAL. Calcd for  $C_{10}H_9NO_7$ : C, 48.17%; H, 4.38%; N, 4.68%. Found: C, 47.79%; H, 4.25%; N, 4.59%.

The infrared spectrum had carbonyl bonds at  $5.78 \mu$  (ester) and  $2.85 \mu$  (aliphatic hydroxyl). The NMR spectrum in perdeuterodimethyl sulfoxide showed a triplet at 3.78 ppm (four aliphatic protons), a triplet at 4.44 ppm (four aliphatic protons), and a singlet at 8.84 ppm (three aromatic protons).

### Polymers

All of the acceptor polymers were prepared by the low-temperature solution procedure as previously reported.<sup>1</sup>

### Charge-Transfer Spectra

The donor polymers which were complexed with the acceptor polymers discussed above are described in an earlier paper.<sup>1</sup>

Since polymer solutions and blends were compatible, two methods were used to determine the charge transfer absorption maxima of the donor polymer-acceptor polymer mixtures. Since it was found that the aryliminodiethanol polymers had maximum absorptions below  $300 m\mu$  while the nitropolyesters had maxima at  $\sim 330 m\mu$ , the latter materials were placed in the reference beam of the Cary 14 spectrophotometer. In the first procedure, concentrated solutions of the polymers were prepared at 0.1-0.5 *M* in 1,2-dichloroethane or 1,1,2,2-tetrachloroethane. The spectra were determined by scanning a mixture of donor polymer and acceptor polymer solu-

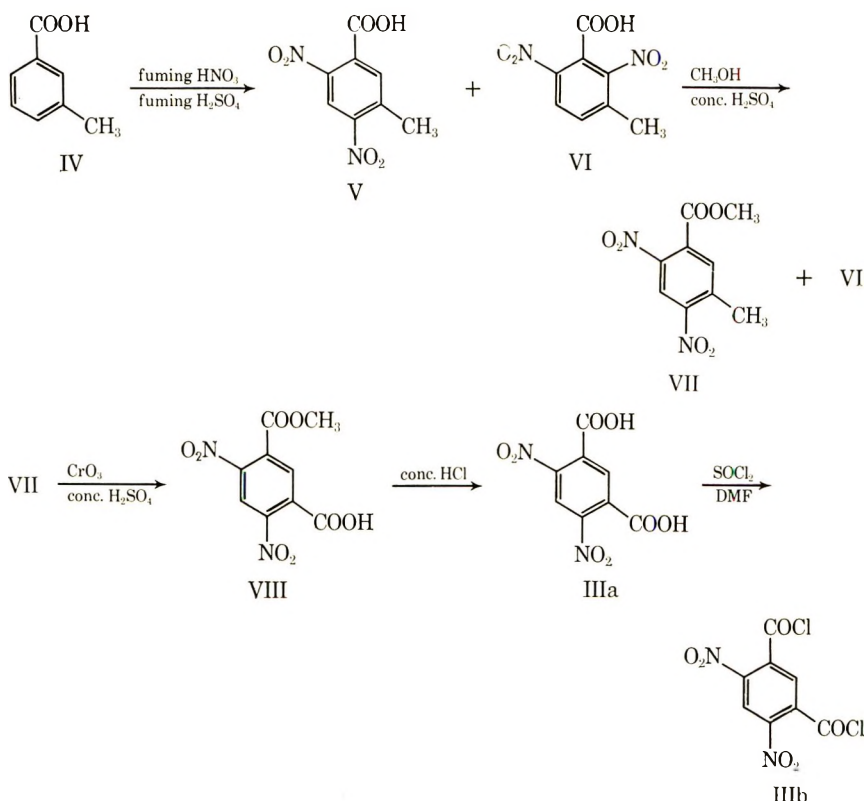
tions in a 1-cm cell against a 1-cm cell containing the acceptor polymer solution.

The other method used films of uniform thickness which were cast from chloroform solution. After drying, a film of a mixture and a film of the acceptor were placed in the sample and reference beams, respectively, and the spectra determined. Both techniques gave identical results.

## RESULTS AND DISCUSSION

### Synthesis

Both 5-nitrosophthalic and nitroterephthalic acids are readily available and were routinely converted to the acid chlorides with thionyl chloride in the presence of *N,N*-dimethylformamide. The preparation of 4,6-dinitroisophthaloyl chloride, which was a modification of Blatt's procedure,<sup>11</sup> is a multistep synthesis starting from *m*-toluic acid (IV). Nitration of IV gives equal amounts of the isomeric dinitro acids, V and VI.



Esterification of the mixture with methanol in the presence of sulfuric acid gave methyl 4,6-dinitro-*m*-toluate exclusively, since sterically hindered VI does not react under these conditions. After separating the acid VI from the ester VII, the latter was oxidized with chromic acid to the half ester

TABLE II  
Properties of High Molecular Weight Polynitrophthalates<sup>a</sup>

No.	Polymer	RV <sup>b</sup>	$T_g$ , °C <sup>c</sup>	$T_m$ , °C <sup>d</sup>	Tensile modulus, psi	Tensile strength, psi	Elongation, %	Impact, ft-lb./in. <sup>3</sup>
1	Poly(1,6-hexanediol 5-nitroisophthalate)	0.73	50	100	90,000	2800	290	10
2	Poly(bisphenol A 5-nitroisophthalate)	0.41	120	225	240,000	5500	4	20
3	Poly[bis(2-hydroxyethyl)5-nitroisophthalate-bisphenol A carbonate]	0.40	70-80	—	260,000	5200	5	—
4	Poly(1,6-hexanediol nitroterephthalate)	0.46	25	—	5,300	1400	630	—
5	Poly(bisphenol A nitroterephthalate)	0.62	225	—	260,000	9800	44	350

<sup>a</sup> Determined on films cast from chloroform.

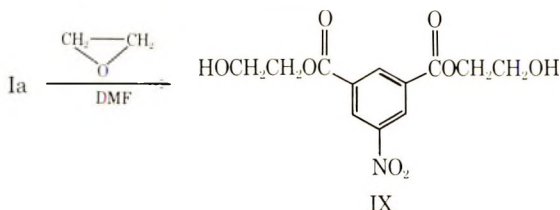
<sup>b</sup> Reduced viscosity in chloroform at 25°C at 0.2 g/100 ml of solvent.

<sup>c</sup> The glass transition temperature was measured by determining recovery characteristics as a function of temperature.<sup>14</sup>

<sup>d</sup> Crystalline melting point.

(VIII). Hydrolysis and reaction with thionyl chloride afforded 4,6-dinitroisophthaloyl chloride (IIIb).

In order to prepare polycarbonates containing nitrophthalate segments along the polymer chain, the bis(2-hydroxyethyl) derivatives of 5-nitrophthalic acid was prepared (IX).



The polymer syntheses were performed by the low-temperature, solution process which was described in a previous paper.<sup>1</sup>

## Physical Properties

### *Acceptor Polymers*

The mechanical properties of the five high molecular weight nitrophthalate polymers which were prepared are given in Table II. The effect of the nitro group on the polymer properties is seen by comparing the  $T_g$  of polymer 5 in Table II (22.5°C) with the reported softening temperature for poly(bisphenol A terephthalate) of 350°C.<sup>13</sup> This nitro group causes, as expected, a large decrease in  $T_g$  because it is in an unsymmetrical position (X). The symmetrically disposed nitro group in poly(bisphenol A 5-nitroisophthalate), however, also lowers the softening temperature con-

TABLE III  
Nitrophthalic Acid Polymers

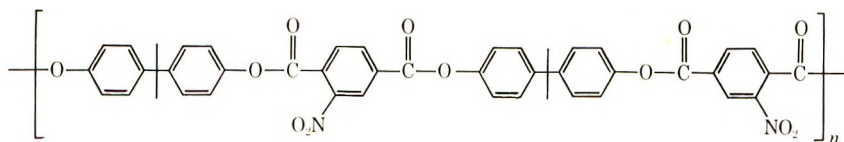
Number	Polymer	RV <sup>a</sup>
1	Poly(1,4-butanediol-5-nitroisophthalate)	0.11
2	Poly(1,6-hexanediol 5-nitroisophthalate)	0.73
3	Poly(bisphenol A 5-nitroisophthalate)	0.41
4	Poly(1,6-hexanediamine 5-nitroisophthalamide)	0.33 <sup>b</sup>
5	Poly(1,6-hexanediol nitroterephthalate)	0.46
6	Poly(bisphenol A nitroterephthalate)	0.62
7	Poly(resorcinol nitroterephthalate)	0.27 <sup>c</sup>
8	Poly(1,6-hexanediol 5-nitroisophthalate- co-nitroterephthalate) (1:1)	0.35
9	Poly(1,6-hexanediol 4,6-dinitroisophthalate)	0.28
10	Poly(bisphenol A 4,6-dinitroisophthalate)	0.09 <sup>b</sup>
11	Poly[bis(2-hydroxyethyl)5-nitroisophthalate- bisphenol A carbonate]	0.40

<sup>a</sup> Reduced viscosity at 25°C at 0.2 g/100 ml of chloroform except where noted.

<sup>b</sup> In *N,N*-dimethylformamide.

<sup>c</sup> In *m*-cresol.

siderably (250°C to 120°C).<sup>13</sup> This is presumably caused by the bulky nature of the nitro group.



X

A complete list of the nitrophthalic acid polymers prepared is given in Table III.

### Polymer Mixtures

The physical properties of the following three donor polymer-acceptor polymer mixtures are given in Tables IV, V, and VI:

- A { poly(phenyliminodiethanol isophthalate) (XI)  
 poly(1,6-hexanediol-5-nitroisophthalate) (XII)
- B { poly(*p*-anisyliminodiethanol isophthalate) (XIII)  
 poly(bisphenol A-5-nitroisophthalate) (XIV)
- C { poly(*p*-anisyliminodiethanol-bisphenol A carbonate) (XV)  
 poly[bis(2-hydroxyethyl)-5-nitroisophthalate-  
 bisphenol A carbonate] (XVI)

TABLE IV  
 Properties of Donor Polymer XI, Acceptor Polymer XII, and a 50:50 Mixture

Property	Donor XI	50:50 mixture	Acceptor XII
Color	Colorless	Yellow	Colorless
Lowest energy absorption maximum, $m\mu$	298	391	330
Reduced viscosity	0.60	0.50	0.40
Glass transition temp $T_g$ , °C	50	50	60
Tensile modulus, psi	90,000	260,000	Low

TABLE V  
 Properties of Donor Polymer XIII, Acceptor Polymer XIV, and a 50:50 Mixture

Property	Donor XIII	50:50 mixture	Acceptor XIV
Color	Colorless	Yellow-orange	Colorless
Lowest energy absorption maximum, $m\mu$	298	398	330
Reduced viscosity	0.41	0.31	0.22
Glass transition temp $T_g$ , °C	120	90	50
Tensile modulus, psi	240,000	235,000	Too low in molecular weight to measure

TABLE VI  
Properties of Donor Polymer XV, Acceptor Polymer XVI, and a 50:50 Mixture

Property	Donor XV	50:50 mixture	Acceptor XVI
Color	Colorless	Yellow-orange	Colorless
Lowest energy absorption maximum, $m\mu$	298	398	330
Reduced viscosity	0.80	0.60	0.40
Glass transition temp $T_g$ , $^{\circ}C$	50-60	60-70	70-80
Tensile modulus, psi	335,000	360,000	260,000

These polymers, which were all prepared at film forming molecular weights, are representative of the many possible combinations, since both polyesters and polycarbonates were used.

### Solution Viscosities

To further elucidate the chain to chain complexing of donor and acceptor polymers, solution viscosities of mixtures were determined and compared

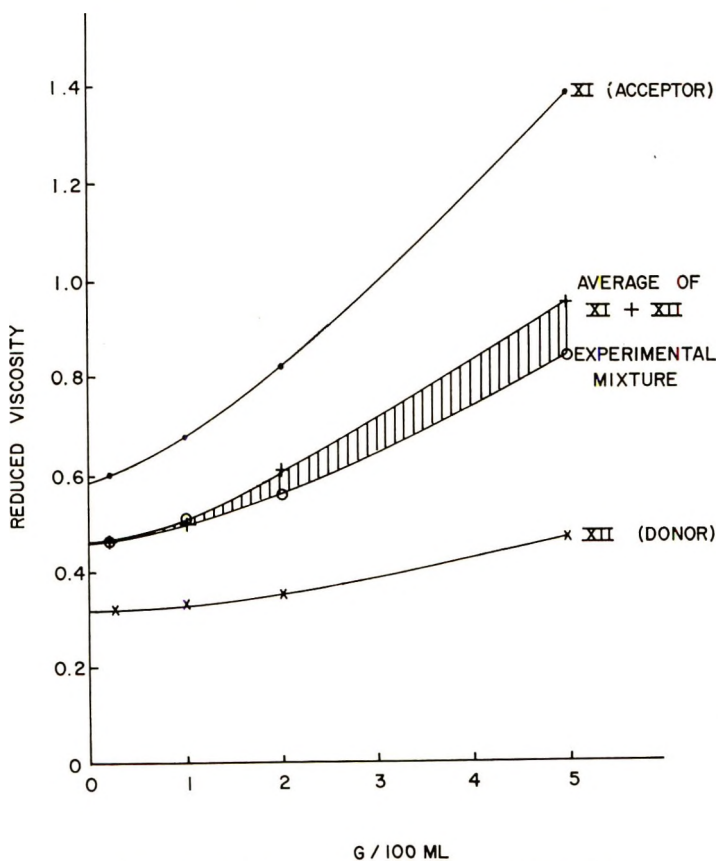
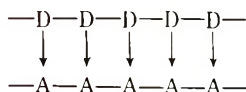
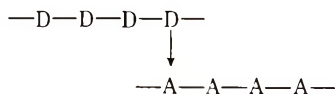


Fig. 1. Reduced viscosity vs. polymer concentration.

with the data for the individual polymers. In Figure 1, the reduced viscosities of the materials are plotted against the corresponding polymer concentrations for donor polymer XI, acceptor polymer XII, and a 50:50 mixture of the two. A comparison of the latter with the predicted average shows that the deviation, although small, increases with increasing concentration. Since charge transfer interactions are very concentration-dependent, it is quite reasonable to expect that at 5 g/100 ml the chain to chain interactions are important. The observed decrease in viscosity is consistent, therefore, with a model that predicts a decrease in the polymer volume:<sup>15</sup>



The other model is one that predicts an increased volume (increased viscosity) because of the increased importance of chain end interactions:



### Electrical Conductivity

The electrical conductivities of several donor polymer-acceptor polymer mixtures were determined and are presented in Table VII. The decreased

TABLE VII  
Volume Resistivities of Donor Polymer-Acceptor Polymer Mixtures

Number	Polymer mixture	Form <sup>a</sup>	Volume resistivity, ohm-cm <sup>b</sup>
1	XV	Film	$1.3 \times 10^{16}$
2	XI	Film	$1 \times 10^{13}$
3	XII		
3	XIII	Film	$1 \times 10^{13}$
4	XII		
4	Poly(3,4,5-trimethoxyphenyl- iminodiethanol isophthalate)		
	XVII	Film	$1 \times 10^{12}$
	XII		
5	XIII	Film	$2.7 \times 10^{13}$
	Table II, no. 5		
6	XVII	Disk	$1 \times 10^{12}$
	Table III, no. 9		
7	Table VIII, no. 5	Disk	$2.5 \times 10^{11}$

<sup>a</sup> Equimolar amounts of polymer were mixed in chloroform and films cast from solution. If the mixture did not form a coherent film, discs were compression-molded at 10,000 psi.

<sup>b</sup> Determined by Dr. M. M. Labes and Dr. P. L. Kronick at the Franklin Institute, Philadelphia, Pa.



resistivity of the mixtures (numbers 2-6) as compared to the uncomplexed donor (number 1) is about  $10^3$  ohm-cm. This increased conductivity is significant because of the relatively weak interactions which are observed. Number 7 represents a single polymer containing both donor and acceptor groups. Its conductivity is even higher than that of the blends and, hence, represents an area of future, continued interest.

### Donor-Acceptor Polymers

Table VIII contains a list of polymers, which were prepared from aryliminodiethanols and the nitrophthaloyl chlorides, containing both donor and acceptor groups along the polymer chain. They were not obtained at high molecular weight, however, even though the reactants were previously

TABLE VIII  
Donor-Acceptor Polymers<sup>a</sup>

Number	Polymer	RV <sup>b</sup>	Yield, %
1	Poly(phenyliminodiethanol 5-nitroisophthalate)	0.07	75
2	Poly(phenyliminodiethanol nitroterephthalate)	0.15	92
3	Poly( <i>p</i> -anisyliminodiethanol 5-nitroisophthalate)	0.08	77
4	Poly( <i>p</i> -anisyliminodiethanol nitroterephthalate)	0.10	92
5	Poly(2,5-dimethoxyphenyliminodiethanol 5-nitroisophthalate)	0.06	43

<sup>a</sup> The polymers were prepared by the pyridine-catalyzed reaction between the appropriate aryliminodiethanol with either 5-nitroisophthaloyl or nitroterephthaloyl chloride.

<sup>b</sup> Reduced viscosity in chloroform at 25°C at 0.2 g/100 ml of solvent.

used to prepare high molecular weight polymers (see Table II and reference 1). Possible explanations are either the loss of reactivity or mobility of the growing polymer chains when complexed with each other. This would change the effective stoichiometry and lead to lower molecular weight polymers.

### CONCLUSIONS

High molecular weight polyesters and polycarbonates were prepared which contained nitrated phthalates as the structural feature of interest. These electron-acceptor polymers were mixed with previously prepared electron-donor aryliminodiethanol polymers to give unique charge-transfer polymer mixtures. Chain-to-chain complexing of these mixtures due to charge transfer interaction was demonstrated by studying their visible spectra, mechanical properties, solution viscosities, and electrical conductivity.

We gratefully acknowledge the highly competent technical assistance of Mr. Peter J. Degen.

### References

1. T. Sulzberg and R. J. Cotter, *Macromolecules*, **2**, 146 (1969) (Part II).
2. T. Sulzberg and R. J. Cotter, *Macromolecules*, **2**, 150 (1969) (Part III).
3. G. Smets, V. Balogh, and Y. Castille, in *Macromolecular Chemistry, Paris 1963* (*J. Polym. Sci. C*, **4**), M. Magat, Ed., Interscience, New York, 1963, p. 1467.
4. N. C. Yang and Y. Gaoui, *J. Amer. Chem. Soc.*, **86**, 5022 (1964).
5. C. R. Noller, *Chemistry of Organic Compounds*, Saunders, Philadelphia, 1957, p. 451.
6. E. V. Kuznetsov, A. P. Gil, I. M. Shermergorn, and S. F. Kuznetsova, *Vysokomol. Soedin.*, **6**, 31 (1964); *Chem. Abstr.*, **60**, 10801d (1964).
7. H. Schnell, *Angew. Chem.*, **68**, 633 (1956).
8. A. I. Vogel, *Practical Organic Chemistry*, Wiley, New York, 1956, p. 874.
9. K. F. Jennings, *J. Chem. Soc.*, **1957**, 1172.
10. M. A. Soderman and T. B. Johnson, *J. Amer. Chem. Soc.*, **47**, 1393 (1925).
11. A. H. Blatt, *J. Org. Chem.*, **25**, 2030 (1960).
12. P. Ruggli and O. Schmid, *Helv. Chim. Acta*, **18**, 247 (1935); *Chem. Abstr.*, **29**, 3668 (1935).
13. V. V. Korshak and S. V. Vinogradova, *Polyesters*, Pergamon Press, London, 1965.
14. A. Brown, *Textile Res. J.*, **25**, 891 (1955).
15. H. Morawetz, *Macromolecules in Solution*, Interscience, New York, 1965, p. 368.

Received March 19, 1970

Revised April 15, 1970

## Poly-2-oxazolidones: Preparation and Characterization

J. E. HERWEH and W. Y. WHITMORE, *Research and Development Center, Armstrong Cork Company, Lancaster, Pennsylvania 17604*

### Synopsis

Poly-2-oxazolidones were synthesized by the 1,3-cycloaddition of bisglycidyl ethers to diisocyanates with the use of *N,N*-dimethylformamide and lithium chloride as solvent and catalyst, respectively. A variety of arylene and alkylene diisocyanates and co-reactant bisepoxides were used in the polymer-forming reaction. The polymers, obtained in high yield, were generally soluble in methylene dichloride, chloroform, *N,N*-dimethylformamide, and dimethyl sulfoxide. They had intrinsic viscosities up to 0.42 dl/g and could be cast into films. In several cases molecular weights were determined by vapor pressure osmometry. The poly-2-oxazolidone based upon 1,6-hexamethylene diisocyanate and the bisglycidyl ether of isopropylidene diphenol gave the highest molecular weight. Confirmation that the base unit of the polymers contains the 2-oxazolidone ring was obtained by elemental analysis, infrared and NMR spectroscopy. The poly-2-oxazolidones synthesized were found to be amorphous by x-ray diffraction. Thermogravimetric analyses indicated that a majority of the poly-2-oxazolidones were stable in dry air up to 300°C. In a number of cases *T<sub>g</sub>*'s were also determined by using differential scanning calorimetry.

### INTRODUCTION

The purpose of this investigation was to examine the reaction of diisocyanates with bisglycidyl ethers to obtain poly-2-oxazolidones more amenable to characterization. Adaptation of the 1,3-cycloaddition reaction of epoxides to isocyanates to give poly-2-oxazolidones has been reported.<sup>1-6</sup> In most cases, however, thorough characterization of the reaction products was hindered by their insolubility. As a result, prior workers have utilized two alternate routes to obtain more tractable poly-2-oxazolidones. These alternate syntheses are the polyaddition-condensation between bisepoxides and difunctional urethanes,<sup>7</sup> and the dehydrochlorination with base of high molecular weight polyurethanes with chloromethyl side chains.<sup>8,9</sup>

This paper describes the preparation of a number of new poly-2-oxazolidones. In addition, some polymers previously reported were also synthesized to allow for an assessment and comparison of alternate reaction routes and/or to obtain products that would better lend themselves to characterization. The identification of the reaction products as poly-2-oxazolidones is based on elemental analyses, viscosity, and molecular weight determina-

tions coupled with previously reported<sup>10,11</sup> NMR and infrared results with model mono- and di-2-oxazolidones.

## EXPERIMENTAL SECTION

### General

The proton NMR spectra were determined on a Japan Electron Optics Lab 4H-100 spectrometer with tetramethylsilane (TMS) as an internal standard. Infrared absorption spectra were obtained on KBr disks with the use of a Perkin-Elmer Model 337 spectrophotometer. A Cannon-Ubbelohde dilution viscometer (50-N409) was employed for viscosity determinations in *N,N*-dimethylformamide (DMF) at 30°C. Intrinsic viscosity was determined by extrapolating to zero concentration a plot of reduced specific viscosity versus concentration. Molecular weights were determined by Galbraith Laboratories, Inc., Knoxville 21, Tenn., by vapor-pressure osmometry (DMF as the solvent). Elemental analyses were also performed by Galbraith Laboratories.

Thermogravimetric analyses (TGA) were determined in dry air at 6°C per min, using an American Instrument Co. Thermo-Grav. Differential scanning calorimetry (DSC) results were obtained using a Perkin-Elmer differential scanning calorimeter.

### Materials

The diisocyanates used were obtained from commercial sources and were distilled prior to use: 2,4-tolylene diisocyanate (bp 116–117°C/10 mm), 1,6-hexamethylene diisocyanate (bp 96.5–97°C/1.4 mm), 4,4'-methylene bis(phenyl isocyanate) (bp 147–149°C/0.03 mm), 4,4'-methylene bis(cyclohexyl isocyanate) (bp 149–153°C/0.03 mm), isophorone diisocyanate (bp 113–114°C/0.85 mm) and 2,4,4-(2,2,4)-trimethylhexamethylene diisocyanate (mixture of isomers) (bp 108.5–110°C/1.0 mm).

The diglycidyl ether of 4,4'-isopropylidene diphenol (Bisphenol-A) (DGBA), obtained from the Dow Chemical Co. under the designation DER 332 LC as a low-melting crystalline solid, was used as received. The diglycidyl ethers of 1,4-butanediol and resorcinol were distilled prior to use (bp 100–102°C/0.2 mm and bp 146–155°C/0.01 mm, respectively). The purity of the epoxides was confirmed by functional group (oxirane oxygen) analysis by a reported procedure.<sup>12</sup>

DMF was dried over calcium hydride and subsequently distilled from a fresh portion of the hydride before use. Lithium chloride was dried *in vacuo* in the presence of phosphorus pentoxide for 24 hr prior to use.

### Preparation of Poly-2-oxazolidones (II)

An example of the synthesis of a poly-2-oxazolidone (II) is given below. All of the poly-2-oxazolidones (II) studied (Table I) were prepared by this procedure or minor variations of it.

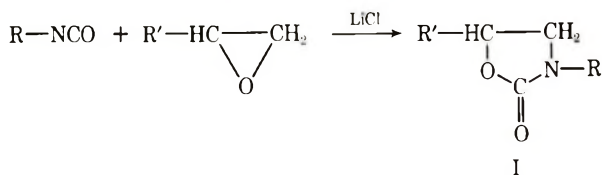
A solution of 1,6-hexamethylene diisocyanate (33.6 g, 0.2 mole) and the diglycidyl ether of 4,4'-isopropylidene diphenol (DGBA) (68 g, 0.2 mole) in 250 ml of DMF was added dropwise in 1 hr to a stirred and refluxing solution of DMF (300 ml) containing 0.08 g of lithium chloride under a nitrogen atmosphere. Upon completing the addition, the reaction mixture was refluxed for 12 hr and then cooled to room temperature. A major portion of the solvent (400 ml) was distilled from the clear amber reaction mixture at reduced pressure (16 mm). The viscous, pale amber residual oil was added with stirring to 4 liters of cold water and a white granular solid precipitated. The filtered white solid was washed with portions of fresh water using a Waring Blendor to achieve good mixing. The solid was air-dried overnight and finally dried to constant weight *in vacuo* at 50°C in the presence of phosphorus pentoxide. The polymeric reaction product (II-1) (97.4 g) softened at 110°C and melted over a broad range (130–170°C). Flexible, somewhat brittle films were melt-pressed on a Preco Press at a platen temperature of 400°F and a pressure of 20,000 psi.

A portion (10 g) of the crude poly-2-oxazolidone (II-1) was precipitated twice from DMF solution by addition to water and after drying gave 6.5 g of analytically pure II-1.

## RESULTS AND DISCUSSION

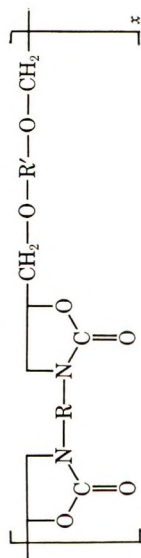
### Formation of Poly-2-oxazolidones

The synthesis of model oxazolidones (I) from isocyanates and epoxides was previously investigated in this laboratory.<sup>10,11</sup> As a result of that study a procedure was developed that optimized the use of DMF and LiCl as solvent and catalyst, respectively, for the preparation of mono- and di-oxazolidones.<sup>10,11</sup> Briefly, the procedure entails addition of an isocyanate to a refluxing solution of the epoxide and catalyst (LiCl) in DMF:



The procedure was modified for preparing poly-2-oxazolidones (II), in that a mixture of the diisocyanate and diglycidyl ether was added to refluxing DMF containing a catalytic amount of lithium chloride. The polymer-forming reaction proceeded without the formation of a precipitate and was terminated after varying periods of time by concentrating the reaction mixture and then adding the concentrate to water. Using this procedure, a variety of poly-2-oxazolidones (II) were prepared and isolated, usually as white to cream-colored powders. Table I summarizes reaction times used, yields, melting points, intrinsic viscosities, molecular weights (in some cases), and analytical data.

TABLE I  
Poly-2-oxazolidones (II)



Polymer	R	R'	Reaction time, hr	Yield, % <sup>a</sup>	Softening and melting range, °C <sup>b</sup>	C, %		H, %		N, %		$[\eta]$ , dl/g <sup>b</sup>	$M_n^b$
						Calcd	Found	Calcd	Found	Calcd	Found		
II-1			12	96	90, 125-180	68.5	68.2	7.1	7.3	5.5	5.3	0.34	4700 4750
II-2			12	78	Viscous oil	58.4	57.7	8.2	8.3	7.6	8.1	—	—
II-3			12	88 <sup>c</sup>	285, 303-305 70, 92-150	61.5	61.6	6.7	6.7	7.2	7.1	0.03	—
II-4			21	95	134, 145-160	73.2	73.4	6.1	6.1	4.7	5.6	0.13	—
II-5			12	89	83, 88-100	66.4	68.0	6.6	6.6	6.2	6.8	0.12	—

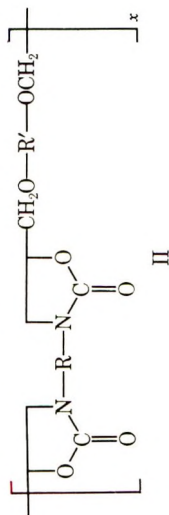
II-6			12	92	125, 135-175	68.6	68.5	5.3	5.3	5.9	6.1	0.11	1340 1360
II-7			12	98	123, 130-145	70.0	70.4	6.6	6.6	5.9	6.1	0.09	—
II-8			24	97.5	160, 175-195	71.7	71.7	7.6	7.6	4.7	4.7	0.21	3000
II-9			24	95	157, 170-195	70.4	70.2	7.8	7.8	5.0	5.1	0.16	3250
II-10			24	97	100-112	69.8	70.3	7.8	7.9	5.1	5.1	0.25	—

<sup>a</sup> Reported yields are for crude reaction products.

<sup>b</sup> Determined on reaction products (II) precipitated from DMF solution by addition to water.

<sup>c</sup> Yield includes 5.6% of a high-melting (285-305°C) crystalline solid fraction. The viscosity determination indicates that the high-melting solid is of relatively low molecular weight.

TABLE II  
Effect of Reaction Time on Degree of Polymerization of Poly-2-oxazolidones



Polymer	R	R'	Reaction time, hr	Yield, %	Softening and melting range, °C	$[\eta]$ dl/g
II-1	$-(\text{CH}_2)_6-$		6 12 24 48	98 96 95 96	98, 110-123 100, 125-180 100, 125-140 100, 130-180	0.16 0.34 0.39 0.42
II-4			6 21 48	95 95 96	140, 145-160 134, 145-160 135, 145-158	0.14 0.15 0.14



The poly-2-oxazolidones (II) were generally of relatively low molecular weight as evidenced by viscosity and molecular weight determinations. In several cases (Table II) involving polymers prepared from the reaction of hexamethylene diisocyanate and 4,4'-methylene bis(phenyl isocyanate) with the diglycidyl ether of 4,4'-isopropylidene diphenol efforts were made to increase the degree of polymerization by extending reaction time. In the case of the poly-2-oxazolidone (II-1) based upon the aliphatic diisocyanate longer reaction times increased the degree of polymerization as judged by intrinsic viscosity values (Table II). The degree of polymerization for the poly-2-oxazolidone (II-4) based upon the aromatic diisocyanate failed to increase.

Confirmation of the reaction products as poly-2-oxazolidones (II) was obtained by infrared spectra, NMR, and elemental analysis. The infrared spectra of the polymers (II) exhibited a very strong somewhat broad absorption in the region 1735 to 1750  $\text{cm}^{-1}$ . This absorption is characteristic of the carbonyl group of the oxazolidone ring.<sup>13</sup> In no case was there any absorption in the 2242–2274  $\text{cm}^{-1}$  region attributed to the isocyanate group.

NMR spectra of the poly-2-oxazolidones (II) (Tables III and IV) show ill-defined complex multiplets in the region 4.70 to 5.0 ppm. The field position of this absorption corresponds reasonably well with that previously established for the methine proton ( $H_A$ ) of the 2-oxazolidone ring in the model compounds.<sup>10,11</sup> As previously demonstrated, the methine proton ( $H_A$ ) is characterized by a double doublet when only the adjacent methylene protons of the 2-oxazolidone ring are available for interaction as in the case of 5-phenyl-*N-p*-tolyl-2-oxazolidone (I,  $R = p$ -tolyl,  $R' = \text{phenyl}$ ). In cases where oxymethylene protons ( $H_D$ ) are also present (in 2-oxazolidones based on oxymethylene glycidyl ethers), the splitting pattern becomes complex.

Other factors may also influence the nature of the methine proton ( $H_A$ ) signal. Earlier studies involving model compounds established that 4- and/or 5-isomeric 2-oxazolidones can result from the cycloaddition of isocyanates to epoxides.<sup>10</sup>

It was further demonstrated that the field position of the  $H_A$  proton of the 4-isomer is shifted upfield, when compared to its position in the 5-isomer. This shift involves ca. 0.2 ppm in the cases examined. The relatively broad complex signal observed for the polymers may then be due in part to the presence of 4- and 5-isomeric 2-oxazolidone rings in the polymer chain.

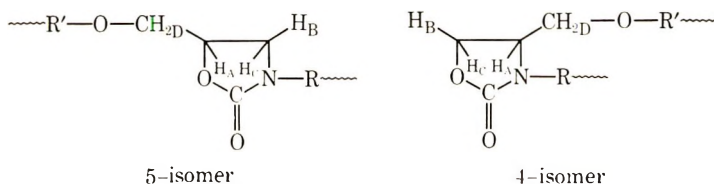
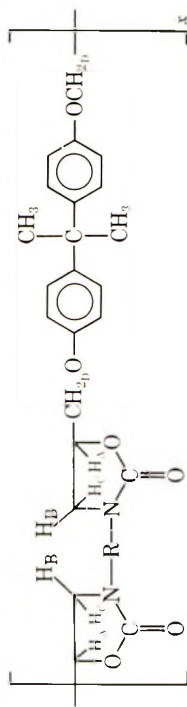

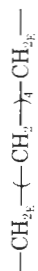

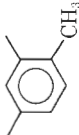


TABLE III  
NMR Data and Assignments for Poly-2-oxazolidones (II) Based on Various  
Diisocyanates and the Diglycidyl Ether of Bisphenol A



Polymer	R	Chemical shifts, ppm ( $\delta$ ) (TMS=O)				
		H <sub>A</sub>	H <sub>B</sub> , H <sub>C</sub>	H <sub>D</sub>	H <sub>E</sub>	
II-10 <sup>a</sup>		4.74 (complex multiplet)	3.25 (complex multiplet) 3.61 (complex multiplet)	4.06 (d) $J = 5.0$	3.15 (complex multiplet)	
II-9 <sup>a</sup>		4.78 (complex multiplet)	3.6 (complex multiplet)	4.08 (broad)	3.0 (complex multiplet)	

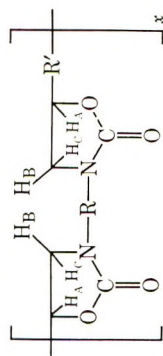
II-8 <sup>b</sup>				See H <sub>A</sub> , H <sub>B</sub>
II-1 <sup>c</sup>		4.75 (complex multiplet) 4.76 (complex multiplet)	3.45 (complex multiplet) 3.35 (d,d) $J_{BA} = 6.5$ ; $J_{BC} = 8.0$ 3.63 (t) $J_{CA} = J_{CB} = 8.0$	4.09 (d) $J = 5.0$ 4.07 (d) $J = 4.5$ 3.14 (multiplet)
II-4 <sup>b</sup>		4.95 (complex multiplet)	3.9-4.0 (complex multiplet)	4.18 (d) $J = 4.5$
II-7 <sup>b</sup>		5.0 (complex multiplet)	3.37 (complex multiplet) 4.0 (complex multiplet)	4.23 (d) $J = 5.0$

<sup>a</sup> Spectrum determined in deuteriochloroform (15% w/v) at 50°C.

<sup>b</sup> Spectrum determined in hexadeuterated DMSO (15% w/v) at 80°C.

<sup>c</sup> Spectrum determined in hexadeuterated DMSO (10% w/v) at 80°C.

TABLE IV  
Nmr Data and Assignments for Poly-2-oxazolidones (II)<sup>a</sup>



Polymer	R	R'	Chemical shifts, ppm ( $\delta$ ) (TMS=O)				
			H <sub>A</sub>	H <sub>B</sub> ,H <sub>C</sub>	H <sub>D</sub>	H <sub>E</sub>	
II-3			4.75 (complex multiplet)	3.37 (d,d) $J_{BA} = 6.0$ $J_{BC} = 8.5$ 3.66 (t) $J_{CA} = J_{CB} = 8.5-9.0$	4.11 (d) $J = 4.5$	3.16 (m)	
II-6			4.99 (complex multiplet)	3.85 (m) 4.15 (m)	4.21 (d) $J = 5.0$	—	
II-5			4.70	3.75 (complex multiplet)	—	—	

<sup>a</sup> Spectra determined in hexadeuterated DMSO (10% w/v) at 80°C.

The NMR signals attributed to the methylene protons ( $H_B$  and  $H_C$ ) in the polymers (II) are also broad and complex in the majority of cases. The field position of these protons ( $H_B$  and  $H_C$ ) is in general agreement with that found for model compounds. The splitting patterns of the methylene protons are due primarily to interaction with each other and the methine proton ( $H_A$ ). In addition, the situation is compounded by the similar field positions of the oxymethylene protons ( $H_D$ ) and the *N*-methylene or methine protons ( $H_E$ ) attached to the 2-oxazolidone ring; the latter protons being present only in those cases where an aliphatic diisocyanate is used as a coreactant.

In the majority of poly-2-oxazolidones (II) examined, deuterated dimethyl sulfoxide (DMSO) was used as the solvent at a probe temperature of 80°C in order to obtain improved resolution. Under these conditions definite splitting patterns could be discerned for the methylene protons ( $H_B$  and  $H_C$ ) of several poly-2-oxazolidones (Tables III and IV). As in the case of the model compounds, the lower field signal is a triplet assigned to the  $H_C$  protons and the upfield signal a double doublet assigned to  $H_B$ . The reason for the assignments and the disposition of the splitting patterns has been discussed.<sup>10</sup> The magnitude of the coupling constants for  $H_B$  and  $H_C$  protons of the polymers (II) is similar to that of the simple 2-oxazolidones.

The signals for other protons of the repeating structural unit of II are at the expected field positions. The oxymethylene protons ( $H_D$ ) adjacent to the 2-oxazolidone ring, for example, are in most instances readily observed as a doublet in the region 4.06 to 4.23 ppm. The magnitude of the coupling constant involved is, as expected, 4.5–5.0 Hz. Integration of the areas for the various proton signals is in general agreement with the number of protons associated with the assigned recurring structural unit of a given polymer (II). In summary the nature and disposition of the proton signals along with their integration was taken as supporting evidence for the assigned structures.

The possibility of formamidine ( $RN=CH-NMe_2$ ) formation, resulting from the reaction of isocyanate with DMF,<sup>14</sup> was briefly considered in regard to the nature of the end groups of the low molecular weight poly-2-oxazolidones (II). Such a reaction would cause chain termination and contribute to low molecular weight products (II). The presence of a formamidine function should manifest itself in the NMR spectra of II (particularly the lower molecular weight polymers) by a signal (sharp singlet) for the  $-NMe_2$  protons. The position of this signal was established for the model compound, *N,N*-dimethyl-*N'*-*p*-tolyl formamidine, as being at 2.89 ppm. A signal ( $2.85 \pm 0.05$  ppm, singlet) that may be attributed to  $-NMe_2$  protons was observed in the NMR spectra of the low molecular weight poly-2-oxazolidones (II-4, 5, 6, and 7, Table I) based upon aromatic diisocyanates. The NMR spectra of some of the relatively higher molecular weight poly-2-oxazolidones (II-1, 3, 8, 9, and 10, Table I) prepared from aliphatic diisocyanates exhibited weak signals in the region expected for  $-NMe_2$  protons.

Both *N,N*-dimethyl-*N'*-*p*-tolyl and —*N'*-phenyl formamides exhibit strong absorptions in the infrared at 1635 and 1600  $\text{cm}^{-1}$  attributed to  $>\text{N}=\text{C}=\text{N}-$  and  $>\text{C}=\text{N}-$ , respectively.<sup>15</sup> The infrared spectra of poly-2-oxazolidones (II-4, 5, 6, and 7, Table I) showed absorptions in the 1630 and 1590  $\text{cm}^{-1}$  regions suggestive of the formamide function. Some of the polymers (II-1, 8, 9, and 10) based upon aliphatic diisocyanates gave infrared absorptions in the 1605 and 1580  $\text{cm}^{-1}$  regions that may also be attributed to formamides.

Convincing evidence for other possible chain terminating functions such as hydroxy, amino and chloromethyl carbamate groups was sought but none could be found. The evidence obtained suggests that if a nonreactive solvent could be found for the reaction a higher degree of polymerization would result.\*

### Properties of Poly-2-oxazolidones (II)

Most of the poly-2-oxazolidones (II) are soluble in DMF at room temperature. The polymers (II) are insoluble in benzene and alcohol. Tetrahydrofuran dissolves II-9 and II-10, but not the remaining polymers; in

TABLE V  
Solubilities of Poly-2-oxazolidones (II)

Polymer	Solubility <sup>a</sup>					
	$\text{CH}_2\text{Cl}_2$	$\text{CHCl}_3$	DMF	$\text{C}_6\text{H}_6$	THF	EtOH
II-1	S <sup>b</sup>	S	S	IS (s)	IS (s)	IS (s)
II-2	—	S	S (d)	—	—	—
II-3	S	S (d)	S (d)	IS (s)	IS (s)	IS (s)
II-4	S <sup>b</sup>	S	S	IS	IS (s)	IS
II-5	S	S	S	IS (s)	IS (s)	IS
II-6	IS (s)	IS (s)	S	IS	IS	IS
II-7	S <sup>b</sup>	S	S	IS	IS (s)	IS
II-8	S <sup>b</sup>	S	S	IS (s)	IS (s)	IS
II-9	S <sup>b</sup>	S	S	IS	S	IS
II-10	S <sup>b</sup>	S	S	IS (s)	S	IS

<sup>a</sup> S (soluble), IS (insoluble), IS (s) insoluble but softens, S (d) soluble but with difficulty; determined at 25°C by using 0.1 g of the poly-2-oxazolidone and 1 ml of solvent.

<sup>b</sup> Films can be cast from solution.

the latter cases softening and swelling usually occur. Most of the poly-2-oxazolidones possess some solubility in chloroform and methylene dichloride. Some qualitative solubilities for II are summarized in Table V.

The x-ray diffraction patterns for a number of the polymers (II-1, 7, 8, 9, and 10) indicate that they are amorphous. The amorphous nature of the

\* The preparation of poly-2-oxazolidone (II-1, Table I) was repeated in DMSO. The characteristics (solubility, molecular weight as judged by inherent viscosity values and thermal properties) of the light-brown solid reaction product indicated possible solvent interaction to yield a product of even lower molecular weight than that obtained in DMF.

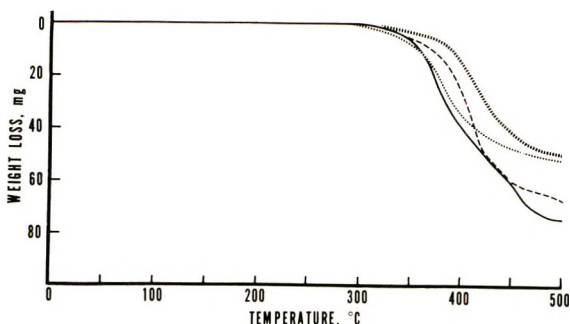


Fig. 1. Thermogravimetric curves of poly-2-oxazolidones (—) II-3, (...) II-4, (---) II-6, and (-·-) II-7 (Table I) to 500°C at 6° C/min in dry air.

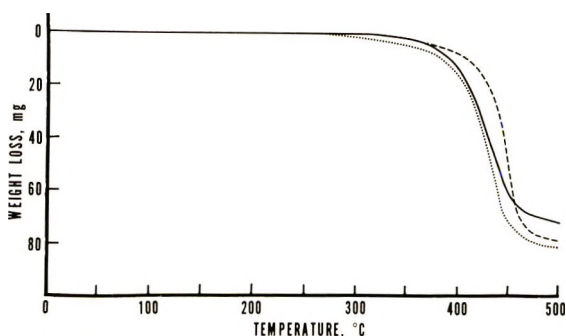


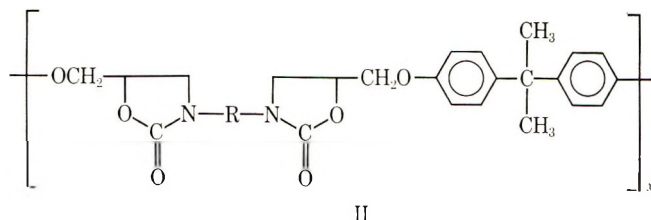
Fig. 2. Thermogravimetric curves of poly-2-oxazolidones (—) II-1, (---) II-8, and (...) II-9 (Table I) to 500°C at 6° C/min in dry air.

poly-2-oxazolidones is indicative of irregular structure, the presence of 4- and 5-isomeric oxazolidone rings, and possible unsymmetrical repeating units in which d- and l- configurations can occur randomly along the polymer chain.

The thermal behavior of the poly-2-oxazolidones (II) was examined by thermogravimetric analysis, but failed to indicate any definite relationship between apparent stability and structure of the repeating unit. In all cases the initial inflection point occurs in the range of 265–335°C, with a majority of the polymers exhibiting an initial weight loss at 300–310°C. Furthermore, under the conditions used the thermograms of II fail to indicate a stepwise thermolysis that might point to loss of carbon dioxide and accompanying aziridine formation. Instead, the thermograms are generally characterized by a relatively smooth curve, indicating an initial relatively slow weight loss followed by an increase in rate of weight loss. Similar results are obtained for the model compounds described previously.<sup>10,11</sup> The thermograms for some of the poly-2-oxazolidones (II) are given in Figures 1 and 2.

In a number of cases the poly-2-oxazolidones (II) were further characterized as to their thermal behavior by obtaining their glass transition temper-

TABLE VI  
Glass Transition Temperature of Some Poly-2-oxazolidones (II)  
as Determined by DSC<sup>a</sup>



Polymer	R	$T_g$ , °C <sup>b</sup>
II-1	$-(\text{CH}_2)_6-$	84
II-10	$-\text{CH}_2-\overset{\text{CH}_3}{\underset{ }{\text{CH}}}-\text{CH}_2-\overset{\text{CH}_3}{\underset{\text{CH}_3}{ }{\text{C}}}-\text{CH}_2\text{CH}_2-$	85.5
II-9		154
II-8		162
II-7		122

<sup>a</sup> Heating rate, 20°C/min.

<sup>b</sup> Determined on quenched samples. All samples were preheated (>110°C but <230°C) prior to determining  $T_g$ .

atures ( $T_g$ ). The  $T_g$ 's were determined by DSC and are tabulated in Table VI.

### Fabrication of Poly-2-oxazolidones (II)

The ability of the poly-2-oxazolidones to form films and fibers was briefly examined. In several cases films were solution-cast and melt-pressed, and somewhat brittle fibers were manually melt-spun. The film-forming qualities of poly-2-oxazolidone (II-1) were examined in some detail. Films were cast from dichloroethane solution containing 20% by weight of polymer. After drying at room temperature, the resulting films exhibit high gloss and good adhesion to glass and tin plate.



## References

1. G. P. Speranza and W. J. Peppel, *J. Org. Chem.*, **23**, 1922 (1958).
2. R. Oda, S. Tokiura, A. Miyasu, and M. Okano, *Kobunshi Kagaku*, **17**, 72 (1960); *Chem. Abstr.*, **55**, 16516a (1961).
3. M. Yokoyama and S. Konya, paper presented at International Symposium on Macromolecular Chemistry, Tokyo and Kyoto, 1966; *Preprints*, **5**, 22 (1966).
4. S. Sandler, F. Berg, and G. Kitazawa, *J. Appl. Polym. Sci.*, **9**, 1994 (1965).
5. S. Sandler, *J. Polym. Sci. A-1*, **5**, 1481 (1967).
6. R. Dileone, paper presented before the 155th National Meeting of the American Chemical Society, San Francisco, April 1968; *Polym. Preprints*, **9**, No. 1, 642 (1968).
7. Y. Iwakura, S. Izawa, and F. Hayano, *J. Polym. Sci. A-1*, **4**, 751 (1966).
8. Y. Iwakura, A. Nabeya, F. Hayano, and K. Kurita, *J. Polym. Sci. A-1*, **5**, 1865 (1967).
9. C. H. Schramm (to J. T. Baker Chemical Co.), U. S. Pat. 3,383,358 (May 14, 1968).
10. J. E. Herweh, T. A. Foglia, and D. Swern, *J. Org. Chem.*, **33**, 4029 (1968).
11. J. E. Herweh, *J. Heterocycl. Chem.*, **5**, 687 (1968).
12. E. C. Dearborn, R. M. Fuoss, A. K. Mackenzie, and R. G. Shepherd, *Ind. Eng. Chem.*, **45**, 2715 (1953).
13. M. E. Dyen and D. Swern, *Chem. Rev.*, **67**, 197 (1967).
14. M. L. Weiner, *J. Org. Chem.*, **25**, 2245 (1960).
15. C. N. R. Rao, *Chemical Applications of Infrared Spectroscopy*, Academic Press, New York, 1963, p. 267.

Received December 4, 1969

Revised February 9, 1970

## Stereospecific Polymerization of Isobutyl Vinyl Ether by $\text{AlR}_3\text{-VCl}_n$ Catalysts. I. Influence of Preparative Conditions of the Catalysts\*

YASUSHI JOH,† HEIMEI YUKI, and SHUNSUKE MURAHASHI,  
*Department of Polymer Science, Faculty of Science, Osaka University,  
Toyonaka, Osaka 560, Japan*

### Synopsis

The polymerization of isobutyl vinyl ether by the  $\text{VCl}_n\text{-AlR}_3$  system was carefully studied. The vanadium components were prepared by the reaction between  $\text{VCl}_4$  and  $\text{AlEt}_3$  or  $n\text{-BuLi}$  as a reducing agent.  $\text{VCl}_3\cdot\text{LiCl}$  and  $\text{VCl}_2\cdot 2\text{LiCl}$  are the effective catalysts for the stereospecific polymerization of isobutyl vinyl ether. When  $\text{VCl}_5\cdot\text{LiCl}$  is combined with  $\text{AlR}_3$ , a new catalytic system is formed. The effect of the preparative conditions of the various vanadium component in the  $\text{AlR}_3\text{-VCl}_n$  system shows that the effective vanadium component is trivalent. In the polymerization by  $\text{VCl}_3\cdot\text{LiCl-Al}(i\text{-Bu})_3$  system, a change of the polymerization mechanism may occur at  $\text{Al}(i\text{-Bu})_3/\text{VCl}_3\cdot\text{LiCl}$  ratio at around 5. When the ratio is lower than 5, a cationic polymerization by  $\text{VCl}_3\cdot\text{LiCl}$  takes place predominantly, while at ratios higher than 5, it is suggested that the polymerization proceeds by means of a  $\text{VCl}_3\cdot\text{LiCl-Al}(i\text{-Bu})_3$  complex by a coordinated anionic mechanism. The polymers obtained by these catalysts are highly crystalline. Styrene was also polymerized by using the same catalysts.  $\text{VCl}_3\cdot\text{LiCl}$  and  $\text{VCl}_3\cdot\text{LiCl-THF}$  complex yielded amorphous polymer by cationic polymerization. When  $\text{VCl}_3\cdot\text{LiCl}$  was combined with 6 mole-eq of  $\text{Al}(i\text{-Bu})_3$ , the resulting polystyrene was highly crystalline and had an isotactic structure, while the  $\text{VCl}_2\cdot 2\text{LiCl-Al}(i\text{-Bu})_3$  (1:6) system yielded traces of polymer of extremely low stereoregularity. The results indicate that the effective vanadium component at  $\text{Al/V} \geq 6$  is trivalent and that the mechanism is a coordinated anionic one.

### INTRODUCTION

Considerable literature data on the synthesis of crystalline poly(vinyl ethers) have been reported since the pioneering work of Schildknecht et al.,<sup>1,2</sup> who polymerized the vinyl ethers in a hydrocarbon solvent at  $-80^\circ\text{C}$  to  $-60^\circ\text{C}$  by using boron trifluoride-diethyl ether or other ether complexes. Natta and co-workers<sup>3,4</sup> have stated that such a polymer has an isotactic structure.

Vandenberg<sup>5</sup> has obtained highly crystalline poly(vinyl ethers) with high melting points by using vanadium chloride-triisobutyl aluminum catalyst

\* Presented at the Symposium of Polymer Science, Tokyo, Japan, 1961.

† Present address: Research Department, Mitsubishi Rayon Co., Ltd., Otake, Hiroshima, 739-06, Japan.

system. Shostakovskii and co-workers<sup>6,7</sup> also reported the polymerization of vinyl ether with heterogeneous catalysts based on  $\text{TiCl}_4$  or  $\text{VOCl}_3$ ,  $\text{LiC}_3\text{H}_7$ , and  $\text{Al}(i\text{-Bu})_3$ . We have also studied the stereospecific polymerization of isobutyl vinyl ether by heterogeneous catalysts.<sup>8-10</sup> This paper deals with the polymerization of isobutyl vinyl ether by trialkyl-aluminum-vanadium chloride systems and shows the influence of the preparative conditions of the catalysts on the polymerization. The effective vanadium component in this catalytic system was found to be trivalent.

In the polymerization by the  $\text{AlR}_3\text{-VCl}_3\cdot\text{LiCl}$  system, it is presumed that, when the molar ratio of  $\text{AlR}_3$  to  $\text{VCl}_3\cdot\text{LiCl}$  is lower than 5, a cationic polymerization by  $\text{VCl}_3\cdot\text{LiCl}$  predominates, while at  $\text{AlR}_3/\text{VCl}_3\cdot\text{LiCl}$  ratio higher than 5, the polymerization may proceed by so-called coordinated anionic mechanism by  $\text{VCl}_3\cdot\text{LiCl-AlR}_3$  complex.

## EXPERIMENTAL

### Monomer

Isobutyl vinyl ether was a commercial product which was refluxed under a nitrogen atmosphere for 8 hr and distilled once.

The distillate was further refluxed over  $\text{LiAlH}_4$  for 5 hr and fractionally distilled immediately before use under a nitrogen atmosphere, bp  $82.5^\circ\text{C}$ ,  $n_{25}^D = 1.3931$  (lit.<sup>11</sup> 1.3938).

Commercial styrene was purified by successive washing with 1% sodium hydroxide aqueous solution followed by water. After being dried over anhydrous magnesium sulfate, it was fractionally distilled immediately before use under nitrogen.

### Solvents

*n*-Heptane and toluene were treated with fuming sulfuric acid and concentrated sulfuric acid, respectively, then washed with alkali aqueous solution followed by water. The solvents were then distilled over metallic sodium under nitrogen. Diethyl ether and tetrahydrofuran were refluxed over metallic sodium for 8 hr and distilled immediately before use in an atmosphere of nitrogen.

### Reagents

**Vanadium Tetrachloride ( $\text{VCl}_4$ ).** A commercial product was distilled under nitrogen; the fraction distilling at  $148^\circ\text{C}$  was used.

***n*-Butyllithium (*n*-BuLi).** A *n*-hexane solution of *n*-BuLi was prepared from *n*-butyl chloride and metallic lithium according to Ziegler's procedure.<sup>12</sup> The concentration was determined by the double titration method<sup>13</sup> and stored at  $-20^\circ\text{C}$ .

**Triethylaluminum,  $\text{AlEt}_3$ , and Triisobutylaluminum  $\text{Al}(i\text{-Bu})_3$ .** Triethylaluminum and triisobutyl aluminum supplied by Ethyl Corporation were used without further purification.

### Vanadium Component of the Catalysts

**Reduction of  $VCl_4$  by  $AlEt_3$ .** All manipulations were carried out under nitrogen.  $VCl_4$  (0.6 mmole) was dissolved in 10 ml of *n*-heptane in a three-necked Schlenk vessel, and to this a prescribed amount of  $AlEt_3$  was added dropwise by an injection syringe under vigorous stirring. On addition of  $AlEt_3$ , a purple dispersion of precipitates was formed simultaneously. The color of the precipitate changed further to brown according to the amount of  $AlEt_3$  used. The reaction mixture was allowed to stand overnight at room temperatures, then it was heated for 8 hr at 90°C. After a supernatant liquid was removed out by means of an injection syringe, the precipitate was washed five times by using 30 ml of purified, air free *n*-heptane. Thus, soluble materials were thoroughly removed. The precipitate was finally suspended in 10 ml of *n*-heptane and used as a vanadium component of the catalysts.

**Reduction of  $VCl_4$  by *n*-BuLi.**  $VCl_4$  was reduced by *n*-BuLi by a method similar to that mentioned above. In order to obtain the vanadium component in a uniform reduction state, reaction vessels should be shaken as vigorously as possible during the dropwise addition of *n*-BuLi.

When an equimolar amount of BuLi to  $VCl_4$  was used, a violet vanadium trichloride ( $VCl_3 \cdot LiCl$ ) was obtained. The yellow-brown color of  $VCl_4$  in heptane solution disappeared at the endpoint of the dropwise addition of *n*-BuLi. After the addition was completed the reaction mixture was boiled for 10 min in order to complete the reaction and then was allowed to cool. The suspension was used as the vanadium component of the catalysts.

### Polymerization

**Polymerization of Isobutyl Vinyl Ether.** Polymerizations were carried out in a Schlenk vessel with the use of a catalyst composed of  $AlEt_3$  and the vanadium components. Polymerization procedures used were either (A) or (B) described below.

(A) The polymerizations were carried out under a nitrogen atmosphere at 30°C in 20 ml of heptane. Monomer,  $AlR_3$ , and the vanadium component were added in that order. Here, the amount of  $AlR_3$  was 6 mole-*eq* to  $VCl_4$  used for the preparation of the vanadium component.

(B) The polymerizations were the same except as described below. In this procedure, a prescribed amount of  $Al(i-Bu)_3$  was first added to 20 ml of *n*-heptane followed by an equimolar amount of monomer to the  $Al(i-Bu)_3$ . To this mixture, the  $VCl_3 \cdot LiCl$  suspension in heptane which had been previously prepared was introduced.

After aging of the mixture for 10 min, monomer was added so that the total amount of the monomer including the one previously added to  $Al(i-Bu)_3$  should be a prescribed amount.

After the polymerization had been performed for a given period, the reaction mixture was poured into a large amount of methanol containing a

small amount of HCl and phenyl- $\beta$ -naphthylamine, and it was allowed to stand over night at room temperatures to decompose the catalyst. The polymer precipitated was collected, washed with ethanol, and dried.

The polymer was extracted in 100 ml of acetone per gram of the polymer at its boiling point for 4 hr.

The percentage of insoluble material was used as one measure of the stereospecificity of the polymerization. It was confirmed from x-ray diffraction measurement of the stretched samples and also infrared spectra that the insoluble fractions are crystalline.

**Polymerization of Styrene.** A given amount of  $\text{Al}(i\text{-Bu})_3$  was dissolved in 30 ml of *n*-heptane and to this, an equimolar amount of diethyl ether was added so as to depress the reducing power of  $\text{Al}(i\text{-Bu})_3$ . The suspension of  $\text{VCl}_3 \cdot \text{LiCl}$  was then introduced. After aging of the mixture for 10 min at 30°C, the polymerization of styrene was performed under nitrogen for 4 hr at 30°C. After being polymerized for a given period, the reaction mixture was poured into acidic methanol to decompose the catalyst. A 1-g portion of the polymer was extracted in 100 ml of methyl ethyl ketone, and the percentage of insoluble material was determined. The insoluble fraction is crystalline by x-ray examination, showing isotactic structure. This is used as a measure of the stereoregularity of the polymer.

### Viscosity Measurements

The reduced viscosity ( $\eta_{sp}/c$ ) was determined at 30°C in benzene solution for the insoluble fraction of poly(isobutyl vinyl ether) at a concentration of 1 g/100 ml.

## RESULTS

### Valence of Vanadium Component and Catalytic Activity

**Vanadium Component Reduced by  $\text{AlEt}_3$ .** Vanadium components of different reduction states were prepared by the reaction between a fixed amount of  $\text{VCl}_4$  and various amounts of  $\text{AlEt}_3$  (as reducing agent). The polymerization was carried out by procedure A by using the catalyst system comprising the vanadium components thus prepared and additional  $\text{AlEt}_3$ . To avoid confusion between  $\text{AlR}_3$  used in the preparation of the vanadium components with that used in the polymerization, we intend to denote by  $(\text{AlR}_3)_R$  the  $\text{AlR}_3$  used as a reducing agent in the vanadium component preparations.

The results of the polymerizations are shown in Figures 1 and 2. Both total conversion and the acetone-insoluble fraction gave maxima at the molar ratio of  $(\text{AlEt}_3)_R/\text{VCl}_4$  of around 0.6.

The viscosities of the polymers were almost constant regardless of the molar ratio  $(\text{AlEt}_3)_R/\text{VCl}_4$ , as shown in Figure 2.

Figure 3 shows the results of the polymerization by the procedure A with the same catalyst system in which the vanadium components were

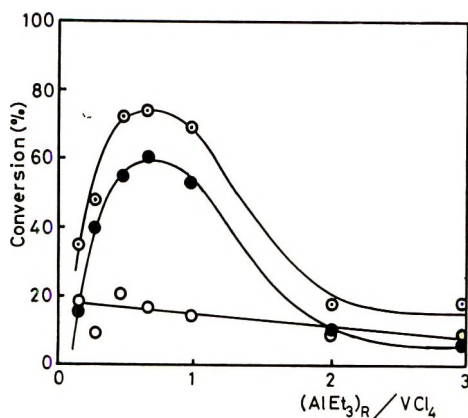


Fig. 1. Influence of  $(\text{AlEt}_3)_R/\text{VCl}_4$  ratio in the vanadium component preparation ( $\text{VCl}_4$  0.0006 mole, fixed,  $(\text{AlEt}_3)_R$  varied). (○) Total conversion, (●) acetone-insoluble, (○) acetone-soluble. Polymerization conditions: *n*-heptane 10 ml, isobutyl vinyl ether 3g, polymerization temperature 10°C, polymerization time 24 hr.,  $\text{AlEt}_3 = 0.0036$  mole

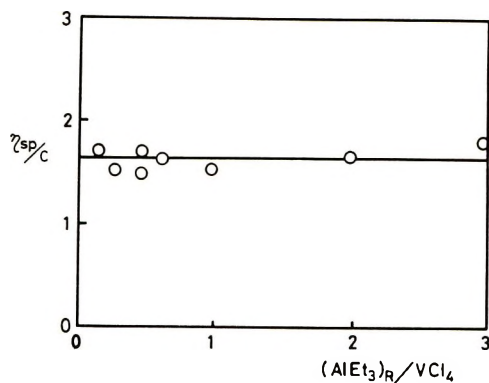


Fig. 2. Influence of  $(\text{AlEt}_3)_R/\text{VCl}_4$  in the vanadium component preparation on the viscosity of the resulting polymer ( $\text{VCl}_4$  0.0006 mole, fixed,  $(\text{AlEt}_3)_R$  varied).  $\eta_{sp}/c$  ( $c = 1.0$ ) was measured at 30°C in benzene solution. The polymerization conditions are those given in Fig. 1.

prepared by the reaction between various amounts of  $\text{VCl}_4$  and a fixed amount of  $\text{AlEt}_3$ .

Both total conversion and the acetone-insoluble fraction increased approximately in proportion to  $\text{VCl}_4$  in the range of  $\text{VCl}_4/(\text{AlEt}_3)_R < 1$ , but these became approximately constant when the ratio is higher than 2. Figure 4 shows that the viscosities of the polymers decreased slightly as the  $\text{VCl}_4$  increased.

**Vanadium Component Reduced by *n*-BuLi.** Polymerizations were carried out according to procedure A by using catalyst systems comprising  $\text{Al}(i\text{-Bu})_3$  and vanadium components which were prepared by the reduction of  $\text{VCl}_4$  by *n*-BuLi.

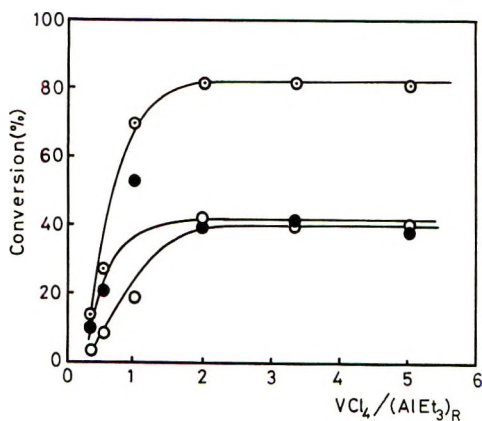


Fig. 3. (○) Total conversion, (●) acetone-insoluble, (○) acetone-soluble. Influence of  $VCl_4/(AlEt_3)_R$  ratio in the vanadium component preparation [ $VCl_4$  varied,  $(AlEt_3)_R$  0.0006 mole, fixed]. The polymerization conditions; *n*-heptane 10 ml., monomer 3 g, polymerization temperature 10°C, polymerization time 24 hr.,  $AlEt_3 = 0.0036$  mole.

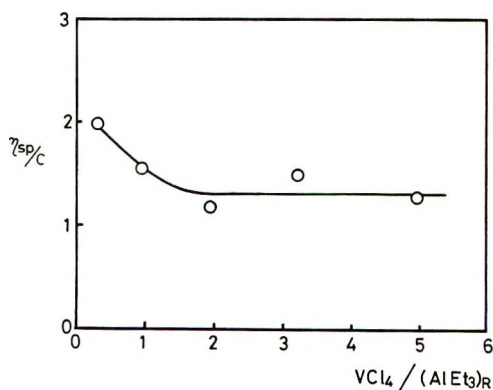


Fig. 4. Influence of  $VCl_4/AlEt_3$  ratio in the vanadium component preparation [ $VCl_4$  varied,  $(AlEt_3)_R$  fixed, 0.0006 mole] on the viscosity of the resulting polymer.  $\eta_{sp}/c$  was measured at 30°C in benzene solution at  $c = 1.0$ . The polymerization conditions are those given in Fig. 3.

Figure 5 shows the results of the polymerization. The vanadium components were prepared with a fixed amount of  $VCl_4$  and various amounts of *n*-BuLi.

As a result, a similar trend was observed as in the case when  $(AlEt_3)_R$  was used as a reducing agent. Both total conversion and the acetone-insoluble fraction reached maxima when the molar ratio of *n*-BuLi to  $VCl_4$  was just unity.

Interestingly, even if the vanadium components were prepared at the conditions of  $(BuLi)_R/VCl_4 < 1$ , if the precipitated products were boiled for about 30 min before washing by *n*-heptane, the polymerization resulted

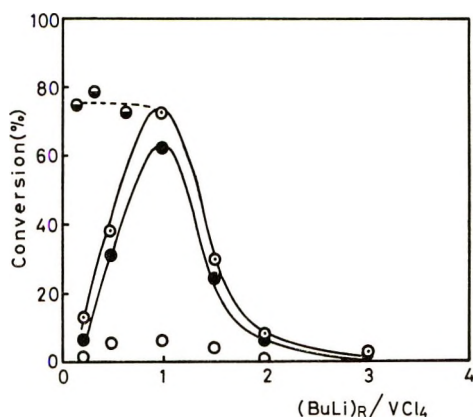


Fig. 5. Influence of  $(\text{BuLi})_R/\text{VCl}_4$  ratio in the vanadium component preparation ( $\text{VCl}_4$  0.00025 mole, fixed,  $(\text{BuLi})_R$  varied). (○) Total conversion, (●) acetone-insoluble, (◐) acetone-soluble, (◑) total conversion by boiled vanadium component. Polymerization conditions; *n*-heptane 10 ml, monomer 3 g,  $\text{Al}(i\text{-Bu})_3$  0.0015 mole, polymerization temperature  $30^\circ\text{C}$ , polymerization time 1 hr.

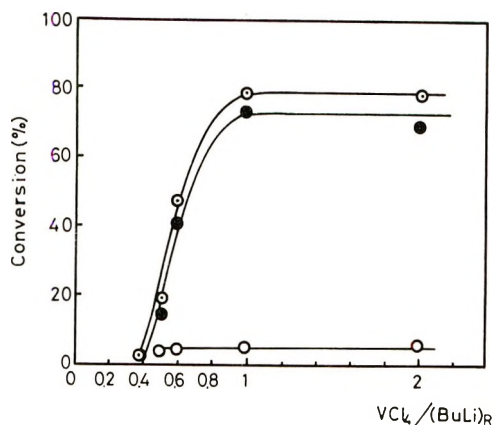


Fig. 6. Influence of  $\text{VCl}_4/(\text{BuLi})_R$  ratio in the vanadium component preparation [ $\text{VCl}_4$  varied,  $(\text{BuLi})_R$  0.00025 mole, fixed]. (○) Total conversion, (●) acetone-insoluble, (○) acetone-soluble. Polymerization conditions are those given in Fig. 3.

in comparable conversion to that obtained by using the vanadium component prepared at  $(\text{BuLi})_R/\text{VCl}_4 = 1$ . Here,  $(\text{BuLi})_R$  denotes the BuLi used as a reducing agent in the vanadium component preparations. It should be noted, however, that the greater part of the resulting polymer was soluble in acetone, showing the polymer to be of lower stereoregularity.

Alternatively, the polymerizations were carried out in the same manner by using the vanadium components prepared by the reaction between various amounts of  $\text{VCl}_4$  and a fixed amount of *n*-BuLi. The results are shown in Figure 6. Similar to the case of  $(\text{AlEt}_3)_R$ , both total conversion and the acetone-insoluble fractions increased approximately in proportion



to the  $\text{VCl}_4$  used in the range of molar ratio  $\text{VCl}_4/(\text{n-BuLi})_R < 1$ , while these became almost constant in the range of  $\text{VCl}_4/(\text{BuLi})_R \geq 1$ .

### Polymerization of Isobutyl Vinyl Ether with Various Vanadium Chlorides without $\text{AlR}_3$

The polymerization of isobutyl vinyl ether was performed with various vanadium chlorides of different valences without  $\text{AlR}_3$ . The results are shown in Table I. It was found that isobutyl vinyl ether can be polymerized by  $\text{VCl}_4$ ,  $\text{VCl}_3 \cdot \text{LiCl}$ , and  $\text{VCl}_2 \cdot 2\text{LiCl}$ , but not by the vanadium component prepared by  $\text{VCl}_4$  and 3 mole-eq of *n*-BuLi.

TABLE I. Polymerization<sup>a</sup> of Isobutyl Vinyl ether by  $\text{VCl}_n$

Kind	Catalyst color	Concentration (millimole)	Elevation of temp. at monomer addition (°C)	Conversion (%)	Property of polymer	Solubility in hot acetone
$\text{VCl}_4$ <sup>b</sup>	red brown	0.5	40	40.0	very sticky	soluble
$\text{VCl}_3$ <sup>b</sup>	violet	5.4	20	35.0	very sticky	soluble
$\text{VCl}_2$ <sup>b</sup>	brown	5.0	0	26.0	sticky	soluble
$\text{VCl}_3 \cdot \text{LiCl}$ <sup>c</sup>	violet	0.5	40	85.6	sticky	mostly soluble
$\text{VCl}_3 \cdot \text{LiCl}$ <sup>c</sup>	violet	0.5	0 <sup>d</sup>	92.0	not sticky	partly soluble
$\text{VCl}_2 \cdot 2\text{LiCl}$ <sup>c</sup>	brown	0.5	40	86.0	slightly sticky	mostly soluble
$\text{VCl}_2 \cdot 2\text{LiCl}$ <sup>c</sup>	brown	0.5	0 <sup>d</sup>	92.0	not sticky	partly soluble
$\text{VCl} \cdot 3\text{LiCl}$ <sup>c</sup>	dark brown	0.5	0	0	—	—

<sup>a</sup> Polymerization conditions: *n*-heptane 10 ml, monomer 3 g, polymerization temp. 1 hr.

<sup>b</sup> Commercial product.

<sup>c</sup>  $\text{VCl}_3 \cdot \text{LiCl}$ ,  $\text{VCl}_2 \cdot 2\text{LiCl}$ ,  $\text{VCl} \cdot 3\text{LiCl}$  were prepared by the reduction  $\text{VCl}_4$  with stoichiometric amount of BuLi.

<sup>d</sup> Elevation of temperature was depressed by cooling.

Interestingly, heterogeneous catalysts such as  $\text{VCl}_3 \cdot \text{LiCl}$  and  $\text{VCl}_2 \cdot 2\text{LiCl}$  can form crystalline polymers even at 30°C. From the characteristic of these catalysts, it is reasonably considered that the polymerization takes place by a cationic mechanism.

### Polymerization by $\text{VCl}_3 \cdot \text{LiCl} - \text{Al}(i\text{-Bu})_3$ System

Polymerizations were carried out according to procedure B by using the catalyst system comprising  $\text{Al}(i\text{-Bu})_3$  and  $\text{VCl}_3 \cdot \text{LiCl}$ , which was prepared by the reduction of  $\text{VCl}_4$  with an equimolar amount of *n*-BuLi.

An equimolar mixture of  $\text{Al}(i\text{-Bu})_3$  and isobutyl vinyl ether in 20 ml of *n*-heptane was first prepared, and to this,  $\text{VCl}_3 \cdot \text{LiCl}$  suspension was introduced. The effect of aging time from the addition of  $\text{VCl}_3 \cdot \text{LiCl}$  at 30°C on the polymerization was carefully examined. The amount of  $\text{Al}(i\text{-Bu})_3$  used was 6 mole-eq relative to  $\text{VCl}_3 \cdot \text{LiCl}$ , and the polymerizations were carried out at 30°C. It was found that total conversion, the acetone-

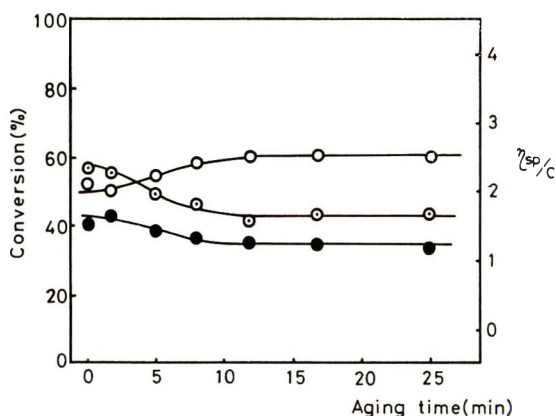


Fig. 7. Influence of the aging time in  $\text{Al}(i\text{-Bu})_3\text{-VCl}_3\cdot\text{LiCl}$  (6:1) system. (○) Total conversion, (●) acetone-insoluble, (○)  $\eta_{sp}/c$  of the acetone-insoluble portion measured at  $30^\circ\text{C}$  in benzene at  $c = 1.0$ . Polymerization procedure; 20 ml of *n*-heptane,  $\text{Al}(i\text{-Bu})_3$  0.0030 mole, monomer 0.0030 mole,  $\text{VCl}_3\cdot\text{LiCl}$  0.0005 mole were mixed in this order and aged for a given time, then monomer 0.027 mole was added to start the polymerization. Polymerization time 3 hr, polymerization temperature  $30^\circ\text{C}$ .  $\eta_{sp}/c$  ( $c = 1.0$ ) was measured at  $30^\circ\text{C}$  in benzene solution.

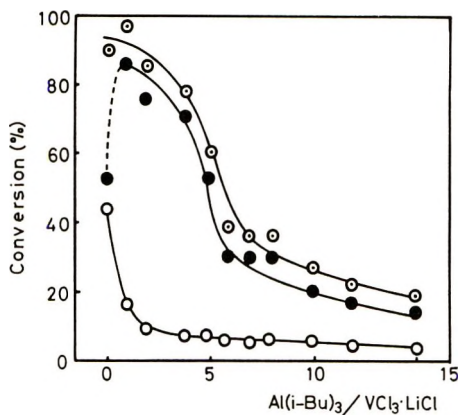


Fig. 8. Influence of  $\text{Al}(i\text{-Bu})_3/\text{VCl}_3\cdot\text{LiCl}$  ratio on the polymerization of isobutyl vinyl ether. (○) Total conversion, (●) acetone-insoluble, (○) acetone-soluble. Polymerization conditions; *n*-heptane 20 ml,  $\text{Al}(i\text{-Bu})_3$  varied,  $\text{VCl}_3\cdot\text{LiCl}$  0.00025 mole, monomer 3 g, polymerization temperature  $30^\circ\text{C}$ , polymerization time 1 hr.

insoluble fraction, and also the acetone-soluble fraction decreased with aging time during the initial 10 min, while the viscosity of the polymers increased during the same period. After about 10 min all of these values became constant and were kept constant over a long period of aging time. The results are shown in Figure 7.

Figure 8 shows the result of the polymerizations by the  $\text{Al}(i\text{-Bu})_3\text{-VCl}_3\cdot\text{LiCl}$  systems [ $\text{VCl}_3\cdot\text{LiCl}$  fixed (0.25 mmole),  $\text{Al}(i\text{-Bu})_3$  varied].

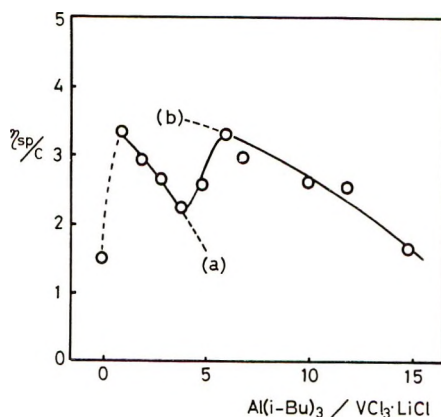


Fig. 9. Influence of Al (*i*-Bu)<sub>3</sub>/VCl<sub>3</sub>·LiCl ratio on the viscosity of the resulting polymer.  $\eta_{sp}/c$  ( $c = 1.0$ ) was measured for the acetone-insoluble fractions in benzene solution at 30°C.

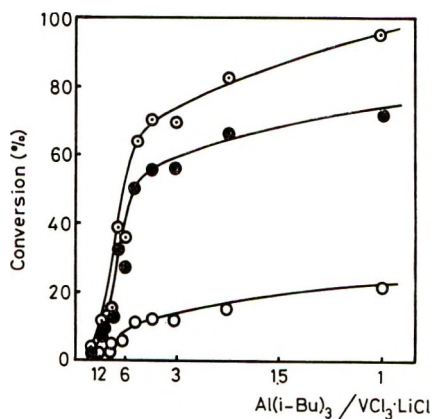


Fig. 10. Influence of Al (*i*-Bu)<sub>3</sub>/VCl<sub>3</sub>·LiCl ratio on the polymerization of isobutyl vinyl ether. (○) Total conversion, (●) acetone-insoluble, (○) acetone-soluble, Al(*i*-Bu)<sub>3</sub> 0.0015 mole, fixed, VCl<sub>3</sub>·LiCl varied. Polymerization conditions; *n*-heptane 20 ml, monomer 3 g, polymerization temperature 30°C, polymerization time 1 hr.

The total conversion and the acetone-insoluble fraction decreased with increasing molar ratio of Al(*i*-Bu)<sub>3</sub> to VCl<sub>3</sub>·LiCl, especially with a rapid decrease at a molar ratio of Al(*i*-Bu)<sub>3</sub>/VCl<sub>3</sub>·LiCl of around 5. Elevation of temperature in the reaction medium was observed when the polymerizations were carried out at Al(*i*-Bu)<sub>3</sub>/VCl<sub>3</sub>·LiCl < 4, while this phenomenon was not observed at Al(*i*-Bu)<sub>3</sub>/VCl<sub>3</sub>·LiCl > 5.

Figure 9 shows that the molecular weight of the acetone-insoluble fractions showed a minimum at Al(*i*-Bu)<sub>3</sub>/VCl<sub>3</sub>·LiCl of 4 and a maximum at Al(*i*-Bu)<sub>3</sub>/VCl<sub>3</sub>·LiCl of 6, then it gradually decreased as the molar ratio of Al/V increased further than 6.

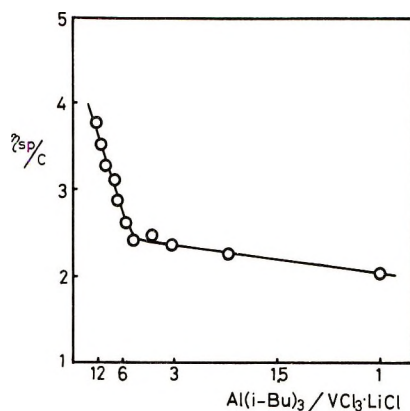


Fig. 11. Influence of  $\text{Al}(i\text{-Bu})_3/\text{VCl}_3 \cdot \text{LiCl}$  ratio on the viscosity of the resulting polymer.  $\eta_{sp}/c$  ( $c = 1.0$ ) was measured at  $30^\circ\text{C}$  in benzene solution. Polymerization conditions are those given in Fig. 10.

Alternatively, the polymerizations were carried out by using the same catalytic system with a fixed amount of  $\text{Al}(i\text{-Bu})_3$  (1.5 mmole) and various amounts of  $\text{VCl}_3 \cdot \text{LiCl}$ . Results are shown in Figure 10. The total conversion and the acetone-insoluble fraction rapidly increased with increasing  $\text{VCl}_3 \cdot \text{LiCl}$  in the range of  $\text{Al}(i\text{-Bu})_3/\text{VCl}_3 \cdot \text{LiCl} > 5$ . The acetone-soluble fractions changes in a similar way with increasing  $\text{VCl}_3 \cdot \text{LiCl}$  concentration; however, the ratio of the insoluble part to the soluble part was approximately constant, regardless of the  $\text{Al}(i\text{-Bu})_3/\text{VCl}_3 \cdot \text{LiCl}$  ratio.

Figure 11 shows that the molecular weight of the acetone-insoluble fractions decreased rapidly with increasing  $\text{VCl}_3 \cdot \text{LiCl}$  in the range of  $\text{Al}(i\text{-Bu})_3/\text{VCl}_3 \cdot \text{LiCl} > 5$  while the decrease became slower at  $\text{Al}(i\text{-Bu})_3/\text{VCl}_3 \cdot \text{LiCl} < 5$ .

### Polymerization of Styrene

Table II shows that the results of the polymerizations of styrene which were carried out at  $30^\circ\text{C}$  with the same catalyst systems used in the polymerization of the isobutyl vinyl ether. The  $\text{VCl}_3 \cdot \text{LiCl}$  alone showed high catalytic activity for the polymerization of styrene, however, the polymers obtained were easily soluble in methyl ethyl ketone and were found to be all amorphous.

On the other hand, with the  $\text{VCl}_3 \cdot \text{LiCl}-\text{Al}(i\text{-Bu})_3$  catalyst, a crystalline polystyrene was obtained. This fact shows that  $\text{VCl}_3 \cdot \text{LiCl}-\text{Al}(i\text{-Bu})_3$  has a high catalytic activity for the stereospecific polymerization of styrene, while with the  $\text{VCl}_2 \cdot 2\text{LiCl}-\text{Al}(i\text{-Bu})_3$  system, only traces of polystyrene of extremely low stereoregularity were obtained. The fact indicates that vanadium component useful for the stereoregular polymerization of styrene was trivalent  $\text{VCl}_3 \cdot \text{LiCl}$ , similar to the polymerization of isobutyl vinyl ether.

TABLE II. Polymerization<sup>a</sup> of Styrene by  $\text{Al}(i\text{-Bu})_3\text{-VCl}_n \cdot m\text{LiCl}$  ( $n = 2, 3, n + m = 4$ ) and  $\text{VCl}_3$  Catalyst

Catalyst	Solvent	Al/V ratio	Conversion (%)	Stereo-specificity <sup>c</sup> (%)	Melt point <sup>e</sup> of polymer (°C)
$\text{Al}(i\text{-Bu})_3\text{-VCl}_2 \cdot 2\text{LiCl}$	toluene	6	0.7	2.1	150
$\text{Al}(i\text{-Bu})_3\text{-VCl}_3 \cdot \text{LiCl}$	toluene	6	7.9	74.9	229
$\text{Al}(i\text{-Bu})_3\text{-VCl}_3 \cdot \text{LiCl}$	<i>n</i> -heptane	6	8.0	78.0	229
$\text{VCl}_3 \cdot \text{LiCl}^b$	<i>n</i> -heptane	—	23.4	0	—
$\text{VCl}_3 \cdot \text{LiCl}\text{-THF}$	<i>n</i> -heptane	1 <sup>f</sup>	0.8 <sup>d</sup>	0	—

<sup>a</sup> Polymerization conditions; solvent 30 ml,  $\text{VCl}_3$  0.0005 mole, styrene 5 ml, polymerization temperature 30°C, polymerization time 4 hr.

<sup>b</sup> Prepared by the reduction of  $\text{VCl}_4$  by stoichiometric amount of *n*-BuLi.

<sup>c</sup> Insoluble part in methyl ethyl ketone/total polymer  $\times 100$ .

<sup>d</sup> Polymerization time 3 hr.

<sup>e</sup> Melting point of the methyl ethyl ketone insoluble fraction.

<sup>f</sup> THF/ $\text{VCl}_3$  ratio.

## DISCUSSION

Vanadium compounds can be reduced much easier than titanium compounds. Natta et al.<sup>14</sup> reported that  $\text{VCl}_3$  was readily reduced to  $\text{VCl}_2$  by the action of  $\text{R}_3\text{Al}$  at temperatures above 60°C; at 100°C, surface reduction occurred so that all of the active centers on its surface could be reduced from trivalent to divalent after 60 min. They also reported that when  $\text{Et}_2\text{AlCl}$  was used instead of  $\text{AlEt}_3$ , no reduction of  $\text{VCl}_3$  was detectable after 180 min at 90°C.

On the other hand, Bier<sup>15</sup> et al. reported that  $\text{TiCl}_4$  was reduced to  $\text{TiCl}_3$  by an equimolar amount of  $\text{AlR}_3$  at 25°C after 1 hr, while  $\text{VCl}_4$  could be reduced to  $\text{VCl}_{2.3}$ , on the average, under the same conditions. When  $\text{R}_2\text{AlCl}$  was used instead of  $\text{R}_3\text{Al}$ ,  $\text{VCl}_4$  was reduced to  $\text{VCl}_{2.7}$ . From these facts it is considered that when  $\text{VCl}_4$  is allowed to react with  $\text{AlR}_3$ , the resulting  $\text{VCl}_3$  is further reduced by  $\text{R}_2\text{AlCl}$  formed:



Vandenberg<sup>5</sup> also reported that a purple dispersion obtained by the reduction of  $\text{VCl}_4$  by  $\text{AlEt}_3$  under the condition of  $\text{VCl}_4/\text{Et}_3\text{Al} = 1:0.36$  (molar ratio) for 16 hr at 80°C was an effective catalyst for the stereospecific polymerization of vinyl ethers, and 80% of the vanadium was present in the trivalent form (remainder of vanadium divalent). The chocolate-colored dispersion obtained by the further reduction of this purple dispersion by  $(i\text{-Bu})_3\text{Al}\text{-THF}$  complex\* at  $\text{Al/V} = 2$  for 20 hr at room temperature has higher catalytic activity, and 12% of the vanadium component in this catalytic system was trivalent and 88% was divalent.

As mentioned above, vanadium compounds are very easily reduced; therefore, in this investigation,  $\text{VCl}_4$  was treated beforehand with  $\text{R}_3\text{Al}$  or

\* It is reported that a reaction time of 5 min is sufficient in the case of  $\text{Al}(i\text{-Bu})_3$  instead of  $(i\text{-Bu})_3\text{Al}\text{-THF}$ .

BuLi in stoichiometric proportions to give vanadium chlorides of prescribed reduction states, then additional  $R_3Al$  was further introduced to this in the presence of monomer so as to form the complex polymerization catalyst.

It is conceivable that further reduction of the vanadium component by  $R_3Al$  was depressed in the presence of the monomer, since the color of the vanadium compound does not change during the polymerization, and that the aging time of the catalyst mixture does not influence the polymerization except the initial 10 min of aging as shown in Figure 7.

Figures 5 and 6 show that when  $n$ -BuLi was used as a reducing agent in the preparation of the vanadium component the stereospecific polymerization activity of the catalyst ( $AlR_3-VCl_n \cdot mLiCl$ ) was highest when  $(n\text{-BuLi})_R/VCl_n$  was just unity, either when BuLi was kept constant and  $VCl_4$  was varied, or vice versa. The color of the vanadium component prepared at  $(n\text{-BuLi})_R/VCl_4 = 1$  was violet.

A rapid decrease in the stereospecific polymerization activity was observed when the ratio of  $(n\text{-BuLi})_R/VCl_4$  increased to 1.5, at which ratio the color of the vanadium component changed from violet to chocolate brown. This strongly suggests that the effective vanadium component in this catalytic system is trivalent, and when it was reduced to a lower state, the catalytic system loses its stereospecific polymerization activity. Our results differ from those by Vandenberg at this point.

Alternatively, when  $Et_3Al$  was used as reducing agent in the preparation of the vanadium component, the catalytic activity reached a maximum when the ratio of  $(Et_3Al)_R/VCl_4$  was 0.5–0.6, as shown in Figures 1 and 3.

From the above results, the active vanadium component in this catalytic system was considered to be trivalent:



It can also be regarded that  $EtAlCl_2$  did not reduce the  $VCl_3$  further under the reaction condition employed here, namely, at  $90^\circ C$  for 8 hr. When  $(n\text{-BuLi})_R$  or  $(AlEt_3)_R$  was fixed and  $VCl_4$  was varied in the vanadium component preparation, the polymerization activity of the  $Al(i\text{-Bu})_3-VCl_n$  system was approximately constant if the  $VCl_4$  was present in sufficient amounts. This can be reasonably explained if the excess of soluble  $VCl_4$  was removed by washing and therefore, a constant amount of  $VCl_3$ , which corresponds to the amount of the reducing agent, acted as an effective catalyst component.

Even if  $(n\text{-BuLi})_R/VCl_4$  was less than unity, when the reaction mixture in the preparation was boiled before washing, the catalyst system  $Al(i\text{-Bu})_3-VCl_n$  showed a comparable activity to that prepared at  $(n\text{-BuLi})_R/VCl_4$  of unity, probably because the unreduced  $VCl_4$  was thermally decomposed to  $VCl_3$ , which acted as an effective catalyst component.

However, it should be noted that the greater part of the polymers obtained by the boiled catalyst at  $(BuLi)_R/VCl_4 < 1$  is soluble in acetone. This indicated that thermally decomposed  $VCl_3$  is not an effective catalyst

for the stereospecific polymerization, although the polymerization activity seems comparable.

Figure 8 gives the results of the polymerization by  $\text{Al}(i\text{-Bu})_3\text{-VCl}_3\text{-LiCl}$  [ $\text{VCl}_3\text{-LiCl}$  fixed,  $\text{Al}(i\text{-Bu})_3$  varied] showing the rapid decrease of the total conversion and of the acetone-insoluble fraction at the  $\text{Al}(i\text{-Bu})_3/\text{VCl}_3\text{-LiCl}$  ratios of around 4–5. Figure 9 shows that the viscosity of the acetone-insoluble fraction gave minimum value at the  $\text{Al}(i\text{-Bu})_3/\text{VCl}_3\text{-LiCl}$  ratio of 4. This strongly suggests that some sort of a change in the polymerization mechanism has taken place at the  $\text{Al}(i\text{-Bu})_3/\text{VCl}_3\text{-LiCl}$  ratio of around 5.

In fact, a marked temperature elevation of the polymerization medium was observed at  $\text{Al}(i\text{-Bu})_3/\text{VCl}_3\text{-LiCl}$  ratio lower than 4, and in this region the polymerization rate was extremely fast, while at  $\text{Al}(i\text{-Bu})_3/\text{VCl}_3\text{-LiCl}$  ratio higher than 5 the polymerization rate became moderate and that very little rise of temperature in the polymerization medium was observed.

It is interesting that  $\text{VCl}_3\text{-LiCl}$  alone could polymerize isobutyl vinyl ether to a high molecular weight, crystalline polymer in a similar manner without the action of  $\text{AlR}_3$  when the temperature rise during the polymerization was depressed by cooling.

It should be noted that the stereospecific polymerization took place with  $\text{VCl}_2\text{-2LiCl}$  without  $\text{Al}(i\text{-Bu})_3$ , similar to polymerization with  $\text{VCl}_3\text{-LiCl}$ .

It may be that in case of the  $\text{Al}(i\text{-Bu})_3\text{-VCl}_3\text{-LiCl}$  system,  $\text{Al}(i\text{-Bu})_3\text{-VCl}_3\text{-LiCl}$  complex might be formed on the surface of  $\text{VCl}_3\text{-LiCl}$  particles. At low  $\text{Al}(i\text{-Bu})_3$  concentration, free  $\text{VCl}_3\text{-LiCl}$  might be still present in addition to the complex, and hence the polymerization would proceed by both the  $\text{Al}(i\text{-Bu})_3\text{-VCl}_3\text{-LiCl}$  complex and free  $\text{VCl}_3\text{-LiCl}$ .

In this case, it is believed that the polymerization by  $\text{VCl}_3\text{-LiCl}$  proceeds by a cationic mechanism much faster than that by the  $\text{Al}(i\text{-Bu})_3\text{-VCl}_3\text{-LiCl}$  complex. Accordingly, at lower concentration of  $\text{Al}(i\text{-Bu})_3$ , the polymerization occurred predominantly by  $\text{VCl}_3\text{-LiCl}$ .

Alternatively, when the concentration of  $\text{Al}(i\text{-Bu})_3$  increases so that all of the catalytic sites on the surface of  $\text{VCl}_3\text{-LiCl}$  particles may form the complex with  $\text{Al}(i\text{-Bu})_3$ , the polymerization proceeds at a much more moderate rate, most predominantly with the complexes.

Presumably, the change of the polymerization mechanism might occur at around an  $\text{Al}(i\text{-Bu})_3/\text{VCl}_3\text{-LiCl}$  ratio of 4–5.

As already mentioned above, in the  $\text{R}_3\text{Al-VCl}_n$  catalyst system used in this investigation, trivalent vanadium is effective and it becomes inactive by further reduction to divalent vanadium, which differs from the results of Vandenberg.<sup>5</sup> However, Vandenberg used his complex catalyst,  $\text{R}_3\text{Al-VCl}_n$  (80% trivalent) at a ratio of  $\text{AlR}_3/\text{VCl}_n = 2$ . According to our results, he discussed the catalytic activity in the region at which the cationic polymerization is still predominant.

It is evident from our results that the divalent  $\text{VCl}_2\text{-2LiCl}$  is sufficiently active in this region (see Table I). Another difference between Vandenberg's catalyst and ours is the mode of preparation of the vanadium component. In our catalyst the vanadium component was prepared by the

reduction of  $VCl_4$  with  $BuLi$ . It seems quite advantageous that our vanadium component contains  $LiCl$  which has no cationic character, while in Vandenberg's catalyst, the vanadium component coexists with aluminum compounds such as  $(i-Bu)_2AlCl$ ,  $(i-Bu)AlCl_2$ , and perhaps  $AlCl_3$ , all of which are sufficiently cationic in nature to induce cationic polymerization.

Shostakovskii and co-workers<sup>6,7</sup> has reported the stereoregular polymerization of vinyl ethers at room temperature by using similar catalysts composed of  $TiCl_4-LiC_3H_7-Al(i-Bu)_3$  (1:1.5:0.5), and  $VOCl_3-LiC_3H_7-Al(i-Bu)_3$  (1:1.5:3). The catalyst preparation and the polymerization procedure were quite similar to ours, namely, the catalyst was best prepared by reducing  $TiCl_4$  with  $LiC_3H_7$  followed by addition of  $Al(i-Bu)_3$ ; this procedure avoided the formation of  $R_2AlCl$ , which is advantageous for the stereospecific polymerization. Their polymerization conditions, however, seem to be in the cationic region, therefore, these are different from our polymerization conditions, that is,  $Al(i-Bu)_3/VCl_3 \cdot LiCl \geq 6$ . Figures 10 and 11 also show that remarkable change in the polymerization behavior at  $Al(i-Bu)_3/VCl_3 \cdot LiCl$  ratio of around 5. This again suggests that there is a change in the polymerization mechanism between lower and higher  $Al(i-Bu)_3/VCl_3 \cdot LiCl$  ratio of 5.

At  $Al(i-Bu)_3/VCl_3 \cdot LiCl$  ratios higher than 5, the catalytic activity depends substantially on the concentration of  $VCl_3 \cdot LiCl$ ; accordingly, the conversion increased approximately in proportion to the  $VCl_3 \cdot LiCl$  used.

It appears that there is something which should be noted in the change in viscosity of the polymer produced under the various polymerization conditions as shown in Figures 9 and 11, but the reason for this change is not clear at present.

The change in viscosity in Figure 9 might be explained by considering that the curve might be an overall result of a duplication of two lines (*a*) and (*b*). This is a reasonable explanation for this extraordinary viscosity behavior, since as we discussed, the change of mechanism of the polymerization might occur at an  $Al(i-Bu)_3/VCl_3 \cdot LiCl$  ratio of around 5. The decrease in viscosity with increasing  $Al(i-Bu)_3$  concentration might be due to chain transfer to  $Al(i-Bu)_3$ .

The change in the viscosity in Figure 11 also suggests that the change of mechanism of the polymerization might occur at  $Al(i-Bu)_3/VCl_3 \cdot LiCl$  ratio of around 5, since the slope of the curve changed at this point.

A great increase in viscosity at lower  $VCl_3 \cdot LiCl$  concentration might be the result of an influence of low effective catalyst concentration.

Interestingly, when styrene was polymerized by  $VCl_3 \cdot LiCl$  only amorphous polystyrene was obtained, probably by a cationic mechanism. It is therefore considered that in the stereospecific polymerization of vinyl ether by  $VCl_3 \cdot LiCl$  or  $VCl_2 \cdot 2LiCl$ , the coordination of the monomer to the catalyst might play an important role in the similar mechanism which Vandenberg proposed on his catalyst.<sup>5</sup>

However, the catalytic complexes in  $Al(i-Bu)_3-VCl_3 \cdot LiCl$  system which were completely formed at the  $Al(i-Bu)_3/VCl_3 \cdot LiCl$  ratio higher than 5 could polymerize styrene to a crystalline polymer with predominantly iso-



tactic structure. This indicates that the reaction mechanism by  $\text{VCl}_3 \cdot \text{LiCl}$  alone and  $\text{Al}(i\text{-Bu})_3\text{-VCl}_3 \cdot \text{LiCl}$  is quite different.

In the polymerization of isobutyl vinyl ether by the  $\text{VCl}_3 \cdot \text{LiCl-Al}(i\text{-Bu})_3$  system, one can consider that  $\text{Al}(i\text{-Bu})_3$  acts as a Lewis base to depress the catalytic activity of  $\text{VCl}_3 \cdot \text{LiCl}$  like the action of tetrahydrofuran with  $\text{VCl}_3 \cdot \text{LiCl}$ .  $\text{VCl}_3 \cdot \text{LiCl-THF}$  complex<sup>16</sup> is indeed an effective catalyst in the stereospecific polymerization of isobutyl vinyl ether, the mechanism of which is surely cationic.

However, as shown in Table II,  $\text{VCl}_3 \cdot \text{LiCl-THF}$  could not produce crystalline polystyrene, in spite of the much lower activity of the catalyst than  $\text{VCl}_3 \cdot \text{LiCl-Al}(i\text{-Bu})_3$  complex. From this fact, it is considered that  $\text{VCl}_3 \cdot \text{LiCl-Al}(i\text{-Bu})_3$  (1:6) must form a new type of complex catalyst in which  $\text{Al}(i\text{-Bu})_3$  does not merely act as a Lewis base to depress the catalytic activity but acts as a complexing agent to form another type of the catalytic complex, probably a coordinated anionic polymerization catalyst.

In the  $\text{Al}(i\text{-Bu})_3\text{-VCl}_3 \cdot \text{LiCl}$  catalyst system at  $\text{Al}(i\text{-Bu})_3/\text{VCl}_3 \cdot \text{LiCl}$  ratios higher than 6, the presence of the catalytic sites of so-called coordinated anionic polymerization is undeniable. However, we could not make clear in this investigation whether the polymerization of isobutyl vinyl ether proceeds by the same mechanism as the polymerization of styrene; however, a coordinated anionic polymerization mechanism is strongly suggested.

### References

1. C. E. Schildknecht and S. T. Gross, *Ind. Eng. Chem.*, **41**, 1998 (1949).
2. C. E. Schildknecht and P. H. Dunn, *J. Polym. Sci.*, **20**, 597 (1956).
3. G. Natta, P. Pino, and G. Mazzanti, *Chim. Ind. (Milan)*, **37**, 927 (1955).
4. G. Natta, I. Bassi, and P. Corradini, *Makromol. Chem.*, **18/19**, 455 (1956).
5. E. J. Vandenberg, in *First Biannual American Chemical Society Polymer Symposium (J. Polym. Sci. C, 1)*, H. W. Starkweather, Jr., Ed., Interscience, New York, 1963, p. 207.
6. M. F. Shostakovskii, A. V. Bogdanova, A. V. Golvin, and S. Shamakhmudova, *Izv. Akad. Nauk SSSR, Otd. Khim. Nauk*, **1962**, 1813.
7. M. F. Shostakovskii, A. V. Bogdanova, and S. Shamakhmudova, *Izv. Akad. Nauk SSSR, Otd. Khim. Nauk*, **1964**, 363.
8. S. Murahashi, H. Yuki, and Y. Joh, paper presented at Polymer Symposium, Tokyo, Japan, 1961; *Preprints*, p. 233.
9. S. Murahashi, H. Yuki, and Y. Joh, *Sen-i Kagaku Kenkyusho Nenpo, Osaka Univ.*, **15**, 145 (1962).
10. S. Murahashi, H. Yuki, and Y. Joh, *Sen-i Kagaku Kenkyusho Nenpo, Osaka Univ.*, **15**, 147 (1962).
11. C. E. Schildknecht, A. O. Zoss, and A. Makinley, *Ind. Eng. Chem.*, **39**, 180 (1947).
12. K. Ziegler and H. G. Gellart, *Ann.*, **567**, 179 (1950).
13. H. Gilman and A. H. Hanbein, *J. Am. Chem. Soc.*, **66**, 1515 (1944).
14. G. Natta, G. Mazzanti, D. E. Luca, U. Ginnini, and F. Bandini, *Makromol. Chem.*, **76**, 54 (1964).
15. G. Bier, A. Gumboldt, and G. Schleitzer, *Makromol. Chem.*, **58**, 43 (1962).
16. Y. Joh, K. Harada, H. Yuki, and S. Murahashi, *J. Polym. Sci.*, in press.

Received October 28, 1969

Revised March 23, 1970

## Salt-Catalyzed Reaction between Styrene Oxide and Silk Fibroin

HIDEKI SHIOZAKI\* and YOSHIO TANAKA, *Research Institute for Polymers and Textiles, Kanagawa, Yokohama, Japan*

### Synopsis

The addition reaction of styrene oxide (StO) with silk fibroin was studied in the presence of various salts in different solvents at 45–75°C. Some water was required to make StO react with silk padded with various salt solutions. The reaction rate increased with the salt concentration and reached a maximum value at a certain concentration of the salt. Padding with solutions of thiosulfate, cyanide, thiocyanate, bicarbonate, or carbonate resulted in high add-ons (to 65 mole, 10<sup>5</sup> g) and low solubilities in HCl and NaOH aqueous solutions. The weight gains increased with the epoxide concentration and reached a constant value at a certain concentration of StO solution in ethanol, while they decreased slightly with epoxide concentration over 10% of StO solution in *n*-hexane. Histidine, lysine, arginine, tyrosine, and aspartic and glutamic acids were found to react. The reaction rate decreased with increasing solubility parameter of the solvent used, reached a minimum value about at 10 or at the solubility parameter of the epoxide, and then increased with the parameter. The StO–silk reaction may depend on the distribution of StO between aqueous salt and an organic solvent phases, and on the swelling of silk fiber in different aqueous salt solutions or in various organic solvents. The mechanism for this epoxide–silk reaction and the reactivity difference between StO and phenyl glycidyl ether toward silk fibroin are discussed in the light of the observed phenomena.

### INTRODUCTION

Although the literature contains some references to the epoxide–silk reaction in the presence of NaOH,<sup>1,2</sup> BF<sub>3</sub>,<sup>3a</sup> SnCl<sub>4</sub>,<sup>3b</sup> and tertiary amines such as diethylaminopropylamine,<sup>4</sup> it is not clear what kinds of amino acid residues of the silk fibroin react with an epoxide, and there is no information on the reaction between an epoxide and silk fibroin in the presence of a neutral or a weakly basic salt. Unlike the cellulose reaction, a strongly basic salt like sodium hydroxide should be an unsuitable catalyst for the reaction of the protein fibers such as silk and wool under any conditions, because the fibers become yellow and are degraded. An acidic salt or Lewis acid like SnCl<sub>4</sub> and BF<sub>3</sub> may also not be suitable, since the epoxide–protein fiber reaction occurs only at high temperature, resulting in degradation of the fiber. On the other hand, the tertiary amine gives no

\* Present address: Industrial Research Institute of Kanagawa, 3173 Tomioka, Kanazawa, Yokohama, Japan.

degenerative effect on the fibroin but has been found to be ineffective for the epoxide-silk reaction.<sup>4</sup>

Phenyl glycidyl ether was found, previously, to react with ease with the silk fibroin in the presence of the salt,<sup>5</sup> and the mechanism for the epoxide-silk reaction has been discussed in the light of the observed phenomena.<sup>6</sup> The present paper reports the silk fibroin reaction with styrene oxide, for which the polar and steric factors are different from those of phenyl glycidyl ether, and discusses the reactivity difference between styrene oxide and phenyl glycidyl ether in the epoxide-silk reaction.

## EXPERIMENTAL

### Materials

Reagent grade styrene oxide (StO) was used after distillation under reduced pressure. All other chemicals were of reagent grade and were used without further purification. Degummed and bleached Habutae silk (ca. 1 g/10 cm<sup>2</sup>) was treated with a 0.3% aqueous solution of Marseilles soap, hot water, and with a 0.1% aqueous solution of Na<sub>2</sub>CO<sub>3</sub> at 50–60°C, neutralized with diluted acetic acid solution, and then washed with hot and cold distilled water completely. Purified 9 cm × 9 cm silk fabric was used throughout.

### Reaction Procedure

A 0.8 g swatch was padded with the desired aqueous salt solution to an approximate 100% wet pickup through the roll mangle. The loosely rolled swatch was then dropped into a graduated glass tube containing 15 ml of a StO solution in various solvents such as carbon tetrachloride, *n*-hexane, and ethanol; this was attached to a reflux condenser, held in a thermostatically controlled bath at the desired temperature, and occasionally shaken during the reaction time.

At the end of the reaction, the swatches were washed with the solvent used, extracted with boiling acetone for 30 min, and washed successively with methanol, tap water, and finally distilled water. The epoxide and its oligomer produced in the fabric are quickly replaced by hot acetone, and could be recovered. The washed and air-dried swatches were dried in a forced draft oven at 100–105°C, placed in a desiccator over silica gel for 30 min, and weighed. Before tests were made, the samples were equilibrated for 24 hr.

### Test Methods

The dried silk fabrics (ca. 200 mg) untreated and treated with epoxide were completely hydrolyzed by heating for 6 hr at 100°C in 30 ml of 6*N* HCl aqueous solution.<sup>6</sup> The amino acid contents were determined with the buffered solution (pH, 2.2) of the hydrolyzates (0.2 mg/0.1 ml) by using a Sibata AA-600 Type Rapid Amino Acid Analyzer (column filled with

Aminex resin), a modified Stein-Moore apparatus.<sup>7</sup> Since the contents of proline, leucine, isoleucine and methionine are low in silk fibroin and were not important in our investigation,<sup>6</sup> these amino acids were not determined accurately. Basic amino acids like histidine, lysine, and arginine were determined with 10-fold concentrated solution of the hydrolyzates (2 mg/0.1 ml); tryptophan was not determined in the present study.

The add-ons of StO on the silk fabrics were calculated from the oven-dried weights of the samples before and after the treatments, a correction being made for the weight loss on treatment with the catalyst alone.

### RESULTS AND DISCUSSION

The effect of reaction time was investigated; results are shown in Figure 1. The reaction between silk fibroin and StO (1.7*M*) was carried out at 75–76°C with the use of 1*N* Na<sub>2</sub>S<sub>2</sub>O<sub>3</sub> aqueous solution in carbon tetrachloride or ethanol. The add-ons under these conditions varied with time and reached about 50 mole/10<sup>5</sup> g for 6 hr in ethanol or 20 hr in carbon tetrachloride.

Figure 2 illustrates the variations of the reacted StO on the silk fibroin at various concentrations (10–100%) of StO, where *n*-hexane, ethanol, and tetrahydrofuran were used as solvents and the initial concentration of Na<sub>2</sub>S<sub>2</sub>O<sub>3</sub> was kept constant at 1*N*. The add-ons of StO on silk varied markedly with the epoxide concentration and the kinds of solvents used.

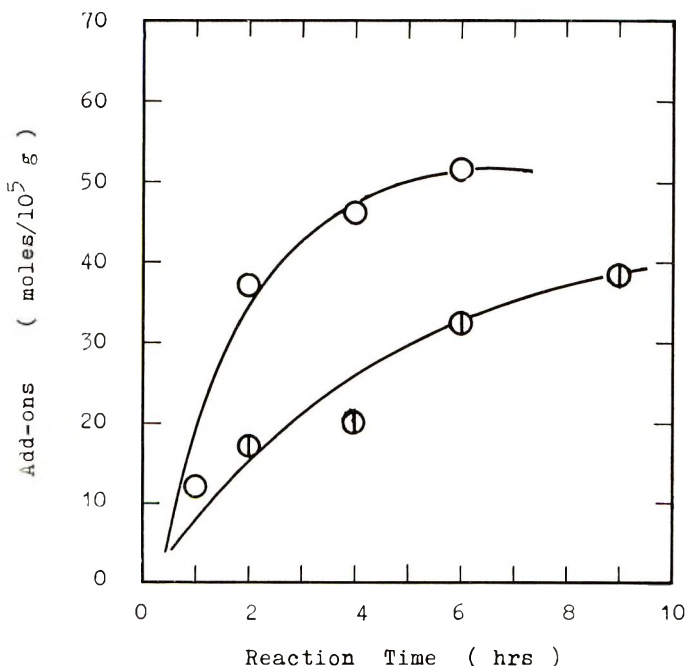


Fig. 1. Effect of reaction time on the add-on of StO at 75°C: (○) in ethanol; (⊙) in CCl<sub>4</sub>. Add-on of 47.3M/10<sup>5</sup>g was obtained with reaction for 20 hr in CCl<sub>4</sub>.

Treatment with 10% StO solution in *n*-hexane gave the highest rate of add-on, and the add-ons decreased with the epoxide concentration. With solution in ethanol, the add-ons increased markedly with increasing concentration of StO up to 20% and then reached an equilibrium. No reaction occurred at 20% or less concentration of StO in tetrahydrofuran, and use of 40% or more concentration of the epoxide resulted in an increase in rate of add-ons with concentration of the epoxide. The suitable concentration of the epoxide seems to be dependent on the characteristics of the solvents and the reaction temperature.

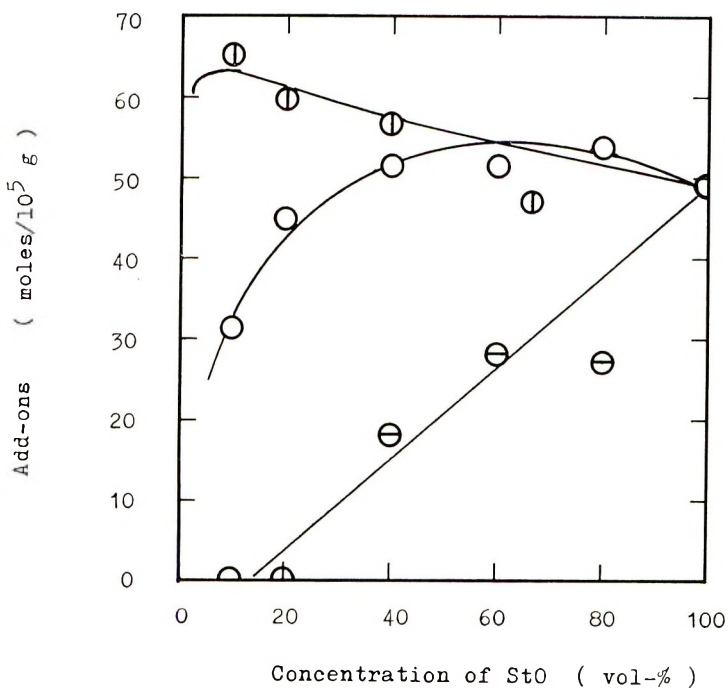


Fig. 2. Effect of concentration of StO on the add-on of StO at 75°C: (○) in ethanol; (⊖) in tetrahydrofuran; (⊕) at 69°C in *n*-hexane. 1*N* Na<sub>2</sub>S<sub>2</sub>O<sub>3</sub> was used as a catalyst.

Water may play an important part in the silk-epoxide reaction as shown in Figure 3. Silk fibroin was treated with 1*N* Na<sub>2</sub>S<sub>2</sub>O<sub>3</sub> aqueous solution to 100% wet pickup, dried in air oven or sprayed with water to 0-200% of water, and then treated in 1.7*M* StO solution in *n*-hexane at 69-70°C for 6 hr. The extraction of water after pretreatments with dilute Na<sub>2</sub>S<sub>2</sub>O<sub>3</sub> before application of StO solution failed to produce the desired weight gains. Similar application of the epoxide solution to the silk swatch with 70-80% of water resulted in the highest add-ons after a reaction time of 6 hr. It is also of interest to note that pretreatment of fibroin with excess water before immersion in the epoxide solution in *n*-hexane under the same reaction condition resulted in decreased add-ons.

The effect of the salt concentration on the reaction is shown in Figure 4. The silk swatch was padded with different concentrations of  $\text{Na}_2\text{S}_2\text{O}_3$  in aqueous solution from 0.25 to 2.0*N* to an approximate 100% wet pickup, and then treated with 1.7*M* StO solution in *n*-hexane at 69–70°C or in ethanol at 75–76°C for 6 hr. Use of concentrations of  $\text{Na}_2\text{S}_2\text{O}_3$  as low as 0.5*N* resulted in much smaller add-ons in above both solutions. As might be expected, increasing salt concentration resulted in increasing add-ons of StO; and the maximum add-ons were reached at about a concentration of 1*N* in the case of ethanol as a solvent and of 1.5*N*, when *n*-hexane was used as a solvent.

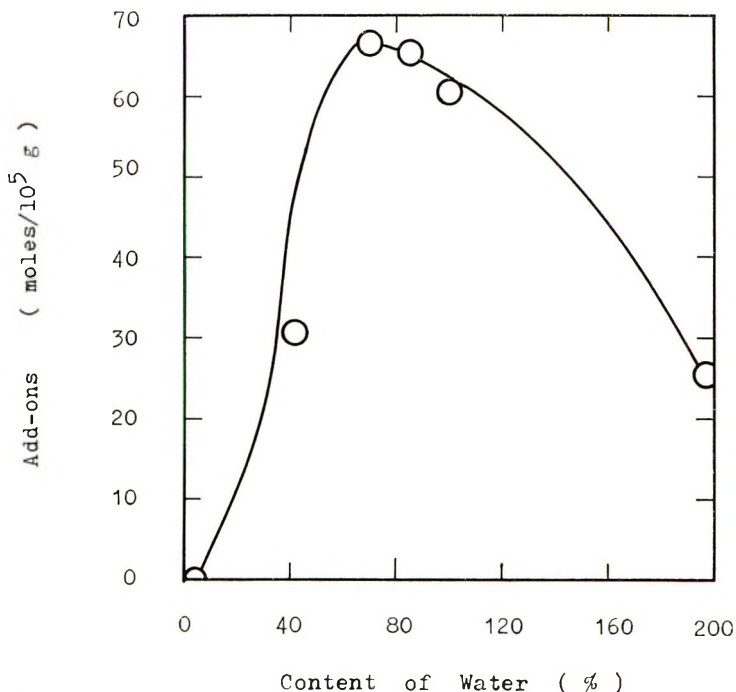


Fig. 3. Effect of water in silk fibroin on the add-on of StO at 69°C. 1*N*  $\text{Na}_2\text{S}_2\text{O}_3$  and *n*-hexane were used as catalyst and solvent, respectively, with the reaction time of 6 hr.

Previous work<sup>6</sup> and experiments presently under way have shown that the reaction may proceed in an aqueous phase containing salt, epoxide, and an organic solvent dissolved in water. The reaction in these cases, of course, is considered to be heterogeneous, because of the existence of the fabrics. Epoxide have been found to react with various carboxylic acids, phenols, alcohols, and amines in various organic solutions,<sup>8</sup> but in this case, the reaction in the organic phase can be negligible as the reaction rate decreases and approaches zero as the water is removed completely (Fig. 3). The add-ons obtained with various alcohols as solvents may suggest that the reaction at the interface of the aqueous and organic phases is negligibly small (Table I).

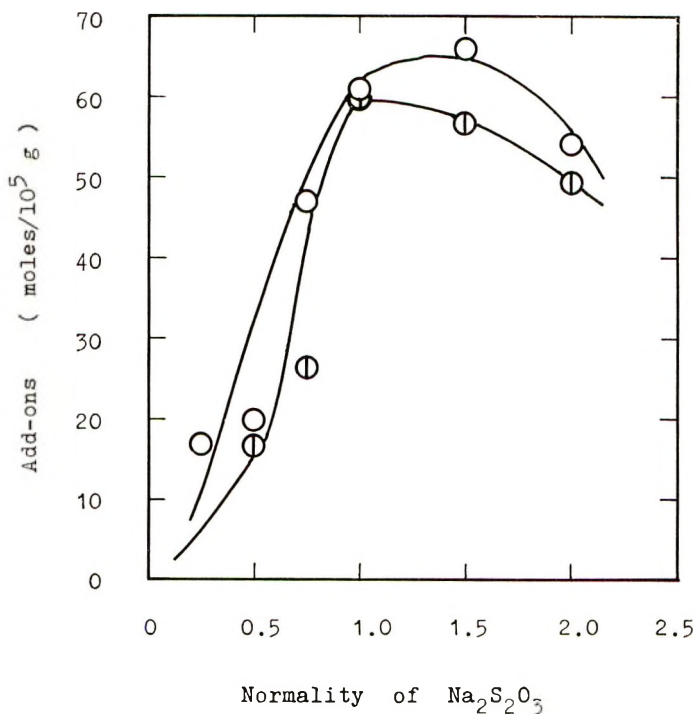


Fig. 4. Effect of concentration of  $\text{Na}_2\text{S}_2\text{O}_3$  on the add-on of StO: (O) at 75°C in ethanol; (⊖) at 69°C in *n*-hexane.

That the reaction under consideration is ionic and catalytic is easily shown by the facts that low add-ons were obtained in the reaction between the epoxide and silk fibroin without a salt, and that when water was extracted from the system, the reaction rate decreased and approached zero as the water was removed completely. However, it is not clear why the amount of epoxide add-on is dependent on the salt content of the fibroin, and why the add-ons reach a maximum value at a certain concentration of the salt. The simplest explanation of the phenomenon is that maximum add-on occurs in the region of maximum salt swelling of the silk. Hence, more surface is presented to the entering epoxide in the heterogeneous reaction.

The effect of solvents was found to be most marked in this salt-catalyzed silk reaction with epoxide. Table I shows the add-ons obtained by treating the fabrics, which were padded with 1*N*  $\text{Na}_2\text{S}_2\text{O}_3$  solution, with 1.7*M* StO solutions in various solvents for 6 hr at 75–76°C or at the boiling points of the solvents used. *n*-Hexane, cyclohexane, toluene, methyl ethyl ketone, *n*-butanol, ethanol, isopropanol, isoamyl alcohol, *n*-hexyl alcohol, and *n*-octyl alcohol were found to be better for this reaction, resulting in add-ons of 50–60 mole/ $10^5$  g. Carbon tetrachloride, ethyl acetate, dioxane, cyclohexanone, *tert*-butyl alcohol, and methanol gave smaller add-ons of 30–35

TABLE I  
Effect of Solvent on Reaction of Styrene Oxide with Silk Fibroin<sup>a</sup>

Solvent	Solubility parameter <sup>b</sup>	Dielectric constant <sup>c</sup>	Add-on mole/10 <sup>5</sup> g
<i>n</i> -Hexane <sup>d</sup>	7.3	1.89	59.5
Cyclohexane	8.2	2.05	49.4
Carbon tetrachloride	8.6	2.21	32.3
Toluene	8.9	2.24	61.3
Ethyl acetate	9.1	6.02	32.8
Tetrahydrofuran	9.1	7.0	0
Methyl ethyl ketone	9.3	15.45	54.5
Cyclohexanone	9.9	18.3	32.9
Dioxane	10.0	2.21	35.1
Isoamyl alcohol	10.0	15.3	54.5
<i>n</i> -Octyl alcohol	10.3	10.34	55.3
<i>tert</i> -Butanol	10.6	11.4	34.3
<i>N,N</i> -dimethylformamide	12.1	37.0	26.9
<i>n</i> -Hexyl alcohol	10.7	13.3	58.4
Cyclohexanol	11.4	15.0	3.25
<i>n</i> -Butanol	11.4	17.1	55.9
Isopropanol	11.5	18.6	52.7
Benzyl alcohol	12.1	13.0	17.3
Ethanol	12.7	25.7	60.8
Methanol <sup>e</sup>	14.5	31.2	31.8

<sup>a</sup> The swatch was padded with 1*N* Na<sub>2</sub>S<sub>2</sub>O<sub>3</sub> aqueous solution to an approximate 100% wet pickup and then made to react with a solution of StO (3 cc) in various solvents (12 cc) at 75–76°C for 6 hr.

<sup>b</sup> See ref. 9.

<sup>c</sup> See ref. 10.

<sup>d</sup> The swatch was reacted at 69–70°C for 6 hr.

<sup>e</sup> Reaction at 64–65°C.

mole/10<sup>5</sup> g. In cyclohexanol and tetrahydrofuran, no reaction of StO with silk fibroin occurred in the presence of the thiosulfate.

The dielectric constant of the solvent does not appear to give a clue to the reaction mechanism, unlike the case of homogeneous reaction of the epoxide in various solutions.<sup>8</sup> When the add-ons were plotted against the solubility parameters<sup>9</sup>  $\delta$  of solvents, a similar relationship was observed, as in the case of phenyl glycidyl ether (PGE),<sup>6</sup> although the dispersion in this relationship was larger in StO than in the PGE reaction reported previously.<sup>6</sup> The dispersion may suggest that the add-ons or the reaction rates cannot be interpreted by the solubility parameter only, but by another factor. This relationship can be estimated as follows, as in the cellulose-epoxide reaction. The concentration of the epoxide in the aqueous phase may have a minimum value in the case of a solvent whose solubility parameter is similar to that of the epoxide. Therefore, the reaction rate should reach a minimum value in such solvent, if it is the epoxide in the aqueous phase which reacts with silk fibroin and if the reaction rate depends on the concentration of epoxide. The swelling of the silk fibroin



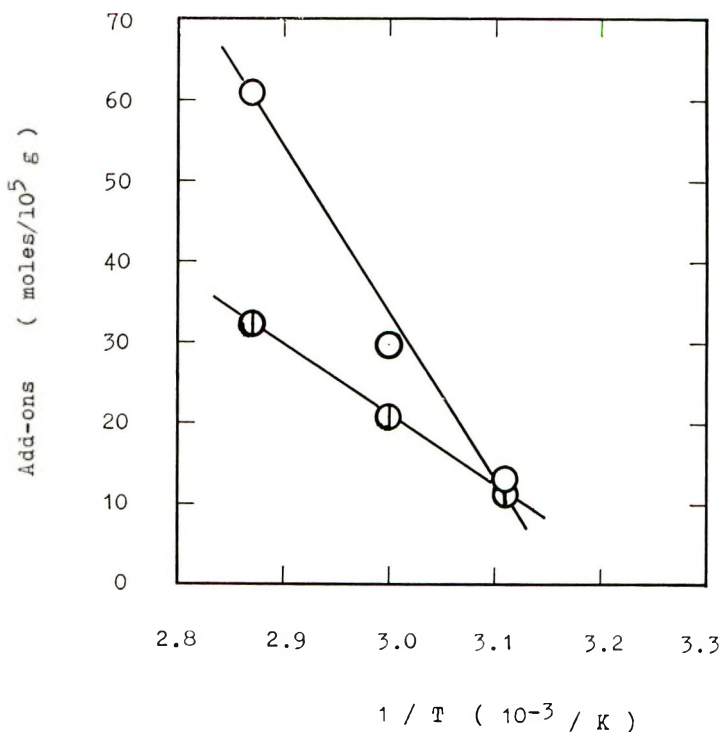
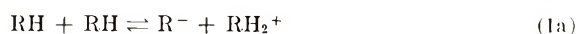


Fig. 5. Effect of temperature on the add-ons of StO: (O) in ethanol; (⊖) in CCl<sub>4</sub>. Na<sub>2</sub>S<sub>2</sub>O<sub>3</sub> was used as a catalyst.

may have a maximum value in the solvents whose solubility parameters are similar to that of silk. Hence, more surface is presented to the entering epoxide in the heterogeneous reaction, and the maximum add-on or the maximum reaction rate occurs in the region of maximum swelling of the silk.

In order to determine the effect of reaction temperature on StO add-ons, silk fibroin padded with 1*N* Na<sub>2</sub>S<sub>2</sub>O<sub>3</sub> solution was treated with 1.7*M* StO solution in ethanol or in carbon tetrachloride. The result is shown in Figure 5. Almost the same add-on was obtained in both solvents at 45°C, but the rates of the add-ons were found to be higher in ethanol than in carbon tetrachloride at temperatures above 45°C. Stirring favors diffusion, but the temperature effect shown in the figure is conclusive in demonstrating that the reaction rate is governed by activated collisions with the surface and not by diffusion.

Proteins are generally assumed to be multivalent zwitterions [see eq. (1a)] containing a large number of positively and negatively charged



groups at their isoelectric point,<sup>11</sup> which depends on the number of ionized groups and on their ionization constants. Here RH is a proton-supplying

TABLE II  
Amino Acid Contents of Silk Fibroins Treated with Styrene Oxide

Catalyst soln <sup>a</sup>	Solvent <sup>b</sup>	Add-on, mole/ 10 <sup>5</sup> g	Amino acid contents, mole/10 <sup>5</sup> g											
			Gly- cine	Ala- mine	Ser- ine	Tyro- sine	Aspar- tic acid	Glu- tamic acid	Va- line	Phenyl- ala- mine	Argi- nine	Ly- sine	Histi- dine	Threo- nine
	Untreated	0	566	365	139	63.1	18.4	13.6	23.0	6.64	4.87	2.32	1.63	13.5
1 <i>N</i> Na <sub>2</sub> S <sub>2</sub> O <sub>4</sub>	EtOH	11.9	565	366	138	63.6	20.9	14.9	22.0	6.70	4.53	1.75	1.34	13.3
"	"	13.3	565	362	137	62.0	20.0	14.4	21.9	6.65	4.41	1.41	1.54	13.6
"	"	29.6	566	360	135	60.5	20.1	14.5	21.6	6.64	4.45	1.21	0.96	13.1
"	"	37.0	566	364	136	60.0	19.8	14.0	21.5	6.41	3.98	1.06	0.88	13.8
"	"	60.8	562	363	135	56.7	18.9	13.9	20.1	6.30	2.47	0.61	0.21	13.5
1.5 <i>N</i> Na <sub>2</sub> S <sub>2</sub> O <sub>4</sub>	<i>n</i> -Hexane	57.6	570	370	131	57.1	16.4	12.6	20.0	6.65	0.67	2.44	0.20	11.7
2 <i>N</i> Na <sub>2</sub> S <sub>2</sub> O <sub>4</sub>	<i>n</i> -Hexane	53.8	572	376	127	52.8	15.0	12.0	19.1	6.76	—	—	—	11.3
"	EtOH	53.8	575	373	129	53.1	17.4	13.5	19.4	6.66	1.27	0.43	Trace	10.0
1 <i>N</i> Na <sub>2</sub> SCN	<i>n</i> -Hexane	37.3	569	363	136	59.1	20.1	14.3	21.7	6.69	4.21	1.07	0.24	13.0
1 <i>N</i> Na <sub>2</sub> CO <sub>3</sub>	<i>n</i> -Hexane	55.8	558	365	135	62.5	19.2	14.1	22.9	6.70	4.57	0.77	0.40	13.9

<sup>a</sup> Aqueous catalyst solution for padding.

<sup>b</sup> Solvent used in treating with styrene oxide.

group, such as COOH, OH, NH, or NH<sub>2</sub> of an amino acid residue. The carboxylic groups may derive from aspartic and glutamic acids, the phenolic hydroxyl groups from tyrosine, the NH groups from histidine, the NH<sub>2</sub> groups from arginine and lysine, and the alcoholic hydroxyl groups from serine and threonine. These acidic and basic groups, however, are easily found to be 99–100% ionized<sup>12</sup> under these experimental conditions, while the phenolic and alcoholic hydroxyl groups are evidently very weak acids and practically unchanged in neutral solutions.

Serine, tyrosine, aspartic and glutamic acids, threonine, arginine, lysine, histidine, tryptophan, and the endgroups of the amino acid residues can be expected to be reactive sites for an epoxide. The silk fibroin treated and untreated with StO was hydrolyzed with 6*N* HCl solution to determine the amino acid contents. As shown in Table II, the alcoholic hydroxyl groups may be inactive to the epoxide under these conditions, because no or a little change was observed in contents of serine and threonine. The reaction rate of StO with the phenolic hydroxyl groups of tyrosine was found to be very low, while the reaction with the amino groups from arginine, lysine, and histidine proceeded rapidly. Tryptophan could not be analyzed because of its decomposition under the acidic hydrolysis. The acidic groups from aspartic and glutamic acids should react with StO to produce esters, which could be hydrolyzed easily under acidic conditions to give the original carboxylic groups. In consequence, the reaction of StO with these carboxylic groups can not be estimated. However, ethylene and propylene oxides have been found to react with egg albumin to give esters under similar condition,<sup>13</sup> and the reaction rate of StO with acetic acid has been observed to be higher than that of propylene oxide.<sup>8</sup> Thus, the reactivity of StO to the carboxylic groups from aspartic and glutamic acids seems to be quite high.

Padding with more concentrated salt solutions (1.5 or 2.0*N* Na<sub>2</sub>S<sub>2</sub>O<sub>3</sub> aqueous solution) resulted in more decreases of aspartic and glutamic acids, valine and threonine of the silk fibroin treated with StO (see Table II). These decreases in contents of some amino acids may come from a partial dissolution of the fibroin by a catalytic action of a base produced from the reaction of the epoxide with the salt as shown in eq. (2):



where X<sup>-</sup> is an ion from the salt. The addition reaction of the ion to the epoxide has been studied by many workers<sup>15</sup> and is used for determination of the epoxide. Consequently, the reaction curves shown in Figure 4 can be partly explained by the partial dissolution of the protein fiber mentioned above.

A number of salts in aqueous solutions at constant concentration of 1*N* were used as pretreatments to catalyze the silk–StO reactions in *n*-hexane at 69–70°C. Salts such as thiosulfate, thiocyanate, cyanide, carbonate, and bicarbonate could be classed as good catalysts in this reaction, and ones

TABLE III  
Effect of Salt on Reaction of Styrene Oxide with Silk Fibroin<sup>a</sup>

No.	Salt	$E_N$ of anion <sup>b</sup>	Add-on, moles/10 <sup>5</sup> g
1	NaNO <sub>3</sub>	0.29	20.6
2	Na <sub>2</sub> SO <sub>4</sub>	0.59	21.3
3	NaOCOCH <sub>3</sub>	0.95	22.1
4	Na <sub>2</sub> CO <sub>3</sub>	—	55.8
5	NaHCO <sub>3</sub>	—	48.3
6	NaCl	1.24	10.8
7	KCl	1.24	17.7
8	LiCl	1.24	22.4
9	NH <sub>4</sub> Cl	1.24	10.5
10	KBr	1.51	4.61
11	LiBr	1.51	28.3
12	NaSCN	1.83	37.3
13	KSCN	1.83	37.8
14	Ca(SCN) <sub>2</sub>	1.83	39.8
15	KOCN	—	27.1
16	NaI	2.06	13.1
17	KI	2.06	25.9
18	CaI <sub>2</sub>	2.06	18.2
19	Na <sub>2</sub> S <sub>2</sub> O <sub>3</sub>	2.52	59.5
20	KCN	2.79	62.1

<sup>a</sup> The swatch was padded with 1*N* aqueous salt solution to an approximate 100% wet pickup and then reacted with a solution of StO (3 cc) in *n*-hexane (12 cc) at 69–70°C for 6 hr.

<sup>b</sup> See ref. 20.

like LiCl, LiBr, KI, Na<sub>2</sub>SO<sub>4</sub>, NaNO<sub>3</sub>, KOCN, and NaOCOCH<sub>3</sub> caused lower add-ons, as shown in Table III. The salt effects on this reaction are associated with the cations in the following order of efficiency, although the difference in ions is small except ammonium ion:  $Ca^{++} \geq Li^+ \geq K^+ > Na^+ > NH_4^+$ . The anions of the added salts caused enhanced add-ons of the silk treated with StO in the following order of efficiency:  $CN^- > S_2O_3^{--} > CO_3^{--} > HCO_3^- > SCN^- > CH_3CO_2^-$ ,  $SO_4^{--}$ ,  $NO_3^- \geq I^-$ ,  $Br^-$ ,  $Cl^-$ .

The effect order of the cations is similar to the Hofmeister or the lyotropic series,<sup>16</sup> and can be elucidated partly by the hydration ability of the cations.<sup>17</sup> The salt effect on the swelling of the silk fiber must be associated with the cations in the order:  $K^+ > Na^+ > Li^+ > H^+ \text{ m } Ca^{++}$ . The add-ons, therefore, can be elucidated by the swelling of the silk fibroin.

The effect of anions on this reaction can be described partly by the hydration ability of the anions, and more extensively by the reactivity of these anions in nucleophilic substitution reactions such as the Swain-Scott parameters<sup>18</sup>  $n$ , or the Edwards parameter<sup>19</sup>  $E_N$ . Figure 6 shows a typical relationship between add-ons and the Edwards' nucleophilic parameters  $E_N$ , obtained as described in a recent review.<sup>20</sup> The lower efficacy of  $I^-$  with a significant higher nucleophilicity ( $E_N = 2.05$ ) is probably due to its

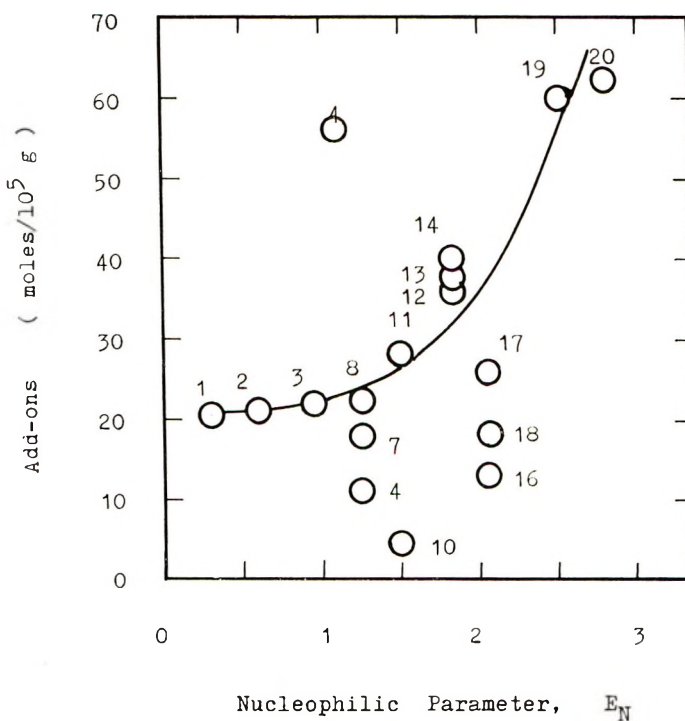
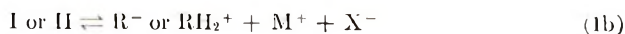
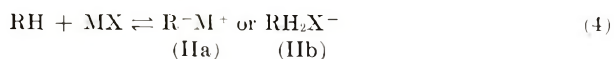
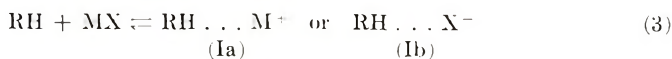


Fig. 6. Effect of the anions in the padding solutions on the add-ons of  $\text{SiO}$ . See also Table III.

lower  $H_N$  value of  $-9.00$ ,  $H_N$  being another parameter of Edwards which is a measure of the basicity of the nucleophile.<sup>19</sup> On the other hand, the considerably higher effect of  $\text{CO}_3^-$  with a lower nucleophilicity ( $E_N \geq 1.10$ ) can be described by its higher basicity. The use of  $\text{S}_2\text{O}_3^{--}$  and  $\text{CN}^-$  resulted in exceedingly high add-ons, and these high efficiencies can be explained by both high basicity ( $H_N = 3.60-10.88$ ) and high nucleophilicity ( $E_N = 2.52-2.79$ ). However, the  $H_N$  parameters of Edwards cannot elucidate the efficacy of the anions, and the dispersion in this relationship suggests that a higher order interaction term of the hydration ability, the nucleophilicity of the anions, or yet another factor plays a part in the epoxide-silk reaction catalyzed by the anions. Similar effects of added salts have been studied by Korchagin<sup>21</sup> on the hydrolyzing action of sodium hydroxide and of hydrochloric acid on the silk.

In the process of adsorbing counterions the ionized groups of the protein become neutralized,<sup>22</sup> as shown by eqs. (1), (3), and (4):



where MX is a salt, and RH is a proton-donating group as mentioned above. The electrochemical properties of the protein have been found to depend on the kind and concentration of the various ions present,<sup>23,24</sup> partly due to the secondary effect of the salt by the ionic strength of the solution as shown in the dissociation equilibrium of glycolic acid.<sup>25</sup> This secondary salt effect can describe one of the concentration effects of the salt, shown in Figure 4, because the concentration of active species such

as  $\overline{R'CHCH_2O} \dots H^+$  has been found to depend on the concentration of the proton.<sup>15</sup> Some solvents such as alcohol change the dissociation constants of the proton-supplying groups and shift the isoelectric point to lower or higher pH values, thus changing the reaction rate, as shown in Table I. As shown in the previous paper,<sup>6</sup> an interpretation of the effects of the water, salt, and solvent can be also gained from a consideration of the salting-in and the salting-out phenomena of a lyophilic sol.<sup>11,16</sup>

The existence of ion-pairs II or complexes I of silk fibroin with ions can be suggested from the fact that proteins combine readily not only with hydrogen ions, but also with other ions present on the solution.<sup>11</sup> The combination of proteins with the ions is attributable to electrostatic forces of the ionic groups. Anions are bound to positively charged  $NH_2^+$  or  $NH^+$  groups of the silk, while cations are attracted by the negatively charged  $CO_2^-$  groups. The linkages which they form depend chiefly on their valence and are so stable that the ions are removed neither by dialysis or by electrophoresis, although it may be possible to remove them by electrodiagnosis.<sup>11</sup> Hence, the active species in this reaction may be ion-pairs such as IIa for the carboxylic group and IIb for the amino groups and complexes like I for hydroxyl groups.

In order to explain the available data, the following reaction sequence, suggested by us in the previous paper,<sup>6</sup> is proposed:



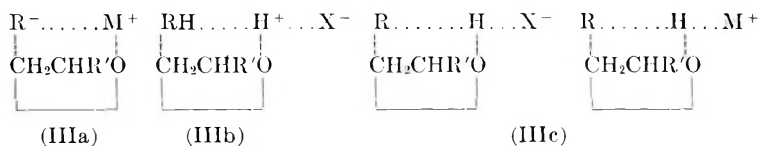
where,  $R'$  is  $C_6H_5$ , and  $R$  is  $R''CO_2$  in eq. (5),  $R''NH$  or  $R''N$  in eq. (6), and  $R''O$  in eq. (7),  $R''$  being any of the possible organic moieties of the proteins. In the reaction shown by eq. (5), protons may be supplied from the complexes I or the ion-pairs IIb, and possibly also from the water. Besides the above main processes, the following sequence may occur in some degree too:



where  $R$  is  $R''NH$  or  $R''N$ . In the reaction of eq. (7),  $RH$  is the phenolic hydroxyl group from tyrosine or the carboxyl group from aspartic and glutamic acids.

Since StO was virtually unreactive with the serine and threonine residues of the fibroin and reacted very slowly with tyrosine (see Table II), the reaction of the epoxide with the complexes I may occur under limited conditions. For example, treatment of the silk with an anion like  $S_2O_3^{--}$ ,  $SCN^-$ , or  $CN^-$  and with the use of a solvent such as ethanol, *n*-butanol, or *n*-hexane resulted in the StO reaction with the tyrosine residue at 75°C. In spite of the nucleophilic differences of various ions such as ammonium, carboxylate, hydroxide, phenolate, and inorganic ions, it is found<sup>15</sup> that all ring-opening reactions under basic or neutral conditions are essentially similar, involving the attack of a nucleophile on one of the epoxide carbon atoms. Since inorganic ions used as catalysts and phenolic hydroxyl groups, carboxylate, and ammonium ions are present in this reaction mixture, they enter into competitive reactions with the epoxide.

If the transition-state species or activated complex is of type IIIb or IIIc, the catalytic efficiency of the anions can be elucidated by their basicity which is a measure of the nucleophilic reactivity



towards protons, or by their nucleophilicity towards carbon atom. The basicity may play an important part for the transition-state species IIIb, while the nucleophilic reactivity towards carbon atom, such as the Swain-Scott parameters  $n$  and the Edwards parameter  $E_N$  must play a part for an activated complex such as IIIc,<sup>20</sup> because the steric constraint in IIIc should be greater than it is in the corresponding ion-pairs of type IIIb. In this epoxide-silk reaction, a transition-state species of type IIIc may play a more important role than IIIb, because the add-ons depend on the conversion of undissociated phenolic hydroxyl groups of tyrosine (see Table II); therefore, the add-ons can not be explained by the basicity, but by the nucleophilicity (Fig. 6). The dispersion in this relationship, however, may suggest the contribution of other factors such as the basicity and the electrochemical effects of the anions on the silk fibroin, as discussed above. The hydroxyl groups produced in reactions (5)–(8) seem to be unreactive to epoxides or less reactive than those of serine under these conditions.

The ring-opening reaction of the epoxide can be generally explained by the modified Taft equation:<sup>15</sup>

$$\log k - \log k_0 = \rho_p \sigma^* + \rho_s E_s \quad (9)$$

where  $k_0$  is the rate constant for the reaction of a given compound,  $k$  is the rate constant for the same reaction of one of its substituted derivatives,  $\sigma^*$  is the polar substituent constant characteristic of the substituent,  $E_s$  is the steric substituent constant,  $\rho_p$  is the polar reaction constant, and  $\rho_s$  is

the reaction constant as a measure of the susceptibility of the reaction to the steric effects of substituents. As a linear relationship has been observed between the polar substituent constant  $\sigma^*$  and the basicity of ethers,<sup>26</sup> the basicity or the nucleophilicity of the epoxides should increase in the order: PGE < StO. Thus, the reactivity towards nucleophilic species will decrease and that towards electrophilic reagents may increase as the basicity of the epoxide increases, i.e., as the  $\sigma^*$  value decreases. The  $\sigma^*$  values for StO and PGE are 0.620 and 0.850, respectively,  $\sigma^*$  for propylene oxide being 0. Therefore, the reactivity of StO towards the phenolic hydroxyl group can be considered to be higher than that of PGE.<sup>6</sup> This is not so in this reaction. The lower reactivity of StO may be explained by the larger steric effect ( $E_s = -0.90$ ) of the substituent than that ( $E_s = -0.33$ ) of PGE. Thus, the steric factor of the substituent of the epoxide seems to play a more important role in the salt-catalyzed reaction of the epoxide with the silk fibroin. A discussion involving other epoxides will be reported in near future.

The authors are grateful to Drs. R. Murase, M. Suzuki, G. Shirota, and A. Okada for their discussion and direction on this study, and wish to express thanks to Prof. Dr. H. Zahn for his interest on this investigation.

### References

1. T. Ikemura, *Sen-i Gakkaishi*, **24**, 531 (1968).
2. S. Imazu, I. Nishigori, and S. Ogawa, *Tokkyo Koho*, **38**, 25198 (1963).
3. M. Oku and A. Shimizu, *Kinu no Goseijushi Kako Sonota Shori no Kenkyu (Studies on Treatments of Silk with Synthetic Resins and Others)*, Department of Sericulture of Agriculture of Japanese Government, Tokyo, 1953, (a) p. 98 (b) p. 63.
4. M. Oku, H. Ishibashi, and Y. Matsudaira, *Jushikako*, **5**, 585 (1956).
5. H. Shiozaki and Y. Tanaka, *J. Polym. Sci. B*, **7**, 325 (1969).
6. Y. Tanaka and H. Shiozaki, *Makromol. Chem.*, **129**, 12 (1969).
7. Shibata Chemical App. Mfg. Co. Ltd., Catalogue No. 7506 (1967).
8. Y. Tanaka and H. Kakiuchi, *Yukigosei Kagaku Kyokaiishi*, **26**, 37 (1968).
9. J. Brandrup and E. H. Immergut, *Polymer Handbook*, Interscience, New York, 1966, p. IV-347.
10. *Yozai Pokketo-bukku (Pocket-book of Solvents)*, The Society of Synthetic Organic Chemistry, Japan, Ohmu Sha, 1967.
11. F. Haurowitz, *Chemistry and Biology of Proteins*, Academic Press, N. Y., Chapter 5, 1950.
12. A. Albert and E. P. Serjeant, *Ionization Constants of Acids and Bases*, Methuen, London, 1st ed., 1962, Chap. 7.
13. H. Fraenkel-Conrat, *J. Biol. Chem.*, **154**, 227 (1944); *Chem. Abstr.*, **38**, 5509 (1944).
14. H. Fraenkel-Conrat and H. S. Olcott, *J. Amer. Chem. Soc.*, **66**, 1420 (1944).
15. R. E. Parker and N. S. Isaacs, *Chem. Revs.*, **59**, 737 (1959).
16. S. Glasstone, *The Elements of Physical Chemistry*, 7th ed., Maruzene, Tokyo, 1954, Chap. 17.
17. J. P. Hunt, *Metal Ions in Aqueous Solution*, Benjamin, New York, 1963, p 16.
18. C. G. Swain and C. B. Scott, *J. Amer. Chem. Soc.*, **75**, 141 (1953).
19. J. O. Edwards, *J. Amer. Chem. Soc.*, **76**, 1540 (1954); *ibid.*, **78**, 1819 (1956).
20. J. E. Leffer and E. Grunwald, *Rates and Equilibria of Organic Reactions*, Wiley, New York, 1963, p. 243.



21. M. V. Korchagin, *Zh. Priklad. Khim.*, **25**, 212 (1952).
22. H. G. B. de Jong, *Kolloid-Beih.*, **48**, 33 (1938).
23. E. L. Smith, *J. Biol. Chem.*, **108**, 187 (1935).
24. B. D. Davis and E. J. Cohn, *J. Amer. Chem. Soc.*, **61**, 470 (1941).
25. H. M. Dawson and W. Lowson, *J. Chem. Soc.*, **135**, 1217 (1921).
26. Y. Tanaka, *J. Macromol. Sci. (Chem.)*, **A1**, 1059 (1967).

Received December 18, 1969

Revised March 11, 1970

## Polymerization of Monolayers of Vinyl and Divinyl Monomers

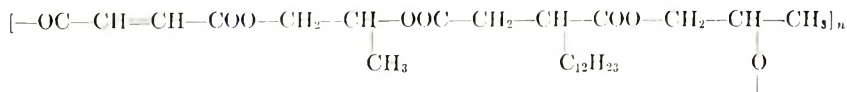
N. BEREDJICK\* and W. J. BURLANT, *Scientific Research Staff, Ford  
Motor Company, Dearborn, Michigan 48121*

### Synopsis

Monolayer balance techniques have been used to study "two-dimensional" polymerization of monomolecular films of octadecyl methacrylate and a divinyl ester. Polymerizations were initiated with ultraviolet radiation, and reaction rates and properties of the product evaluated from surface pressure-area isotherms. The polymerization rate of the acrylate in argon is linear up to 70% conversion; the product obtained in this way exhibits an isotherm which may reflect the packing and orientation of the starting monolayer. Rate data for the divinyl system—the product of which should be a sheet-like, two-dimensional analog of a network system—exhibit no unusual features.

Techniques to initiate monolayer polymerizations are described in the literature, although structural characteristics of these interesting systems have not been investigated: polymerization of vinyl isobutyl ether by gaseous boron trifluoride or benzoyl peroxide dissolved in the film;<sup>1</sup> oxidative polymerization of the adduct of  $\beta$ -eleostearin with maleic anhydride;<sup>2,3</sup> polycondensation of stearaldehyde deposited on dilute solutions of polyfunctional amines;<sup>4</sup> and polymerization of 4-vinylpyridine intercalated in clay;<sup>5</sup> and a variety of vinyl compounds adsorbed on clay.<sup>6,7</sup>

This paper describes surface pressure-area isotherms of starting materials and products for the ultraviolet-initiated polymerization of monolayers of two vinyl monomers: octadecyl methacrylate, and the divinyl ester derived from dodecanyl succinic anhydride, maleic anhydride, and propylene glycol.



This starting material was calculated on the basis of stoichiometric material balances and cryoscopic molecular weight determinations to have a double-bond concentration of 1.5/molecule and a number average molecular weight of 900. It should be noted that some of the double bonds are on side chains and their location is uncertain.

\* Present address: United Nations Industrial Development Organization (UNIDO), Box 20, Grand Central P. O., New York, New York 10017.

## EXPERIMENTAL

### Starting Materials

Commercially available octadecyl methacrylate was washed with 1% sodium hydroxide solution to remove inhibitor, dried over  $\text{CaCl}_2$ , and distilled twice *in vacuo* over copper powder; the fraction boiling at  $195.5^\circ$  (4.5 mm) used in these experiments.

ANAL. Calcd for octadecyl methacrylate,  $\text{C}_{22}\text{H}_{42}\text{O}$ : C, 78.1%; H, 12.4%. Found: C, 77.8%, H, 12.3%.

A degassed mixture of monomer (4.0 g) and azobis isobutyronitrile (0.030 g) in benzene (20 g) was polymerized at  $68^\circ\text{C}$  for 24 hr; polymer (II) was isolated by precipitation with methanol and purified by freeze drying from benzene. Its density was 0.964 g/ml; intrinsic viscosity, 0.15 dl/g in benzene, at  $30^\circ\text{C}$ .

ANAL. Calcd for poly(octadecyl methacrylate),  $(\text{C}_{22}\text{H}_{42}\text{O}_2)_n$ : C, 78.1%; H, 12.4%. Found: C, 78.2% H, 12.4%.

The ultraviolet absorption spectrum of this monomer exhibited a shoulder at  $3000 \text{ \AA}$  with gradual increase in absorption in the region of 2600 to  $3500 \text{ \AA}$ .

Divinyl monomer (I) was synthesized from reagent grade dodecenyl succinic anhydride, maleic anhydride, and propylene glycol.<sup>8</sup> Double bond concentration of 1.5/molecule of number average molecular weight of 900 was estimated from stoichiometric material balances and cryoscopic molecular weights in benzene. A broad absorption band is noted in the 2500–3500  $\text{ \AA}$  region. The monomer was freeze-dried before use.

Benzene, used for spreading the monolayer films, was distilled twice before use. Distilled water to fill the modified Langmuir trough was twice distilled from quartz and purged with argon for at least 24 hr; pH 6.7–6.9; specific resistance,  $1.8\text{--}2.0 \times 10^6$  ohms.

### Surface Pressure–Area Measurements

The modified Langmuir trough apparatus and manipulative techniques have been described.<sup>9–12</sup> The temperature was maintained at  $24 \pm 1^\circ\text{C}$ . The reproducibility of the measurements is estimated to be  $\pm 0.002$  dyne/cm.

The monolayer film—starting monomer or polymer—was deposited on water from dilute benzene solution, and confined between a heavy moveable barrier on one end and a float-torsion wire bridge on the other. After a waiting period of 15–20 min to permit solvent evaporation, the area was reduced in small decrements and from the corresponding angular deflection of a pointer connected to the bridge surface, pressures in dynes/centimeter were calculated. Measurements were made at intervals of 30 or 60 sec. The film was compressed until collapse—indicated by a constant or declining pressure—was noted.

The cross-sectional area, film thickness or the vertical dimension of the oriented molecule, collapse pressure, and compressibility can be obtained from a typical pressure area isotherm. Cross-sectional area is obtained by extrapolating to the  $x$  axis the slope from the steepest portion of the curve, near collapse, and is expressed as  $\text{m}^2/\text{mg}$  or  $\text{\AA}^2/\text{molecule}$  or  $\text{\AA}^2/\text{monomer unit}$ . Film volume is obtained by assuming that the tightly compressed monolayer has the same density as the bulk monomer or polymer. Thickness calculated from volume and cross-sectional area represents the vertical dimension of the oriented molecule. Collapse pressure is that pressure at which either a sudden decline or a leveling off is noted during compression; rigid or solidlike films undergo collapse abruptly, whereas mobile or liquidlike films reach a constant pressure plateau gradually. The change in surface area with pressure (compressibility of the film) is  $(a_0 - a_1)/(a_0 f_1)$ , where  $a_0$  is the cross-sectional area and  $a_1$  the smaller area at pressure  $f_1$ .

### Polymerization of Monomolecular Films

After a monolayer was deposited, the sealed cabinet was flushed with argon until the oxygen level had fallen to about  $0.10\% \pm 0.05\%$ , as measured with a Beckman Model 778 process oxygen analyzer. The monovinyl or divinyl monomer was compressed to a predetermined pressure, and polymerization was initiated by ultraviolet light from a Hanovia 5654A mercury-vapor lamp in an aluminum reflector 6 in. above the surface of the monolayer; this lamp emits radiation in the range (2500–3500  $\text{\AA}$ ) in which the monomers absorb.

From surface measurements of artificial mixtures of octadecyl methacrylate and its conventionally prepared polymer, the relation between surface area/monomer unit and monomer concentration was found to be linear (data from Table II below); consequently the extent of polymerization in the present study was monitored by the change in area, or pressure, with time. Reaction was considered complete when no pressure change occurred over a 10-min period.

## RESULTS AND DISCUSSION

Monolayer properties reflect the geometry of the system, its steric configuration, location of polar groups, and cohesive and adhesive properties.<sup>13</sup> From studies of mixtures, information is obtainable about packing, compatibility, and coiling and folding of the components.<sup>14–18</sup>

### Octadecyl Methacrylate

The monomer exhibits a liquidlike surface pressure–area isotherm (Fig. 1, Table I): pressure rises gradually from about 1 dyne/cm at  $1.1 \text{ m}^2/\text{mg}$ . At about 11 dyne/cm pressure and  $0.46 \text{ m}^2/\text{mg}$  area, an inflection occurs to produce a slight change in slope. More intimate and tighter packing of the long chain hydrocarbon groups probably begins at this stage. Collapse takes place at 15–16 dyne/cm. The cross-sectional area of 47–49

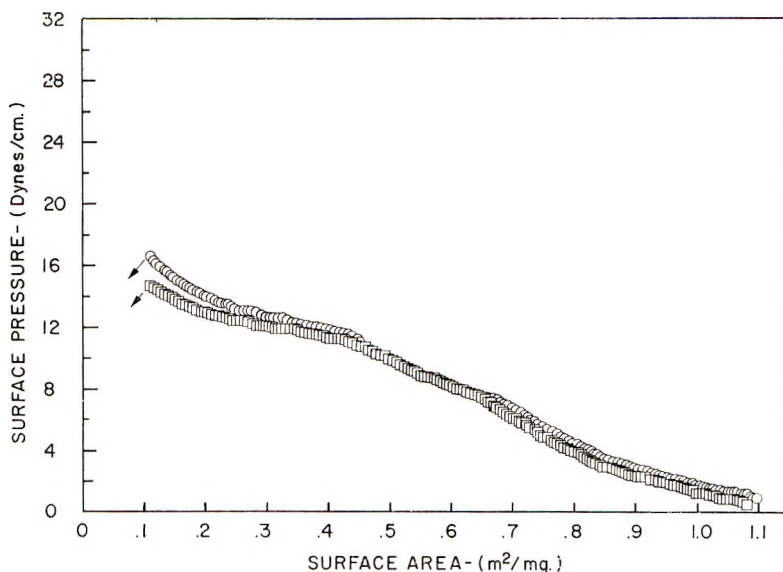


Fig. 1. Surface pressure-area isotherms for octadecyl methacrylate.

$\text{\AA}^2/\text{molecule}$  at extrapolated zero pressure suggests the increased spatial requirements of the methacryloxy group, compared with the straight-chain hydrocarbon alcohol group alone ( $22 \text{\AA}^2/\text{molecule}$ ). The value obtained for the film thickness ( $13\text{--}14 \text{\AA}$ ) is lower than expected and indicates that a portion of the hydrocarbon chain is in the water phase. The general contour of the isotherm is that of an expanded liquid film with fair compressibility ( $0.0586\text{--}0.0548 \text{ cm/dyne}$ ).

#### Poly(octadecyl Methacrylate) (Bulk-Polymerized)

This polymer affords an isotherm (Fig. 2) that is practically flat from  $1.08 \text{ m}^2/\text{mg}$  to  $0.62 \text{ m}^2/\text{mg}$ , where a point of inflection occurs; pressure rises steeply to about  $8 \text{ dyne/cm}$ , then more rapidly to about  $29 \text{ dyne/cm}$ ,

TABLE I  
Properties of Monolayer Mixtures of Octadecyl Methacrylate,  
Monomer and Polymer

Monomer concentration, %	Area at extrapolated zero pressure		Collapse pressure, dynes/cm	Compressibility, cm/dyne
	$\text{m}^2/\text{mg}$	$\text{\AA}^2/\text{molecule}$		
100	0.84-0.88	47-49	15-16	0.0586 0.0548
80	0.80	45	18	0.0446
60	0.69	39	22	0.0373
22	0.54	30	25	0.0217
0	0.50	28 <sup>a</sup>	29	0.0114

<sup>a</sup> Per monomer unit.

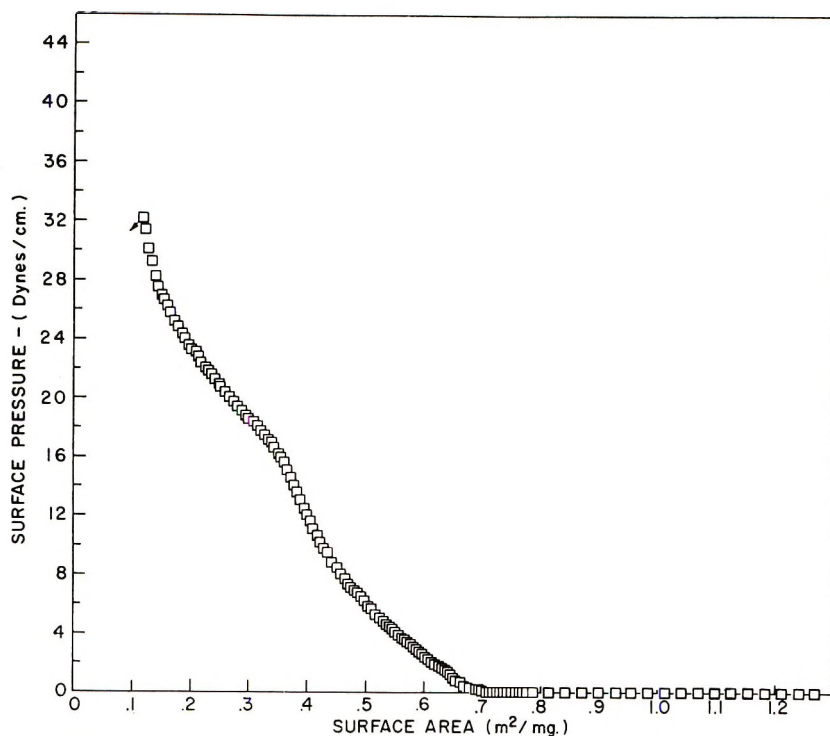


Fig. 2. Surface pressure-area isotherms for bulk-polymerized poly(octadecyl methacrylate).

when collapse is observed. The cross-sectional area of  $28 \text{ \AA}^2$ /monomer unit agrees with the reported value.<sup>19</sup> Higher collapse pressures, such as those reported previously, are obtained only for rapid compressions. The polymer film is significantly less compressible than that of the monomer, i.e.,  $0.0114$  compared to  $0.0548 \text{ cm}^2/\text{dyne}$ . Film thickness is about  $21 \text{ \AA}$ .

### Mixtures of Octadecyl Methacrylate and its Bulk Polymer

During polymerization of a monolayer, the experimental pressure observed is a function of the surface pressure of both monomer and polymer molecules. To gain some insight of these effects, a series of mixtures of monomer with increasing amount of the "bulk" polymer were prepared and the monolayer film characteristics determined over a range of surface areas (Fig. 3, Table I).

With the exception of the homopolymer, the isotherms have a common inflection point at about  $11 \text{ dyne/cm}$  pressure. For the present purpose, it is helpful to consider regions below and above that pressure: At areas greater than  $0.45 \text{ m}^2/\text{mg}$ , and below  $11 \text{ dyne/cm}$  pressure, a gradual transition is observed from a liquid-type film to a more condensed structure, with increasing polymer concentration. Thus, surface pressure is noted

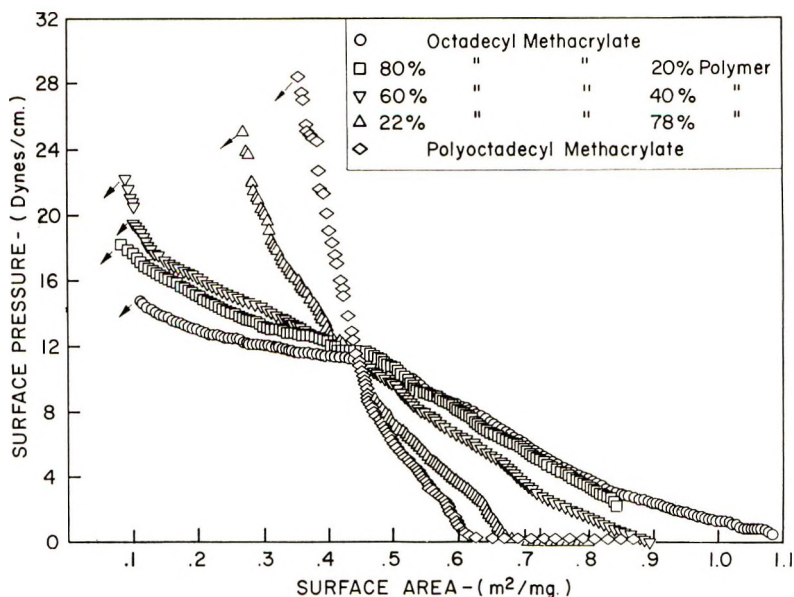


Fig. 3. Surface pressure-area isotherms for mixtures of monomer and poly(octadecyl methacrylate).

for the monomer at areas as large as  $1.1 \text{ m}^2/\text{mg}$ , where a majority of the hydrocarbon chains are probably in disarray and interfere with each other and with the polar groups. The reduction of the carbon-carbon double bond to a single bond chain "condenses" the film. The free motion of monomer molecules across the water surface gradually gives way to a chain of segments exhibiting a great deal of rigidity; this also is evident in the gradual decrease in compressibility values. At the inflection point, a phase or conformational change (helix to helix, or random coil to helix) appears to occur.

At pressures higher than the inflection point, surface pressure characteristics are opposite to those observed below  $11 \text{ dyne/cm}$ . Now at any given area, the increased concentration of polymer contributes to higher surface pressures. Surface pressure under these conditions probably is controlled by intimate packing of the hydrocarbon side chains; compared with the monomer, such packing is more limited in the polymer because of the restrictive effect of the backbone chain. This effect further is indicated by the observed gradual decrease in area, at extrapolated zero pressure, with increasing amounts of polymer. That the backbone chain stabilizes the film is indicated by the increase in collapse pressure with increase in polymer concentration.

#### Ultraviolet-Initiated Polymerization of Monomer in Argon

A monolayer of octadecyl methacrylate was compressed to  $8.5 \text{ dyne/cm}$ , and polymerization initiated by ultraviolet irradiation. Figure 4 shows

two conversion curves of pressure change with time, and indicates the reproducibility of this measurement. When no further change in pressure was noted, irradiation was discontinued and the heavy metal bar withdrawn to the far end of the trough.

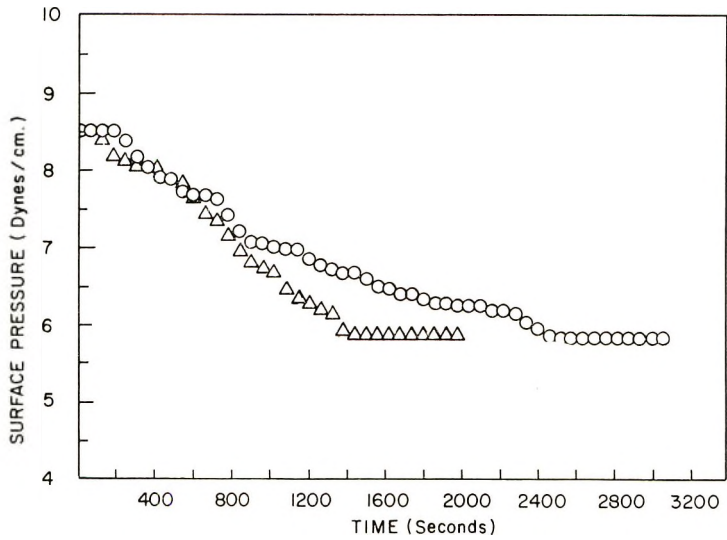


Fig. 4. Surface pressure-time conversion curves for ultraviolet polymerization of octadecyl methacrylates in argon.

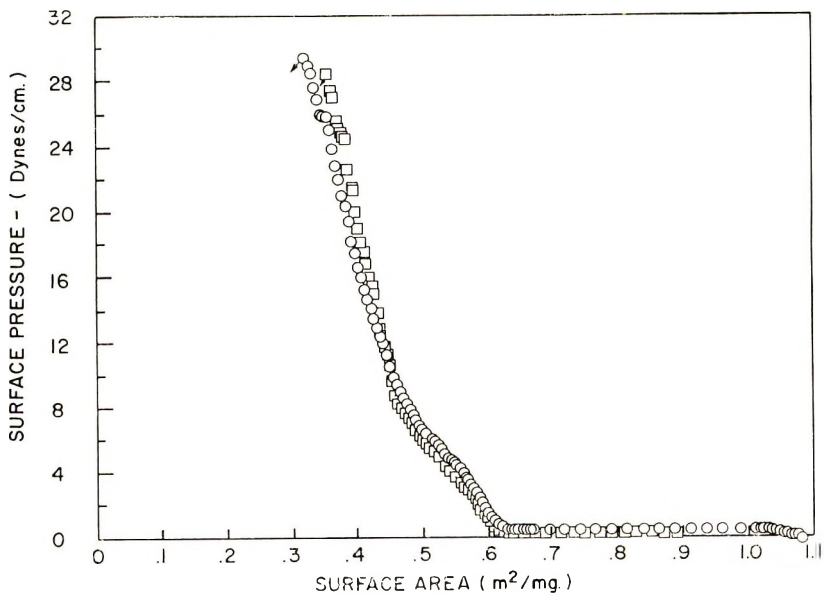


Fig. 5. Surface pressure-area isotherm derived from polymerization of the monolayer for poly(octadecyl methacrylate).



The cross-sectional area at extrapolated zero pressure of the polymer so obtained,  $0.57 \text{ m}^2/\text{mg}$ , is about equal to that of the bulk-polymerized material ( $0.50 \text{ m}^2/\text{mg}$ ), thus indicating in fact complete conversion of unsaturation at the point at which no further pressure change is noted. The rate curve is characterized by (a) a linear portion up to 70% conversion and (b) the absence of a Trommsdorff effect which, while noted for bulk polymerizations, is not expected to be present in the case of the monolayer reaction. The change in monomer concentration with time,  $d\alpha/dt$ , calculated from the linear region is  $0.62 \times 10^{-2} \text{ sec}^{-1}$ .

The polymer film obtained in this manner was permitted to expand over the increased surface area on the trough. After a waiting period of 30 min, compression was begun and the pressure-area isotherm determined of the polymer monolayer (Fig. 5).

This isotherm can be divided into two regions—one below and one above 16 dyne/cm. Surface pressure first is noted at about  $0.65 \text{ m}^2/\text{mg}$ —the same as that of the bulk polymerized material (Fig. 2), although the pressure rise is slower for the former. A point of inflection occurs at about 16 dyne/cm, ascribable perhaps to chain folding; film collapse occurs at 32 dyne/cm. The cross-sectional area at the extrapolated zero pressure is  $0.57 \text{ m}^2/\text{mg}$  or  $32 \text{ \AA}^2/\text{monomer unit}$ ; film thickness is about  $18 \text{ \AA}$ ; compressibility is  $0.0278 \text{ cm/dyne}$ . Although these values are of the same order of magnitude as those for the bulk polymer, a comparison of the shape of the two isotherms reveals differences in contour, which may be associated with the stereochemical structure of the polymers: The bulk polymer probably is atactic, while the monolayer derived from the polymer may have a more regular distribution of pseudo-asymmetric centers in the backbone, since chain growth was initiated while the monomer molecules were packed and oriented. This point requires further substantiation by other physicochemical means.

### Monolayer Polymerization of Octadecyl Methacrylate in Air

At  $50^\circ\text{C}$ , methacrylate radicals react with oxygen much more rapidly than with monomer.<sup>20</sup> It is likely that the monolayer polymerization of octadecyl methacrylate in air also affords a polymeric peroxide (Fig. 6) since the increase in surface pressure noted is in accord with the greater molar volume expected for copolymerization with oxygen. The initial overall rate of reaction,  $d\alpha/dt$ , is  $2.0 \times 10^{-3} \text{ sec}^{-1}$ —about three times as rapid as in the absence of oxygen.

The isotherm for the polymeric peroxide is shown in Figure 7. Surface pressure rises from about  $0.85 \text{ m}^2/\text{mg}$ , and a point of inflection, perhaps due to chain folding, occurs at 23 dyne/cm; thereafter the isotherm rises to 37 dyne/cm where collapse occurs. The area at the extrapolated zero pressure is  $0.54 \text{ m}^2/\text{mg}$  or about  $32 \text{ \AA}^2/\text{monomer unit}$ , assuming an equimolar copolymer with oxygen. The film thickness is about  $19 \text{ \AA}$  and its compressibility is  $0.0210 \text{ cm/dyne}$ .

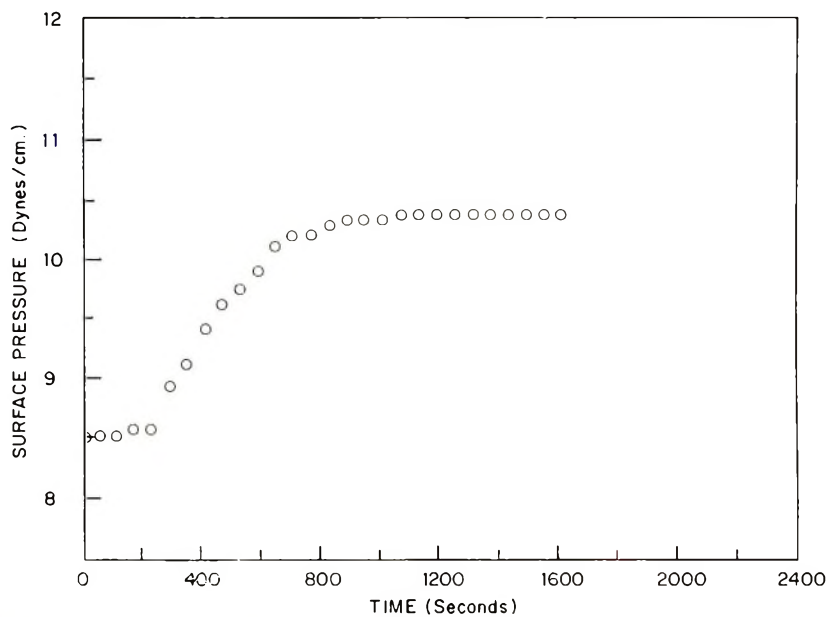


Fig. 6. Surface pressure-time conversion curves for monolayer polymerization of octadecyl methacrylate in air.

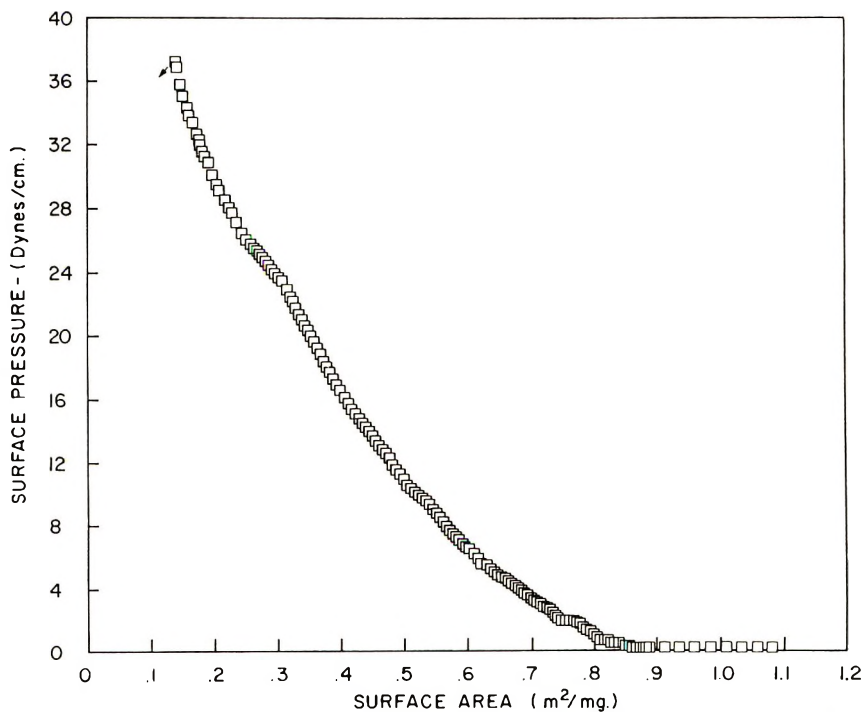


Fig. 7. Surface pressure-area isotherm for poly(octadecyl methacrylate) obtained from polymerization of the monolayer in air.

TABLE II  
Monolayer Properties of Octadecyl Methacrylate and Its Polymer

Monolayer	Area at extrapolated zero pressure		Collapse pressure, dyne/ cm	Film thick- ness, Å	Compressibility, cm/dyne
	m <sup>2</sup> /mg	Å <sup>2</sup> /mono- mer unit			
Octadecyl methacrylate	0.84-0.88	47-49	15-16	13-14	0.0586-0.0548
Poly(octadecyl methacrylate) <sup>a</sup>	0.50	28	29	21	0.0114
Poly(octadecyl methacrylate) <sup>b</sup>	0.57	32	32	18	0.0278
Poly(octadecyl methacrylate peroxide) <sup>c</sup>	0.54 <sup>d</sup>	32 <sup>e</sup>	37	19	0.0210
	0.65 <sup>f</sup>	39		16	

<sup>a</sup> Product of radical initiated bulk polymerization.

<sup>b</sup> Product of ultraviolet-initiated monolayer polymerization in argon.

<sup>c</sup> Product of ultraviolet-initiated monolayer polymerization in air.

<sup>d</sup> From the upper portion of Figure 7.

<sup>e</sup> Assuming a 1:1 copolymer with oxygen.

<sup>f</sup> From the lower portion of Figure 3.

Monolayer data on which the preceding discussions are based are summarized in Table II.

### Divinyl Ester

Surface characteristics of the divinyl monomer containing the dodecyl chain are shown in Figure 8. The film exhibits properties different from the other monomer: side chains pack as the film is compressed to position

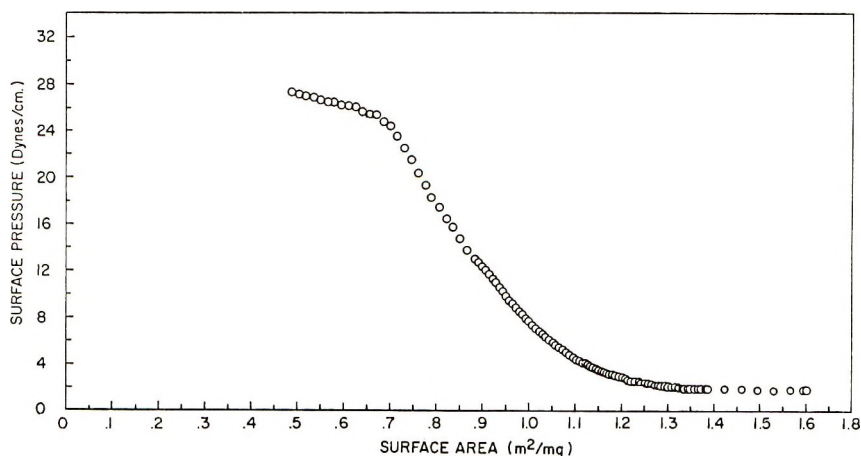


Fig. 8. Surface pressure-area isotherms for starting divinyl ester (I).

A; at this point, the backbone appears to fold with collapse becoming imminent.

Polymerization in a monolayer may be expected to lead to a sheetlike, two-dimensional analog of the crosslinked network obtained from the bulk

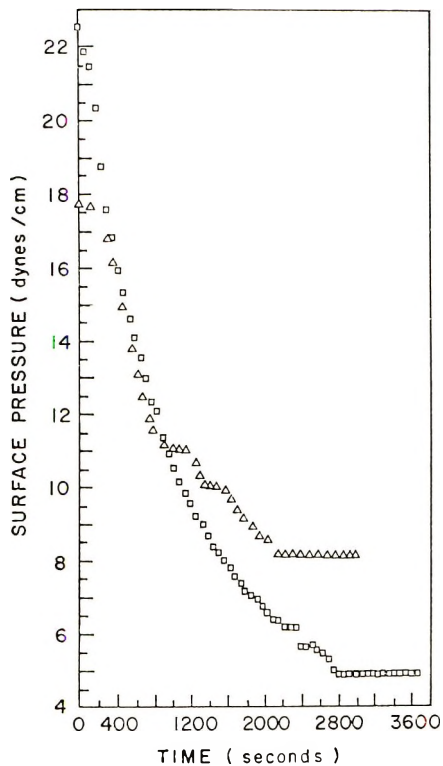


Fig. 9. Surface pressure-time conversion curves for polyester (I) polymerized (□) in air and (△) in argon.

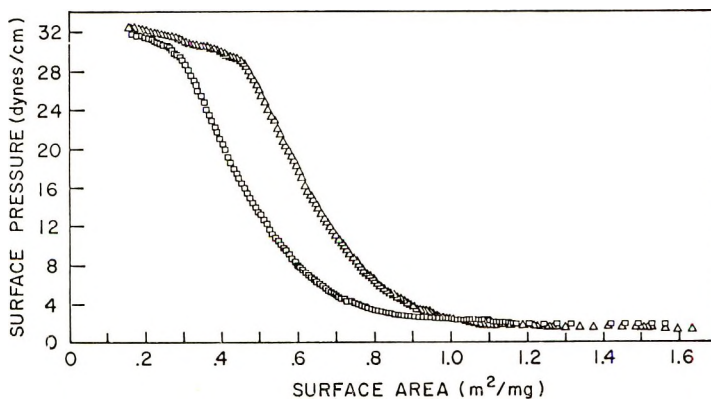


Fig. 10. Surface pressure-area isotherms for polymers obtained by polymerization monolayers of polyester (I) (□) in air and (△) in argon.

reaction. Rate data in air and in argon (Fig. 9) indicate that either oxygen could not be eliminated effectively; the rates of both the polymerization and copolymerization with oxygen are essentially the same. Isotherms of both air- and argon-irradiated polymers (Fig. 10) are similar: the steep portions are characteristic of the hydrocarbon chain; the more gradual region corresponds to the polyethylene backbone, which is a further confirmation of the conclusions reached above from the examination of the rate data in air and in argon.

The experimental assistance of Mrs. M. Katz is gratefully acknowledged.

### References

1. G. Scheibe and H. Schuller, *Elektrochem. Z.*, **59**, 861 (1955).
2. G. Gee, *Proc. Roy. Soc. (London)*, **A153**, 116, 129 (1935).
3. G. Gee, *Trans Faraday Soc.*, **32**, 187 (1936).
4. S. Bressler, M. Judin, and D. Talmud, *Acta Physiocochim. USSR*, **14**, 71 (1941).
5. H. Friedlander and C. Frink, *J. Polym. Sci. B*, **2**, 475 (1964).
6. A. Blumstein, J. Herz, V. Sinn, and C. Sadron, *C. R. Acad. Sci. (Paris)*, **246**, 1846 (1958).
7. A. Blumstein, *Bull. Soc. Chim. France*, **1961**, 899.
8. E. Parker and E. Moffett, *Ind. Eng. Chem.*, **46**, 1615 (1959).
9. H. E. Ries, Jr., and H. D. Cook, *J. Colloid Sci.*, **9**, 535 (1954).
10. H. E. Ries, Jr., and H. D. Cook, *J. Phys. Chem.*, **60**, 1533 (1956).
11. N. K. Adam, *The Physics and Chemistry of Surfaces*, 3rd ed., Oxford Univ. Press, Oxford, 1951.
12. N. Beredjick, in *Newer Methods of Polymer Characterization* B. Ke, Ed., Interscience, New York, 1964.
13. J. Herz, F. Husson, and V. Luzzati, *C. R. Acad. Sci. (Paris)*, **252**, 3462 (1961).
14. H. E. Ries, Jr., and D. C. Walker, *J. Colloid Sci.*, **16**, 361 (1961).
15. N. Beredjick, *J. Appl. Polym. Sci.*, in press.
16. N. Beredjick and H. E. Ries, Jr., *J. Polymer Sci.*, **62**, S64 (1962).
17. N. Beredjick and H. E. Ries, Jr., paper presented to Division of Polymer Chemistry, 142nd National Meeting, American Chemical Society, Atlantic City, N. J., 1962; *Preprints*, **3** No. 2, 263 (1962).
18. H. E. Ries, Jr., N. Beredjick, and J. Gabor, *Nature*, **186**, 883 (1960).
19. D. J. Crisp, *J. Colloid Sci.*, **1**, 161 (1946).
20. M. S. Matheson, E. E. Auer, E. B. Bevilacqua, and E. J. Hart, *J. Amer. Chem. Soc.*, **71**, 497 (1949).

Received March 6, 1969

Revised

## Treatments of Cross-Termination Rate Constants in Radical Copolymerization

KATSUKIYO ITO, *Government Industrial Research  
Institute of Nagoya, Kita-ku, Nagoya, Japan*

### Synopsis

In copolymerization, Arlman's equation was modified to

$$(1 + f_1/r_1)(1 + 1/r_2f_1)k_{tab}/\bar{k}_{tab} = K_1 + K_2/r_1r_2 + K_3f_1/r_1 + K_4/r_2f_1$$

where  $k_{tab}$  is an apparent cross-termination rate constant depending on a ratio  $f_1 = [A]/[B]$ , and  $K_x$  ( $x = 1, 2, 3, 4$ ) is the ratio of each cross-termination rate constant depending on the penultimate unit to the geometric mean  $\bar{k}_{tab}$  of two termination rate constants in homopolymerizations. The calculated values of  $(K_1 + K_2/r_1r_2)$  by using this equation were related to  $K_1 + K_2/r_1r_2 = 18/r_1r_2$ .

### INTRODUCTION

It has been found that an apparent cross-termination rate constant  $k_{tab}$  for the reaction between unlike radical chain ends is significantly larger than the geometric mean  $\bar{k}_{tab}$  of two termination rate constants  $k_{ta}$  and  $k_{tb}$  of the respective homopolymerizations.<sup>1-6</sup> This relationship is given by

$$k_{tab} = l \bar{k}_{tab} \quad l \geq 1 \quad (1)$$

where

$$k_{tab} = (k_{ta}k_{tb})^{1/2}$$

Because  $l$  depends on the ratio  $f_1 = [B]/[A]$  for the concentrations of monomers, Barb<sup>7</sup> pointed out that this dependence is related to the influence of polar repulsion between the penultimate units in copolymeric radicals. Arlman<sup>8</sup> carried out a formulation for the relationship between  $l$  and  $f_1$  in the cross terminations  $ii^* + ^*j$  and  $ji^* + ^*j$ , where  $i, j = A$  or  $B$ .

In homopolymerization, Ito<sup>9</sup> pointed out that the termination rate constant depends theoretically and experimentally on the repulsion between radical chain ends with the net electric charges, i.e., on the effects of the net electric charges in polymeric radicals  $^*ji$  and  $^*nm$  ( $m, n = A$  or  $B$ ) where the influences of the penultimate units,  $i$  and  $m$  are different from  $j$  and  $n$ , respectively. Thus, Arlman's formulation must be modified for the various cross terminations,  $ij^* + ^*nm$  ( $j \neq n$ ).

The aims of this paper are a modified formulation for the relationship between  $l$  and  $f_1$ , and experimental examination of it. Furthermore, the

analysis of the cross-termination rate constants obtained are carried out by using Ito's equation for termination rate constant.

## THEORY

### Formulation for Relationship between $l$ and $f_1$

On denoting termination rate constants by  $k_{ijmn}$  ( $i, j, m, n = a$  or  $b$ ), the termination rate is given by

$$R_t = k_{taaa}[AA^*]^2 + k_{taab}[AA^*][AB^*] + k_{taaba}[AA^*][BA^*] + k_{taabb}[AA^*][BB^*] + k_{tabab}[AB^*]^2 + k_{tabba}[AB^*][BA^*] + k_{tabaa}[AB^*][BB^*] + k_{tbbba}[BB^*][BA^*] + k_{tbbbb}[BB^*]^2 \quad (2)$$

By using previously derived relationships<sup>10</sup>

$$\begin{aligned} [BA^*] &= [AA^*]f_1/r_1 \\ [AB^*] &= [BB^*]/r_2f_1 \\ [A^*] &= [AA^*] + [BA^*] = (1 + f_1/r_1)[AA^*] \\ [B^*] &= [BB^*] + [AB^*] = (1 + 1/r_2f_1)[BB^*] \end{aligned} \quad (3)$$

where  $r_1 = k_{paa}/k_{pab}$  and  $r_2 = k_{pbb}/k_{pba}$ , eq. (2) becomes

$$R_t = \alpha k_{ta} [A^*]^2 + \bar{k}_{tab} [A^*][B^*] + \beta k_{tb} [B^*]^2 \quad (4)$$

where

$$\begin{aligned} \alpha &= [k_{taaaa} + k_{taaba}(f_1/r_1) + k_{tabaa}(f_1/r_1)^2]/(1 + f_1/r_1)^2 k_{ta} \\ \beta &= [k_{tbbbb} + k_{tbbba}/r_2f_1 + k_{tabba}(1/r_2f_1)^2]/(1 + 1/r_2f_1)^2 k_{tb} \end{aligned}$$

and

$$\begin{aligned} \phi &= (1 + f_1/r_1)(1 + 1/r_2f_1)l \\ &= K_1 + K_2/r_1r_2 + K_3f_1/r_1 + K_4/r_2f_1 \end{aligned} \quad (5)$$

where

$$\begin{aligned} K_1 &= k_{taabb}/\bar{k}_{tab} \\ K_2 &= k_{tabba}/\bar{k}_{tab} \\ K_3 &= k_{tbbba}/\bar{k}_{tab} \\ K_4 &= k_{taaab}/\bar{k}_{tab} \end{aligned}$$

In the structure  $ij^*$ , the effect of  $j$  on the net electric charge should be considerably stronger than the effect of  $i$ . The termination rate constant depends exponentially on the net electric charges.<sup>9</sup> Thus, in the termination reaction,  $ij^* + {}^*nm$ , in the case  $n = j$ , it may be possible that  $k_{ijmj}$  should be approximated to  $k_{ijjj}$  ( $= k_{ij}$ ). However, in the case  $n \neq j$ ,

$k_{ti_jmn}$  can not be directly approximated to  $\bar{k}_{tab}$ , and should be significantly larger than  $\bar{k}_{tab}$ .

On the above assumptions, because  $K_3$  and  $K_4$ , respectively, are significantly larger than  $k_{taaba}/k_{ta}$  and  $k_{tbbab}/k_{tb}$ ,  $\phi$  strongly depends on  $f_1$ . On the other hand,  $\alpha$  and  $\beta$ , respectively, do not strongly depend on  $f_1$ . The following equations are available:

$$\alpha \rightarrow k_{taaaa}/k_{ta} = 1 \quad f_1 \rightarrow 0$$

$$\beta \rightarrow k_{tabab}/k_{tb} \simeq 1$$

and

$$\alpha \rightarrow k_{tabaa}/k_{ta} \simeq 1 \quad f_1 \rightarrow \infty$$

$$\beta \rightarrow k_{tbbbb}/k_{tb} = 1$$

These relationships are independent of  $k_{ijji}/k_{ij}$  ( $i \neq j$ ). Because the net electric charge in  $jj^*$  is not equivalent to the net electric charge in  $ij^*$   $k_{ijji}$  may be moderately larger than  $k_{ij}$ . Especially, if  $k_{ijji}/k_{ij}$  is approximated to 2,  $\alpha$  and  $\beta$ , respectively, are approximately to unity. On the above considerations, the experimental results should be treated by eq. (5). When  $f_1$  is a large or small value, eq. (5) is approximated to the following equations:

$$\phi = K_1 + K_2/r_1r_2 + K_3f_1/r_1 \quad K_3f_1/r_1 \gg K_4/r_2f_1 \quad (f_1 \text{ large}) \quad (6)$$

$$\phi = K_1 + K_2/r_1r_2 + K_4/r_2f_1 \quad K_4/r_2f_1 \gg K_3f_1/r_1 \quad (f_1 \text{ small}) \quad (7)$$

If the penultimate unit does not affect the cross-termination rate constant,  $k_{tab}$  is equivalent to  $k_{ti_jmn}$  ( $j \neq n$ ) and

$$l = k_{tab}/\bar{k}_{tab} = K_x \quad (x = 1, 2, 3, 4) \quad (8)$$

### Cross-Termination Rate Constants

According to the previous paper<sup>9</sup> the termination rate constant depends on the segmental diffusion rate constant and the distance  $L$  between radical chain ends for the thermal energy equaling the coulombic energy of interaction of the net electric charges. Fortunately, because the effect of the penultimate unit on the segmental diffusion constant is not comparable with the effect of the penultimate unit on the net electric charge,  $K_x$  should treat the changing net electric charge (accordingly  $L$ ). Because the value of  $L$  for the cross-termination rate constants should be smaller than the value  $L = L_m$  for the geometric mean  $\bar{k}_{tab}$ ,  $K_x$  becomes

$$K_x = L \exp\{(L_m - L)/R\}/L_m(1 - \exp\{-L/R\}) \quad (9)$$

where  $R$  is the average distance for approach of the radical chain ends for bimolecular reaction.

In the past,<sup>5,11</sup> a relationship between cross-termination rate constant and propagation rate constant has been evaluated by

$$l^2 = \text{constant}/r_1r_2 \quad (10)$$



As stated in the introduction, because  $l$  depends on  $f_1$ , eq. (10) is not correct for the relationship between cross-termination rate constant and propagation rate constant. In this paper, eq. (10) is modified to equations applicable to the experimental results.

In the termination reaction,  $AA^* + ^*BB$ , the penultimate unit does not affect the apparent interaction between the net electric charges, and this reaction resembles the propagation reaction,  $A^* + B$  or  $B^* + A$ . Thus, an evaluation

$$K_1 = \text{constant}/r_1r_2$$

should be suitable. In the termination reaction  $BA^* + ^*BA$ , the penultimate unit forces this reaction into a bimolecular reaction between two radical chain ends with the same net electric charges. Thus, for strong influences of the penultimate unit, no strong relationship between  $K_2$  and  $1/r_1r_2$  can be recognized, and an evaluation  $K_2 = \text{constant}$ , should be suitable. These two equations are combined into

$$K_1 + K_2/r_1r_2 = \text{constant}/r_1r_2 \quad (11)$$

In the termination reaction,  $AA^* + ^*BA$  or  $BA^* + ^*BB$ , an evaluation of the influence of the penultimate unit related to  $1/r_1r_2$  is complex and cannot be carried out by a simple relationship.

## APPLICATIONS AND DISCUSSION

### Application of Equations (6) and (7)

In copolymerization<sup>12</sup> of styrene (St) and methyl methacrylate (MMA) with the use of 1,1'-azobiscyclohexacarbonitrile (ACHN) as photosensitizer at 35°C, a linear relationship between  $\phi$  and  $f_1/r_1$  could be obtained (Fig. 1). The following values were calculated:

$$K_1 + K_2/r_1r_2 = 80$$

$$K_3 = 24.3$$

In this experiment, another linear relationship between  $\phi$  and  $1/r_1r_2$  could not be obtained. Thus, by using an approximate linear relationship for  $\phi = 80$  and 202 at  $1/r_2f_1 = 0$  and 13.8, respectively, the following value,  $K_4 = 8.5$  was calculated.

In copolymerization<sup>13</sup> of acrylonitrile (AN) with MMA with ACHN as photosensitizer at 30.5°C, a linear relationship between  $\phi$  and  $f_1/r_1$  was obtained (Fig. 2). The following values were calculated:  $K_1 + K_2/r_1r_2 = 60$  and  $K_3 = 21$ . The calculation of  $K_4$  in this experiment was impossible.

In copolymerization<sup>13</sup> of St and AN with ACHN as photosensitizer at 20°C, a complete linear relationship between  $\phi$  and  $1/r_2f_1$  could be obtained (Fig. 3). The  $K$  values calculated were  $K_1 + K_2/r_1r_2 = 1200$  and  $K_4 = 253$ .

In copolymerization<sup>14</sup> of St and diethyl fumarate (DEF) initiated by 2,2'-azobisisobutyronitrile (AIBN) at 60°C, a linear relationship between

$\phi$  and  $f_1/r_1$  could be obtained (Fig. 4). The following values were calculated:  $K_1 + K_2/r_1r_2 = 500$  and  $K_3 = 17$ .

By using selected data for copolymerization of St and butyl acrylate (BA) from Arlman's paper,<sup>8</sup> a linear relationship between  $\phi$  and  $1/r_2f_1$  could be obtained (Fig. 5). The following values were calculated:  $K_1$

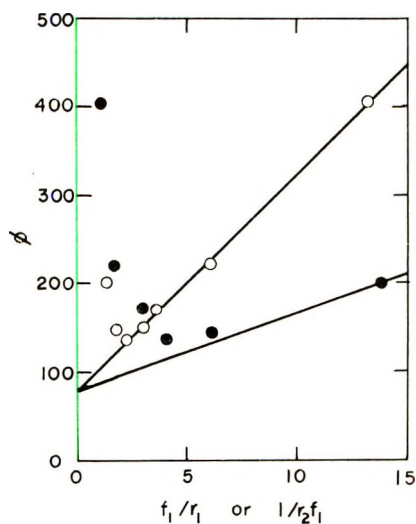


Fig. 1. Relationship between  $f_1/r_1$  or  $1/r_2f_1$  and  $\phi$  in copolymerization of St and MMA with ACHN as photosensitizer at 35°C:<sup>12</sup> (O)  $f_1/r_1$  vs.  $\phi$ , (●)  $1/r_2f_1$  vs.  $\phi$ .

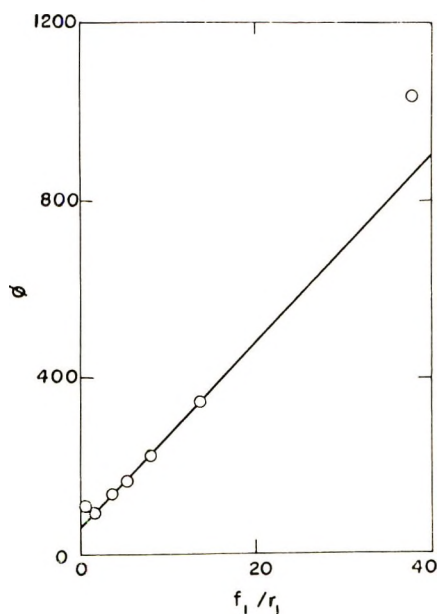


Fig. 2. Relationship between  $f_1/r_1$  and  $\phi$  in copolymerization of AN and MMA with ACHN as photosensitizer at 30.5°C.<sup>13</sup>

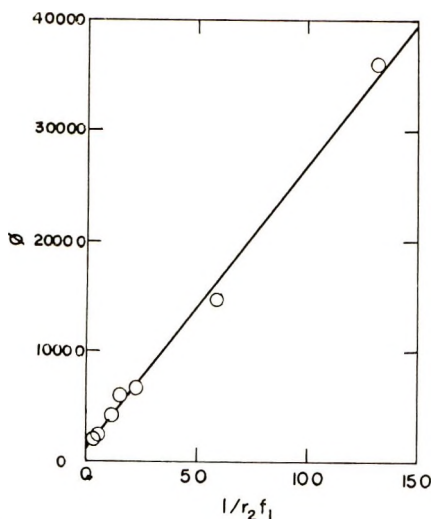


Fig. 3. Relationship between  $1/r_2 f_1$  and  $\phi$  in copolymerization of St and AN with ACHN as photosensitizer at 20°C.<sup>13</sup>

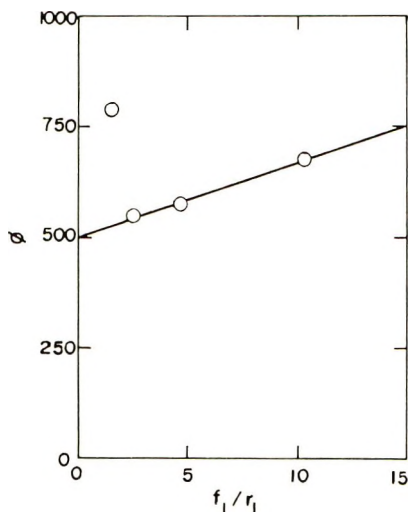


Fig. 4. Relationship between  $f_1/r_1$  and  $\phi$  in copolymerization of St and DEF initiated by AIBN at 60°C.<sup>14</sup>

+  $K_2/r_1 r_2 = 340$  and  $K_4 = 190$ . An example of copolymerization with no influence of the penultimate unit is the system St-*p*-methoxystyrene (pm-St) initiated by AIBN at 60°C.<sup>11</sup> In this copolymerization,  $K_z$  is unity. The results are collected in Table I.

The treatment on the basis of eq. (5) is not applicable to the copolymerization of vinyl acetate with St,<sup>15</sup> AN,<sup>13</sup> or MMA.<sup>12,16</sup> These copolymerizations could not be satisfactorily interpreted by using Arlman's treatment<sup>12,13</sup> or Atherton and North's treatment<sup>16</sup> related to the weak dependence of the composition of the monomer feed on the termination rate

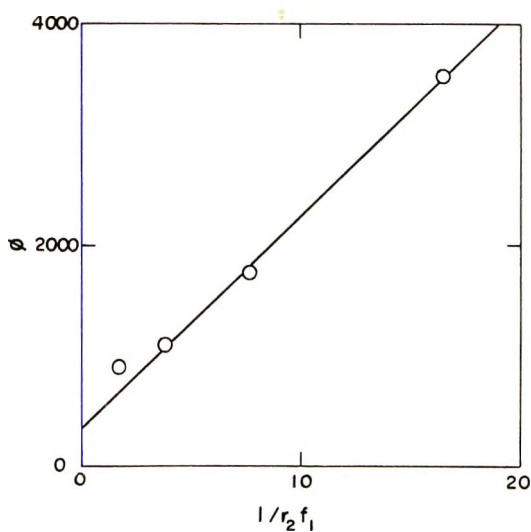


Fig. 5. Relationship between  $1/r_2 f_1$  and  $\phi$  for selected copolymerization data for the system St-BA.<sup>8</sup>

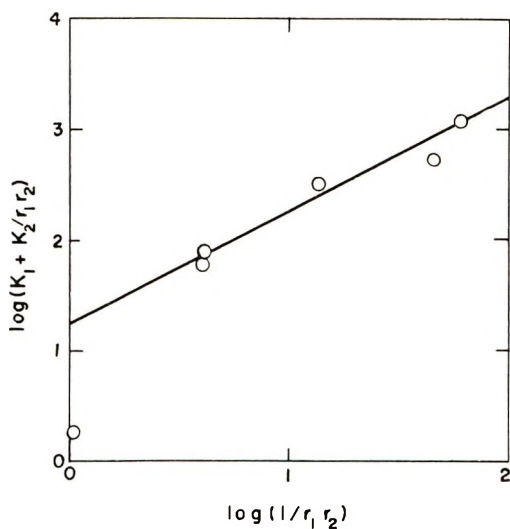


Fig. 6. Relationship related to eq. (11) for the values of  $(K_1 + K_2/r_1 r_2)$  and  $1/r_1 r_2$  in Table I.

constant, because the composition of the monomer feed strongly affects the polymerization rate or termination rate constant. Walling's treatment<sup>15</sup> should be suitable for the interpretation of these copolymerizations, however.

#### Cross-Termination Rate Constant

On setting  $L = 0$  in eq. (9),  $K_x$  becomes

$$K_x = (R/L_m) \exp\{I_m/R\} \quad (12)$$

TABLE I  
Values of  $1/r_1r_2$ ,  $K_1 + K_2/r_1r_2$ ,  $K_3$  and  $K_4$   
for Various Copolymerization Systems

System	$1/r_1r_2$	$K_1 + K_2/r_1r_2$	$K_3$	$K_4$
St-pmSt	1.05	2.05	1	1
AN-MMA	4.08	60	21	—
St-MMA	4.17	80	24.3	8.5
St-BA	13.8	340	—	190
St-DEF	47.6	500	17	—
St-AN	61	1200	—	253

when  $8 \geq L \geq 7$ ,  $K_z$  is calculated to be in the range 160–376. Thus, the calculated value corresponds to the large values  $K_1 = 190$  and 253, respectively, for the copolymerizations of St with BA and St with AN. Medium values of  $K_z$  in the range from 1 to large values for various copolymerizations can be calculated by using eq. (9) with a value of  $L$  in the range 0 to  $L_m$ . However, because the experimental results are not very precise, these evaluations are qualitative. Quantitative evaluations require very precise experimental results.

A linear relationship related to eq. (11) for the values in Table I could be obtained (Fig. 6). Equation (11) becomes

$$K_1 + K_2/r_1r_2 = 18/r_1r_2$$

The theoretical derivation of the equation related to eq. (11) is not known. A simple relationship between  $K_3$  or  $K_4$  and  $1/r_1r_2$  for the values in Table I could not be obtained.

### References

1. E. J. Arlman, H. W. Melville, and L. Valentine, *Rec. Trav. Chim.*, **28**, 945 (1949).
2. E. J. Arlman and H. W. Melville, *Proc. Roy. Soc. (London)*, **A203**, 301 (1950).
3. E. P. Bonsall, L. Valentine and H. W. Melville, *Trans. Faraday Soc.*, **48**, 763 (1952).
4. C. W. Walling, *J. Amer. Chem. Soc.*, **71**, 1930 (1949).
5. H. W. Melville and L. Valentine, *Proc. Roy. Soc. (London)*, **A200**, 337, 358 (1950).
6. J. H. Bradbury and H. W. Melville, *Proc. Roy. Soc. (London)*, **A222**, 468 (1954).
7. W. G. Barb, *J. Polym. Sci.*, **11**, 117 (1953).
8. E. J. Arlman, *J. Polym. Sci.*, **17**, 375 (1955).
9. K. Ito, *J. Polym. Sci. A-1*, in press.
10. E. Merz, T. Alfrey, and G. Goldfinger, *J. Polym. Sci.*, **1**, 75 (1946).
11. E. P. Bonsall, L. Valentine, and H. Melville, *J. Polym. Sci.*, **7**, 39 (1953).
12. M. Suzuki, H. Miyama, and S. Fujimoto, *J. Polym. Sci.*, **37**, 533 (1959).
13. M. Suzuki, H. Miyama, and S. Fujimoto, *Bull. Chem. Soc. Japan*, **35**, 57, 60 (1962).
14. C. Walling and E. A. McElhill, *J. Amer. Chem. Soc.*, **73**, 2819 (1951).
15. C. Walling, *J. Amer. Chem. Soc.*, **71**, 1930 (1949).
16. J. N. Atherton and A. M. North, *Trans. Faraday Soc.*, **58**, 2049 (1962).

Received January 13, 1970

## Polymerization of Vinyl Monomers by Diphenylsulfone-Potassium Complexes\*

TAKUJI HIRAHARA, TAKAAKI SUGIMURA,† and YUJI MINOURA, *Research Institute for Atomic Energy, Osaka City University, Osaka, Japan*

### Synopsis

Diphenylsulfone (DPSO<sub>2</sub>) was found to react with an equimolar amount of potassium in tetrahydrofuran (THF), dimethoxyethane (DME), or diglyme (DG) at reflux or an elevated temperature to yield a reddish-black solution, giving an electron spin resonance (ESR) signal. The signal was attributed to the formation of relatively labile DPSO<sub>2</sub> anion radical. The apparent effects of solvents on the reactivity of DPSO<sub>2</sub> with potassium depended on the polarities and the solvation powers: benzene ≅ toluene ≅ dioxane ≪ tetrahydrofuran < monoglyme < diglyme. The monopotassium complex was found to react further with another molecular amount of the metal to yield a dark blue solution giving no ESR signal.

The monopotassium complex initiated the polymerization of acrylonitrile (AN). It did not, however, initiate the polymerization of methyl methacrylate (MMA), styrene (St), or isoprene (IP). The active species of the monopotassium complex that initiated the polymerization of AN was found from analyses of the reaction products and the infrared spectrum of oily oligomer of AN obtained by the complex to be potassium benzenesulfinate. The dipotassium complex was found to initiate the polymerization of MMA, St, IP and AN. The active species of the dipotassium complex that initiated the polymerization of MMA, St, or IP was found from analyses of the reaction products and the infrared spectrum of the oily oligomer of MMA obtained by the complex to be phenyl potassium.

### INTRODUCTION

Diphenylsulfone (DPSO<sub>2</sub>) is well known to have a very stable sulfonyl group owing to the *dπ-pπ* interaction,<sup>1-4</sup> and the compound can be stable even at 378°C, its boiling point. It is, however, cleaved at the C-S bond with alkali metals(M),<sup>5,6</sup> as shown in eqs. (1) and (2), similar to the cleavage reactions of the organic sulfides by the metals to yield the corresponding mercaptan and alkane.<sup>7-10</sup>



\* This work was presented in part at the 15th annual meeting of the Society of Polymer Science, Japan, Nagoya, May 1966.

† Present address: Central Research Institute of Nippon Zeon, Co., Ltd., Kawasaki, Japan.

It is also known that diarylsulfones are reductively cleaved to thiol and hydrocarbon by lithium metal in methylamine, but when sodium in liquid ammonia is used, aromatic sulfinic acid and hydrocarbon are produced.<sup>10</sup> In general, the use of excess sodium often removes sulfur entirely from the molecule as sodium sulfide,<sup>11</sup> and this fact has been used to advantage as the basis of a quantitative determination of sulfur.<sup>12</sup> Aromatic sulfones are also known to be cleaved by sodium piperidine to give a sulfinic acid and corresponding *N*-arylpiperidine.<sup>13</sup> Diaryl and alkyl aryl sulfones are reductively cleaved with sodium amalgam in boiling ethanol to give sulfinic acid and hydrocarbon,<sup>14</sup> and recently it has been shown that diphenylsulfone as well as diphenyl sulfide can be cleaved with triphenylsilyllithium.<sup>15</sup> More recently DPSO<sub>2</sub> has been known to react with potassium mirror in dimethoxyethane below -70°C to form a radical anion.<sup>16</sup> Other isolated instances of sulfone cleavage are known, usually under vigorous conditions,<sup>17-20</sup> and a review of the older literature has been given by Suter.<sup>21</sup>

The authors also confirmed the cleavage reaction of DPSO<sub>2</sub> by potassium metal in tetrahydrofuran (THF), dimethoxyethane (DME), or diglyme (DG) at reflux or an elevated temperature to yield a reddish-black or a dark blue solution, and further used the complex solution as the anionic catalyst in the polymerization of vinyl monomers. The authors also found that the DPSO<sub>2</sub>-potassium complex solution formed with an equimolar amount of the metal gave an electron spin resonance (ESR) signal when prepared in diglyme, and the complex solution initiated the polymerization of acrylonitrile. The monopotassium complex was found to react further with another equimolecular amount of potassium to yield a dark blue solution giving no ESR signal, and the dipotassium complex was found to initiate the polymerization of methyl methacrylate, styrene, isoprene, and acrylonitrile at the given polymerization conditions.

This paper deals with the investigation of the active species that initiated the polymerization of these vinyl monomers by the analyses of the reaction products obtained by reacting the complexes with benzyl chloride, or the carbonation reaction of the complexes.

## EXPERIMENTAL

### Reagents

**Diphenylsulfone (DPSO<sub>2</sub>).** DPSO<sub>2</sub> was prepared by the Friedel-Crafts reaction from anhydrous aluminum chloride, benzenesulfonyl chloride, and benzene according to the method of Beckurts and Otto.<sup>22</sup>

**Dimethoxyethane (monoglyme).** Methyl cellosolve (1830 g, 24 mol) was added to a three-necked flask equipped with a condenser, a mechanical stirrer and a thermometer, and then 184 g (8.0 mole) of sodium metal was added portionwise with stirring. As sodium dissolved, the mixture thickened and turned dark brown in color. When all the sodium metal dissolved, methyl chloride was passed into the mixture through the inlet tube

at such a rate that very little escaped the reaction. After about 3 hr the reaction was complete, and the liquid portion was distilled off to separate from sodium chloride. Fractional distillation of the liquid gave 550 g of monoglyme, boiling at 83–84°C,  $n_D^{20}$  1.3810 (lit.<sup>23</sup>  $n_D^{20}$  1.3813). The yield, based on sodium metal added, was 76%. Monoglyme obtained was refluxed over small pieces of calcium hydride overnight, and was distilled off immediately before use.

**Diethyleneglycol dimethyl Ether (Diglyme).** Diglyme was prepared in the same way as monoglyme by using diethyleneglycol monomethyl ether and sodium metal.<sup>24</sup> The solvent was also purified in the same way as monoglyme, bp 62–63°C/15 mm Hg.

The monomers and the other solvents were purified by the usual methods and distilled over calcium hydride just before use.

### Polymerization

The polymerizations of the vinyl monomers by the complexes were carried out in the sealed glass tubes. Precautions were taken to remove traces of moisture and air in all the polymerizations. The reaction mixture was poured into a large excess of methanol containing dilute hydrochloric acid after the desired length of time, and then filtered off. The polymers obtained were dried under a reduced pressure at a room temperature to constant weights.

### Measurement of Electron Spin Resonance Spectra

The diglyme solutions of monopotassium and dipotassium complexes were placed in a quartz glass tube by means of a syringe under a stream of argon gas. Measurements of these samples were carried out on a Hitachi MPU-3B Type spectrometer (x-band, 9400 Mcps) with 100 keps modulation.

### Measurement of Infrared Spectra

The measurements of infrared spectra were carried out on a Perkin Elmer 337 Type double-beam infrared spectrometer over the region of 4000 to 600  $\text{cm}^{-1}$ .

### Analysis of Sulfur

The sulfur contents of the compounds were qualitatively confirmed by the sodium fusion method.<sup>25</sup>

### Measurement of Molecular Weight

The molecular weights of the compounds were measured on a Knauer vapor-pressure osmometer.

### Analysis by Chromatography

The reaction mixture obtained was analyzed by thin-layer and column chromatograms.



### Reaction of $\text{DPSO}_2$ with Potassium

$\text{DPSO}_2$ , corresponding amounts of finely divided potassium metal, and freshly distilled solvent were added to a four-necked flask equipped with a condenser, a stirrer, an argon gas inlet, and a thermometer, after purging with a dry argon gas. The mixture was stirred at a refluxed or an elevated temperature. After about  $\frac{1}{2}$  hr, the reaction mixture turned reddish-black or dark blue in color and the metal gradually disappeared. The reaction mixture was filtered through the glass filter under a stream of argon gas after about 5 hr, and the filtrate was immediately used in an argon atmosphere.

### Reaction of Monopotassium Complex with Benzyl Chloride

Freshly distilled benzyl chloride (0.023 moles) was added to 100 ml. of monoglyme solution of monopotassium- $\text{DPSO}_2$  (0.023 moles) complex under a stream of argon gas, and the mixture was left for about 20 hr at the temperature with stirring. The solvent was evaporated off and the residue was washed with distilled water, and the organic layer remained was extracted with chloroform. Distilling off the solvent, the reaction mixture obtained were chromatogramed on alumina in chloroform. The elution with chloroform gave diphenyl (0.0098 mole), phenylbenzylsulfone (0.0065 mole), and benzenesulfinylbenzyl ester (0.0150 mole), identified by mixed melting point, C, H analysis, sodium fusion method, determination of molecular weights, and infrared spectra.

Diphenyl: mp  $69-70^\circ\text{C}$  (lit.<sup>26</sup> mp,  $69-70^\circ\text{C}$ ); IR spectrum: phenyl group:  $1950-1750$ ,  $1600$ ,  $1495$ ,  $1455$ ,  $1027\text{ cm}^{-1}$ .

ANAL. Calcd for diphenyl: C, 93.46%; H, 6.54%; MW, 154. Found: C, 93.37%; H, 6.80%; MW, 154.2.

Phenylbenzylsulfone: mp  $146-147^\circ\text{C}$  (lit.<sup>27</sup> mp,  $147^\circ\text{C}$ ); IR spectrum: phenyl group:  $1950-1750$ ,  $1580$ ,  $1480$ ,  $1450\text{ cm}^{-1}$ ; sulfonyl group:  $1318$ ,  $1307$ ,  $1294$ ,  $1156\text{ cm}^{-1}$ ; C-S bond:  $683\text{ cm}^{-1}$ .

ANAL. Calcd for phenylbenzylsulfone: C, 67.24%; H, 5.17%; MW, 232. Found: C, 67.11%; H, 5.29%; MW, 230.

Benzenesulfinyl benzyl ester: mp  $98-100^\circ\text{C}$  (lit.<sup>28</sup> mp,  $98^\circ\text{C}$ ); IR spectrum: phenyl group:  $1950-1750$ ,  $1580$ ,  $1480$ ,  $1450\text{ cm}^{-1}$ ; S=O bond of sulfinyl ester:  $1125\text{ cm}^{-1}$ .

ANAL. Calcd: C, 67.24%; H, 5.17%; MW, 232. Found: C, 66.98%; H, 5.26%; MW, 228.

### Carbonation Reaction of Dipotassium Complex

A 100-ml portion of monoglyme solution of dipotassium- $\text{DPSO}_2$  (0.023 mole) complex was added to a large excess amount of finely crushed Dry Ice and was left to stand overnight at a room temperature. The solvent was evaporated off and the residue was diluted with 100 ml of distilled

water. The aqueous solution was acidified with 1*N* hydrochloric acid, and the solution was shaken with ferric chloride to remove off phenylsulfonic acid.<sup>28,29</sup> The filtrate was extracted with chloroform to give a white powder (0.020 mole). The compound was found to be benzoic acid, identified by melting point, mixed melting point, C, H analysis, determination of molecular weight, and infrared spectrum. Benzoic acid: mp 122–123°C (lit.<sup>26</sup> mp 122.4°C); IR spectrum: phenyl group: 1950–1750, 1588, 1485, 1450  $\text{cm}^{-1}$ ; carbonyl group: 1670  $\text{cm}^{-1}$ .

ANAL. Calcd: C, 68.84%; H, 4.95%; MW, 122.12. Found: C, 68.21%; H, 5.08%; MW, 122.

## RESULTS AND DISCUSSION

### Reaction of $\text{DPSO}_2$ with Potassium

Diphenylsulfone ( $\text{DPSO}_2$ ) did not react with potassium in a nonpolar medium such as benzene, toluene, or dioxane, even at reflux temperature. When a polar medium such as tetrahydrofuran (THF), dimethoxyethane (DME), or diglyme (DG) was used, however,  $\text{DPSO}_2$  reacted with potassium at the refluxed or an elevated temperature to form a reddish-black solution. A solution of the  $\text{DPSO}_2$ -potassium complex prepared in diglyme at an elevated temperature with the equimolar ratio showed a clear ESR signal shown in Figure 1. Only a weak signal was obtained, however, when THF or DME was used as solvent. Apparently, the effect of the solvents on the reactivity of  $\text{DPSO}_2$  with potassium increased in the order of increasing the polarities and solvation powers:<sup>30</sup> benzene  $\cong$

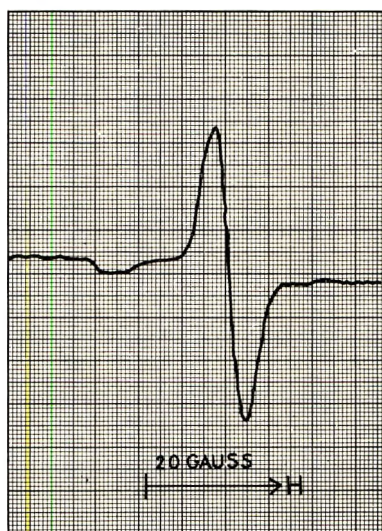
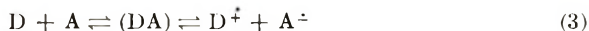


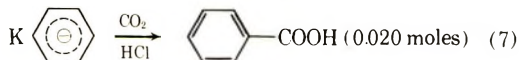
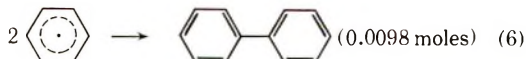
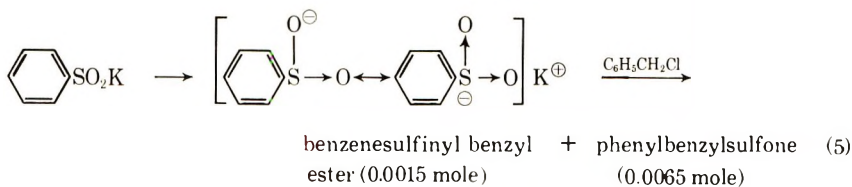
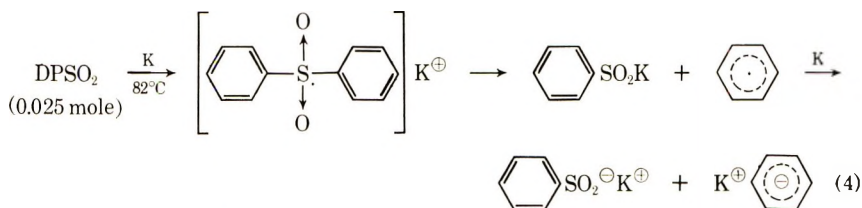
Fig. 1. Electron spin resonance spectrum of  $\text{DPSO}_2$ -monopotassium complex obtained in diglyme solvent at elevated temperature; 100 kcps modulation, X-band = 9400 Mcps, measured at room temperature.

toluene  $\cong$  dioxane  $\ll$  THF  $<$  DME  $<$  DG. The radical ions are known to form from a donor-acceptor interaction via a charge-transfer complex; namely,



where D and A denote the donor and acceptor, respectively. The most important factor in the radical ion formation is the lowered free energy of the free radical ion state due to ion-solvent interaction. This tends to stabilize the free-radical state with respect to the other states of the systems.<sup>31</sup> The solvent interaction also influences the first step, accompanied by an alteration of charge in the complex. The ground state of the complex is a superposition of a "no bond" state and a dative state. Interaction with the solvent enhances the contribution of the dative state and hence lead to a stronger transfer of charge.<sup>31</sup>

The monopotassium complex was found to react further with another molecular amount of potassium to yield a dark blue solution giving no ESR signal. From the reaction product analyses and the ESR spectral results, the reaction of DPSO<sub>2</sub> with potassium under the conditions used here was reasonably expressed in the following schemes (4)–(7), which differ from the results of Kaiser and co-workers, who examined the reaction below  $-70^{\circ}\text{C}$  and found transfer of an electron from potassium metal to the phenyl group.<sup>16</sup>



The first step is assumed to be the transfer of an electron from potassium to the sulfonyl group to form a relatively labile radical anion under the conditions used here. C-S bond scission then occurs to yield benzene sulfinate and phenyl radical. The phenyl radical reacts with another molecular amount of potassium to yield phenyl anion.

The reaction of  $\text{DPSO}_2$  with Li, Na, alkaline earth metals or amalgams of alkaline earth metals was also investigated in DME at the refluxed temperature under a stream of argon gas, however, inferior or nearly no reaction occurred with the metals.

### Polymerization of Vinyl Monomers by $\text{DPSO}_2$ -Potassium Complexes

The monopotassium complex was found to initiate the polymerization of acrylonitrile in benzene, toluene, tetrahydrofuran (THF), dimethoxyethane (DME), or dimethylformamide (DMF) solvent, as may be seen in Table I. However it did not initiate the polymerization of methyl methacrylate, styrene, or isoprene under the conditions applied in Table I. In

TABLE I  
Polymerization of Acrylonitrile in Various Solvents by  $\text{DPSO}_2$ -  
Monopotassium Complex Prepared in DME Solvent<sup>a</sup>

Solvent	Vol. solvent, ml	$[\text{DPSO}_2\text{-K}]$ mole/l.	Reaction time, min	Conversion, %
Benzene	9	$3.00 \times 10^{-2}$	60	0.25
			120	0.32
			180	0.51
Toluene	9	$3.00 \times 10^{-2}$	60	0.25
			120	0.40
			180	0.65
THF	9	$3.00 \times 10^{-2}$	30	3.2
			60	8.0
			90	8.2
DME	10	$3.00 \times 10^{-2}$	30	6.4
			60	8.0
			90	12.1
DMF	7	$9.00 \times 10^{-3}$	10	65.5
			20	80.4
			30	85.8

<sup>a</sup>  $[\text{AN}] = 3.04$  mole/l. at  $0^\circ\text{C}$ . The catalyst was added as DME solution.

view of the low solubilities of the complex and the polymer formed except in DMF solvent, DMF was mainly used for the polymerization of acrylonitrile. To clarify the active species that initiated the polymerization of the monomer, oily oligomer was obtained at a molar ratio of the monomer (0.0912 moles) to the catalyst of 1:5 in DMF solvent under a stream of argon gas with vigorous stirring. The infrared spectrum is shown in Figure 2, from which the active species is clearly concluded to be potassium sulfinate, identical with the reaction products analyses. As already described in our previous paper,<sup>32</sup> the initiation reaction of the anionic polymerization is determined by the following factors: (a) basicity, (b) polarizability, (c)  $\alpha$  effect.

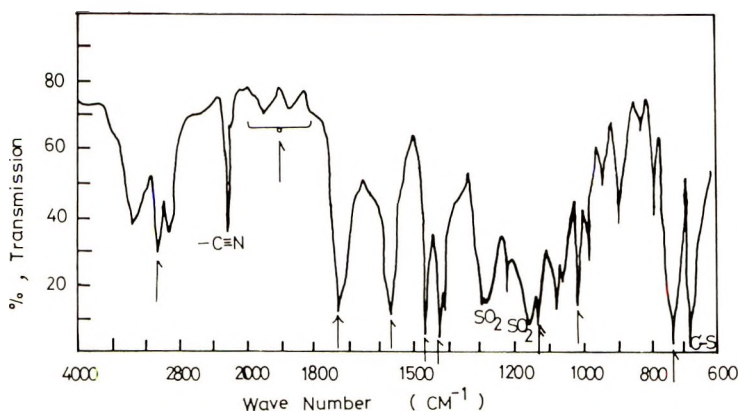


Fig. 2. Infrared spectrum of oily oligomer of acrylonitrile obtained by  $\text{DPSO}_2^-$ -monopotassium complex in DMF at room temperature: ( $\uparrow$ ) phenyl group; ( $\downarrow$ )  $\text{S}=\text{O}$  bond of sulfinyl ester; ( $\uparrow$ ) cyclic  $\beta$ -keto ester.

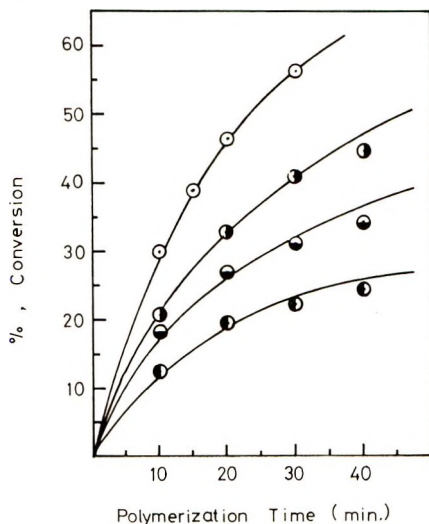
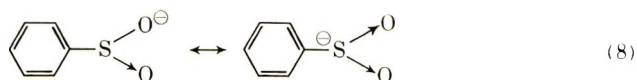


Fig. 3. Polymerization of acrylonitrile by  $\text{DPSO}_2^-$ -monopotassium complex in DMF Solvent at  $0^\circ\text{C}$ ,  $[\text{AN}] = 3.04$  mole/l.: ( $\odot$ )  $[\text{DPSO}_2^- \text{K}] = 9.00 \times 10^{-3}$  mole/l.; ( $\bullet$ )  $[\text{DPSO}_2^- \text{K}] = 6.00 \times 10^{-3}$  mole/l.; ( $\ominus$ )  $[\text{DPSO}_2^- \text{K}] = 5.00 \times 10^{-3}$  mole/l.; ( $\omin�$ )  $[\text{DPSO}_2^- \text{K}] = 4.00 \times 10^{-3}$  mole/l.

The  $\text{p}K_a$  value of benzenesulfonic acid, the conjugate acid of phenylsulfinate, is 1.8–2.0,<sup>33</sup> which is quite a low value. The charge delocalization of benzenesulfinate is also considered in the scheme (8),



as may be seen from scheme (5). However resonance with phenyl nuclei is not so large owing to the unstable  $2p\pi-3p\pi$  interaction. Thus benzene-

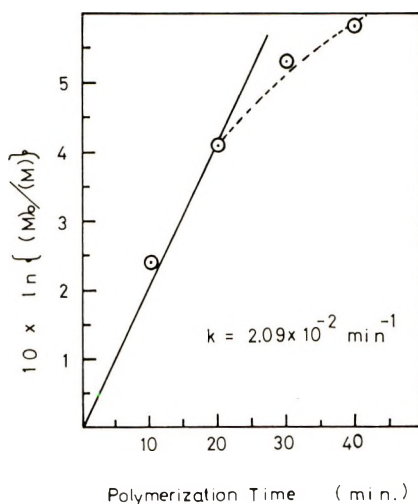


Fig. 4. Relationship between  $\ln ([M]_0/[M])$  and polymerization time;  $[AN] = 3.04$  mole/l.,  $[DPSO_2-K] = 6.00 \times 10^{-2}$  mole/l., in DMF solvent, at  $0^\circ C$ .

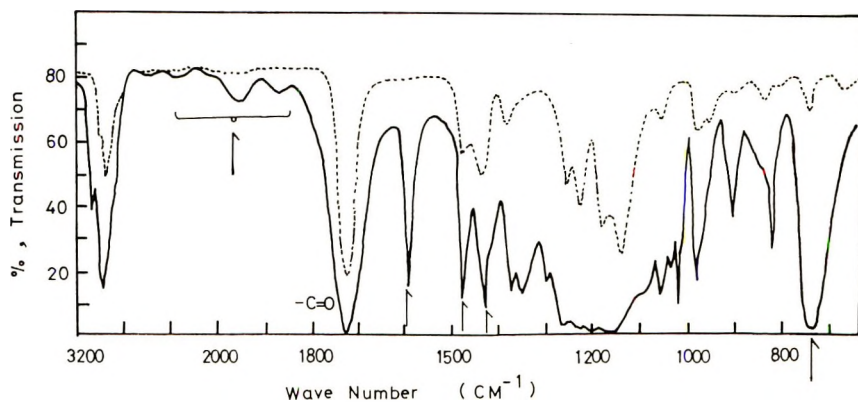


Fig. 5. Infrared spectrum of oily oligomer of methyl methacrylate obtained by  $DPSO_2$ -dipotassium complex in THF at room temperature: (↑) phenyl group.

sulfinate would be highly polarizable.<sup>34</sup> The reactivity of potassium benzenesulfinate for initiating the polymerization of acrylonitrile is hence reasonably appreciable, despite the low  $pK_a$  value. The polymerization of acrylonitrile by the various concentrations of the complex is shown in Figure 3. The relationship between  $\ln ([M]_0/[M])$  and the polymerization time is shown in Figure 4, in which obvious deviations of the plots, specific to the anionic polymerization of acrylonitrile, are observed.

The dipotassium complex was found to initiate the polymerization of MMA, St, IP, and AN, as may be seen in Table II.

Potassium sulfinate, however, did not initiate the polymerization of MMA, St, or IP as described above. The active species that initiated the poly-

TABLE II  
 Polymerization of Vinyl Monomers by  $\text{DPSO}_2$ -Dipotassium  
 Complex in THF Solvent at  $0^\circ\text{C}^a$

Monomer	Reaction time, hr	Conversion, %
AN	Explosively polymerized solution	on adding the catalyst
MMA	4	16.5
	8	34.3
	12	51.0
St	4	5.2
	8	11.3
	12	15.8
IP	4	4.8
	8	11.0
	12	14.6

<sup>a</sup>  $[\text{AN}] = 3.04$  mole/l.,  $[\text{MMA}] = 1.89$  mole/l.,  $[\text{St}] = 1.74$  mole/l.,  $[\text{IP}] = 2.00$  mole/l.,  $[\text{DPSO}_2\text{-2K}] = 1.00 \times 10^{-2}$  mole/l.; 1 ml of the DME solution of the catalyst was added to the reaction mixture of THF and the monomer.

merization of the monomers are hence clearly attributed to phenylpotassium,<sup>35,36</sup> from scheme (4), and Figure 5, where the infrared spectrum of the oily oligomer obtained by dipotassium complex at room temperature with vigorous stirring at a molar ratio of monomer (0.0567 moles) to complex of 1:3.

### References

1. H. P. Koch, *J. Chem. Soc.*, **1949**, 408.
2. G. Leandri, A. Mangini, and R. Passerini, *Gazz. Chim. Ital.*, **84**, 73 (1954).
3. V. Baliah and V. Ramakrishnan, *J. Indian Chem. Soc.*, **35**, 151 (1958).
4. G. Gilento, *Chem. Rev.*, **60**, 143 (1960).
5. W. E. Truce, D. P. Tate and D. N. Burdge, *J. Am. Chem. Soc.*, **82**, 2872 (1960).
6. F. Kraft and W. Vorster, *Ber.*, **26**, 2815 (1893).
7. C. A. Kraus and G. F. White, *J. Amer. Chem. Soc.*, **45**, 768 (1923).
8. F. E. Williams and E. Gebauer-Fueluegg, *J. Amer. Chem. Soc.*, **53**, 352 (1931).
9. R. C. Krug and S. Tocker, *J. Org. Chem.*, **20**, 1 (1955).
10. W. E. Truce and J. J. Breiter, *J. Amer. Chem. Soc.*, **84**, 1621 (1962).
11. R. A. Lečwith and N. McFarlane, *Proc. Chem. Soc. (London)*, **1964**, 108.
12. N. Kharasch, S. J. Potemna, and H. J. Wehrmeister, *Chem. Rev.*, **39**, 269 (1946).
13. W. Bradley, *J. Chem. Soc.*, **1938**, 458.
14. R. E. Dabby, J. Kenyon, and R. F. Mason, *J. Chem. Soc.*, **1952**, 4881.
15. D. Wittenberg, T. C. Wu, and H. Gilman, *J. Org. Chem.*, **23**, 1898 (1958).
16. E. T. Kaiser, M. M. Urberg, and D. H. Eargle, Jr., *J. Amer. Chem. Soc.*, **88**, 1037 (1966).
17. D. T. Gibson, *J. Prakt. Chem. [2]*, **142**, 218 (1935).
18. O. Jacobsen, *Ber.*, **20**, 900 (1887).
19. R. Otto and H. Ostrop, *Ann.*, **141**, 96 (1867).
20. R. Otto, *Ber.*, **18**, 248 (1885).
21. C. M. Suter, *Organic Chemistry of Sulfur*, Wiley, New York, 1944, p. 681.
22. H. Beckurts and R. Otto, *Ber.*, **11**, 2066 (1878).
23. J. V. Capinjola, *J. Amer. Chem. Soc.*, **67**, 1615 (1945).
24. H. C. Brown and B. C. S. Rao, *J. Amer. Chem. Soc.*, **77**, 3161 (1955).

25. L. F. Fieser, *Experiments in Organic Chemistry*, 3rd. ed., Heath, Boston, p. 228.
26. *The Merck Index of Chemicals and Drugs*, 7th ed., Merck & Co. New Jersey, 1960.
27. R. L. Shriner, H. C. Struck, and W. J. Jorrison, *J. Amer. Chem. Soc.*, **52**, 2060 (1930).
28. J. Thomas, *J. Chem. Soc.*, **95**, 342 (1909).
29. S. Krishna and H. Singh, *J. Amer. Chem. Soc.*, **50**, 792 (1928).
30. F. M. Brower and H. W. McCornick, *J. Polymer Sci. A*, **1**, 1749 (1963).
31. I. Isenberg and S. L. Baird, Jr., *J. Amer. Chem. Soc.*, **84**, 3803 (1962).
32. T. Hirahara and Y. Minoura, *J. Polym. Sci. A-1*, in press.
33. R. Burkhard, D. Sellers, F. DeCou, and J. Lambert, *J. Org. Chem.*, **24**, 767 (1959).
34. A. B. Burg, *Organic Sulfur Compounds*, N. Kharasch, Ed., Vol. 1, Pergamon Press, New York, 1961, p. 30.
35. A. Zilkha, S. Barzakray, and A. Ottolenghi, *J. Polym. Sci. A*, **1**, 1813 (1963).
36. A. Zilkha, A. Ottolenghi, and S. Barzakay, *J. Polym. Sci. A*, **1**, 3643 (1963).

Received February 10, 1970



## Calorimetric Investigation of Polymerization Reactions. IV. Curing Reaction of Polyester Fumarate with Styrene

KAZUYUKI HORIE, ITARU MITA, and HIROTARO KAMBE,  
*Institute of Space and Aeronautical Science, University of Tokyo,  
Komaba, Tokyo, Japan*

### Synopsis

The curing reaction of polyester fumarate with styrene was investigated with a differential scanning calorimeter (DSC) operated isothermally. The change in rate of cure was followed over the whole range of conversion. The rate of cure is accelerated by the gel effect to about ten to fifty times the rate of model copolymerization of diethyl fumarate with styrene. This autoacceleration is much enhanced for systems with higher crosslinking densities and at lower temperatures. The results confirm that both termination and propagation steps of the curing reaction are controlled by diffusion of polymeric segments and monomer molecules over almost the whole range of conversion. The final extent of conversion is short of completion for isothermal cure and even for postcure of polyester fumarate with styrene because of crosslink formation. The final conversion of isothermal cure decreases with increasing crosslinking density and shows a maximum with increasing reaction temperature. This temperature dependency of the final conversion is caused by the difference in the activation energies for two propagation rate constants  $k_{pf}$  and  $k_{ps}$ , which were evaluated to be 7–10 and 5–8 kcal/mole, respectively, for the intermediate stage of the curing reaction.

### INTRODUCTION

The copolymerization of polyester fumarate with styrene is well known as a typical crosslinking reaction accompanied by a gel effect. Analyses of the structure of the crosslinked polymers are, in general, difficult because of the insolubility of the cured products.

Hamann, Funke, and Gilch<sup>1</sup> have proposed a hydrolysis method which transforms the crosslinked polyester to a linear copolymer of fumarate with styrene. They have revealed the dependency of final conversion on the styrene content<sup>2</sup> and on the structure of linear polyester fumarate.<sup>3</sup> The change in relative degree of cure with time has been followed by the changes in electrical resistivity,<sup>4,5</sup> viscoelasticity,<sup>6–8</sup> NMR<sup>9</sup> and ESR<sup>10</sup> absorption spectra. Infrared analysis<sup>11–14</sup> has also been used to determine the rate of cure of unsaturated polyester with styrene. As to the mechanism of the curing reaction of unsaturated polyester with styrene, Gordon and McMillan<sup>15</sup> as well as Burlant and Hinsch<sup>12</sup> have proposed that the termina-

tion reaction may not be controlled by diffusion over a wide range of conversion, mainly because the rate of cure seems to be constant at this range in spite of the onset of gelation. Monomer reactivity ratios for the copolymerization of polyester fumarate ( $M_2$ ) with styrene ( $M_1$ ) determined by several investigators have given inconsistent results ( $r_1 = 0.30$ ,  $r_2 = 0.07$ ;<sup>2</sup>  $r_1 = 0.16$ ,  $r_2 = 0$ ;<sup>12</sup>  $r_1 = 0.03$ ,  $r_2 = 3.0$ <sup>16</sup>). Funke and his co-workers<sup>2</sup> have claimed the applicability of monomer reactivity ratios for the styrene–diethyl fumarate system<sup>17</sup> to the curing reaction of fumarate polyester with styrene over a wide range of conversion. However, the monomer reactivity ratios may lose their significance when the propagation reaction becomes controlled by diffusion of monomer molecules.

The fairly ambiguous status of present knowledge regarding the kinetics of this curing reaction would be improved by the absolute determination of the rate of cure over the whole range of conversion and by the clarification of the diffusion-controlled mechanism for the each stage of cure.

In previous papers, the rates of diffusion-controlled polymerization of methyl methacrylate and styrene<sup>18</sup> and of copolymerization of diethyl fumarate with styrene<sup>19</sup> have been determined over the whole range of conversion with a differential scanning calorimeter (DSC). The curing reaction of epoxy resin with diamines<sup>20</sup> has also been investigated by the same technique. The polymerization of methyl methacrylate has been shown to cease at a certain conversion where the glass transition of the polymer–monomer system occurs.<sup>18</sup> The quantitative relationship between the final conversion and the glass transition phenomenon of the system has also been established for the crosslinked epoxy system.<sup>20</sup>

The present paper is concerned with the kinetics of the curing reaction of fumarate polyester with styrene over the whole range of conversion. A large scale of autoacceleration in rate of cure and the interesting dependency of final conversion on the curing temperature were observed and are discussed in relation to the diffusion behavior of styrene monomer and the polymeric segments containing fumaric units in them.

## EXPERIMENTAL

### Materials

Linear polyester fumarates of different degrees of unsaturation were prepared by the condensation of diethylene glycol with mixtures of fumaric and succinic acids in different compositions. The preparation was carried out with stirring under nitrogen by heating to 150°C in an hour, then at 190°C for more than several hours until the acid value of the polyester became about 25–30. Water and residual glycol were removed at a reduced pressure and the product was cooled under nitrogen to give a white, jelly-like solid. No inhibitor was added to the system. The average molecular weight was determined by the chemical analysis for hydroxyl and carboxyl ends of the polyester.<sup>21</sup> The monomer compositions and the number-

average molecular weight of the linear polyesters are shown in Table I, together with the composition of styrene used for crosslinking.

Styrene monomer was freed of inhibitor, dried, and purified by distillation under nitrogen at a reduced pressure. The middle fraction was collected and stored in an icebox.

TABLE I  
Composition of Polyester Fumarate and Styrene

	Polyester fumarate			$\bar{M}_n$	Styrene, mole
	Fumaric acid, mole	Succinic acid, mole	Diethylene glycol, mole		
PES 1	0.30	0.70	1.05	3,300	1.00
PES 2	0.60	0.40	1.05	2,800	1.00
PES 3	1.00	0	1.05	2,300	1.00
PES 0	0	1.00	1.05	2,700	1.00

Benzoyl peroxide (BPO) was recrystallized from chloroform-methanol solution in a usual manner.

### Procedure

Polyester fumarate was copolymerized with styrene in bulk at 60–100°C with 0.10 mmole/g BPO. The copolymerization was carried out in a modified sample pan of a Perkin-Elmer differential scanning calorimeter (DSC-1), operated isothermally.

Details of the procedure with the DSC as well as the calibration performance are similar to those described previously.<sup>19</sup> In the case of reactions with very large rate of cure at 90 or 100°C, the sample holder assembly in DSC was cooled with liquid nitrogen from outside the ordinal cover in order to improve the cooling capacity of the apparatus. Temperature equilibrium at sample and reference holders was attained within half a minute or so after setting the apparatus at a certain temperature.

The rate of cure and the final conversion for curing reactions of polyester fumarate with styrene were determined from the DSC thermograms by using the values of heat of copolymerization of diethyl fumarate with styrene<sup>19</sup> at each monomer composition.

After an isothermal cure in DSC had been completed, temperature scanning at 8°C/min was carried out on the same sample up to 200°C. An exothermic peak due to the postcure of remained monomers began to appear just beyond the temperature of isothermal cure.

A long-time postcure for the isothermally cured sample was compared with the postcure with temperature scanning. The postcure at 100°C for 2 hr and successively at 160°C for 24 hr forced the reaction to almost the same extent of conversion as the postcure by temperature scanning did, and temperature scanning with DSC was adopted as a convenient method for determining the extent of postcure.

### Residual Fumarate Content

The content of residual fumarate was measured by infrared spectrophotometry. A Shimadzu IR-50A type infrared spectrophotometer was used for the determination of the absorbance at  $1650\text{ cm}^{-1}$  for the fumaric C=C bond in the isothermally cured film. The C=O stretching band of polyester at  $1730\text{ cm}^{-1}$  was used as an internal reference, and the ratios of optical densities of the two bands  $D_{1650}/D_{1730}$  for the starting linear polyesters were ascertained to obey the Beer's law.

The residual styrene content was calculated from the final conversion determined by DSC together with the content of residual fumarate by infrared spectrophotometry.

### Dynamic Viscoelasticity of Cured Polyester Fumarate

Dynamic modulus and  $\tan \delta$  for the isothermally cured polyester fumarate films were measured at a constant frequency (10 cps) by a Rion RV-02B type rheometer at temperatures from 20 to  $180^\circ\text{C}$ . The storage modulus in a rubbery region was related to the crosslinking density.

## RESULTS AND DISCUSSION

### Rate of Cure

The curing reaction of polyester fumarates with styrene was carried out isothermally at  $60\text{--}100^\circ\text{C}$ .

Typical DSC curves for the cure of polyester fumarate with styrene at various temperatures are shown in Figure 1. Typical change in rate of cure of polyester fumarates with styrene over the whole range of conversion is illustrated in Figure 2. Autoacceleration in rate of cure is much enhanced for the cases of PES 2 and PES 3 with styrene. The curing reactions of

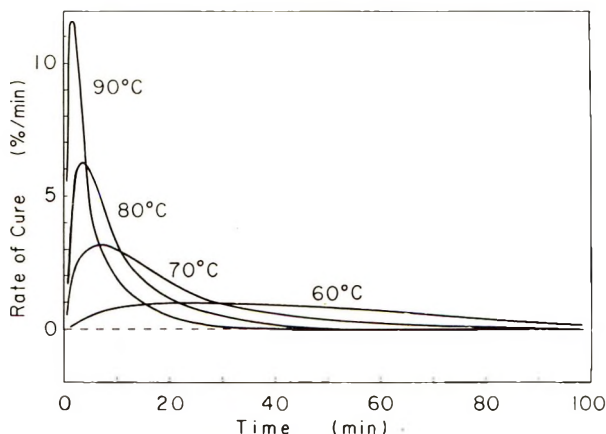


Fig. 1. DSC curves for curing reaction of polyester fumarate (PES 1) with styrene at various temperatures indicated beside the curves.

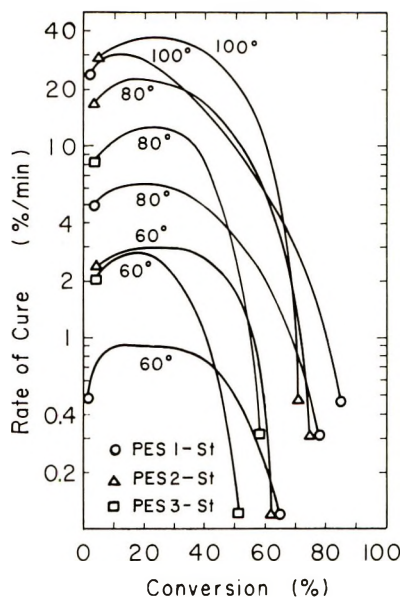


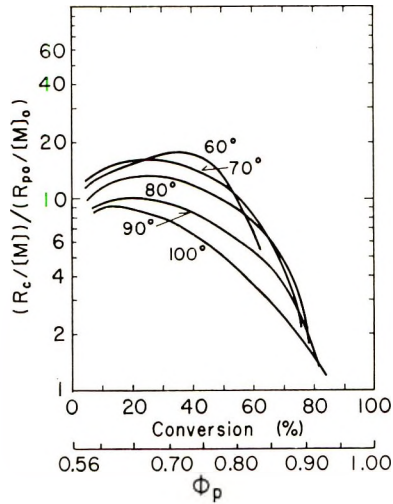
Fig. 2. Change in rate of cure against conversion for curing reaction of polyester fumarates with styrene. Curing temperatures ( $^{\circ}\text{C}$ ) are as indicated.

PES 1 and PES 2 with styrene at  $60^{\circ}\text{C}$  seem remain at a constant rate of cure up to about 40% conversion, in agreement with the reported observations<sup>12, 15</sup> on the rate of cure of unsaturated polyester with styrene.

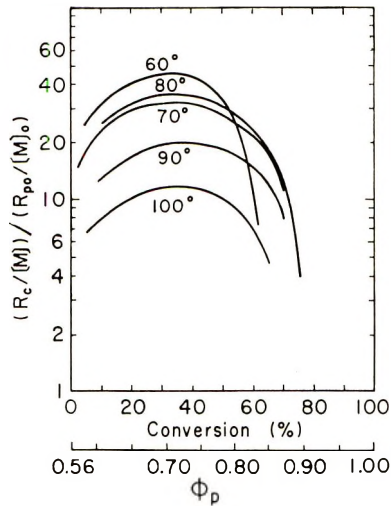
To observe the gel effect separately in the rate curves, the rate of cure  $R_c$ , namely the rate of monomer consumption, was divided by total concentration of monomers  $[M]$ , i.e., the sum of concentrations of styrene and unreacted fumarate units in polyester. The reduction was carried out also with the initial rate of copolymerization per initial total concentration of monomers in model reaction, that is, copolymerization of diethyl fumarate with styrene.<sup>19</sup> The reduced curves for the rate of cure against conversion are shown in Figures 3a-d. In the case of PES O with styrene (Fig. 3d), the polyester without unsaturation acts as a viscous medium for the polymerization of styrene.

It is clear that the rates of cure are accelerated about ten to fifty times those of uncrosslinked model reactions in the range of zero to intermediate conversion. The autoacceleration is more enhanced at lower reaction temperatures as has been shown for the polymerization of methyl methacrylate.<sup>18</sup> The increase in crosslinking density also results in a more distinct gel effect. This is evidence supporting diffusion-controlled termination in this curing reaction. The occlusion and accumulation of polymeric radicals in the curing reaction of unsaturated polyester with styrene have been demonstrated by ESR spectrometry.<sup>10</sup>

Thus, the termination reaction between polymeric radicals  $k_t$  and hence the propagation reaction of a fumarate unit in polyester chain to a growing



(a)

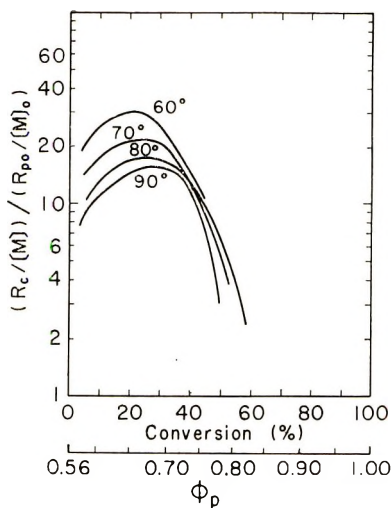


(b)

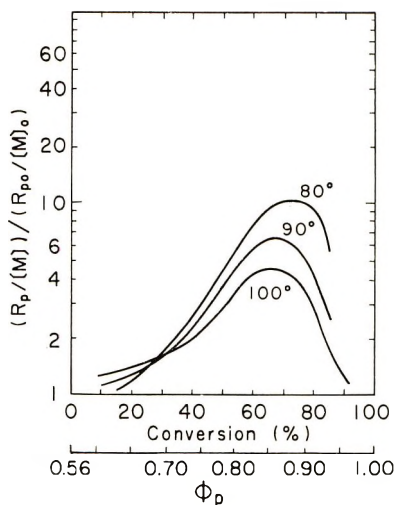
Figure 3 (continues)

polymeric radical  $k_{pf}$  are controlled by diffusion of polymeric segments from the very onset of the reaction.

It has been shown for the polymerization of methyl methacrylate<sup>18</sup> that the autoacceleration due to diffusion control for termination begins when the volume fraction of polymer in the system  $\phi_p$  is nearly equal to 0.20, diffusion control for propagation starts at  $\phi_p \approx 0.40$ , and the abrupt decrease in diffusion coefficients of monomer and primary radical of initiator occurs at  $\phi_p \approx 0.80$ . The  $\phi_p$  for the polyester fumarate-styrene system is indicated on the abscissas in Figures 3a-d. By comparing the change in reduced rate of cure against  $\phi_p$  with that for the polymerization of methyl methacrylate,



(c)



(d)

Fig. 3. Reduced rate curves against conversion or volume fraction of polymer ( $\phi_p$ ) for curing reaction of polyester fumarates (PES) with styrene (St): (a) PES 1-St; (b) PES 2-St; (c) PES 3-St; (d) PES 0-St. Curing temperatures are as indicated.

it may be concluded that the rate of propagation of styrene monomer to a polymeric radical  $k_{ps}$  is controlled by the diffusion of monomer molecule immediately after the onset of the curing reaction, since the  $\phi_p$  is larger than 0.5 at zero conversion. Though the average molecular weight of linear polyester and the kinetic chain length of curing reaction are fairly small in comparison with those of poly(methyl methacrylate), the formation of crosslinking will immediately make the viscosity of the system high enough

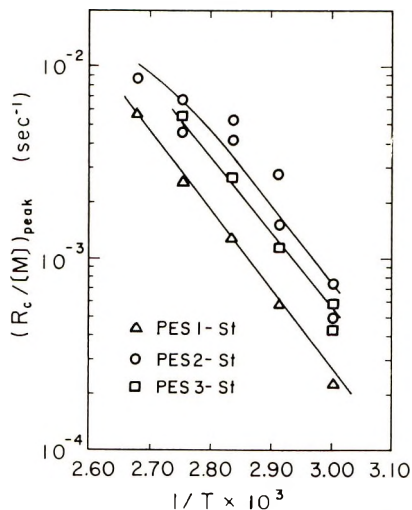


Fig. 4. Maximum rate of cure against reciprocal temperature for curing reaction of polyester fumarates with styrene.

for the diffusion control of  $k_{ps}$ . The recombination of primary radicals of the initiator is supposed to become predominant at  $\phi_p = 0.7-0.8$ . Thus, the observed constancy in rate of cure at  $60^\circ\text{C}$  can be attributed, contrary to the former discussion,<sup>12,15</sup> to the balanced effects of two diffusion-controlled reactions, that is, termination and propagation reactions. In this range of  $\phi_p$ , as has been shown previously,<sup>18</sup> the diffusion coefficient of monomer in the polymer-monomer system does not decrease so rapidly with increasing  $\phi_p$ .

The discussion of monomer reactivity ratios for the bulk curing reaction of polyester fumarate with styrene is not significant if propagation reactions as well as termination reaction are proved to be controlled by diffusion over the whole range of conversion. In this case, the propagation rate constant of fumarate unit to polymeric radical  $k_{pf}$  and that of styrene monomer to polymeric radical  $k_{ps}$  should be employed for the kinetic investigation.

Arrhenius plots of the maximum values of the rate of cure  $(R_c/[M])_{\text{peak}}$  against reciprocal temperature are shown in Figure 4. The overall activation energies were determined to be about 19 kcal/mole for all polyester fumarate-styrene systems. The activation energies for the two diffusion-controlled propagation reactions as well as the termination reaction will be discussed in the following section on the basis of the individual final degrees of conversion of styrene monomer and fumarate unit.

### Final Conversion

The final conversion  $X_f$  of isothermal cure of various polyester fumarates with styrene and the total conversion  $X_t$  as a result of adding to  $X_f$  the conversion of postcure by the temperature scanning are plotted in Figure 5



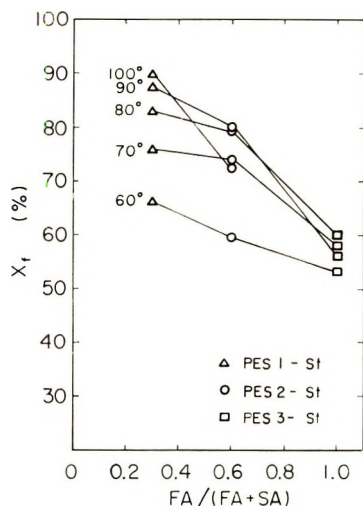


Fig. 5. Final conversion of isothermal cure ( $X_t$ ) against mole fraction of fumarate (FA) in linear polyester fumarate-succinate (SA). Temperatures of isothermal cure are as indicated.

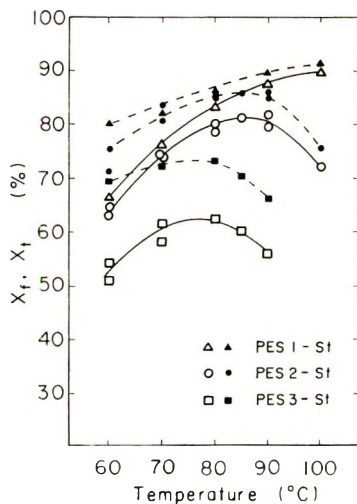


Fig. 6. Final conversion of isothermal cure  $X_t$  (open symbols) and total conversion added by temperature scanning  $X_t$  (filled symbols) against the temperature of isothermal cure.

against the fumarate content in polyesters and in Figure 6 against the reaction temperature of isothermal cure.

The final conversion of isothermal cure markedly decreases with the increase in the content of fumarate units, that is, the crosslinking density of the system. The glass transition temperatures  $T_g$  of these styrene-cured polyester fumarates are in the range of about 0 to 40°C by dilatometry.<sup>22</sup> The isothermal curing reactions did not reach 100% conversion, though all

reactions were carried out at temperatures above the  $T_g$  of the resulting crosslinked polyester. This fact would suggest that the final conversion of crosslinking reaction is regulated mainly by the crosslinking density of the system. This was also ascertained by the results of the postcure (Fig. 6). In spite of the postcure during long times at high temperatures, the reaction substantially ceased at a certain conversion, which depended mainly on the crosslinking density of the system. This has been also the case for the curing reaction of epoxy resin with diamines<sup>20</sup> and would be observed for other polymerization reactions accompanied by the network formation.

The final conversion of isothermal cure plotted against curing temperature indicates a maximum (Fig. 6). The decrease in final conversion of isothermal cure of PES 2 and PES 3 with styrene at high reaction temperatures was an unexpected result, because the mobility of polymeric segments and monomer molecules would increase to some extent at higher temperatures, which should have resulted in higher final conversions.

It is supposed, however, that the activation energy for  $k_{pf}$  would be larger than that for  $k_{ps}$  on the basis of the concept of diffusion-controlled propagation reactions over the almost whole range of conversion, together with the assumption of bigger activation energies for the diffusion of larger molecules. If this is really the case, the larger amount of fumarate units will be involved into copolymerization chains at higher temperatures, resulting in higher crosslinking densities for equal conversion. Thus, the lower final conversion will be provided for higher temperatures by assuming the cessation of reaction at equal crosslinking density in the system. This effect due to the difference of activation energies of the two propagation rate constants would be marked at 80–100°C for highly crosslinked systems, and the ordinal effect of temperature on the final conversion is predominant in other cases.

In order to verify the above supposition, the final conversion of fumarate units for the curing reaction of polyester fumarate with styrene at various reaction temperatures was determined by infrared spectroscopy. The crosslinking density of cured polyester films was also estimated by the dynamic viscoelasticity measurements.

TABLE II  
Extent of Conversion for Fumarate Units (F) and Styrene (S)  
Determined from Infrared and DSC Data

Curing temperature, °C		$\frac{D_{1650}}{D_{1730}} \times 100$	$F_p/F_0$	$S_p/S_0$	$X_f = \frac{F_p + S_p}{F_0 + S_0}$	$\frac{F_0}{F_0 + S_0}$	$\frac{F_p}{F_p + S_p}$
PES 2	Prepolymer	12.3 ± 0.4					
PES 2-St	60	6.9 ± 0.2	0.44	0.76	0.64	0.38	0.26
PES 2-St	100	5.7 ± 0.1	0.54	0.83	0.72	0.38	0.28
PES 3	Prepolymer	19.8 ± 0.4					
PES 3-St	60	12.4 ± 0.4	0.37	0.68	0.53	0.50	0.36
PES 3-St	90	11.0 ± 0.5	0.45	0.68	0.56	0.50	0.40

The fractions of reacted fumarate and styrene to the initial contents of each monomer,  $F_p/F_0$  and  $S_p/S_0$ , respectively, are calculated from the infrared analysis and summarized in Table II. The mole fraction of fumarate units in the crosslinked copolymer  $F_p/(F_p + S_p)$  apparently increases at higher reaction temperatures for the curing reaction of both PES 2 and PES 3 with styrene, supporting the above-mentioned supposition.

The dynamic modulus and  $\tan \delta$  of the cured film of PES 2 with styrene are shown in Figure 7. As the dynamic modulus  $E'$  in rubbery region should be proportional to the crosslinking density according to the theory of rubber elasticity,<sup>22</sup> the crosslinking density of the sample cured at 100°C is found to be larger by 30% than that of the sample cured at 60°C.

The reduced rate of cure with the diffusion-controlled propagation step can be expressed as the sum of the terms concerning the fumarate units and the styrene monomer and is given by eq. (1).

$$\begin{aligned} R_c/[M] &= (R_c/[M])_f + (R_c/[M])_s \\ &= k_{pf}[P\cdot]([F]/[M]) + k_{ps}[P\cdot]([S]/[M]) \end{aligned} \quad (1)$$

The maximum value of reduced rate of cure  $(R_c/[M])_{\text{peak}}$  was divided into the two terms with the same proportion as the mole fraction of each monomer in the copolymer shown in Table II. The monomer compositions at the conversion of maximum rate  $([F]/[M])_{\text{peak}}$  and  $([S]/[M])_{\text{peak}}$  were calculated from the monomer compositions in feed, those in copolymer and the conversion at the peak. By using these values the temperature dependences of  $k_{pf}[P\cdot]$  and  $k_{ps}[P\cdot]$  were calculated, and therefrom the difference of activation energies of two propagation rate constants  $\Delta E_p = E_{pf} - E_{ps}$  was determined to be 1–2 kcal/mole, as is shown in Table III.

TABLE III  
Activation Energies for Rate Constants and Diffusion Coefficients  
in Curing Reaction of Polyester Fumarate with Styrene

	$\Delta E_p =$ $E_{pf} -$					
	$E_{pf} + E_{[P\cdot]}$	$E_{ps} + E_{[P\cdot]}$	$E_{ps}$	$E_{\text{peak}}$	$E_{Df}$	$E_{Ds}$
	kcal/mole	kcal/mole	kcal/mole	kcal/mole	kcal/mole	kcal/mole
PES 2-St	15.8	15.1	0.7	18.6	7–9	6–8
PES 3-St	19.4	17.9	1.5	18.5	7–10	5–8

The above discussion is valid under the condition that the relative diffusibility of fumarate units in the polyester chain to styrene molecules does not change in the course of curing reaction. This condition would be satisfied for the range of volume fraction of polymer  $\phi_p = 0.5$ – $0.8$ . Moreover, for the systems of these volume fractions, the displacement of monomer molecules is necessarily accompanied by displacement of polymeric segments. In a simplified model for the polymer–monomer system according to Kelley and Bueche,<sup>23</sup> the two self-diffusion coefficients, i.e., that for the monomer molecules and that for the polymeric segments, will be derived

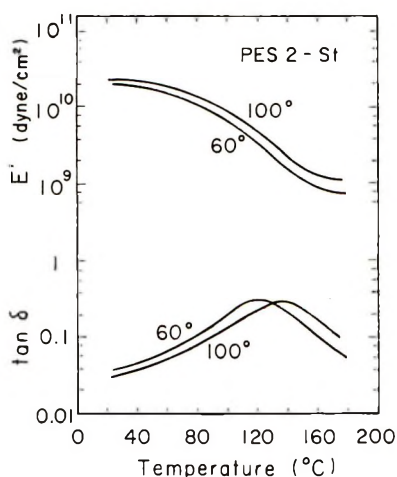


Fig. 7. Dynamic modulus  $E'$  and  $\tan \delta$  for films of PES 2 cured at 60 and 100°C with styrene.

from a single mutual diffusion coefficient of the system;<sup>24</sup> hence, the difference in the two activation energies  $\Delta E_p$  should be reduced to zero. The excess local free volume in the vicinity of monomer molecules proposed by Moor and Ferry,<sup>25</sup> which plays an important role in the diffusion-controlled polymerization of methyl methacrylate,<sup>18</sup> will increase the mobility of monomer molecules. As this effect appears more markedly in low temperatures, the excess local free volume is considered to be the cause of the difference in activation energies of the two propagation rate constants.

The overall activation energy  $E$  is expressed in eq. (2) from the ordinal kinetics of radical polymerization,

$$E = E_p + (E_d - E_t)/2 \quad (2)$$

where  $E_p$ ,  $E_d$ , and  $E_t$  are activation energies for chain propagation, initiator decomposition, and chain termination, respectively. The activation energy of propagation  $E_p$  is composed of two different activation energies  $E_{pf}$  and  $E_{ps}$ .

The activation energies for diffusion of polymeric radicals  $E_{Df}$  and styrene monomer  $E_{Ds}$  were estimated from the overall activation energies of curing reaction at maximum rates  $E'_{\text{peak}}$  in Figure 4, and the values of  $\Delta E_p$  together with  $E_d = 30$  kcal/mole for BPO.<sup>26</sup> The following two relations corresponding to the limiting cases where  $E_p$  is equal to  $E_{pf}$  and where  $E_p$  is equal to  $E_{ps}$ , respectively, were introduced into eq. (2) for the calculation:

$$E_p = E_t = E_{Df} = E_{Ds} + \Delta E_p$$

$$E_p = E_t - \Delta E_p = E_{Ds} = E_{Df} - \Delta E_p$$

The actual activation energies should lie between the values calculated for these two cases. The results are summarized also in Table III. The

values for  $E_{D_s}$  is in good accord with the activation energy for diffusion of styrene monomer in the polystyrene-styrene system ( $E = 6-8$  kcal/mole for  $\phi_p = 0.6-0.7$ ).<sup>27</sup>

The crosslinking density at final conversion  $\nu_{final}$  was calculated by considering the difference in activation energies of two propagation rate constants and is plotted in Figure 8 against mole fraction of fumarate in linear polyester fumarate-succinates.

The crosslinking densities for the hypothetical complete conversion of the samples are indicated for reference by filled symbols in Figure 8. The

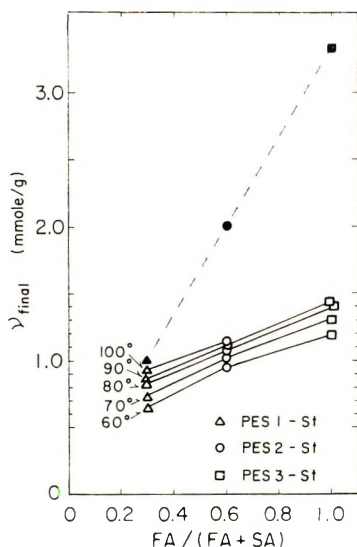


Fig. 8. Crosslinking density at final conversion ( $\nu_{final}$ ) against mole fraction of fumarate (FA) in linear polyesters composed of FA and succinate (SA). Filled symbols represent  $\nu$  at 100% conversion. Curing temperatures are as indicated.

final crosslinking density where further reaction is forbidden by the restriction of segmental mobility due to crosslinking varies slightly with temperature. The values of  $\nu_{final}$  for the curing reactions of PES 1 and PES 2 with styrene are smaller than those for the PES 3-styrene system. This may be attributed to the entanglements produced during the curing reactions by the relatively long linear segments between crosslinking points in PES 1-styrene and PES 2-styrene systems. The average number of physical entanglements per chemically crosslinked point is supposed to be 0.7 and 0.3 for PES 1-styrene and PES 2-styrene systems, respectively, by assuming that no physical entanglement occurs for PES 3-styrene system and that the isothermal curing reactions cease at certain conversions of equal crosslinking density. The iso-crosslinking density assumption about the final conversion of the curing reaction of polyester fumarate with styrene may be supported by plausible results on the average number of physical entanglements. Future investigations will deal with these aspects.

It is concluded from the above results that the propagation step as well as termination step in the curing reaction of polyester fumarate with styrene is controlled by diffusion over the almost whole range of conversion and the kinetics for this curing reaction should be reexamined from this point of view. The activation energies for the diffusion coefficients of polymeric segments and monomer molecules in the system were determined to be 7–10 and 5–8 kcal/mole, respectively. The final conversion of isothermal cure is short of completion. Its temperature dependence can be explained by the difference in the activation energies for two propagation rate constants  $k_{pf}$  and  $k_{ps}$  and by the iso-crosslinking density assumption for the cease of the curing reaction.

### References

1. K. Hamann, W. Funke, and H. Gilch, *Angew. Chem.*, **71**, 596 (1959).
2. W. Funke, S. Knödler, and R. Feinauer, *Makromol. Chem.*, **49**, 52 (1961).
3. S. Knödler, W. Funke, and K. Hamann, *Makromol. Chem.*, **57**, 192 (1962).
4. R. W. Warfield and M. C. Petree, *S. P. E. Trans.*, **1**, 3 (1961).
5. N. C. W. Judd, *J. Appl. Polym. Sci.*, **9**, 1743 (1965).
6. A. Turapov, *Vysokomol. Soedin. A*, **9**, 1525 (1967).
7. J. H. L. Henson, A. J. Lovett, and G. S. Learmonth, *J. Appl. Polym. Sci.*, **11**, 2543 (1967).
8. G. S. Learmonth, G. Pritchard, and J. Reinhardt, *J. Appl. Polym. Sci.*, **12**, 619 (1968).
9. V. F. Chuvayev, L. V. Ivanova, and P. I. Zubov, *Vysokomol. Soedin.*, **6**, 1501 (1964).
10. K. Demmler and J. Schlag, *Kunststoffe*, **57**, 566 (1967).
11. I. A. Alekseeva, G. A. Semernera, and S. S. Spasskii, *Vysokomol. Soedin.*, **5**, 1297 (1963).
12. W. Burlant and J. Hunsch, *J. Polym. Sci. A*, **2**, 2135 (1964).
13. P. Fijolka and Y. Shabab, *Kunststoffe*, **56**, 174 (1966).
14. T. Imai, *J. Appl. Polym. Sci.*, **11**, 1055 (1967).
15. M. Gorcon and I. D. McMillan, *Makromol. Chem.*, **23**, 188 (1957).
16. A. V. Tokarev and S. S. Spasskii, *Zh. Fiz. Khim.*, **33**, 249 (1959).
17. F. Lewis, C. Walling, W. Cumming, E. Briggs, and F. Mayo, *J. Amer. Chem. Soc.*, **70**, 1519 (1948).
18. K. Horie, I. Mita, and H. Kambe, *J. Polym. Sci. A-1*, **6**, 2663 (1968).
19. K. Horie, I. Mita, and H. Kambe, *J. Polym. Sci. A-1*, **7**, 2561 (1969).
20. K. Horie, H. Hiura, M. Sawada, I. Mita, and H. Kambe, *J. Polym. Sci. A-1*, **8**, 1357 (1970).
21. W. R. Sorenson and T. W. Campbell, *Preparative Methods of Polymer Chemistry*, Interscience, New York, 1968, p. 155.
22. K. Shibayama and Y. Suzuki, *J. Polym. Sci. A*, **3**, 2637 (1965).
23. F. N. Kelley and F. Bueche, *J. Polym. Sci.*, **50**, 549 (1961).
24. H. Fujita, *Fortschr. Hochpolym.-Forsch.*, **3**, 1 (1961).
25. R. S. Moor and J. D. Ferry, *J. Phys. Chem.*, **66**, 2699 (1962).
26. C. G. Swain, W. H. Stockmayer, and J. T. Clarke, *J. Amer. Chem. Soc.*, **72**, 5426 (1950).
27. A. E. Chalykh and R. M. Vasenin, *Vysokomol. Soedin.*, **8**, 1908 (1966).

Received January 13, 1970

## Syntheses and Reactions of Ferrocene-Containing Polymers. III. Cyclopolymerization of 1,1'-Divinylferrocene

TOYOKI KUNITAKE, TOSHIHIDE NAKASHIMA, and CHUJI ASO,  
*Department of Organic Synthesis, Faculty of Engineering, Kyushu University,  
Fukuoka, 812, Japan*

### Synopsis

1,1'-Divinylferrocene was polymerized with  $\text{BF}_3\text{OEt}_2$  and AIBN initiators. Polymers were separated into benzene-soluble and benzene-insoluble fractions, the latter probably being crosslinked. The polymers obtained with  $\text{BF}_3\text{OEt}_2$  were shown by infrared and NMR spectroscopy to contain both cyclized (70–80%) and uncyclized units, whereas the radical polymer consisted of more than 96% cyclized units. The benzene-soluble fraction of the cationically obtained polymer softened at temperatures below 150°C, but the insoluble fraction decomposed at 240°C. The radical polymers were stable up to 250–280°C (dec).

### INTRODUCTION

Quite recently we published some results on the cationic polymerization and copolymerization of vinylferrocene.<sup>1</sup> This monomer polymerized readily with Friedel-Crafts catalysts, consistent with the large negative  $e$  value obtained in the radical copolymerization with styrene.<sup>2</sup> Since we have been interested for some time in cyclopolymerizations of divinyl compounds,<sup>3</sup> the polymerization behavior of divinylferrocene was an interesting extension of the previous studies. At the same time, investigation on the properties of polymers containing bridged ferrocene units was considered to be of particular interest.

In this paper we report on the cationic and radical polymerizations of 1,1'-divinylferrocene. During the course of the present investigation, Sosin et al.<sup>4</sup> reported that 1,1'-diisopropenylferrocene with  $\text{BF}_3\text{OEt}_2$  catalyst gave partially soluble polymers having a cyclic structure. Very recently, while this paper was being written, they also showed that 1,1'-divinylferrocene yielded partially soluble polymers with  $\text{BF}_3\text{OEt}_2$  and azobisisobutyronitrile (AIBN), although details were not given.<sup>5</sup>

### EXPERIMENTAL

#### Materials

The monomer was prepared from ferrocene as follows. Ferrocene was acetylated with acetyl chloride and  $\text{AlCl}_3$  in methylene chloride.<sup>6</sup> The

resulting 1,1'-diacetylferrocene was reduced with  $\text{LiAlH}_4$  in tetrahydrofuran to give 1,1'-di( $\alpha$ -hydroxyethyl)ferrocene,<sup>7</sup> mp 69.0–70.1°C (lit.<sup>7</sup> 69–71°C). Divinylferrocene was then obtained by dehydrative sublimation of the dihydroxy derivative at 155°C in the presence of activated neutral alumina (Merck, Grade I) under reduced pressure (13 mm Hg).<sup>8</sup> Crude monomer obtained was purified by additional sublimation at 40°C/0.1 mm Hg, yielding red needles, mp 33.5–34.5°C (lit.<sup>8</sup> 40–41°C).

ANAL. Calcd for  $\text{C}_{14}\text{H}_{14}\text{Fe}$ : C, 70.61%; H, 5.94%. Found: C, 70.28%; H, 6.24%.

$\text{BF}_3\text{OEt}_2$  was purified by repeated distillations and AIBN was recrystallized from ethanol. Toluene, methylene chloride, and benzene were purified by the usual methods and dried over Linde molecular sieve, 3A.

### Polymerization Procedures

Cationic polymerizations were carried out in glass-stoppered Schlenk-type tubes. Solvent, a monomer solution, and a catalyst solution were charged into the polymerization vessel under nitrogen. The reaction mixture was allowed to stand at the required temperature and poured onto excess methanol after a given polymerization period. The polymer recovered was extracted with benzene. The benzene-soluble fraction was reprecipitated by methanol and dried *in vacuo*. The benzene-insoluble fraction was washed with benzene and dried.

Radical polymerizations were performed in sealed ampoules. The polymerization mixture was degassed by the freeze-thaw method under nitrogen and sealed *in vacuo*. The polymerization was terminated by pouring onto methanol containing a small amount of 2,6-di-*tert*-butyl-*p*-cresol. The work-up of the products was the same as in the cationic polymerization.

### Determination of Pendent Double Bond

The content of pendent double bonds in polymers was determined from NMR spectra in  $\text{CS}_2$  by using the ratio of the peak area at 5.3–6.1 ppm (vinyl protons) to that at 3.0–4.6 ppm (ferrocene ring protons). The lower limit of detection in this method was estimated to be about 4%, from measurement of the vinyl proton of a mixture of the polymer possessing 18% of the pendent double bond and the completely cyclized polymer.

### Characterization

Infrared and NMR spectra were obtained with Jasco DS 301 or DS 403G spectrometer and with a Varian A-60 spectrometer, respectively. Molecular weight was measured with a vapor-pressure osmometer (Mechrolab Co., Model 301A) at 37°C in benzene.



## RESULTS AND DISCUSSION

### Polymerization

In the cationic polymerization with  $\text{BF}_3\text{OEt}_2$  catalyst at  $0^\circ\text{C}$ , both benzene-soluble and benzene-insoluble fractions were obtained, as shown in Table I. The rate of polymerization appears to be much higher in methylene chloride than in toluene. The benzene-soluble fraction increased with decreasing monomer concentration and it was obtained in greater amount in methylene chloride than in toluene. The infrared spectra of the two fractions were indistinguishable, indicating that these fractions are structurally quite alike. The benzene-insoluble fractions are possibly crosslinked, since they were insoluble in common organic solvents and in concentrated sulfuric acid. (Uncrosslinked ferrocene-containing polymers such as polyvinylferrocene are readily dissolved in concentrated sulfuric acid, undergoing oxidation to the corresponding ferricinium compounds). Crosslinking probably resulted from the reaction of the pendent vinyl group. In the cationic polymerization in toluene at  $-73^\circ\text{C}$ , some precipitates were formed, but no polymer was recovered by pouring onto methanol. Some oligomeric products, however, were detected on a thin layer chromatogram.

The results of radical polymerization with AIBN are given in Table II. The relative amount of benzene-soluble fraction increased with decreasing monomer concentration in this system also.

The softening point of the soluble fraction varied widely. The soluble fraction of a polymer obtained with  $\text{BF}_3\text{OEt}_2$  (MW 3800, Table I, run 3) softened at  $110\text{--}120^\circ\text{C}$ , and a higher softening temperature ( $140\text{--}150^\circ\text{C}$ ) was observed with a sample of higher molecular weight (MW 10,000, run 4). The soluble polymers obtained with AIBN decomposed at  $250\text{--}280^\circ\text{C}$  without softening. This thermal behavior was similar to that of the benzene-insoluble fractions obtained in the radical and cationic catalyst systems [ $240\text{--}280^\circ\text{C}$  (dec)]. These data suggest that the softening temperature of the soluble polymers is determined by the molecular weight and/or extent of cyclization.

### Polymer Structure

Infrared spectra of benzene-soluble polymers are shown in Figure 1. The characteristic peak of the double bond stretching at  $1630\text{ cm}^{-1}$  disappeared, being hidden in the broad peak group at  $1600\text{--}1700\text{ cm}^{-1}$ . The peaks at  $890$  and  $980\text{ cm}^{-1}$  characteristic of the vinyl group are barely discernible for polymers obtained with  $\text{BF}_3\text{OEt}_2$ , but are completely lost in the radical polymer. Neuse and co-workers<sup>9</sup> observed that a broad absorption at around  $815\text{ cm}^{-1}$  exhibited by ferrocene derivatives split into two peaks at  $800$  and  $860\text{ cm}^{-1}$  in a large number of heterobridged ferrocene compounds. Accordingly, partial splitting of the  $820\text{ cm}^{-1}$  peak to  $810$  and  $850\text{ cm}^{-1}$ , which was observed in the cationically obtained polymer, probably shows the existence of the cyclized structure. These in-

TABLE I  
 Polymerization of 1,1'-Divinylferrocene with  $\text{BF}_3\text{OEt}_2$  at 0°C

Run	$[\text{BF}_3\text{OEt}_2]$ , mole/l.	[Monomer], mole/l.	Solvent	Time, hr	Conversion, % <sup>a</sup>	M.W.	PDB, % <sup>b</sup>	Polymer		Softening point, °C
								$D_{810}/D_{820}$	$D_{850}/D_{820}$	
1	0.05	1.0	toluene	0.5	S, 1.5 I, 2.5	—	—	—	—	100-110 240 (dec)
2	0.025	0.5	toluene	0.67	I, 9	—	—	—	—	240 (dec)
3	0.01	0.2	toluene	13.0	S, 11 <sup>c</sup> I, 24	3,800	33	0.68	0.17	110-120 240 (dec)
4	0.01	0.2	$\text{CH}_2\text{Cl}_2$	8.5	S, 73 I, 1	10,000	18	0.83 <sup>d</sup>	0.22 <sup>d</sup>	140-150 240 (dec)

<sup>a</sup> S and I denote percentage conversions of the benzene-soluble and benzene-insoluble fractions, respectively.

<sup>b</sup> Pendent double bond content as determined from NMR peaks in  $\text{CS}_2$  solution.

<sup>c</sup> ANAL. Calcd for  $(\text{C}_{14}\text{H}_{14}\text{Fe})_n$ : C, 70.61%; H, 5.94%. Found: C, 71.00%; H, 5.97%.

<sup>d</sup> After partial hydrogenation,  $D_{810}/D_{820} = 0.83$  and  $D_{850}/D_{820} = 0.23$ .

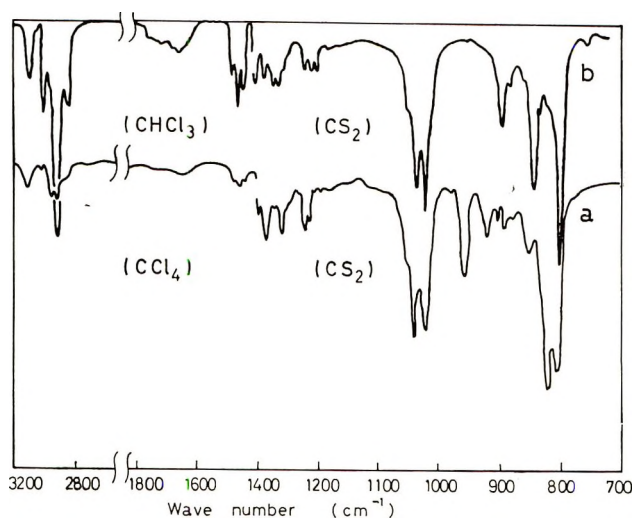
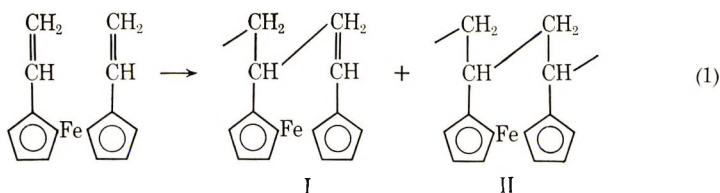


Fig. 1. Infrared spectra of polydivinylferrocene: (a) Table I, run 4, soluble fraction; (b) Table II, run 8, soluble fraction;

frared data indicate that the polymers obtained with  $\text{BF}_3\text{OEt}_2$  catalyst consist of the cyclized and uncyclized units (I and II), as shown in eq. (1).



Since the above splitting was almost complete in the radical polymer and a peak at  $820 \text{ cm}^{-1}$  was very small as seen in Figure 1b, the radical polymer may be composed almost completely of the cyclic units. New peaks appeared at  $800$  and  $840 \text{ cm}^{-1}$  for the radical polymer. Thus, the relative intensities  $D_{800}/D_{820}$  and  $D_{840}/D_{820}$  in the infrared spectrum may be related to the extent of cyclization. For example, a  $\text{BF}_3\text{OEt}_2$  polymer (run 4) showed smaller values ( $D_{810}/D_{820} = 0.8$ ,  $D_{850}/D_{820} = 0.25$ ) than radical polymers ( $D_{800}/D_{820} \geq 3.95$ ,  $D_{840}/D_{820} \geq 1.98$ ), as shown in Table II.

This is further supported by the NMR data. The NMR spectrum of polymers obtained with  $\text{BF}_3\text{OEt}_2$  (Fig. 2a) clearly shows the presence of the pendent vinyl group (peaks at 5.3–6.1 ppm), together with the ferrocene ring protons (3.0–4.6 ppm) and the aliphatic protons. The ratio of the peak area of vinyl plus aliphatic protons to that of ring protons (0.75) agreed well with the calculated value of 0.75. The amounts of the pendent double bond (PDB), which were determined by comparing the peak area of vinyl protons with that of ring protons, are included in Table I.

TABLE II  
Polymerization of 1,1'-Divinylferrocene in Benzene with AIBN at 60°C

Run	[AIBN] × 10 <sup>3</sup> mole/l.	[Mono- mer], mole/l.	Time, hr	Conver- sion, % <sup>a</sup>	Polymer		Decom- position temp, °C
					IR data in CS <sub>2</sub>		
					<i>D</i> <sub>800</sub> / <i>D</i> <sub>820</sub>	<i>D</i> <sub>840</sub> / <i>D</i> <sub>820</sub>	
5 <sup>b</sup>	2.0	1.00	22	S 9	—	—	270
				I 35	—	—	270
6	0.66	0.50	20	S 8	3.95	1.98	270
				I 23	—	—	270
7	0.41	0.35	20	S 10	4.78	2.34	280
				I 15	—	—	260
8	0.25	0.20	20	S 11 <sup>c</sup>	6.26	3.11	280
				I 8	—	—	280
9	0.34	0.14	8	S 6 <sup>d</sup>	—	—	250
10	0.10	0.08	40	S 18	6.87	3.49	280
				I 5	—	—	270

<sup>a</sup> S, I as in Table I. The pendent double bond was not detected in the NMR spectra of the soluble fractions. The limit of detection was about 4%.

<sup>b</sup> Polymerization temperature 70°C.

<sup>c</sup> ANAL. Found: C, 70.77%; H, 6.17%.

<sup>d</sup> Molecular weight: 21,000.

The PDB content varied with the polymerization conditions. With BF<sub>3</sub>OEt<sub>2</sub> catalyst, it was 33% in toluene and 18% in methylene chloride. Such a solvent effect on cyclization is very interesting, because a similar effect was observed in the cationic cyclopolymerization of *o*-divinylbenzene.<sup>10</sup> The vinyl proton was not detected in the radical polymers, as seen from Figure 2*b*. Since the limit of detection of the PDB content was about 4% in the present experimental technique, the PDB content of the radical polymers was concluded to be less than 4% (Table II). On the other hand, the *D*<sub>800</sub>/*D*<sub>820</sub> and *D*<sub>840</sub>/*D*<sub>820</sub> values in the infrared spectra of these polymers increased with decreasing monomer concentration, as shown in Table II.

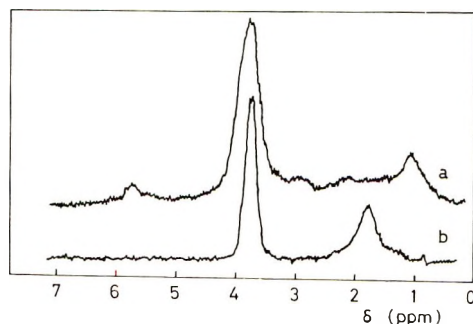


Fig. 2. NMR spectra of polydivinylferrocene in CS<sub>2</sub>: (a) Table I, run 4, soluble fraction; (b) Table II, run 10, soluble fraction.

Accordingly, it may be that these ratios are quite sensitive to the content of the cyclic unit and reflect small differences in the extent of cyclization which are difficult to detect by NMR spectroscopy.

Interestingly, aliphatic proton patterns in NMR spectra are different for the polymers obtained with  $\text{BF}_3\text{OEt}_2$  and AIBN (Figs. 2a and 2b). This may reflect a difference in the polymer conformation influenced by the degree of cyclization.

Attempted hydrogenation of the pendent double bond met with partial success. When a benzene solution of a  $\text{BF}_3\text{OEt}_2$  polymer (Table I, run 4) was hydrogenated over Raney Ni (1 atm, room temperature, 72 hr.), the PDB content decreased from 18% to 13%, as measured by NMR spectroscopy, and the intensity of the infrared vinyl absorptions at 890 and 980  $\text{cm}^{-1}$  decreased. However, the  $D_{810}/D_{820}$  and  $D_{850}/D_{820}$  values remained unchanged, supporting the above-mentioned supposition that these intensity ratios can be measures of the extent of cyclization.

In conclusion, 1,1'-divinylferrocene was shown to polymerize with cationic and free-radical initiators, yielding polymers containing both cyclized and uncyclized units. The extent of cyclization varied with the polymerization conditions. It would be interesting to know what factors affect the extent of cyclization, as was determined previously for *o*-divinylbenzene. The relation between the extent of cyclization and the polymerization conditions is currently being investigated in these laboratories.

### References

1. C. Aso, T. Kunitake, and T. Nakashima, *Makromol. Chem.*, **124**, 232 (1969).
2. C. Aso, T. Kunitake, and T. Nakashima, *Kogyo Kagaku Zasshi*, **72**, 1411 (1969).
3. C. Aso, *Kogyo Kagaku Zasshi*, **70**, 1920 (1967).
4. S. L. Sosin, V. V. Korshak, and T. M. Frunze, *Dokl. Akad. Nauk SSSR*, **179**, 1124 (1968).
5. S. L. Sosin and L. V. Dzhashi, paper presented at IUPAC Symposium on Macromolecular Chemistry, Budapest, 1969; *Preprints*, I, p. 327 (1969).
6. M. Rosenblum and R. B. Woodward, *J. Amer. Chem. Soc.*, **80**, 5443 (1958).
7. K. Yamakawa, H. Ochi, and K. Arakawa, *Chem. Pharm. Bull. (Japan)*, **11**, 905 (1963).
8. M. D. Rausch and A. Siegel, *J. Organometal. Chem.*, **11**, 317 (1968).
9. E. Neuse, R. K. Crossland, and K. Koda, *J. Org. Chem.*, **31**, 2409 (1966).
10. C. Aso, T. Kunitake, Y. Matsuguma, and Y. Imaizumi, *J. Polymer Sci. A-1*, **6**, 3049 (1968).

Received August 19, 1969

Revised February 17, 1970

## Studies on Polyesterification Reactions: Calculation of the Rates of Reverse Reactions

I. VANCSÓ-SZMERCSÁNYI, E. MAKAY-BÖDY, E. SZABÓ-RÉTHY,  
and P. HIRSCHBERG, *Research Institute for the Plastics Industry,  
Budapest, Hungary*

### Synopsis

Reactions between dicarboxylic acids and diols in the melt and leading to an equilibrium yield quantitative results which may be applied to the kinetics of some partial reactions of polyesterification. The relationship of the rate constants of the forward and the reverse reaction as well as of the equilibrium constant furnish valid results both in the absence of catalyst and in the presence of acid or basic catalysts. The values obtained for the energy of activation of the forward and the reverse reaction and of the overall reaction ( $13 \pm 1$  kcal/mole) also are in good agreement.

In our previous papers<sup>1-3</sup> we described qualitative results and some considerations in connection with the overall polyesterification reaction, with the reverse reaction, and with polyesterification as an equilibrium reaction. We established a connection between the hydrolysis sensitivity of the ester bonds and the rate of the reverse reaction.

Our next endeavor is to give a quantitative form to the qualitative results and to complement the available results according to novel points of view.

### EXPERIMENTAL RESULTS AND DISCUSSION

#### Calculating the Kinetic Data of the Reverse Reaction from Polyesterification Leading to Equilibrium

Reactions between various diols and dicarboxylic acids were carried out according to the previously described experimental method up to the establishment of equilibrium.<sup>1</sup> Kinetic calculations were carried out from the decrease of the COOH concentration, determined as a function of time, on the basis of the following considerations.

In an equilibrium condensation process the overall reaction rate is determined by the difference of the rates of the forward reaction and of hy-

drolysis. Assuming a second-order reaction,\* eq. (1) may be written for equivalent initial amounts of diol and dicarboxylic acid:

$$dx/dt = k_d(a - x)^2 - k_h x^2 \quad (1)$$

where  $x$  is the amount of COOH groups having reacted by time  $t$  (moles COOH/1000 g) or the number of ester bonds formed by time  $t$  (ester bonds/1000 g),  $a$  is the initial acid concentration (moles COOH/1000 g), and  $k_d$  and  $k_h$  are, respectively, the rate constants of the forward reaction and hydrolysis.

Solving the differential equation, eq. (1), yields eq. (2):

$$\frac{a - 2c}{2c(a - c)} \ln \frac{[(a - 2c)/a]x - (a - c)}{x - (a - c)} = (k_d - k_h)t \quad (2)$$

where  $c$  is the equilibrium concentration of acid (moles COOH/1000 g).

By substituting into eq. (2) the related values of  $t$  and  $x$  which were measured during the condensation which leads to an equilibrium, but before this equilibrium, the difference of the two rate constants,  $k_d - k_h$ , may be calculated. The determination of the equilibrium constant, on the other hand, also yields the ratio of the two rate constants:

$$K = k_d/k_h \quad (3)$$

From eqs. (2) and (3) the values of  $k_d$  and  $k_h$  may be determined separately.

In view of the experimental conditions (condensation in a melt), we had some reservations at first concerning the applicability of the presented method of calculation. However, the results showed a surprising and convincing logical connection as well as agreement with previous experimental data.

### Kinetic Data Obtained from the Equilibrium Condensation of Various Pairs of Reagents

The data obtained by the described calculation are presented in Table I.

The quantitative results obtained as a function of the chain length of the reagents are in accordance with the previously described qualitative considerations.<sup>1,2</sup> Figures 1 and 2 present some results of Table I. Figure 1 shows the effect of the chain length of glycol. The adopted values are referred to the kinetic constants obtained with ethylene glycol. Thus it is

\* In our previous paper, a reaction order of 2.5 was determined for polyesterifications of succinic, adipic, or sebacic acid with diols.<sup>1</sup> They were protoncatalytic reactions. For equilibrium condensations however, conversion of COOH groups of the above dicarboxylic acids did not exceed 60%, as described in a previous paper.<sup>2</sup> Thus, formation of polyesters could not be considered. Kinetically, this initial stage of the reaction can be treated as mono- or diesterification. It is reasonable from the experimental results as well as from the fact that a high amount of free COOH is present in the initial stage which leads to the conclusion that this reaction is not controlled by the proton concentration. Accordingly, to this initial stage or to the equilibrium esterification, second-order kinetics apply.

TABLE I  
Kinetic Data Calculated from the Esterification to an Equilibrium Value of Various Dicarboxylic Acids and Diols at 180°C

System	$K_{eq}$	$k_d \times 10^3,$ (eq/1000 g) <sup>-1</sup> min <sup>-1</sup>	$k_h \times 10^3,$ (eq/1000 g) <sup>-1</sup> min <sup>-1</sup>	$k_d - k_h$ $\times 10^3,$ (eq/1000 g) <sup>-1</sup> min <sup>-1</sup>
Succinic acid-ethylene glycol	1.37	4.65	3.40	1.25
Succinic acid-1,6-hexane-diol	4.18	8.64	2.07	6.56
Adipic acid-ethylene glycol	1.47	3.70	2.58	1.13
Adipic acid-butylene glycol	2.71	4.64	1.71	2.93
Adipic acid-diethylene glycol	1.40	3.45	2.47	0.98
Adipic acid-1,6 hexane-diol	3.48	5.48	1.57	4.09
Adipic acid-triethylene glycol	1.44	3.09	2.15	0.95
Sebacic acid-ethylene glycol	1.41	3.09	2.19	0.89
Sebacic acid-1,4 butylene glycol	2.65	4.32	1.63	2.69
Sebacic acid-1,6 hexane-diol	3.77	6.37	1.69	4.68

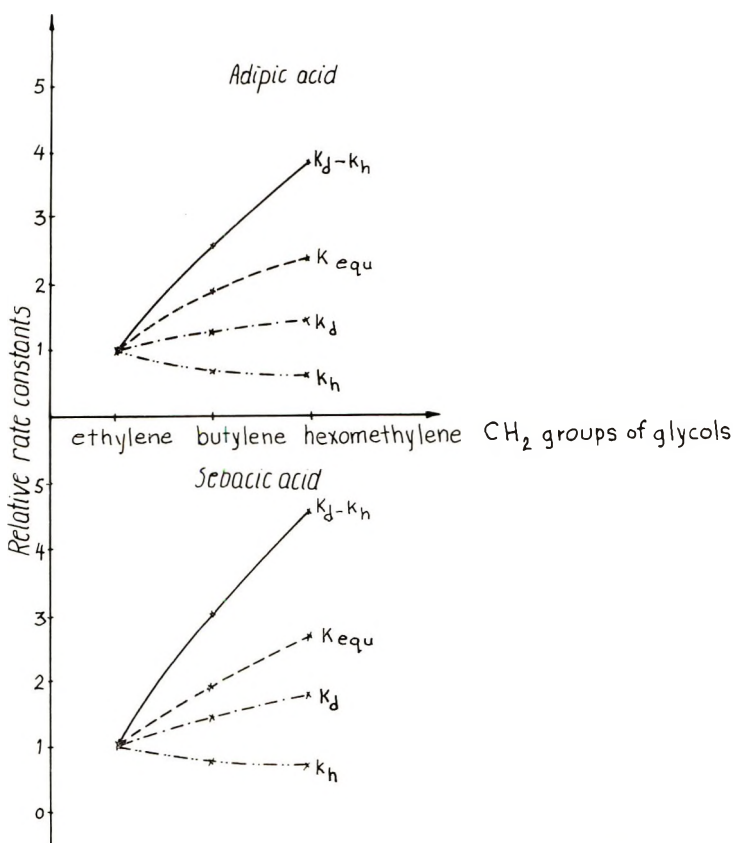


Fig. 1. Effect of the chain length of the glycols on kinetic data.



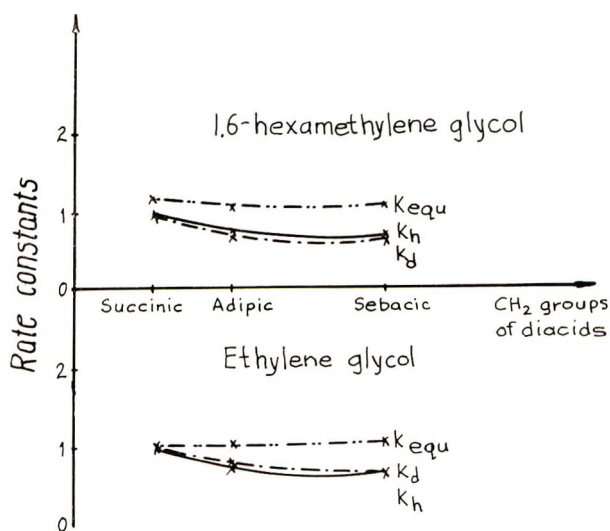


Fig. 2. Effect of the chain length of the acids on kinetic data.

not possible to compare the curves with each other; each curve must be analyzed by itself. The figures prove that the rate constants of the forward reaction and the values of the equilibrium constants increase considerably with the growth of the chain length of the glycol; at the same time the rate constant of hydrolysis decreases.

Figure 2 shows the effect of the chain length of the acid. The rate constants decrease with increasing chain length, with the exception of the equilibrium constant, which is practically independent of chain length in the examined cases.

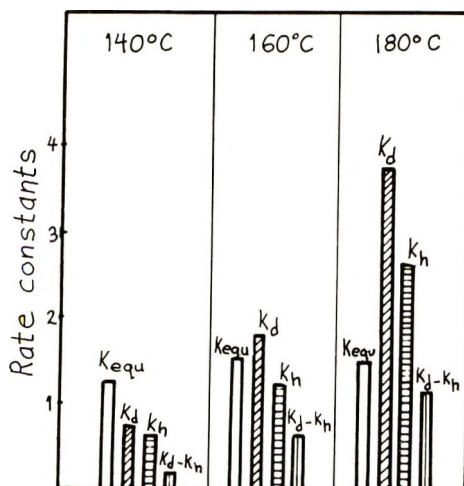


Fig. 3. Kinetic data obtained in the equilibrium reaction of adipic acid and ethylene glycol at various temperatures.

### Influence of Temperature on the Reaction Rate

Figure 3 shows the kinetic data obtained in the equilibrium reaction of adipic acid and ethylene glycol at various temperatures. As can be seen, the equilibrium constant is practically independent of temperature. This is possible only if the energies of activation of the forward and reverse reactions are identical.

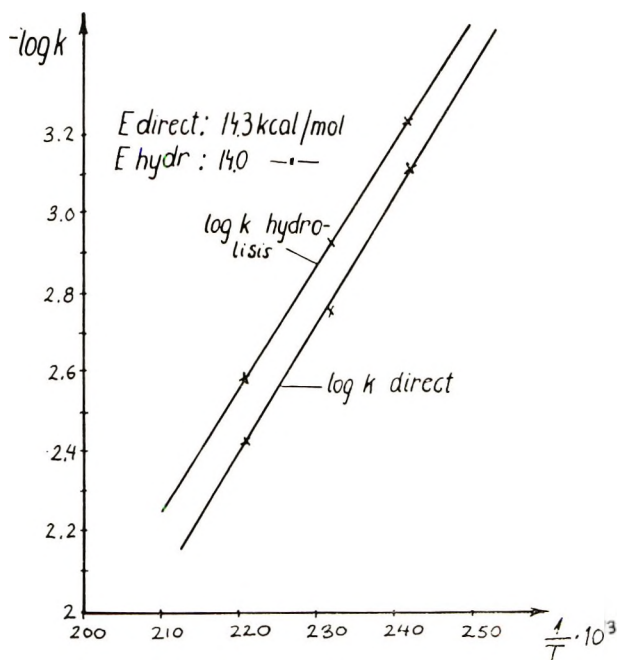


Fig. 4. Plot of  $\log k_d$  and  $\log k_h$  as a function of  $1/T$ .

When the values of the logarithms of the rate constants of hydrolysis and of the direct reaction are plotted as a function of the reciprocal of absolute temperature (Fig. 4), the obtained lines are parallel to each other. The computed values are: for direct esterification,  $E = 14.3$  kcal/mole; for hydrolysis,  $E = 14.0$  kcal/mole. In our previous work<sup>4</sup> we obtained values of about 13 kcal/mole for the energy of activation of polyesterification of numerous pairs of reagents. Considering further the fact that an energy of activation of 13.5 kcal/mole has been calculated for the basic hydrolysis of the polyester prepared from adipic acid and hexanediol, the agreement is really surprising.

### Influence of Catalysts on the Reaction Rate

Esterification leading to an equilibrium has been carried out in some cases also in the presence of basic or acid catalysts. The calculated kinetic constants are logical also in these cases. Basic catalysts (e.g., KOH)

generally did not influence the rate of the forward reaction or increased or even decreased it slightly; the value of the rate constant of hydrolysis, was increased, however. An acid catalyst (*p*-toluenesulfonic acid) considerably increased the rate constant of hydrolysis and even more definitely the rate of the forward reaction; e.g., in the reaction of adipic acid with ethylene glycol at 140°C. without a catalyst we obtained

$$k_d = 0.73 \times 10^{-3}/\text{eq}/1000 \text{ g}/\text{min}$$

$$k_h = 0.59 \times 10^{-3}/\text{eq}/1000 \text{ g}/\text{min}$$

$$k_d/k_h = 1.3$$

while under the influence of para toluene sulfonic acid the respective constants were

$$k_d = 3.69 \times 10^{-3}/\text{eq}/1000 \text{ g}/\text{min}$$

$$k_h = 2.04 \times 10^{-3}/\text{eq}/1000 \text{ g}/\text{min}$$

$$k_d/k_h = 1.8$$

The influence of alcoholysis on the reverse reaction rate has not yet been studied; however we intend to do so in the future.

### References

1. E. Makay-Bödi and I. Vancsó-Szmercsányi, *Europ. Polym. J.*, **5**, 145 (1969).
2. I. Vancsó-Szmercsányi, K. Maros-Gréger, and E. Makay-Bödi, *Europ. Polym. J.*, **5**, 155 (1969).
3. E. Makay-Bödi and I. Vancsó-Szmercsányi, *Magyar Kémiai Polyóirat*, **75**, 27 (1969).
4. I. Vancsó-Szmercsányi and E. Makay-Bödi, in *Macromolecular Chemistry, Prague 1965 (J. Polym. Sci. C, 16)*, O. Wichterle and B. Sedláček, Eds., Interscience, New York, 1968, p. 3709.

Received December 12, 1969

## Polymérisation et Copolymérisation Cationiques des Methylindenes

ERNEST MARÉCHAL, *Institut National Supérieur de Chimie Industrielle  
de Rouen, Mont-Saint-Aignan 76, France*

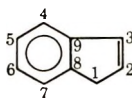
### Synopsis

A study of cationic polymerization and copolymerization of methylindenes has been carried out by experimental methods and by means of quantum chemistry. The study showed a great variation among initiators in efficiency for the various monomers. The study of the effect of temperature on polymerization was carried out for dimethyl-5,7-indene. Polymerization enthalpies and reactivity ratios were determined; the values that were obtained allowed a classification of methylindenes with regard to their reactivity toward a single cation. Total electron densities, free valences, and mobile bond orders, frontier electron densities, and superdelocalizabilities on position 1 and 2 were calculated for all methylindenes. In determining location energies of the electronic double bond in position 2 and the stabilization energies at the time of the attack by a cation, a theoretical classification of the monomers with respect to their reactivity in cationic polymerization was obtained. The agreement between calculation and experimental results is shown to be satisfactory.

Nous avons depuis plusieurs années entrepris l'étude systématique de l'influence des substituants de l'indène sur sa polymérisation et sa copolymérisation cationiques. La polymérisation des méthyl-1-, méthyl-2- et méthyl-3-indènes<sup>1</sup> nous a montré qu'il y avait un abaissement considérable des masses molaires des polymères obtenus avec ces trois monomères par rapport à ceux obtenus avec l'indène. De plus, la copolymérisation cationique du méthyl-3-indène<sup>2</sup> avec l'indène nous a permis d'établir l'existence d'un effet pénultième.

Dans le travail actuel nous allons d'une part, donner des résultats relatifs à des indènes méthylés sur le noyau phényle, d'autre part, exposer une étude théorique de l'ensemble des méthyl-indènes faite à l'aide des méthodes de la chimie quantique.

Dans tout ce qui suit, la numérotation adoptée pour le cycle indénique est donnée par le schéma I. Les lettres M, D, T, désignent respectivement les dérivés monométhylés, diméthylés, et triméthylés de l'indène. Chacune d'elles est suivie des chiffres indiquant les positions des groupes méthyles.



I

[M], [A] et  $R$  désignent respectivement les concentrations molaires en monomère et en amorceur (exprimées en moles par litre de solution totale) et le rendement en polymère précipité par le méthanol.  $[\eta]$  désigne la viscosité intrinsèque exprimée en 100 ml/g. Toutes les polymérisations sont faites dans le chlorure de méthylène. Les préparations des monomères ont été décrites dans nos travaux précédents.<sup>3-6</sup>

## HOMOPOLYMÉRISATION DES MÉTHYL INDÈNES

### Influence de la Nature de l'Amorceur

Il est remarquable de constater que l'efficacité relative des amorceurs est extrêmement différente lorsqu'on passe d'un monomère à un autre.

Les Tableaux I et II donnent respectivement les résultats obtenus avec divers méthylindènes à  $-30$  et à  $-72^\circ\text{C}$ . Lorsque le rendement n'est pas

TABLEAU I<sup>a</sup>

Nature de l'amorceur	Indène		D <sub>46</sub> [ $\eta$ ]	D <sub>47</sub> [ $\eta$ ]	D <sub>56</sub> [ $\eta$ ]	D <sub>57</sub>		T <sub>4,67</sub> [ $\eta$ ]
	R, %	[ $\eta$ ]				R, %	[ $\eta$ ]	
TiCl <sub>4</sub>	100	0,56	1,35	1,3	0,39	95	0,09	0,25
SnCl <sub>4</sub>	45	0,59	1,50	1,6	0,34	100	0,08	0,23
BF <sub>3</sub> ·O(CH <sub>3</sub> ) <sub>2</sub>	12	—	2,50	3,60	0,46	0	—	0,26
BF <sub>3</sub> ·O(C <sub>2</sub> H <sub>5</sub> ) <sub>2</sub>	—	—	2,20	3,5	0,45	0	—	0,31
H <sub>2</sub> SO <sub>4</sub>	8	0,20	1,15	1,0	0,10	65	0,09	0,38
AlBr <sub>3</sub>	—	—	—	—	—	100	0,12	—
SbCl <sub>5</sub>	—	—	—	—	—	100	0,09	—

<sup>a</sup> Les résultats ont été obtenus avec [M] = 0,224 et [A] = 0,01, la température de polymérisation étant  $-30^\circ\text{C}$ .

TABLEAU II<sup>a</sup>

Nature de l'amorceur	In-dène [ $\eta$ ]	M <sub>7</sub>			D <sub>47</sub>			D <sub>57</sub>			T <sub>4,67</sub> [ $\eta$ ]	
		M <sub>5</sub> [ $\eta$ ]	M <sub>6</sub> [ $\eta$ ]	R, %	D <sub>46</sub> [ $\eta$ ]	R, %	D <sub>56</sub> [ $\eta$ ]	R, %	[ $\eta$ ]			
TiCl <sub>4</sub>	1,57	0,5	2,2	100	0,82	0,95	100	1,8	0,95	95	0,15	0,83
SnCl <sub>4</sub>	0,95	0,8	—	—	—	1,05	100	1,9	1,05	100	0,07	0,65
BF <sub>3</sub> ·O-(CH <sub>3</sub> ) <sub>2</sub>	0	—	2,7	100	0,62	2,40	45	1,5	2,40	0	—	0,95
BF <sub>3</sub> ·O-(C <sub>2</sub> H <sub>5</sub> ) <sub>2</sub>	0	0,8	4,5	90	0,48	2,30	100	3,4	2,30	0	—	1,73
H <sub>2</sub> SO <sub>4</sub>	0,50	<sup>b</sup>	2,2	—	—	1	100	1,3	1,00	65	0,11	0,62
AlBr <sub>3</sub>	—	—	—	—	—	—	—	—	—	100	0,17	—
SbCl <sub>5</sub>	—	—	—	—	—	—	—	—	—	100	0,13	—

<sup>a</sup> Les résultats ont été obtenus en travaillant à  $-72^\circ\text{C}$  et avec [M] = 0,224 et [A] = 0,01. Cependant avec le triméthyl-4,6,7-indène (T<sub>4,67</sub>) on a pris [M] = 0,422 et [A] = 0,02 lorsque les éthers de trifluorure de bore étaient utilisés comme amorceur. Enfin avec les méthyl-5-, méthyl-6- et méthyl-7-indènes on a pris [M] = 0,384 et [A] = 0,05 quand l'amorceur était TiCl<sub>4</sub> ou SnCl<sub>4</sub>.

<sup>b</sup> Le rendement est voisin de zéro, aucune détermination de viscosité n'a pu être faite.

indiqué c'est qu'il est de 100%. Après chaque tableau nous avons indiqué les conditions de concentrations dans lesquelles ont été faites les diverses polymérisations.

### Influence de la Température de Polymérisation

Les résultats sont très variables avec la nature du monomère et même de l'amorceur. Rappelons tout d'abord que pour l'indène<sup>7</sup> (comme pour la plupart des monomères polymérisés cationiquement) on observe une diminution de la masse molaire des polymères obtenus quand la température s'élève.

En ce qui concerne le tétraméthyl-4,5,6,7-indène on a observé, lors de sa polymérisation amorcée par  $\text{TiCl}_4$  une indépendance totale de la valeur de  $[\eta]$  vis à vis de la température de polymérisation.

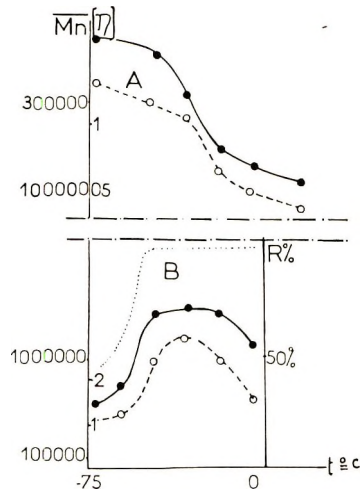


Fig. 1. Influence de la température de polymérisation dans le cas du diméthyl-1,7-indène avec (A) amorceur  $\text{TiCl}_4$ , et (B) amorceur  $\text{BF}_3 \cdot \text{O}(\text{CH}_3)_2$ : (---)  $\overline{M}_n$ ; (—)  $[\eta]$ ; (...)  $R$ .

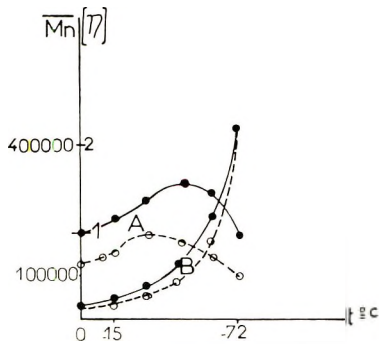


Fig. 2. Influence de la température de polymérisation dans le cas des (A) diméthyl-4,6- et (B) diméthyl-5,6-indènes: (---)  $\overline{M}_n$ ; (—)  $[\eta]$ ; amorceur  $[\text{TiCl}_4] = 0.01$ .

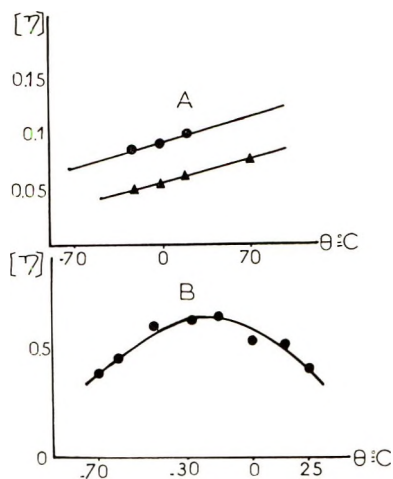


Fig. 3. Influence de la température de polymérisation dans le cas de (A) diméthyl-5,7-indène, amorceur  $\text{SnCl}_4$ , Solvants (●)  $\text{CH}_2\text{Cl}_2$  et (▲) dichloro-1,2-éthane; (B) triméthyl-4,6,7 indène, amorceur  $\text{TiCl}_4$ .

Les variations du rendement et de  $[\eta]$  en fonction de la température de polymérisation sont données par la Figure 1 pour le diméthyl-4,7-indène et par la Figure 2 pour les diméthyl-4,6- et diméthyl-5,6-indènes. Enfin la Figure 3 donne les résultats pour le diméthyl-5,7-indène et le triméthyl-4,6,7-indène.

L'analyse de ces différentes courbes est faite dans la conclusion.

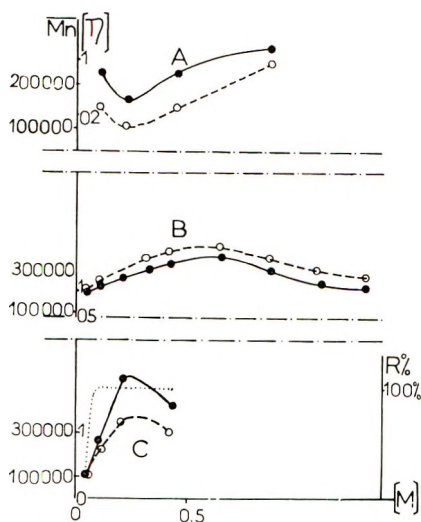


Fig. 4. Influence de la concentration en monomère sur la polymérisation du diméthyl-4,7-indène à (A)  $0^\circ\text{C}$ , (B)  $-30^\circ\text{C}$  et (C)  $-72^\circ\text{C}$ : (---)  $\overline{M}_n$ ; (—)  $[\eta]$ ; (...)  $R$ .  $[\text{TiCl}_4] = 0,01$ .

## Influence de la Concentration en Monomère et en Amorceur

Rappelons tout d'abord que lors de la polymérisation de l'indène<sup>3,7</sup> on observe l'existence d'un maximum de  $[\eta]$  pour une valeur optimum de chacun des deux facteurs  $[M]$  et  $[A]$ . En ce qui concerne le tétraméthyl-

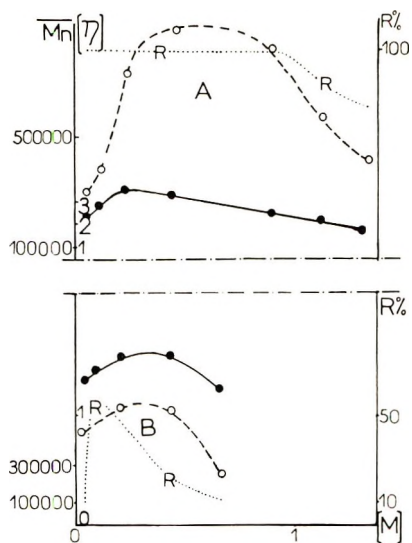


Fig. 5. Influence de la concentration en monomère sur la polymérisation du diméthyl-4,7-indène à (A)  $-30^{\circ}\text{C}$  et (B)  $-72^{\circ}\text{C}$ : (---)  $\overline{M}_n$ ; (—)  $(\eta)$ ; (...)  $R$ .  $[\text{BF}_3, \text{O}(\text{CH}_3)_2] = 0.01$ .

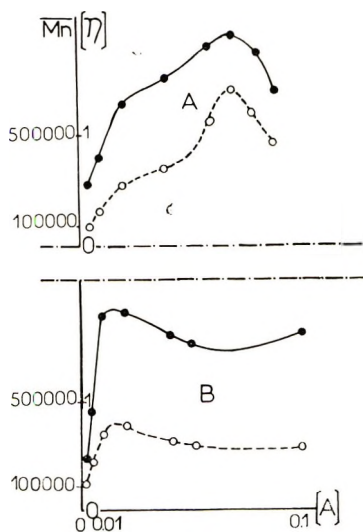


Fig. 6. Influence de la concentration en amorceur sur la polymérisation du diméthyl-4,7-indène à (A)  $-30^{\circ}\text{C}$  et (B)  $-72^{\circ}\text{C}$ : (---)  $\overline{M}_n$ ; (—)  $(\eta)$ .  $[M] = 0,224$ ; amorceur  $\text{TiCl}_4$ .



4,5,6,7-indène on trouve une indépendance à peu près totale de  $[\eta]$  vis à vis de  $[M]$  et une légère croissance de  $[\eta]$  avec  $[A]$ .

Les Figures 4, 5, 6 et 7 donnent les résultats relatifs au diméthyl-4,7-indène, les Figures 8 et 9 ceux relatifs au diméthyl-4,6-indène et enfin les Figures 10 et 11 ceux relatifs au diméthyl-5,6-indène.

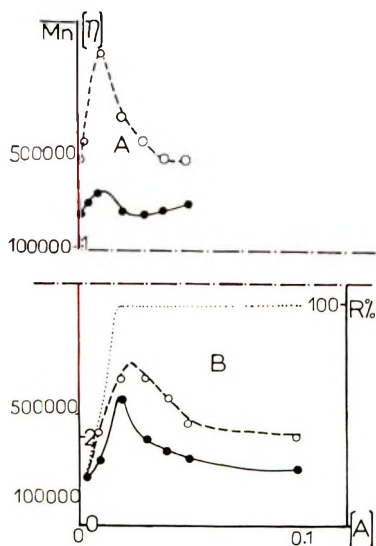


Fig. 7. Influence de la concentration en amorceur sur la polymérisation du diméthyl-4,7-indène à (A)  $-30^{\circ}\text{C}$  et (B)  $-72^{\circ}\text{C}$ : (---)  $\overline{M}_n$ ; (—)  $[\eta]$ .  $[M] = 0,224$ ; amorceur  $\text{BF}_3 \cdot \text{O}(\text{CH}_3)_2$ .

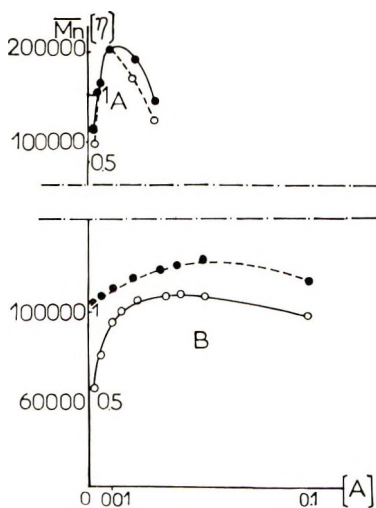


Fig. 8. Influence de la concentration en amorceur sur la polymérisation du diméthyl-4,6-indène à (A)  $-30^{\circ}\text{C}$  et (B)  $-72^{\circ}\text{C}$ : (---)  $\overline{M}_n$ ; (—)  $[\eta]$ .  $[M] = 0,224$ ; amorceur  $\text{TiCl}_4$ .

Dans le cas du méthyl-6-indène (polymérisation amorcée par le tétrachlorure de titane ou l'éthérate de trifluore de bore) on observe une croissance de  $(\eta)$  qui peut atteindre des valeurs très élevées:  $[\eta] = 4,5$  lorsque l'amorceur est l'éthérate éthylique de trifluore de bore avec  $[A] = 0,05$  et  $[M] = 0,384$ .

Pour de diméthyl-5,7-indène,  $[\eta]$  ne dépend pas de  $[M]$  lorsque l'amorceur utilisé est  $AlBr_3$  par contre, lorsque l'amorçage est fait par  $TiCl_4$  il y a existence d'un maximum. L'influence de  $[A]$  est très faible avec ce monomère.

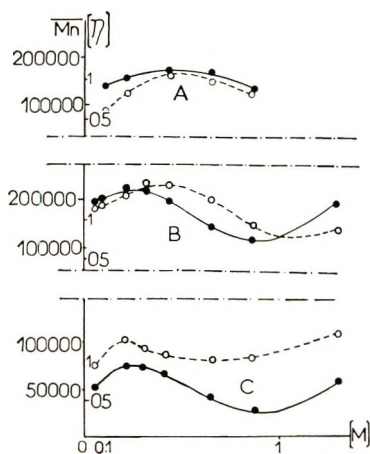


Fig. 9. Influence de la concentration en monomère sur la polymérisation du diméthyl-4,6-indène à (A)  $0^{\circ}C$ , (B)  $-30^{\circ}C$ , et (C)  $-72^{\circ}C$ : (---)  $\overline{M}_n$ ; (—)  $[\eta]$ .  $(TiCl_4) = 0,01$ .

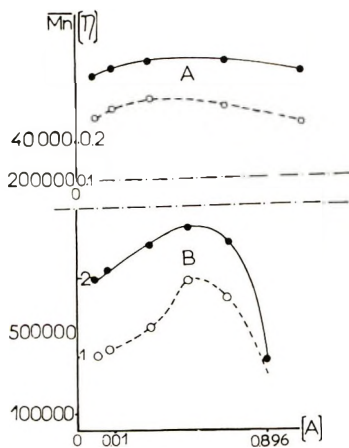


Fig. 10. Influence de la concentration en amorceur sur la polymérisation du diméthyl-5,6-indène à (A)  $-30^{\circ}C$  et (B)  $-72^{\circ}C$ : (---)  $\overline{M}_n$ ; (—)  $[\eta]$ .  $[M] = 0,224$ ; amorceur  $TiCl_4$ .

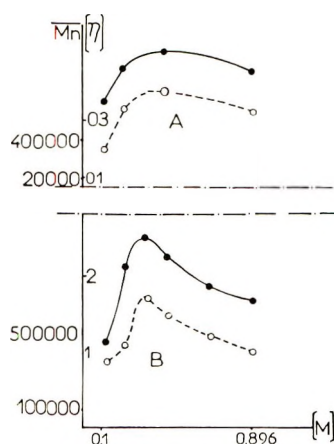


Fig. 11. Influence de la concentration en monomère sur la polymérisation du diméthyl-5,6-indène à (A)  $-30^{\circ}\text{C}$  et (B)  $-72^{\circ}\text{C}$ : (---)  $\bar{M}_n$ ; (—)  $[\eta]$ .  $[\text{TiCl}_4] = 0,01$ .

Enfin avec le triméthyl-4,6,7-indène on observe une croissance de  $[\eta]$  avec  $[M]$  et, que l'amorceur soit  $\text{TiCl}_4$  ou  $\text{SnCl}_4$ , l'existence d'une valeur optimale de  $[A]$  à laquelle correspond un maximum de  $[\eta]$ .

### Valeurs des Enthalpies de Polymérisation

Les mesures ont été faites selon la technique de Chéradame et al.<sup>8</sup> Nous avons pour chaque monomère opéré soit dans un appareil scellé sous vide poussé, soit dans un appareil ouvert sous azote. Les résultats obtenus dans les deux cas sont les mêmes.  $\Delta H_{88}$  désigne l'enthalpie de polymérisation, le monomère et le polymère étant supposés solubles dans le milieu réactionnel. Pour chaque monomère la mesure a été faite avec plusieurs amorceurs et pour diverses valeurs de  $[M]$  et  $[A]$ . Les résultats obtenus ne varient pratiquement pas avec ces différents facteurs. Nous les donnons dans le Tableau III.

En même temps que nous faisons la détermination des enthalpies nous avons relevé les vitesses de début de polymérisation et les temps de demi réaction. La précision des résultats nous permet de donner seulement un ordre de grandeur. Si on prend la vitesse de polymérisation de l'indène

TABLEAU III

Monomère	$\Delta H_{88}$ , kcal/mole
Indène 5	$13,9 \pm 0,6$
$M_6$	$13,7 \pm 0,7$
$M_7$	$14,0 \pm 0,7$
$D_{46}$	$18,5 \pm 0,9$
$D_{47}$	$15,5 \pm 0,9$
$D_{56}$	$18,9 \pm 0,9$
$T_{4567}$	$18 \pm 1$

comme unité, celle des méthyl-6- et diméthyl-4,7-indènes est cinq fois plus grande et celle des diméthyl-4,6-et tétraméthyl-4,5,6,7 indènes huit fois plus grande.

### COPOLYMÉRISATION DES METHYLINDENES AVEC L'INDÈNE ET ENTRE EUX

Les courbes de copolymérisation ont été décrites dans les travaux précédents auxquels nous renvoyons.<sup>3,5,6,9</sup> I désigne l'indène.

Le Tableau IV donne les valeurs des rapports de réactivité, l'indice 1 se rapporte toujours au premier monomère nommé. Le chiffre entre parenthèses après l'amorceur désigne sa concentration molaire. La concentration en monomère [M] et la température sont données pour chaque opération.

TABLEAU IV

Couple de monomères	Amorceur	[M]	Temp, °C	$r_1$	$r_2$
T <sub>4567</sub> /I	TiCl <sub>4</sub> (0,002)	1	0	7,5 ± 0,5	0,20 ± 0,04
D <sub>47</sub> /I	TiCl <sub>4</sub> (0,002)	"	"	3,7 ± 0,3	0,40 ± 0,05
D <sub>56</sub> /I	TiCl <sub>4</sub> (0,002)	"	"	4,2 ± 0,4	0,50 ± 0,10
D <sub>46</sub> /I	TiCl <sub>4</sub> (0,002)	"	"	2,1 ± 0,1	0,40 ± 0,08
T <sub>4567</sub> /I	H <sub>2</sub> SO <sub>4</sub> (0,002)	"	"	16,0 ± 0,5	0,75 ± 0,18
D <sub>47</sub> /I	BF <sub>3</sub> ·O(CH <sub>3</sub> ) <sub>2</sub> (0,002)	"	"	2,5 ± 0,2	0,15 ± 0,03
T <sub>4567</sub> /D <sub>47</sub>	TiCl <sub>4</sub> (0,002)	"	"	2,0 ± 0,2	0,3 ± 0,08
T <sub>4567</sub> /D <sub>46</sub>	TiCl <sub>4</sub> (0,002)	"	"	2,2 ± 0,3	0,53 ± 0,08
D <sub>47</sub> /D <sub>46</sub>	TiCl <sub>4</sub> (0,002)	"	"	0,6 ± 0,04	0,60 ± 0,04
M <sub>6</sub> /I	TiCl <sub>4</sub> (0,05)	0,384	"	2,5 ± 0,25	0,45 ± 0,05
M <sub>5</sub> /I	TiCl <sub>4</sub> (0,05)	"	"	0,85 ± 0,05	1,15 ± 0,05
M <sub>7</sub> /I	TiCl <sub>4</sub> (0,05)	"	"	1,15 ± 0,05	0,8 ± 0,005
D <sub>5.7</sub> /I	TiCl <sub>4</sub> (0,04)	1	-30	3,80 ± 0,04	0,10 ± 0,05
T <sub>4.6.7</sub> /I	TiCl <sub>4</sub> (0,01)	"	"	3,4 ± 0,1	0,15 ± 0,05

### ÉTUDE DE LA POLYMÉRISATION DES METHYLINDENES À L'AIDE DES MÉTHODES DE LA CHIMIE QUANTIQUE

Nous avons trouvé dans la littérature<sup>10</sup> une référence relative à l'étude théorique de certains méthylindènes. Nous avons traité l'indène selon la technique de Pullman et Berthier,<sup>11</sup> c'est à dire que nous avons considéré le CH<sub>2</sub> comme une double liaison C=H<sub>2</sub> pouvant se conjuguer avec les doubles liaisons C=C de la molécule. Le taux de délocalisation de cette liaison est déterminé par la relation  $\beta' = \eta\beta$  dans laquelle  $\beta'$  est l'intégrale d'échange carbone hydrogène et ou  $\beta$  a sa signification habituelle. Il est évident que le choix de  $\eta$  représente un certain arbitraire, mais nous cherchons à comparer entre elles des molécules dérivées de l'indène par substitution et pour lesquelles  $\eta$  peut être considéré comme constant. Nous

avons pris  $\eta = 3$  et pour les deux liaisons partant du carbone en 1 (liaison 1-2 et 1-8)  $\eta = 0,7$ .

Les groupes méthyles ont été traités suivant les deux hypothèses classiques: modèle inductif et modèle hyperconjugué. Pour le premier nous avons pris  $\delta_C = 0,2$  et  $\eta_{C-M_e} = 0$ , pour le deuxième  $\delta_{C_1} = 0,1$ ,  $\delta_{C_2} = 0$ ,  $\delta_{H_3} = 0,2$ ;  $\eta_{C_1C_2} = 0,7$ ,  $\eta_{C_2=H_3} = 2$ .

Les charges, indices de valence libre et indices de liaison mobile sont calculés par les méthodes classiques, les densités frontières et les superdélocalisabilités définies par Yonezawa<sup>12-14</sup> sont établies pour une réaction électrophile.

Les résultats concernant les sommets 2 et 3 sont donnés par le Tableau V pour le modèle inductif et par le Tableau VI pour le modèle hyperconjugué.  $P_{2,3}$  désigne l'indice de liaison mobile entre les sommets 2 et 3.

TABLEAU V

	Charges totales		Densités frontières		Superdelocalisabilités		Indices de Valence libre		
	Mono-mères	Sommet 2	Sommet 3	Sommet 2	Sommet 3	Sommet 2	Sommet 3	$P_{2,3}$	Sommet 2
Indène	1,008	1,006	0,699	0,320	1,251	0,932	0,896	0,661	0,424
M <sub>2</sub>	0,891	1,085	0,645	0,420	1,242	1,178	0,889	0,668	0,431
M <sub>3</sub>	1,087	0,921	0,799	0,333	1,459	0,928	0,893	0,664	0,430
M <sub>4</sub>	1,023	1,002	0,701	0,303	1,303	0,932	0,896	0,660	0,424
M <sub>5</sub>	1,006	1,006	0,689	0,312	1,250	0,932	0,896	0,660	0,425
M <sub>6</sub>	1,019	0,003	0,679	0,283	1,303	0,932	0,896	0,661	0,425
M <sub>7</sub>	1,006	1,005	0,682	0,310	1,250	0,931	0,895	0,660	0,425
D <sub>45</sub>	1,021	1,002	0,698	0,301	1,301	9,932	0,896	0,660	0,425
D <sub>46</sub>	1,035	1,001	0,687	0,269	1,430	0,932	0,896	0,660	0,424
D <sub>47</sub>	1,020	1,002	0,670	0,284	1,301	0,930	0,895	0,661	0,424
D <sub>56</sub>	1,019	1,004	0,665	0,271	1,302	0,931	0,896	0,660	0,425
D <sub>57</sub>	1,007	1,007	0,680	0,306	1,252	0,933	0,897	0,659	0,424
D <sub>67</sub>	1,020	1,003	0,661	0,271	1,306	0,931	0,896	0,660	0,425
T <sub>456</sub>	1,034	1,001	0,682	0,265	1,357	0,932	0,895	0,661	0,426
T <sub>457</sub>	1,001	1,022	0,657	0,284	1,304	0,931	0,895	0,661	0,426
T <sub>467</sub>	1,035	1,001	0,657	0,251	1,362	0,931	0,896	0,661	0,424
T <sub>567</sub>	1,021	1,004	0,654	0,262	1,308	0,931	0,897	0,660	0,424
T <sub>4567</sub>	1,034	1,001	0,657	0,249	1,324	0,932	0,896	0,661	0,424

En plus nous avons calculé l'énergie de localisation de la liaison éthylénique en position 2 pour chaque monomère (puisque c'est sur le sommet 2 que se fait l'attaque du carbocation). Nous l'avons déterminée sur le modèle inductif en faisant la différence entre l'énergie du monomère dans son état normal et son énergie lorsque la double liaison a basculé en position 2.

Enfin nous avons également classé les monomères selon la méthode de Yonezawa.<sup>15,16</sup> D'après cet auteur si un monomère R forme (par son

TABLEAU VI

Mono- mères	Charges totales		Densités frontières		Superdélocali- sabilités			Indices de valence libre	
	Som- met 2	Som- met 3	Som- met 2	Som- met 3	Som- met 2	Som- met 3	$P_{2,3}$	Som- met 2	Som- met 3
Indène	1,007	1,006	0,699	0,320	1,307	1,058	0,896	0,660	0,424
M <sub>2</sub>	0,948	1,152	0,607	0,401	1,213	1,106	0,869	0,692	0,445
M <sub>3</sub>	1,054	0,963	0,784	0,322	1,422	0,910	0,875	0,681	0,456
M <sub>4</sub>	1,016	1,002	0,685	0,286	1,291	0,916	0,894	0,663	0,424
M <sub>5</sub>	1,006	1,004	0,684	0,309	1,249	0,931	0,895	0,661	0,427
M <sub>6</sub>	1,016	1,005	0,659	0,272	1,291	0,932	0,896	0,661	0,423
M <sub>7</sub>	1,007	1,005	0,677	0,307	1,251	0,931	0,896	0,660	0,425
D <sub>45</sub>	1,016	1,002	0,684	0,292	1,291	0,935	0,893	0,662	0,424
D <sub>46</sub>	1,024	1,002	0,654	0,255	1,331	0,929	0,894	0,663	0,422
D <sub>47</sub>	1,016	1,004	0,643	0,271	1,293	0,931	0,895	0,662	0,423
D <sub>56</sub>	1,014	1,004	0,638	0,256	1,277	0,930	0,894	0,662	0,425
D <sub>57</sub>	1,006	1,004	0,671	0,301	1,249	0,931	0,896	0,659	0,427
D <sub>67</sub>	1,015	1,004	0,632	0,256	1,291	0,937	0,895	0,661	0,425
T <sub>456</sub>	1,025	1,002	0,650	0,249	1,333	0,929	0,894	0,662	0,423
T <sub>457</sub>	1,016	1,004	0,645	0,271	1,293	0,931	0,895	0,660	0,423
T <sub>467</sub>	1,024	1,002	0,612	0,231	1,331	0,928	0,894	0,662	0,423
T <sub>567</sub>	1,015	1,005	0,620	0,246	1,292	0,931	0,896	0,657	0,423
T <sub>4567</sub>	1,024	1,003	0,614	0,230	1,354	0,925	0,894	0,661	0,423

TABLEAU VII

Monomère	Energie de localisation		
	CH <sub>3</sub> Inductif	CH <sub>3</sub> Hyperconjugué	( $\Delta E$ ) <sub>rs</sub> CH <sub>3</sub> inductif
Indène	1,824	1,824	0,898
M <sub>2</sub>	—	1,892	0,891
M <sub>3</sub>	1,710	1,712	1,017
M <sub>4</sub>	1,796	1,802	0,927
M <sub>5</sub>	1,826	1,824	0,893
M <sub>6</sub>	1,794	1,802	0,920
M <sub>7</sub>	1,824	1,824	0,897
D <sub>45</sub>	1,798	1,804	0,926
D <sub>46</sub>	1,766	1,780	0,960
D <sub>47</sub>	1,798	1,798	0,926
D <sub>56</sub>	1,796	1,804	0,927
D <sub>57</sub>	1,826	1,828	0,898
D <sub>67</sub>	1,796	1,800	0,928
T <sub>456</sub>	1,768	1,778	0,958
T <sub>457</sub>	1,792	1,798	0,928
T <sub>467</sub>	1,766	1,784	0,961
T <sub>567</sub>	1,796	1,802	0,930
T <sub>4567</sub>	1,766	1,776	0,961

sommet  $r$ ) une liaison avec le sommet  $s$  du cation S il en résulte une énergie de stabilisation  $(\Delta E)_{r,s}$  donnée par:

$$(\Delta E)_{r,s} = -2 \left\{ \sum_m^{occ} \sum_n^{inocc} - \sum_m^{inocc} \sum_n^{occ} \right\} \frac{(a_c^m)^2 (b_s^n)^2 (\beta_{rs})^2}{E_m - F_n}$$

dans lequel les notations "occ" et "inocc" indiquent respectivement des sommations sur toutes les orbitales totalement occupées ou totalement vides, où  $E_m$  et  $F_n$  sont les valeurs propres de la  $m^{\text{ème}}$  orbitale de R et de la  $n^{\text{ème}}$  orbitale de S.  $\beta_{rs}$  est l'intégrale de résonance pour la liaison établie entre  $r$  et  $s$ . Enfin  $a_r^m$  et  $b_s^n$  sont les coefficients de la  $r^{\text{ème}}$  et de la  $s^{\text{ème}}$  orbitales atomiques dans la  $m^{\text{ème}}$  et la  $n^{\text{ème}}$  orbitales moléculaires du monomère et du cation.

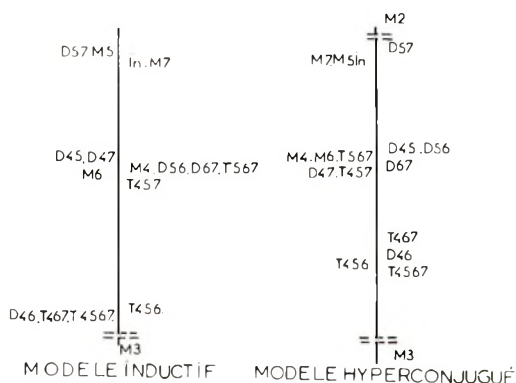


Fig. 12. Comparaison des réactivités des méthylindènes déduites de leurs énergies de localisation. La réactivité est d'autant plus élevée que l'énergie est plus faible, elle va donc en croissant du haut vers le bas ( $M_2$  vers  $M_3$ ).

Les résultats sont donnés par le Tableau VII.

Il nous a semblé qu'il serait plus commode de représenter ces valeurs sur un graphique afin de classer les monomères par ordre de réactivité, c'est ce que nous avons fait sur la Figure 12.

### ANALYSE DES RESULTATS; CONCLUSIONS

En ce qui concerne le tétraméthyl-4,5,6,7-indène on remarque l'indépendance de la masse molaire relativement à la nature de l'acide de Lewis, et les valeurs plus élevées obtenues dans le cas de l'acide sulfurique.

D'une façon générale, on constate que le diméthyl-5,6-indène a un comportement voisin de celui de l'indène alors que les diméthyl-4,6- et les diméthyl-4,7-indènes donnent des polymères de masses moléculaires plus élevées, particulièrement grandes dans le cas de l'amorçage par les éthers de trifluorure de bore.

On observe d'autre part, que le tétraméthyl-4,5,6,7-indène donne à la fois les vitesses les plus grandes et les masses moléculaires les plus faibles.

Ceci ne semble pouvoir être attribué qu'à l'une des causes suivantes: soit à un transfert au monomère relativement plus important dans le cas de ce méthylindène, soit à l'absence de réaction de ramification sur ce polymère, les ramifications se produisant par contre, pour l'indène et surtout pour les indènes diméthylés en 4,7 et 4,6.

Cette dernière hypothèse paraît la plus vraisemblable car on observe par ailleurs, une indépendance des masses moléculaires vis à vis de la nature du catalyseur de Friedel et Crafts, dans le cas du tétraméthylindène, alors qu'il existe une différence appréciable dans le cas de l'indène et du diméthyl-5,6-indène et une grande diversité des résultats en ce qui concerne les diméthyl-4,7- et diméthyl-4,6-indènes. Les éthérates de trifluorure de bore conduiraient aux taux de ramification les plus élevés. La présence de ramifications dans les polyindènes obtenus avec  $TiCl_4$  a déjà été montrée par des méthodes physicochimiques. En ce qui concerne les diméthyl-indènes leur intervention est confirmée par le fait que les polymères du diméthyl-4,7-indène obtenu à  $-72^\circ C$  sont insolubles lorsque la concentration en monomère devient supérieure à 1 mole/litre.

Les résultats les plus caractéristiques sont à notre avis, ceux qui concernent les variations de  $[\eta]$  avec la température de polymérisation. Ils confirment les hypothèses que nous avons faites au sujet du branchement important qui apparaît sur certains polyméthylindènes par attaque des cycles benzéniques par les cations terminaux des chaînes croissantes.

Ainsi, si on observe une variation normale de  $[\eta]$  en fonction de la température de polymérisation pour le diméthyl-5,6-indène ( $[\eta]$  croît quand la température de polymérisation décroît) il n'en est pas de même avec les diméthyl-4,6-, diméthyl-4,7-, et triméthyl-4,6,7-indènes pour lesquels on observe d'abord une croissance de  $[\eta]$  avec la température de polymérisation, puis une décroissance après passage par un maximum. Nous expliquons ce phénomène de la façon suivante: il y aurait d'abord accroissement de la masse molaire par augmentation du branchement avec la température, puis la décroissance classique des masses molaires quand la température augmente finirait par l'emporter. Ceci expliquerait l'existence du maximum. Nos travaux sur ce point sont actuellement poursuivis avec le diméthyl-5,7-indène dans le sens suivant: extension des intervalles de température de polymérisation utilisés dans le but de mettre en évidence un éventuel extrémum; étude des polymérisations à diverses températures pour des concentrations très faibles en amorceur et de l'aptitude de l'indane correspondant à être substitué par réaction de Friedel et Crafts.

Il est d'ailleurs certain que suivant les conditions de polymérisation (température, nature de l'amorceur) un même monomère doit donner des polymères de structure différentes (chaînes peu ramifiées ou au contraire très ramifiées). Ceci est en accord avec les études de diffusion de lumière que nous faisons actuellement et explique que pour une même valeur de  $\bar{M}_n$  on puisse avoir, dans le cas du diméthyl-4,7-indène, des valeurs de  $[\eta]$  différentes suivant les conditions de préparation des polymères.



Les courbes donnant la variation de  $[\eta]$  avec la concentration en monomère sont en accord avec ces remarques. En effet on observe dans tous les cas à basse température ( $-72^{\circ}\text{C}$ ) un maximum très net, caractéristique de la polymérisation cationique de l'indène.<sup>7</sup> Par contre, quand la température s'élève il y a atténuation de ce maximum et même inversion de courbure. Ceci est très probablement dû à ce qu'aux températures plus élevées le phénomène de branchement par attaque des cycles aromatiques par les cations terminaux prend une importance de plus en plus grande. D'ailleurs, dans le cas de la polymérisation du diméthyl-4,6-indène amorcée par  $\text{TiCl}_4$  (courbes 9B et 9C) on observe pour les concentrations élevées en monomère ( $[M] = 0,9$ ) une augmentation des viscosités intrinsèques et des masses molaires, qui suit le premier maximum et est attribuable au branchement sur les cycles phényles.

En ce qui concerne l'influence de la concentration en amorceur on observe dans tous les cas le maximum caractéristique de la polymérisation de l'indène.<sup>7</sup> Dans le cas du diméthyl-4,7-indène des perturbations de même origine que les précédentes apparaissent pour les valeurs élevées de  $[A]$ .

L'examen de la Figure 12 montre que les méthylindènes se classent en trois groupes: monomères très réactifs ( $M_3$ ,  $D_{46}$ ,  $T_{467}$ ,  $T_{4567}$ ,  $T_{456}$ ); monomères de réaction moyenne ( $D_{45}$ ,  $D_{47}$ ,  $M_4$ ,  $D_{56}$ ,  $D_{67}$ ,  $T_{567}$ ,  $T_{457}$ ,  $M_6$ ); monomères de faible réactivité ( $D_{57}$ ,  $M_5$ , indène,  $M_7$ ).

Or, si nous classons les monomères en comparant les valeurs de  $1/r_2$  données par le Tableau IV nous trouvons le même classement. Il y a donc un bon accord entre les résultats expérimentaux et les résultats théoriques, seul le diméthyl-5,7-indène semble beaucoup plus réactif théoriquement que ne le laisse prévoir l'expérience.

Yonezawa a déterminé les énergies de localisation d'autres monomères. Les ordres de grandeur sont les mêmes que les nôtres. Cependant la valeur trouvée pour le styrolène est légèrement inférieure à celle que nous avons pour l'indène. Ceci peut étonner car la détermination des rapports de réactivité<sup>1</sup> montre que l'indène a, vis à vis du cation indénique, une réactivité égale à deux fois celle du styrolène, cependant que la réactivité de ces deux monomères est égale vis à vis du cation styrolénique. A vrai dire, comme le fait remarquer Yonezawa à propos de l' $\alpha$ -méthylstyrolène, il est difficile de faire des comparaisons d'une série à une autre, car les résultats sont très influencés par le choix des paramètres.

## PARTIE EXPERIMENTALE

### Technique de Polymérisation

Les polymérisations cationiques ont été faites suivant la technique de Sigwalt.<sup>7</sup> Le monomère en solution dans le solvant choisi est placé dans un réacteur muni d'une agitation, d'une circulation d'azote et d'un dispositif permettant de repérer la température. L'amorceur est introduit en solution dans le solvant de polymérisation après que la solution de mono-

mère ait été amenée à température convenable. Une fois le temps de réaction écoulé on traite par une solution de méthanol dans le chlorure de méthylène et on précipite par une nouvelle addition de méthanol.

### Determination des Viscosités Intrinsèques

Elles ont été faites à 25°C dans le benzène à l'aide d'un viscosimètre d'Oswald.

### Determination des Masses moléculaires moyennes en Nombre

Elles ont été faites sur osmomètre Mechrolab 501, dans le toluène à 37,5°C.

### Spectres infra-rouge

Ils ont été enregistrés sur appareil Beckmann IR<sub>4</sub>; pour les dosages relatifs à la détermination des rapports de réactivité, nous avons travaillé en densité optique.

### Références

1. E. Maréchal, J. J. Basselier, et P. Sigwalt, *Bull. Soc. Chim. France*, **1964**, 1740.
2. P. Sigwalt et E. Maréchal, *Europ. Polym. J.*, **2**, 15 (1966).
3. E. Maréchal, P. Evrard, et P. Sigwalt, *Bull. Soc. Chim. France*, **1968**, 2049.
4. E. Maréchal, P. Evrard, et P. Sigwalt, *Bull. Soc. Chim. France*, **1969**, 1981.
5. P. Caillaud, J. M. Huet, et E. Maréchal, *Bull. Soc. Chim. France*, sous presse.
6. A. Anton, J. Zwegers, et E. Maréchal, *Bull. Soc. Chim. France*, sous presse.
7. P. Sigwalt, *J. Polym. Sci.*, **52**, 15 (1961).
8. H. Chéradame, J. P. Vairon, et P. Sigwalt, *Europ. Polym. J.*, **6**, 5753 (1967).
9. E. Maréchal et P. Evrard, *Bull. Soc. Chim. France*, **1969**, 2039.
10. Yu. N. Polovii, *Teor. Eksp. Khim.*, **3**, 516 (1967).
11. B. Pulmann et G. Berthier, *Bull. Soc. Chim. France*, **1968**, 55.
12. K. Fukui, T. Yonezawa, et H. Shingu, *J. Chem. Phys.*, **20**, 722 (1952).
13. K. Fukui, T. Yonezawa, et H. Shingu, *J. Chem. Phys.*, **26**, 831 (1957).
14. K. Fukui, C. Nagata, T. Yonezawa, et K. Morokuma, *J. Chem. Phys.*, **34**, 230 (1961).
15. T. Yonezawa, T. Higashimura, K. Katagiri, K. Hayashi, S. Okamura, et K. Fukui, *J. Polym. Sci.*, **26**, 311 (1957).
16. T. Yonezawa, *Rev. Macromol. Chem.*, **1**, 1 (1966).

Received January 9, 1970

Revised March 23, 1970

## Isocyanate-Catalyst and Hydroxyl-Catalyst Complex Formation

S. L. REEGEN and K. C. FRISCH, *Polymer Institute, University of Detroit, Detroit, Michigan 48221*

### Synopsis

As part of an investigation for evidence of isocyanate-catalyst and alcohol-catalyst complex formations, determinations of molecular weights were made by means of the freezing point depression of benzene solutions. Mixtures of 1-methoxy-2-propanol and dibutyltin dilaurate and mixtures of 1-methoxy-2-propanol and triethylamine both gave strong evidence of the formation of complexes. Complex formations were also detected when the alcohol was replaced by phenyl isocyanate. Significantly larger concentrations of the catalyst were involved in isocyanate complexes than were shown to be the case with the alcohol complexes. These results appear to be experimental evidence for the previously proposed ternary complex as an intermediate in the metal-catalyzed formation of urethanes.

### INTRODUCTION

In the course of a study of the kinetics of the reaction between alcohols and polyols with isocyanate with the use of metal salt catalysts, the interesting observation was made that the relative rates of the reactions of model hydroxyl compounds (methoxypropanols) with isocyanates were reversed when a lead catalyst (lead naphthenate) was used instead of a tin catalyst (dibutyltin dilaurate).<sup>1-3</sup> The position of the methoxy group, the nature of the hydroxyl group (primary or secondary), and the type of solvent (polar or non-polar) had a pronounced effect on the reaction rates. The apparent differences in the catalytic activity of these two catalysts in the above reactions have led to further investigations into the mechanisms involved, including a search for evidence of complex formation between the catalysts, alcohol, and isocyanate. Infrared spectroscopy yielded no conclusive evidence for complex formation for 1-methoxy-2-propanol-catalyst or phenyl isocyanate-catalyst systems with the use of either dibutyltin dilaurate or stannous 2-ethylhexoate.<sup>3</sup> These findings were contrary to the results reported by Smith<sup>4</sup> and by Pestemer and Lauerer<sup>5</sup> but were in accordance with the data obtained by Farkas and Strohm.<sup>6</sup> Bloodworth and Davies<sup>7</sup> were able to isolate an adduct formed from aryl isocyanates and alkyltin alkoxides and characterized the *N*-stannoyl carbamate having the structure  $\text{ArN}(\text{SnBu}_3)\text{—COOCH}_3$ . Evidence for complex formation

between phenyl isocyanate and butyltin trichloride was reported by Dyer and Pinkerton.<sup>3</sup>

Likewise, a study of the ultraviolet spectra for mixtures of phenyl isocyanate with tertiary amines (tri-*n*-propylamine and triethylamine), in a manner similar to that described by Pestemer and Lauerer<sup>5</sup> and with organometallic catalysts (stannous 2-ethylhexoate and lead naphthenate) failed to disclose any evidence of catalyst-isocyanate complexes.<sup>3</sup> Combinations of amine and metal catalysts also had no effect on the absorption maximum of phenyl isocyanate. Entelis and co-workers<sup>9</sup> reported ultraviolet data (using  $\lambda = 218 \text{ m}\mu$ ) which gave evidence for the existence of alcohol-tin catalyst complexes in a study of the mechanism of the effect of organotin catalysts on the reaction of *p*-chlorophenyl isocyanate and methanol.

On the other hand, shifts in the —OH proton resonance in the NMR spectra clearly indicated complex formation for the system dibutyltin dilaurate-1-methoxy-2-propanol.<sup>3</sup> Similar shifts were observed when dibutyltin dilaurate was replaced by lead naphthenate or triethylamine.<sup>3</sup> Mixtures of dibutyltin dilaurate-triethylamine catalysts caused a greater shift in the —OH proton resonance than that observed for either catalyst alone. This is in accord with the well known synergistic effect of mixtures of metal catalysts and tertiary amines in the preparation of polyurethanes from isocyanates and hydroxyl-terminated polyethers or polyesters. However, when this method was used, no complex formation could be detected for mixtures of phenyl isocyanate and catalysts.<sup>3</sup> Therefore, other methods were studied which would produce experimental evidence for isocyanate-catalyst complexes. The method which was employed for this investigation was the determination of molecular weights by means of freezing-point depression.

## EXPERIMENTAL

### Cryoscopy

The molecular weights of complexes were determined in benzene solution from the freezing point depression of benzene.

Complex formation was detected by determination of molecular weights of mixtures of alcohols or isocyanates and catalysts. The formation of complexes should result in significantly higher molecular weights than would result from no interaction between reactants and catalysts.

In Figure 1, the molecular weight of 1-methoxy-2-propanol is shown to be dependent on its concentration in benzene; hydrogen bonding between the alcohol groups appears to play an important role at concentrations higher than 6.5 g/l., resulting in significantly higher molecular weights than the theoretical value of 90.

In Table I the molecular weight of dibutyltin dilaurate (DBTDL), as determined by the freezing-point depression of benzene, is shown to change very little with increasing concentration of DBTDL. Thus, only a 2.5%

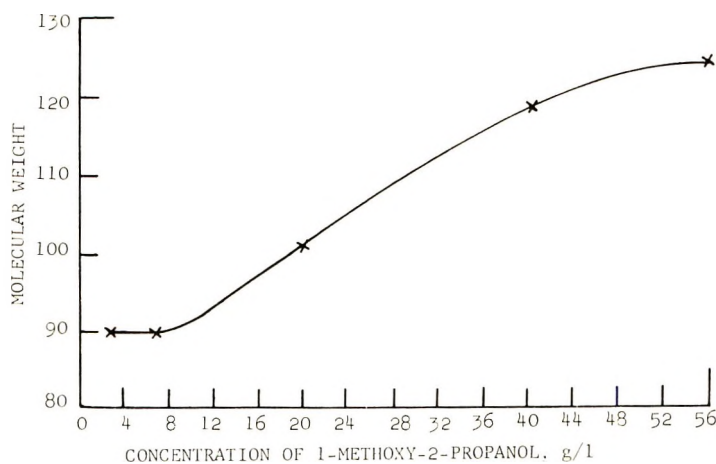


Fig. 1. Molecular weight of 1-methoxy-2-propanol by freezing-point depression of benzene.

TABLE I  
Molecular Weight of Dibutyltin Dilaurate by Freezing-Point Depression of Benzene

Concentration of DBTDL in benzene, g/l.	Molecular weight (theoretical = 599)
80.6	561
160.2	575
241.5	575

TABLE II  
Complex Formation in Mixtures of 1-Methoxy-2-propanol and Dibutyltin Dilaurate by Freezing-Point Depression of Benzene

Concn of 1-methoxy-2-propanol, g/l.	Concn of DBTDL, g/l.	Calculated MW <sup>a</sup>		Experimental MW (c)	Catalyst in complex % [(c - a)/(b - a)] × 100
		No complex (a)	100% complex <sup>b</sup> (b)		
45.0	0	90	—	119	—
45.0	50.5 <sup>c</sup>	204	252	213	19
45.0	178.3 <sup>d</sup>	324	588	352	11
45.0	247.3 <sup>d</sup>	361	680	390	9

<sup>a</sup>  $M_{100} = M_z + M_a$ , where  $M_{100}$  = MW of 100% complex,  $M_z$  = (mole fraction of complex) (MW of complex),  $M_a$  = (mole fraction of excess component) (MW of excess component).

<sup>b</sup> Assuming a 1:1 complex.

<sup>c</sup> MW of DBTDL = 561.

<sup>d</sup> MW of DBTDL = 575.

TABLE III  
Molecular Weight of Triethylamine by Freezing Point Depression of Benzene

Concentration of TEA in benzene, g/l.	Molecular weight (theoretical = 101)
9.1	99
27.3	99
39.4	102
50.5	103
52.5	104

TABLE IV  
Complex Formation in Mixtures of 1-Methoxy-2-Propanol and Triethylamine by  
Freezing Point Depression of Benzene

Concn of 1-methoxy- 2-propanol, g/l.	Concn of TEA, g/l.	Calculated MW		Experi- mental MW (c)	Catalyst in com- plex, % [(c - a)/ (b - a)] × 100
		No complex (a)	100% complex (b)		
54.8	0	90	—	124.5	—
54.8	10.5 <sup>a</sup>	120	149	126	21
54.8	29.3 <sup>a</sup>	114	192	127	17
54.8	40.3 <sup>b</sup>	114	219	128	13

<sup>a</sup> MW of TEA = 99.

<sup>b</sup> MW of TEA = 102.

increase in molecular weight resulted when the concentration of DBTDL was increased from 81 to 242 g/l. These molecular weights were all slightly under the theoretical value of 599.

In Table II the data resulting from mixtures of 1-methoxy-2-propanol and DBTDL are shown. In these determinations, the concentrations of alcohol were maintained constant at 45 g/l., while the concentration of DBTDL was increased in succeeding measurements. The molecular weights that were experimentally determined can be compared with the theoretical values calculated on the basis of (a) no complex formation, and (b) 100% complex formation, assuming a 1:1 complex. It should be noted that a value of 119 was used in calculations for the molecular weight of 1-methoxy-2-propanol, as determined previously for this concentration and values of 561 and 575 were used for the molecular weight of the DBTDL. It is apparent that the molecular weights obtained were, in each case, higher than those calculated for no complex formation and lower than those calculated for 100% complex formation. The experimentally determined molecular weights were significantly higher than the calculated values for no complex formation and are strong evidence of alcohol-Sn complexing in each case. When calculations were made of the concentration of catalyst tied up in complex formation  $[(c - a)/(b - a)] \times 100$ , one can observe that it decreases with increasing DBTDL content in solution.

It should be noted that these determinations of complex formation were made at a concentration of 1-methoxy-2-propanol (45 g/l.) at which there was significant hydrogen bonding (Fig. 1). Determinations at alcohol concentrations at which no hydrogen bonding had been detected (6 g/l.) resulted in no evidence of complex formation with DBTDL.

Similar measurements were made on mixtures of 1-methoxy-2-propanol and triethylamine (TEA). As shown in Table III, the molecular weight of TEA changed very little with increasing concentration (9.1 to 52.5 g/l.). In Table IV the data resulting from mixtures of 1-methoxy-2-propanol and TEA are shown. In these determinations, the concentrations of alcohol were maintained constant at 54.8 g/l., while the concentration of TEA was increased in succeeding measurements. A value of 124.5, as determined previously as the molecular weight of 1-methoxy-2-propanol, and values of 99 and 102 were used as molecular weights of the catalyst, TEA. These molecular weights were significantly higher than the calculated values for no complex formation and appear to be evidence of alcohol-amine complexing in each case. It can also be seen that the concentration of catalyst tied up in the complexes seems to decrease with increasing TEA content in solution.

These molecular weight determinations appear to be significant evidence of complex formation between alcohols (1-methoxy-2-propanol) and catalysts DBTDL and TEA. The results with DBTDL confirm the evidence that was previously obtained<sup>3</sup> by means of NMR data.

Efforts have also been made to find evidence of complex formation between these two catalysts and isocyanates. By the same techniques as described for our alcohol-catalyst work (molecular weights by the freezing point depression of benzene), mixtures of phenyl isocyanate and DBTDL have been studied. It can be seen from Table V that no evidence of complex formation between phenyl isocyanate molecules could be obtained. No change in molecular weight was evident with increasing concentrations of phenyl isocyanate in benzene; the theoretical molecular weight of 119 was obtained in each of the three concentrations shown in Table V.

In Table VI measurements on mixtures of phenyl isocyanate and DBTDL are shown, resulting in molecular weight values that are indicative of a significant amount of complex formation. The measurements indicate that as much as 40-50% of the DBTDL molecules are tied up in complexes with phenyl isocyanate. Significantly larger concentrations of the catalyst

TABLE V  
Molecular Weight of Phenyl Isocyanate by Freezing-Point Depression of Benzene

Concentration of phenyl isocyanate in benzene, g/l.	Molecular weight (theoretical = 119)
47.6	118.6
52.4	119.1
63.1	119.0

TABLE VI  
Complex Formation in Mixtures of Phenyl Isoocyanate and Dibutyltin Dilaurate by Freezing Point Depression of Benzene

Concn of phenyl isocyanate, g/l.	Concn of DBTDL, g/l.	Calculated MW		Experimental MW (c)	Catalyst in complex, % [(c - a)/(b - a)] × 100
		No complex (a)	100% complex (b)		
47.6	0	119	—	119	—
52.4	44.9 <sup>a</sup>	187	222	204	49
70.2	157.1 <sup>b</sup>	266	392	322	44
46.4	224.4 <sup>b</sup>	350	691	482	39

<sup>a</sup> MW of DBTDL = 561.

<sup>b</sup> MW of DBTDL = 575.

seem to be involved in isocyanate complexes than were previously shown to be the case with the alcohol complexes.

In Table VII are listed measurements indicative of the ability of TEA to form complexes with phenyl isocyanate. The molecular weight values indicate that a significant amount of complex formation has been obtained. It is again of interest to note that a higher amount of complexing between phenyl isocyanate and amine takes place than between 1-methoxy-2-propanol and catalyst.

TABLE VII  
Complex Formation in Mixtures of Phenyl Isoocyanate and Triethylamine by Freezing Point Depression of Benzene

Concn of phenyl isocyanate, g/l.	Concn of TEA, g/l.	Calculated MW		Experimental MW (c)	Catalyst in complex, % [(c - a)/(b - a)] × 100
		No complex (a)	100% complex (b)		
61.9	0	119	—	119	—
61.9	8.9 <sup>a</sup>	116	132	120	25
61.9	18.8 <sup>a</sup>	113	156	122	21
61.9	27.7 <sup>a</sup>	112	172	132	33

<sup>a</sup> MW of TEA = 99.

TABLE VIII  
Complex Formation in Mixtures of *n*-Nonane and Dibutyltin Dilaurate by Freezing Point Depression of Benzene

Concn of <i>n</i> -nonane g/l.	Concn of DBTDL, g/l.	Calculated MW		Experimental MW	Catalyst in complex, %
		No complex	100% complex		
10.2	0	128	—	127.5	—
10.2	241.5	503	597	502	0
41.0	241.5	381	673	383	0



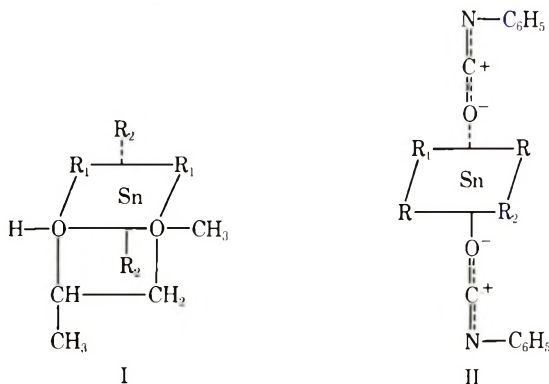
In order to assure ourselves that these molecular weight values were really evidence of complex formation, a system was selected that would not produce complexes. The system studied was nonane-DBTDL. Measurements were made to determine whether the experimentally determined molecular weights agree with the calculated values with the assumption of no complex formation. The data in Table VIII show that the experimentally determined molecular weights agree with the calculated values with the assumptions of no complex formation. These results lend supporting evidence for complex formation between catalyst and alcohol and between catalyst and isocyanate and provide confidence in the sensitivity of the technique that was utilized.

### Mechanisms of Complex Formation

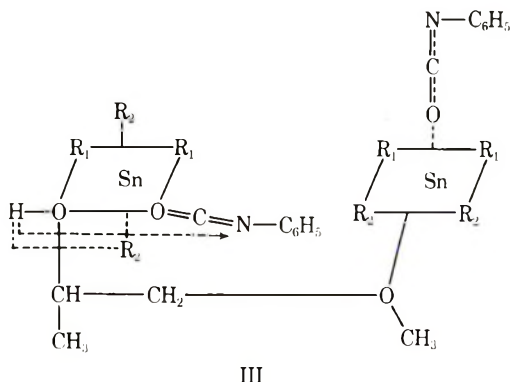
The results of our experimental work with tertiary amines show clearly complex formation between the amine and the isocyanate as well as between the amine and the hydroxyl component. These findings are in accordance with the mechanism postulated by Baker et al.<sup>10-17</sup>

The results which we obtained for complex formation between organo-metallic catalysts such as tin and lead compounds, and 1-methoxy-2-propanol and phenyl isocyanate, respectively, were strong experimental confirmation for ternary complex formation which was first proposed by Britain and Gemeinhardt.<sup>18</sup> Smith<sup>4</sup> has criticized this mechanism because it requires an attack of one electron-deficient center on another, and, therefore, would be unlikely to occur. He proposed an alternate mechanism in which the metal complexes with the alcohol at some site other than the reactive hydroxyl group.

In the case of 1-methoxy-2-propanol we are dealing with what Robins<sup>19</sup> calls an "activated" alcohol; the introduction of a functional methoxy group in a position  $\alpha$  or  $\beta$  to the carbon atom carrying the reactive hydroxyl group could be expected to have the following influence: it would increase the stability of the alcohol-metal ion complex when either five-, six-, or seven-membered chelate rings can be formed, and it also would allow the hydroxyl group to retain a larger portion of its nucleophilicity, particularly in complexes such as I, which contain the more electronegative metal ions.



Postulated structures for tin complexes with 1-methoxy-2-propanol and with phenyl isocyanate are shown in I and II, respectively. Reaction between the ligands of these complexes presumably takes place by an exchange of the ether oxygen in the complex I by an oxygen atom that is part of an isocyanate group as seen in II. This should result in formation of a bridge compound having the structure III. Since it is possible for more than one of the tin-alcohol or tin-isocyanate complexes to interact, this could easily account not only for the presence of bridge compounds of the type AB, but also of the type A<sub>2</sub>B, AB<sub>2</sub>, etc. Urethane formation would then take place by rearrangement of the hydroxyl proton to the nitrogen of the isocyanate group as indicated by the arrow.



Likewise the synergistic action between tin and amine catalysts can be accounted for by structure III, since the isocyanate group can complex with the amine in the manner shown above.

While the relative speed of complex formation is usually very fast, the rate-determining step, the reaction between the ligands after complex formation has taken place, depends upon the coordination number of the metal ion, the configuration of the complex, and the ionic radius of the ion.

### References

1. L. Rand, B. Thir, S. L. Reegen, and K. C. Frisch, *J. Appl. Polym. Sci.*, **9**, 1787 (1965).
2. K. C. Frisch, S. L. Reegen, and B. Thir, in *Macromolecular Chemistry, Prague 1965* (*J. Polym. Sci. C*, **16**), O. Wichterle and B. Sedláček, Eds., Interscience, New York, 1967, p. 2191.
3. K. C. Frisch, S. L. Reegen, W. V. Floutz, and J. P. Oliver, *J. Polym. Sci. A-1*, **5**, 35 (1967).
4. H. A. Smith, *J. Appl. Polym. Sci.*, **7**, 85 (1963).
5. M. Pestemer and D. Lauerer, *Angew. Chem.*, **72**, 612 (1960).
6. A. Farkas and P. F. Strohm, *Ind. Eng. Chem. Fundamentals*, **4**, No. 1, 32 (1965).
7. A. J. Bloodworth and A. G. Davies, *Proc. Chem. Soc.*, **1963**, 264.
8. E. Dyer and R. B. Pinkerton, *J. Appl. Polym. Sci.*, **9**, 1713 (1965).
9. S. C. Entelis, O. V. Nesterov, and R. P. Tiger, *J. Cell Plastics*, **3**, 360 (1967).
10. J. W. Baker and J. B. Holdsworth, *J. Chem. Soc.*, **1947**, 713.

11. J. W. Baker and J. Gaunt, *J. Chem. Soc.*, **1949**, 9.
12. J. W. Baker and J. Gaunt, *J. Chem. Soc.*, **1949**, 19.
13. J. W. Baker, M. M. Davies, and J. Gaunt, *J. Chem. Soc.*, **1949**, 24.
14. J. W. Baker and J. Gaunt, *J. Chem. Soc.*, **1949**, 27.
15. J. W. Baker and D. N. Bailey, *J. Chem. Soc.*, **1957**, 4649.
16. J. W. Baker and D. N. Bailey, *J. Chem. Soc.*, **1957**, 4652.
17. J. W. Baker and D. N. Bailey, *J. Chem. Soc.*, **1957**, 4663.
18. J. W. Britain and P. G. Gemeinhardt, *J. Appl. Polym. Sci.*, **4**, 207 (1960).
19. J. Robins, *J. Appl. Polym. Sci.*, **9**, 821 (1965).

Received January 21, 1970

## Étude de la Cotacticité des Copolymères Acrylonitrile-Méthacrylate de Méthyle par Résonance Magnétique Nucléaire—haute Résolution

PHAM-QUANG-THO et JEAN GUILLOT, *C.N.R.S., Institut de  
Recherches sur la Catalyse, Villeurbanne, Rhône, France*

### Synopsis

A study of the NMR spectra of acrylonitrile-methyl methacrylate copolymers (PAM) with very low percentages of methyl methacrylate (M) allows quantitative determinations of *AMA*, and *MMA* or *AMM* triad sequences from the methoxy resonances. The resolution of the complex  $\alpha$ -methyl resonances of the isolated M units in seven components has been attempted. If our assignments are correct, the analysis of the cotactic pentad sequences (with a M in central position) has revealed that the configurations of the copolymer chain do not follow the Bernoullian or the first-order Markoffian statistics.

### INTRODUCTION

La résonance magnétique nucléaire (RMN) est particulièrement adaptée à l'analyse microstructurale des copolymères. Utilisée dans l'étude des copolymères chlorure de vinylidène-isobutène,<sup>1</sup> chlorure de vinylidène-acétate de vinyle,<sup>2</sup> et styrène-méthacrylate de méthyle,<sup>3</sup> la RMN a permis d'accéder aux distributions de séquences homopolymères dans les copolymères.

Le présent travail a pour but l'étude de la cotacticité des copolymères acrylonitrile-méthacrylate de méthyle (PAM). Dans le PAM, l'influence fortement paramagnétique des groupes ( $-\text{CN}$ ) de l'acrylonitrile (A) se fait nettement sentir sur la valeur de déplacement chimique  $\tau$  des protons méthoxy des unités méthacrylate de méthyle (M) adjacentes.<sup>4</sup> Elle ne peut être qu'exaltée lorsque l'on observe les résonances des groupes  $\alpha$ -méthyles de ces mêmes unités M, résonances qui, déjà, dépendent des configurations en triades isotactiques, hétérotactiques et syndiotactiques de l'homopolymère polyméthacrylate de méthyle (PM).

Pour éviter la complexité certaine due aux effets simultanés des tacticités et cotacticités, nous avons choisi d'analyser les échantillons PAM dans lesquels la quasi-totalité des unités M sont isolées dans la chaîne des copolymères (copolymères à très faibles pourcentages en M, 1-10%).

L'analyse par RMN se porte principalement sur les groupes méthoxy et  $\alpha$ -méthyle, les séquences de PAM étudiées comportent des nombres

impairs d'unités monomères (triades, pentades, ...) avec une unité M centrale. Vu la faible intensité des signaux enregistrés, l'utilisation de la technique d'accumulation s'est avérée indispensable.

## TECHNIQUE EXPERIMENTALE

### Copolymères

Les caractéristiques des copolymères PAM analysés dans cette étude sont rassemblées dans le Tableau I. Les solutions prélevées au cours des copolymérisations sont précipitées par du méthanol, les copolymères obtenus après filtration sont séchés sous vide à une température inférieure à 30°C.

TABLEAU I

Echantillons	Mélange initial		Taux de conversion, % <sup>b</sup>	Composition par CPV		Composition par RMN	
	A, mole	M, mole		A, %	M, %	A, %	M, %
PAM I	1,15	$1,20 \times 10^{-2}$	21	97,5	2,5	97,3	2,7
PAM II	0,97	$1,69 \times 10^{-2}$	19	95,6	4,4	95,4	4,6
PAM III	1,1	$3,9 \times 10^{-2}$	12,3	91,5	8,5	92,9	7,1
PAM IV	—	—	20	—	—	90,6	9,4
PAM V	1,14	0,116	25	80	20	81,7	18,3

<sup>a</sup> Initiateur, azobisisobutyronitrile,  $10^{-3}$  mole/l; solvant, DMF; température de polymérisation, 60°C.

<sup>b</sup> Taux de conversion déterminés par CPV des échantillons analysés par RMN.

### Analyse par RMN-HR

Les spectres RMN à 60 MHz ont été enregistrés par l'unité Varian DA-60-IL à 120-130°C, avec des solutions de PAM (~10%) dans le diméthyle formamide deutérié à 99,6% (DMF-*d*<sub>7</sub>), la référence interne utilisée étant de l'hexaméthyle disiloxane (HMDS,  $\tau_{\text{HMDS}} = 9,95$  ppm). L'amélioration du rapport signal/bruit a été obtenue par l'intermédiaire d'un accumulateur de spectres JEOL-JRA-1. Les décompositions et simulations de spectres RMN des groupes méthoxy et  $\alpha$ -méthyle ont été réalisées grâce à l'analyseur de courbes du Pont de Nemours 310.

En ce qui concerne la décomposition des raies méthoxy et  $\alpha$ -méthyle des PAM, nous avons pris comme raie de référence une lorentzienne dont la largeur à mi-hauteur ( $\delta\nu$ ) peut se mesurer de façon suffisamment précise sur les spectres des PM radicalaires en solution dans le DMF-*d*<sub>7</sub>. ( $\delta\nu$ )<sub>OC<sub>3</sub></sub> est égale à 1,8-2 Hz. Quant à ( $\delta\nu$ ) <sub>$\alpha$ -CH<sub>3</sub></sub>, sa valeur expérimentale mesurée sur les raies des triades hétérotactiques et syndiotactiques est de l'ordre de 3 Hz. L'élargissement expérimentalement observé des raies  $\alpha$ -CH<sub>3</sub> est plutôt dû à l'effet des pentades (spectres à 100 MHz<sup>5</sup> et à 220 MHz<sup>6</sup>). Nous avons donc choisi la valeur de 2 Hz pour ( $\delta\nu$ )<sub>etOC<sub>3</sub></sub> et ( $\delta\nu$ ) <sub>$\alpha$ -CH<sub>3</sub></sub>.

## RESULTATS ET DISCUSSIONS

## Composition des Copolymères PAM

En solution dans le DMF- $d_7$ , les protons méthoxy des PM résonnent à 6,42  $\tau$  et les  $\alpha$ -méthyles des triades isotactiques (i), hétérotactiques (h), et syndiotactiques (s), respectivement à 8,86–8,96 et 9,1 $\tau$  (Fig. 1A). Dans les mêmes conditions, les protons  $\alpha$  du PA apparaissent sous la forme d'un quintuplet ( $J_{AX} \sim 7$  Hz) centré à 6,75  $\tau$ ; les protons  $\beta$  sous la forme apparente de deux triplets enchevêtrés, centrés vers 7,77 et 7,80  $\tau$  attribuables aux diades isotactiques (I) et syndiotactiques (S) respectivement

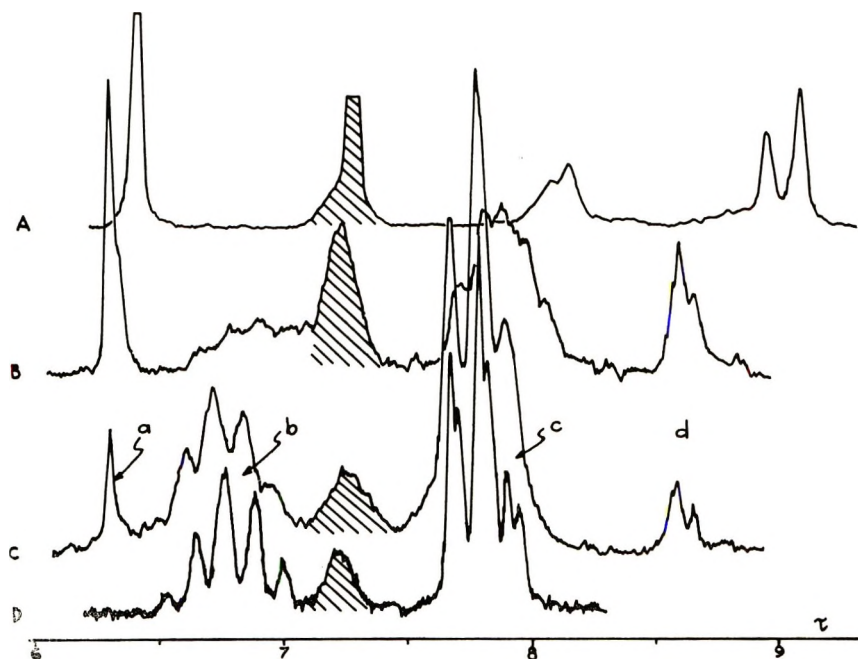


Fig. 1. Spectres RMN à 60 MHz: (A) PM radicalaire; (B) PAM V, (C) PAM II; (D) PA radicalaire. Spectres hachurés: protons résiduels du DMF- $d_7$ .

(Fig. 1D). Cependant l'examen attentif du triplet S (balayage lent) a montré qu'il y a d'une part une légère différence de la valeur de couplage  $J_{AX}$  selon le couple de raies considéré, et d'autre part, il y a élargissement de ces dernières raies. Il est probable que l'on discerne les triades et non les diades, l'élargissement des raies S serait dû à l'effet des triades hétérotactiques (h).

Quant aux spectres RMN des PAM (PAM I à PAM V) (dont les caractéristiques sont consignées dans le Tableau I), on distingue quatre domaines de résonance. Par rapport à PM (Fig. 1A), la raie méthoxy du PAM (raie a, Fig. 1B et 1C) est déplacée vers les basses valeurs en champ; à 6,26  $\tau$ , cette raie devient composite lorsque le pourcentage en M augmente dans

le copolymère (PAM V, Fig. 1B). Entre 6,5 et 7,2  $\tau$  (domaine *b*, Fig. 1B et 1C), on retrouve le quintuplet des protons  $\alpha$  des séquences PA du PAM. Entre 7,5 et 8,5  $\tau$  (domaine *c*, Fig. 1B et 1C), résonnent tous les protons  $\beta$  de A et de M du PAM. Enfin entre 8,5 et 9,0  $\tau$  (domaine *d*, Fig. 1B et 1C), on observe les résonances complexes des  $\alpha$ -méthyles des unités M plus ou moins isolées dans la chaîne du PAM.

En normalisant à 1 proton les différents groupements chimiques de chaque monomère, on a :

$$\begin{aligned} (^{1/3}) \text{ intensité de } a &= (^{1/3}) [a] = [M] \text{ (protons méthoxy)} \\ (^{1/3}) \text{ intensité de } d &= (^{1/3}) [d] = [M] \text{ (protons } \alpha\text{-méthyles)} \\ (^{1/2}) \text{ intensité de } c &= (^{1/2}) [c] = [A + M] \text{ (protons } \beta\text{-méthyléniques)} \end{aligned}$$

d'où

$$M \% = \frac{(^{1/3}) [a]}{(^{1/2}) [c]} \times 100 = \frac{(^{1/3}) [d]}{(^{1/2}) [c]} \times 100 \quad (1)$$

Les pourcentages de M et de A calculés d'après l'éq. (1) sont consignés dans le Tableau I. Ces valeurs sont en accord avec celles déduites des taux de conversion partiels déterminés par chromatographie en phase vapeur (CPV) au moment des prélèvements au cours des copolymérisations.

### Spectre RMN des Méthoxy et $\alpha$ -Méthyle

**Groupe méthoxy.** Le spectra des méthoxy des échantillons PAM IV et PAM V ne sont pas des singlets (raie *a*, Fig. 1B). On peut reconstituer le spectre expérimental en combinant deux lorentziennes de largeur à mi-hauteur égale à 2 Hz environ:  $a_1$  et  $a_2$  centrées respectivement à 6,26 et 6,32  $\tau$  (Fig. 2).  $a_1$  se retrouve dans les spectres des PAM où la totalité des M sont isolés (PAM I et PAM II). On peut attribuer  $a_1$  et  $a_2$  respectivement aux méthoxy des unités M centrales des triades AMA et MMA ou AMM. En effet, il est raisonnable de penser que la valeur  $\tau$  des méthoxy dépend de la nature des unités monomères adjacentes plutôt que de la configuration spatiale de ces dernières. L'existence des triades MMM n'a pas été détectée (leur résonance se trouverait vers 6,42  $\tau$ , soit la même valeur de  $\tau$  que celle des méthoxy des PM analysés dans les mêmes conditions).

Si l'hypothèse précédente est exacte,  $a_1$  est proportionnelle au nombre de séquences à 1 M et  $a_2$ , au nombre de séquences à 2 M. Les valeurs de  $a_1$  et  $a_2$  obtenues par décomposition des spectres RMN sont consignées dans le Tableau II. La comparaison avec les fractions en poids des séquences à une unité M [ $w'(1)$ ] et à deux unités M [ $w'(2)$ ] donne toujours:  $a_1 > w'(1)$  et  $a_2 < w'(2)$ —(valeurs des  $w'(1)$  et  $w'(2)$  calculées à partir des taux de réactivité, voir annexe)—ce qui est normal,  $w'(1)$  et  $w'(2)$  ont été obtenues à partir du rapport molaire  $x_M$  ( $x_M = M/A$ ) du mélange initial en monomères. M se consommant deux à trois fois plus rapidement que A,  $w'(1)$  représente plutôt la limite inférieure pour les séquences à une unité M et  $w'(2)$ , la limite supérieure pour les séquences à deux unités M.

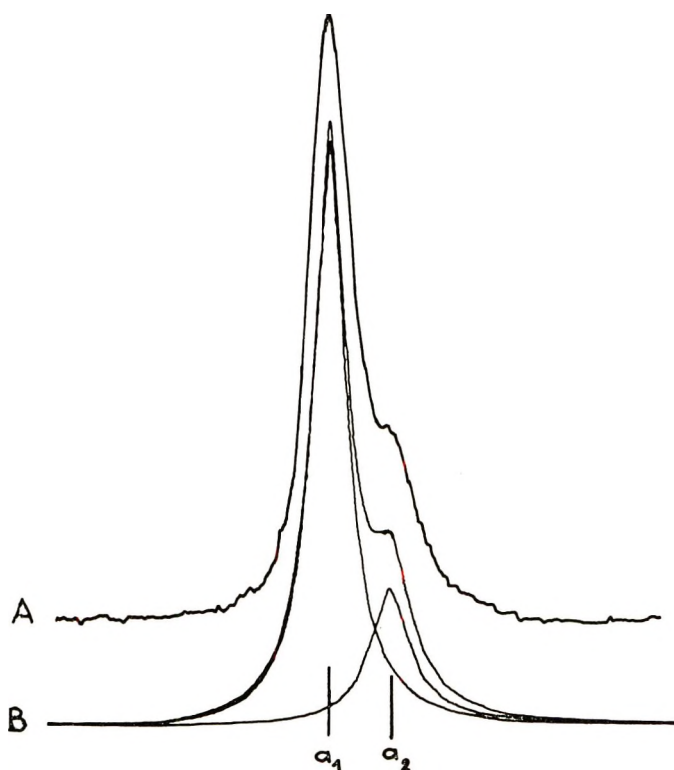


Fig. 2. Spectre RMN des protons méthoxy (largeur de balayage: 100 Hz): (A) spectre expérimental; (B) spectre décomposé.

**Groupe  $\alpha$ -méthyle.** On remarque que les  $\alpha$ -méthyles des M isolés des PAM subissent un déplacement paramagnétique de l'ordre de 0,4 ppm par rapport aux  $\alpha$ -méthyles du PM. Les spectres accumulés des  $\alpha$ -méthyles

TABLEAU II

Pourcentages cumulatifs calculés (par Théorie cinétique) et expérimentaux (par RMN) des Séquences M de Longueur  $n$  des PAM

Echantillons	$x_M^a$	$w'(1),$	$w'(2),$	$w'(3),$	$w'(1)_{RMN}, w'(2)_{RMN},$	
		$\%^b$	$\%^b$	$\%^b$	$n = 1$	$n = 2$
		$n = 1$	$n = 2$	$n = 3$	(raie $a_1$ )	(raie $a_2$ )
PAM I	$1,04 \times 10^{-2}$	97,7	2,2	0,1	—	—
PAM II	$1,74 \times 10^{-2}$	95	5	—	—	—
PAM III	$3,5 \times 10^{-2}$	90	9,8	0,2	95	5
PAM IV	$5,27 \times 10^{-2}$	85,5	13,3	1	93	7
PAM V	0,1	75,5	21,5	2,9	84	16

<sup>a</sup> Rapport molaire  $x_M = M/A$  du mélange initial en monomères.

<sup>b</sup> Pourcentages cumulatifs calculés à partir des valeurs de taux de réactivité déterminés par CPV.

<sup>c</sup> Valeurs obtenues par décomposition des spectres RMN des méthoxy de M.



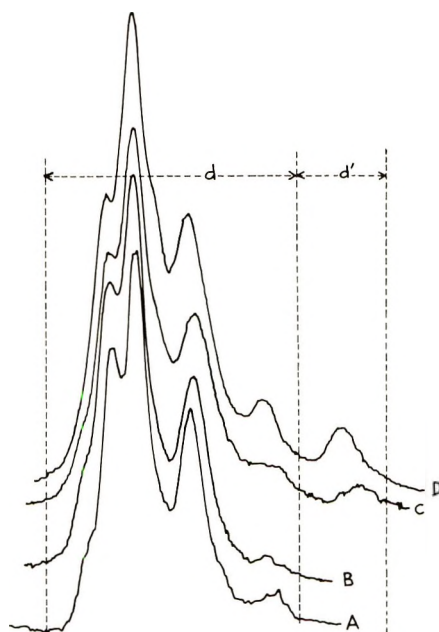


Fig. 3. Spectres RMN accumulés des protons  $\alpha$ -méthyles (largeur de balayage: 100 Hz): (A) PAM I; (B) PAM II; (C) PAM IV; (D) PAM V.

des cinq échantillons PAM (I à V) présentent tous une partie entre 8,46 et 8,8  $\tau$  (domaine  $d$ , Fig. 3) de même allure et un petit dôme centré vers 8,83  $\tau$  (domaine  $d'$ , Fig. 3) dont l'intensité augmente lorsque le pourcentage en M du PAM augmente (PAM IV, Fig. 3C, PAM V, Fig. 3D).  $d'$  appartient probablement aux  $\alpha$ -méthyles des triades MMA ou AMM.

Par le même procédé que précédemment, on peut décomposer le spectre  $d$  en huit raies lorentziennes numérotées par ordre croissant en champ de  $d_1$  à  $d_8$  (Fig. 4). Les pourcentages en intensité obtenus après décomposition sont reportés dans le Tableau III. Pour les échantillons PAM III, PAM IV, PAM V (plus riches en M), pour lesquels les mesures sont plus accessibles, on constate l'égalité suivante en intensités:

$$a_2 \simeq d_8 + d'$$

TABLEAU III  
Décomposition des Spectres RMN des  $\alpha$ -Méthyles des PAM (Fig. 4)

	$d_1$ ( $\tau =$ 8,54)	$d_2$ ( $\tau =$ 8,56)	$d_3$ ( $\tau =$ 8,59)	$d_4$ ( $\tau =$ 8,61)	$d_5$ ( $\tau =$ 8,65)	$d_6$ ( $\tau =$ 8,68)	$d_7$ ( $\tau =$ 8,73)	$d_8$ ( $\tau =$ 8,75)
PAM I, %	4	22	35	4,5	26	1,5	4	2
PAM II, %	4,5	23,5	37,5	5	24	2,5	2	1
PAM III, %	3,5	22	38	3,5	24	2	5	1,5
PAM IV, %	3	24,5	35	6	22,5	3,5	2,5	3
PAM V, %	3	20	32	7,5	23,5	5	4,5	5

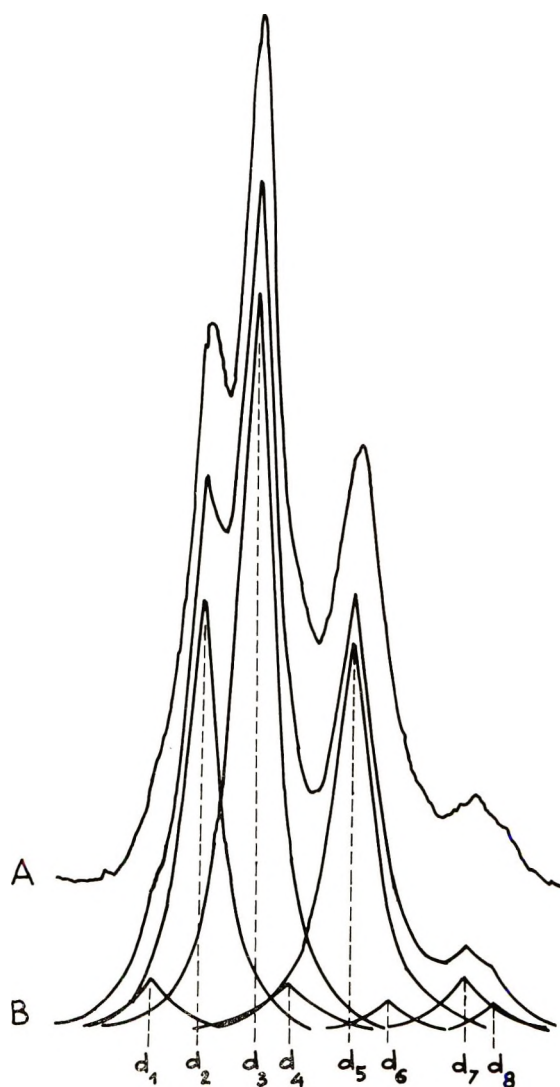


Fig. 4. Spectre RMN accumulé des protons  $\alpha$ -méthyles du PAM III: (A) spectre expérimental; (B) spectre décomposé.

Ainsi, les  $\alpha$ -méthyles des séquences PAM à unité M centrale correspondent aux sept singlets ( $d_1$  à  $d_7$ ). Cette résolution permet, en principe, de discerner les différentes pentades cotaectives ( $-A_{n-2}A_{n-1}MA_{n+1}A_{n+2}-$ ) dont les pourcentages expérimentaux en intensité sont consignés dans le Tableau IV (avec  $\sum_{i=1}^7 d_i = 100\%$ ).

Le calcul des longueurs de séquences moyennes en nombre en monomère A,  $\overline{Ln(A)}$ , des PAM, à partir des résultats cinétiques a donné pour valeurs  $\overline{Ln(A)}$  4,3; 7,7; 11,1; 22,7; 37,3 respectivement pour PAM V; PAM IV, PAM III, PAM II, et PAM I (pour les mêmes raisons que précédemment,

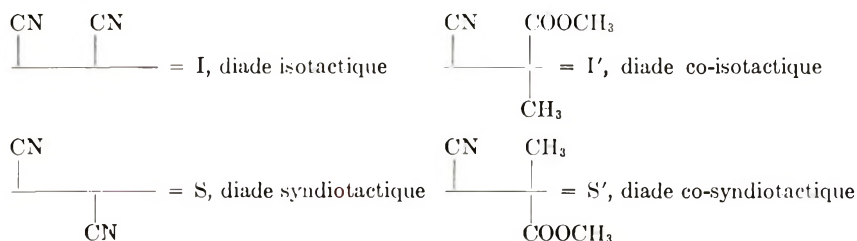
TABLEAU IV  
Attribution des Raies  $\alpha$ -Méthyles des Pentades Cotactiques  
( $-A_{n-2}A_{n-1}M A_{n+1}A_{n+2}$ )

Raie	$\tau$	%	Pentades	Probabilités d'existence
$d_1$	8,53	3,7	SI'I'S	$P(SI'I'S)$
$d_2$	8,56	23,1	II'I'S ou SI'I'I	$P(II'I'S) + P(SI'I'I)$
$d_3$	8,59	36,6	II'I'I	$P(II'I'I)$
$d_4$	8,61	5,5	SI'S'S ou SS'I'S II'S'S ou SS'I'I IS'I'S ou SIS'I IS'I'I ou II'I'S	$\Sigma P(\dots I'S' \dots) + \Sigma P(\dots S'I' \dots)$
$d_5$	8,65	24,7	SS'S'S	$P(SS'S'S)$
$d_6$	8,68	3,0	IS'S'S ou SS'S'I	$P(IS'S'S) + P(SS'S'I)$
$d_7$	8,73	3,7	IS'S'I	$P(IS'S'I)$

ces valeurs ne sont que des limites inférieures—voir annexe), ce qui exclut toute possibilité de perturbation provoquée par la présence des séquences alternées (AMAMAM). On observe cependant un léger élargissement des raies, ce qui est probablement dû à l'influence des courtes séquences A (de longueur inférieure à 4A), lorsque l'on passe de PAM I à PAM V.

En ce qui concerne  $d_8$  et  $d'$  (raie composite), attribuées aux M centraux des triades AMM ou MMA, leur analyse est délicate, d'une part, à cause de l'influence simultanée des tacticité et cotacticité, et d'autre part, il y a enchevêtrement possible avec les  $\alpha$ -méthyles des triades isotactiques i des séquences PM à plus de trois unités M du PAM.

On peut définir les tacticité et cotacticité des diades AA, AM ou MA de la façon suivante:



L'effet de la tacticité et de la cotacticité sur la résonance des  $\alpha$ -méthyles est dû, dans le cas du PM, à l'anisotropie magnétique des groupes ( $-C=O$ ), dans le cas du PAM, aux anisotropies ces groupes ( $-C=O$ ) et ( $-C\equiv N$ ). Il paraît alors raisonnable de penser que, pour les différentes triades cotactiques (à unité M centrale), l'ordre de résonance soit le même que celui du PM:

$$\tau(I'I') < \tau(I'S') = \tau(S'I') < \tau(S'S')$$

L'influence des groupes ( $-C\equiv N$ ) étant plus prononcée que celle des ( $-C=O$ ), d'où l'effet des unités  $A_{n-2}$  et  $A_{n+2}$  sur les  $\alpha$ -méthyles des M centraux des pentades cotactiques.

A cause de la similitude entre ( $-C=O$ ) et ( $-C\equiv N$ ), on peut, en se basant sur l'analyse configurationnelle en pentades des différents PM à 220 MHz,<sup>6,9</sup> admettre que, pour une même triade cotactique centrale ( $-A_{n-1}MA_{n+1}-$ ), l'ordre de résonance des  $\alpha$ -méthyles des différentes pentades cotactiques soit:

$$\tau(S \dots S) < \tau(S \dots I) = \tau(I \dots S) < \tau(I \dots I)$$

Dans le cas présent, au lieu des neuf raies  $\alpha$ -méthyles prévues pour les pentades cotactiques (par raison de symétrie II'S'S et IS'I'S ne seraient pas discernables), on n'en observe que sept. En supposant que les pentades à triades cohétérotactiques centrales ( $\dots I'S' \dots$  et  $\dots S'I' \dots$ ) ne soient pas résolues, l'attribution des singlets  $\alpha$ -méthyles en fonction de  $\tau$  est celle que nous proposons dans le Tableau IV.

Si cette attribution est bonne, l'utilisation des relations statistiques entre les probabilités d'existence des pentades  $P(\dots)$  et les probabilités conditionnelles de placement  $P(\dots/\dots)$  définies par Reimoller et Fox<sup>7</sup> permet de déduire les valeurs de  $P(\dots/\dots)$  reportées dans le Tableau V.

TABLEAU V  
Probabilités conditionnelles de Placements

Pentades cotactiques		$P(S/SI'I')$	0,24
		$P(I/SI'I')$	0,76
		$P(S/II'I')$	0,24
		$P(I/II'I')$	0,76
		$P(S/SS'S')$	0,94
		$P(I/SS'S')$	0,06
		$P(S/IS'S')$	0,29
		$P(I/IS'S')$	0,71
Triades cotactiques	$d_1 + d_2 + d_3$	$P(I'I')$	0,63
	$d_4$	$P(I'S') + P(S'I')$	0,05
	$d_5 + d_6 + d_7$	$P(S'S')$	0,32
		$P(I'/I')$	0,96
		$P(I'/S')$	0,08
		$P(S'/I')$	0,04
		$P(S'/S')$	0,92
Diades cotactiques	$d_1 + d_2 + d_3 + \frac{1}{2}d_4$	$P(I')$	0,66
	$\frac{1}{2}d_4 + d_5 + d_6 + d_7$	$P(S')$	0,34

On constate que:

$$\left. \begin{array}{l} P(I') \neq P(I'/I') \neq P(I'/S') \\ P(S') \neq P(S'/S') \neq P(S'/I') \end{array} \right\} \text{triades } (-A_{n-1}MA_{n+1}-)$$

La probabilité conditionnelle de placement d'une nouvelle unité A sur un radical en croissance terminé par  $-AM^\circ$  dépend de la cotacticité de la diade terminale. La statistique de Bernouilli n'est donc pas applicable. Par ailleurs les valeurs de  $\rho_I$  et de  $\eta_{S'}$  trouvées sont respectivement égales à 8,7 et 2,7 ( $\neq 1$ ), il y a effet penultième net.

En ce qui concerne les pentades ( $-A_{n-2}A_{n-1}MA_{n+1}A_{n+2}-$ ):

$$\begin{aligned} P(I/II'I') &= P(I/SI'I') \neq P(I/SS'S') \neq P(I/IS'S') \\ P(S/II'I') &= P(S/SI'I') \neq P(S/SS'S') \neq P(S/IS'S') \end{aligned}$$

La probabilité conditionnelle de placement d'une nouvelle unité A sur un radical en croissance terminé par  $-A_{n-2}A_{n-1}MA_{n+1}^\circ$  ne dépend pas de la tacticité de la diade ( $A_{n-2}A_{n-1}$ ), ceci seulement dans le cas où la triade terminale est coisotactique. En revanche, dans le cas où la triade terminale est cosyndiotactique, il y a influence de la tacticité de la première diade et l'on observe une certaine dissymétrie. Etant donné l'hypothèse faite sur l'attribution des raies  $\alpha$ -méthyles, l'analyse des pentades à triades centrales cohétérotactiques est impossible.

Il apparaît que, pour les tacticité et cotacticité des PAM, l'entourage immédiat de l'unité M ne suit ni la statistique de Bernoulli, ni la statistique de Markoff d'ordre un.

Le manque de résolution dans le domaine de résonance des protons  $\beta$  n'a pas permis l'exploitation des configurations en diades et en tétrades cotactiques, les hypothèses concernant les pentades cotactiques n'ont pu alors être confirmées, ni infirmées.

### ANNEXE

Un travail précédent,<sup>8</sup> concernant la cinétique de la copolymérisation radicalaire du couple acrylonitrile-méthacrylate de méthyle a permis de mettre en évidence l'existence d'un effet pénultième. Les taux de réactivité expérimentaux sont les suivants:

$$\begin{aligned} r_{MM} &= 1,01 \pm 0,2 \\ r_{AM} &= 1,56 \pm 0,05 \\ r_{AA} &= 0,39 \pm 0,03 \\ r_{MA} &= 0,20 \pm 0,03 \end{aligned}$$

d'où les fractions en poids des séquences PM à  $n$  unités M des PAM:

$$w'(n) = \frac{nP_{MMA}^2 P_{AMM} P_{MMM}^{n-2}}{P_{MMA} + P_{AMM}}$$

avec  $P_{MMA}$  = probabilité d'addition d'un monomère A sur un radical terminé par  $-MM^\circ$ , etc . . .

$$P_{MMA} = \frac{1}{1 + r_{MM}x_M}$$

$$P_{AMA} = \frac{1}{1 + r_{AM}x_M}$$

$$P_{AMM} = \frac{r_{AM}x_M}{1 + r_{AM}x_M}$$

$$P_{MMM} = \frac{r_{MM}x_M}{1 + r_{MM}x_M}$$

avec

$$x_M = M/A$$

$x_M$  étant le rapport molaire du mélange initial en monomères.

Pour les fractions en poids des unités M isolées, on utilise la formule:

$$w'(1) = \frac{P_{MMA}P_{AMA}}{P_{MMA} + P_{AMM}}$$

Les longueurs de séquences moyennes en nombre en A des PAM s'obtiennent, compte-tenu de l'effet pénultième, à l'aide de l'équation suivante:

$$\overline{Ln(A)} = \frac{P_{AAM} + P_{AMM}}{P_{AMM}}$$

### Références

1. T. Fischer, J. B. Kinsinger, et C. W. Wilson III, *J. Polym. Sci. B*, **4**, 379 (1966); *J. Polym. Sci. B*, **5**, 285 (1967).
2. S. Ikuma et H. Kada, *J. Polym. Sci. B*, **6**, 219 (1968).
3. Y. Yamashita et K. Ito, in *International Symposium on Polymer Characterization (Appl. Polym. Symp., 8)*, K. A. Boni and F. A. Sliemers, Eds., Interscience, New York, 1969, p. 245.
4. K. Matsuzaki, T. Uryu, M. Okada, K. Ichigure, T. Ohki, et M. Takeuchi, *J. Polym. Sci. B*, **4**, 487 (1966).
5. J. Guillot, A. Guyot, et Pham Q. T., *J. Macromol. Sci., A*, **2**, 1303 (1968).
6. K. C. Ramey, *J. Polym. Sci. B*, **5**, 857 (1967).
7. M. Reimoller et T. G. Fox, *Am. Chem. Soc. Polymer Preprints*, **7**, 987 (1966).
8. A. Guyot et J. Guillot, *J. Macromol. Sci. A*, **2**, 889 (1968).
9. R. C. Ferguson, *Macromolecules*, **2**, 237 (1969).

Received March 6, 1970

## Mechanism of the Thermal Stabilization of Poly(vinyl chloride) with Metal Carboxylates and Epoxy Plasticizers

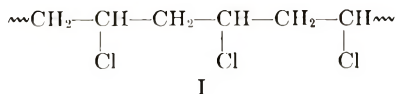
DONALD F. ANDERSON\* and D. A. MCKENZIE,  
*Union Carbide Corporation, Tarrytown Technical Center,  
 Tarrytown, New York 10591*

### Synopsis

The chemical reactions responsible for the retardation of thermal discoloration in poly(vinyl chloride) (PVC) stabilized with a combination of an epoxy plasticizer and a heavy metal soap mixture of Group IIa and IIb metals have been studied. Allylic chlorides (a mixture of 4-chlorohexene-2 and 2-chlorohexene-3) are used as prototypes for the degrading segment of the polymer chain. The results confirm earlier reports that, when a mixture of a covalent and ionic metal soap is used as the stabilizer, the covalent moiety (e.g., Cd and Zn soaps) functions to esterify the allylic site of the degrading PVC model. A synergistic effect displayed by the ionic soap (e.g., Ca or Ba) is caused by a transfer of carboxylate ligands from the ionic soap to the depleting covalent species, which has been largely converted to the corresponding chloride. When an epoxy plasticizer model (cyclohexene oxide) is used in conjunction with the metal soap stabilizer, the preferred reaction is esterification. After a considerable build-up of ester, an  $\alpha$ -chloroether, 2-hexenyl 4-(2-chlorocyclohexyl) ether, is formed by the reaction of cyclohexene oxide with the PVC model. This reaction was found to be catalyzed by cadmium chloride. The esterification and etherification reactions provide an explanation for the synergism observed in the stabilization of PVC containing a combination of an epoxy plasticizer with a covalent and an ionic metal soap.

### INTRODUCTION

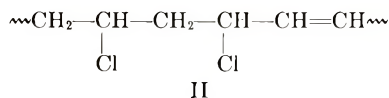
If the structure of the poly(vinyl chloride) were ideally linear with alternating secondary chlorines (I) then stabilization would not be a problem.



A consideration of the polymerization mechanism reveals that thermally unstable structures are expected in the free-radical polymerization of vinyl chloride.<sup>1</sup> Bengough and Norrish<sup>2</sup> reported that chain transfer to monomer is the predominant termination step in the polymerization.

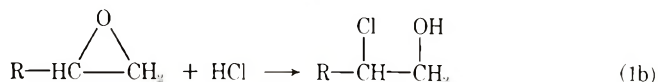
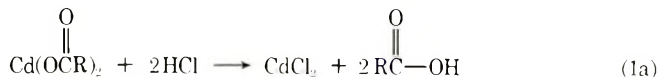
\* Author to whom inquiries should be directed.

An allylic chloride structure (II) which is markedly more labile than the secondary chloride would be expected to result from

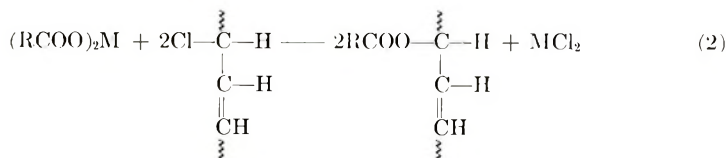


this termination. Tertiary chlorides are also present in polyvinyl chloride as shown by the work of Cotman.<sup>3</sup>

The major function of the stabilizers which have given satisfactory commercial service has been to react with the hydrogen chloride split off from PVC on thermal processing. Several earlier workers had suggested that, in the absence of an acid acceptor, accumulated hydrogen chloride catalyzed further degradation of the polymer.<sup>4,5</sup> However, careful work by Arlmann<sup>6</sup> disclosed no evidence of any degradation catalysis in the presence of hydrogen chloride, and this theory of stabilization has been largely abandoned. Thermal stabilizers employed in present day technology are generally metal salts or soaps capable of reacting with hydrogen chloride. Secondary stabilizers are also used in conjunction with the main components. Some of these are alkyl and aryl phosphites and certain epoxy plasticizers. Typical reactions by which these materials bind hydrogen chloride chemically are shown by eqs. (1a) and (1b).



The first experimental evidence on the chemistry of the stabilization of PVC by metallic soaps was reported by Frye and Horst.<sup>7</sup> They used infrared spectroscopy and radioactive-labeled tracer techniques to show that the labile allylic chlorine on the polymer chain is replaced by a more thermally stable fatty carboxylate [eq. (2)].



This work has been confirmed by others, including Bengough and Onozuka,<sup>8</sup> Shimura,<sup>9</sup> Klemchuk,<sup>10</sup> and most recently, Deanin.<sup>11</sup> Onozuka and Asahina<sup>12,13</sup> have also studied the synergistic stabilization effects observed when a combination of metal soaps is used as a stabilizer. The enhancement of stabilization with this system was attributed to an ester interchange reaction between an alkaline earth metal soap and a covalent



chloride (Ca/Zn) which retards covalent zinc chloride formation and subsequent degradation.

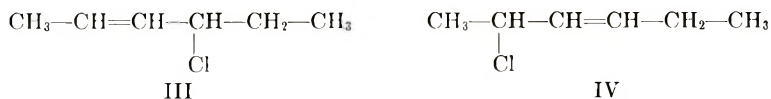
Surprisingly few studies have been reported on the chemistry of stabilization by oxirane compounds. Perry<sup>14</sup> suggested the initial formation of the corresponding chlorohydrin with subsequent regeneration of epoxide in the presence of the metallic soap stabilizers. Hopf<sup>15</sup> has reported the grafting of the oxirane group to double bonds formed by the loss of hydrogen chloride from the polymer. Neither of the above mechanisms have been substantiated.

This paper will present a quantitative study of the chemistry of the thermal stabilization of poly(vinyl chloride). The mechanisms involved are elucidated by ascertaining the products formed on reacting a low molecular weight prototype of the degrading section of a poly(vinyl chloride) molecule with metal carboxylates and with a compound containing the oxirane structure. This work significantly extends the model compound study performed initially by Onozuka with the utilization of the soluble 2-ethylhexanoate salts as metal soap stabilizer models.

## RESULTS AND DISCUSSION

### Selection of Model Systems

Low molecular weight models were selected for this investigation in order to facilitate isolation and identification of the reaction products by distillation, vapor phase chromatography and nuclear magnetic resonance. A mixture of hexenyl allylic isomers, 4-chlorohexene-2 (III) and 2-chlorohexene-3 (IV), synthesized by the treatment of 2-hexene-4-ol with anhydrous hydrogen chloride,<sup>16</sup> was chosen as the degrading poly(vinyl chloride) model. Since the allylic chlorides were difficult to separate into pure isomers, the mixture was used. The two

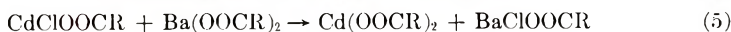
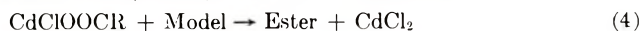


isomers, both having allylic chlorides, are of similar reactivity in the reactions involved in this study. The allylic metal soap stabilizer system is represented by the 2-ethyl hexanoates and acetates of zinc, cadmium, calcium and barium. Cyclohexene oxide was used to simulate an epoxy plasticizer.

### Reactions of Metal Carboxylates with PVC Model

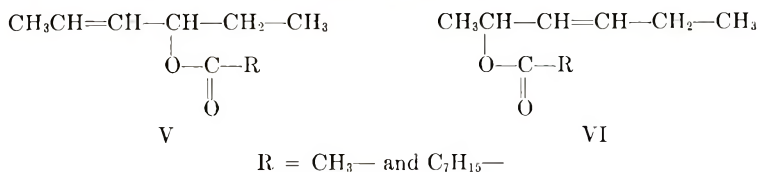
Our work has shown that poly(vinyl chloride) metal soap stabilizers can be divided into two classes, covalent salts and ionic salts. A similar classification was used by Deanin.<sup>11</sup> In the work reported here, cadmium carboxylates have been used as representatives of the covalent moiety, whereas the ionic moiety is represented by the barium carboxylates. It

appears that the covalent member of the stabilizer package is the active species involved in replacing the unstable allylic chloride function with a more thermally stable carboxylate ligand to provide a less easily degradable ester. The ionic carboxylate regenerates the cadmium carboxylate by exchanging a carboxylate ligand for a chloride ion from the cadmium chloride formed in the esterification [eqs. (3)–(6)].



In eqs. (3)–(6), the reactive species in esterification can be either the cadmium carboxylate or the half salt [eqs. (3) and (4)]; however, we have found that the dicarboxylate is the most reactive species.

The reactions of the acetates and 2-ethylhexanoates of cadmium and barium with the allylic hexenyl chlorides were carried out in dilute solutions in tetrahydrofuran at 60°C. The cadmium salt was observed to react rapidly under these conditions to give a clean and efficient conversion to the hexenyl esters, V and VI. The barium salt failed to react under similar conditions. Identical reactions were run with the zinc and



calcium salts and analogous results were obtained although the zinc carboxylates were considerably more reactive than the corresponding cadmium compounds. The calcium carboxylates were inert.

TABLE I  
Reactions of Cadmium Carboxylates with PVC Model  
at 60°C in Tetrahydrofuran;  $[\text{Model}]_0 = 0.26 \text{ M}$

Ligand	Salt/ Model	Reaction time, hr	Ester, % <sup>a</sup>	Olefin, % <sup>c</sup>
Acetate	3/1	0.5	100	None
Acetate	1/1	1	100	None
Acetate	1/2	20	84	16
Acetate	1/10	20	68 <sup>b</sup>	> ester <sup>b</sup>
2-Ethylhexanoate	1/2	0.25	100	None
2-Ethylhexanoate	1/4	0.25	100	None
2-Ethylhexanoate	1/4	20	100	50 <sup>c</sup>

<sup>a</sup> Based on available acetate ligand (2 mole ligand/mole of salt).

<sup>b</sup> Partial conversion of the PVC model to the ester (68%) based on available acetate, before dehydrohalogenation converted excess model to olefin. Olefin yield calculated based on PVC model.

<sup>c</sup> Esterification was complete after 15 min; CdCl<sub>2</sub> catalyzed the decomposition of remaining model to olefin.

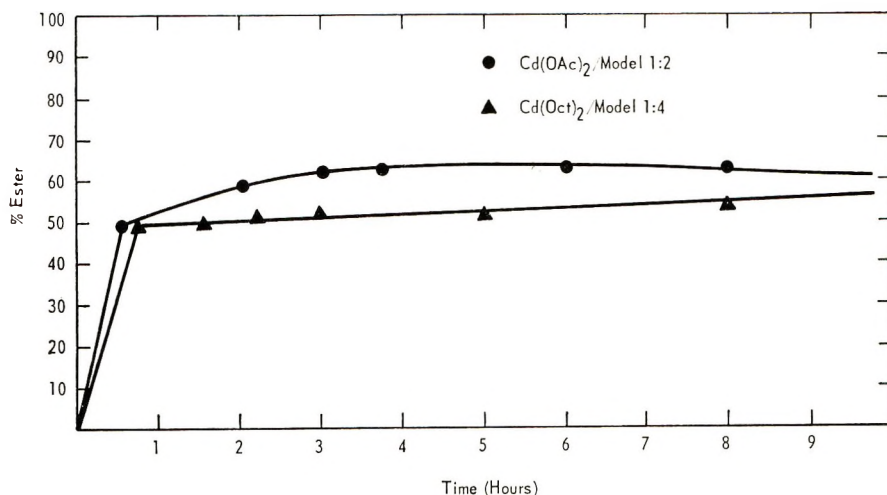


Fig. 1. Plot of ester vs. time for the reaction of cadmium carboxylates with PVC model.

The reactions with cadmium acetate proceeded rapidly when 3:1, 2:1, and 1:1 molar ratios of salt to allylic chloride were used. Vapor-phase chromatographic analysis revealed complete conversion of the chlorides to a mixture of allylic hexenyl acetates (V and VI, see Table I).

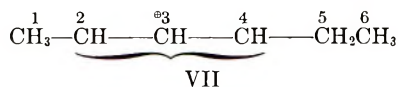
In order to investigate the extent of esterification, a 1:2 ratio of cadmium acetate/PVC model was allowed to react. After 1 hr, half the PVC model had been converted to the ester (Fig. 1); within the next 4 hr, a 20% further conversion to the ester was observed along with some competition from dehydrohalogenation to form 2,4-hexadiene; 16% of the diene formed in 16 hr. Each experiment with the acetate salts involved a heterogeneous reaction mixture in which cadmium acetate was slightly soluble and cadmium chloride was very slightly soluble. It would appear likely that the rate of reaction is solubility dependent, i.e., the amount of available acetate ions in solution determines the speed at which esterification proceeds. At half reaction, the cadmium acetate was converted to the half salt, cadmium chloroacetate ( $\text{CdClOAc}$ ), which is probably less reactive than the diacetate due to its insolubility in the reaction medium. This accounts for the slower reaction after 50% conversion of the allylic chloride to the ester, and consequently, allows the competing dehydrochlorination reaction to become increasingly favorable (Fig. 1).

A 10:1 mixture of allylic chloride:cadmium acetate was found to proceed to about 60% conversion to the ester (based on available acetate). However, the amount of 2,4-hexadiene formed exceeded the ester. This observed dehydrochlorination can be attributed to a secondary reaction in which the cadmium chloride formed after esterification acts as a catalyst for dehydrohalogenation of the model to olefin. To test this hypothesis, a dilute solution of the allylic halide model was treated with cadmium chloride at 60°C. After 2 hr, the PVC model was 50% degraded to 2,4-

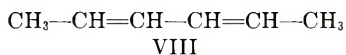
hexadiene. The acetate ester was found to be thermally stable after being heated at 150°C for 48 hr. Onozuka<sup>13</sup> reported the ester, 4-acetoxyhexene-2, decomposes at 230°C.

The above reactions were repeated with the soluble octanoate salt and were found to proceed as described above. However, the rates of conversion to the ester were markedly faster. An experiment in which the molar ratio of salt to model was 1:2 revealed that esterification was complete in 15 min with total conversion to the ester (Table I). A competing reaction in which dehydrochlorination became the major reaction after completion of esterification was similarly observed when a 4:1 molar ratio of PVC model/cadmium 2-ethylhexanoate was employed (Fig. 1, Table I). Several experiments were run with the barium acetate and 2-ethylhexanoate salts and the allylic hexenyl chloride model. The insoluble barium acetate failed to undergo any reaction even after 48 hr; the soluble octanoate salt gave analogous results.

The above observations could easily be explained by the proposed mechanism, in which ionization of the allylic chloride is assisted by the



presence of cadmium ion with delocalization of charge over carbons 2, 3, and 4 (VII). In the presence of excess carboxylate ligands, esterification becomes the predominant reaction by attack at C<sub>2</sub> or C<sub>4</sub>; however, with a deficiency of carboxylate, the incipient carbonium ion may collapse to form 2,4-hexadiene (VIII).



An independent synthesis of the allylic acetate, 4-acetoxyhexene-2, was achieved by the reaction of 2-hexene-4-ol with acetyl chloride. The most important feature of the NMR spectrum of this isomer is a triplet assigned to the C<sub>6</sub> methyl group centered at 0.85 ppm. An NMR spectrum of a mixture of the above isomer with 2-acetoxyhexene-3 obtained by the reaction of the allylic chloride mixture with cadmium acetate showed an additional triplet centered at 1.2 ppm. This difference can be attributed to the C<sub>6</sub> methyl of the 4-acetoxyhexene-2. In all other respects, the two spectra appear identical.

#### Reaction of Ba/Cd Carboxylate Mixtures with PVC Model

Ligand transfer has been postulated to explain the synergism of cadmium and barium soaps observed in the stabilization of the polymer. Experiments designed to demonstrate the extent of ligand transfer were devised and carried out quantitatively with the PVC model and mixtures of barium and cadmium acetates and with the 2-ethyl hexanoate salts. A mixture of barium and cadmium acetates with the PVC model in a molar ratio of 4:1:10 was found to proceed to 30% conversion to form the hexenyl

TABLE II  
Reactions of Cadmium-Barium Carboxylate Mixtures and  
PVC Model at 60°C in Tetrahydrofuran;  $[\text{Model}]_0 = 0.26 M$

Ligand	Salt/ model	Cd/Ba	Reaction time, hr	Ester, % <sup>a</sup>	Olefin, % <sup>b</sup>
Acetate	1/2	1/4	20	30	12.6
Acetate	1/2	0/1	48	None	None
Acetate	1/2	1/3 <sup>c</sup>	24	30 <sup>d</sup>	None
2-Ethylhexanoate	1/2	0/1	24	None	None
2-Ethylhexanoate	1/2	1/4	24	100	None

<sup>a</sup> Based on total available acetate (2 moles ligand/mole of model).

<sup>b</sup> Remainder of reaction mixture was unreacted PVC model.

<sup>c</sup> 0.25 CdCl<sub>2</sub>, 0.75 Ba(OAc)<sub>2</sub>.

<sup>d</sup> Based on available ligand from cadmium acetate (formed by complete ligand exchange of cadmium chloride with barium acetate).

acetates (Table II). No further reaction was observed after 24 hr. This could logically be attributed to poor solubility of the salts in the reaction medium. In spite of the low conversion to ester, the extent of this reaction is clearly greater than would be expected from the amount of available acetate obtainable from cadmium acetate alone; therefore, some ligand exchange must have occurred [eqs. (5) and (6)]. The same reaction was performed by using the soluble 2-ethylhexanoate mixture with identical molar ratios of reactants. After 18 hr, the reaction was complete with

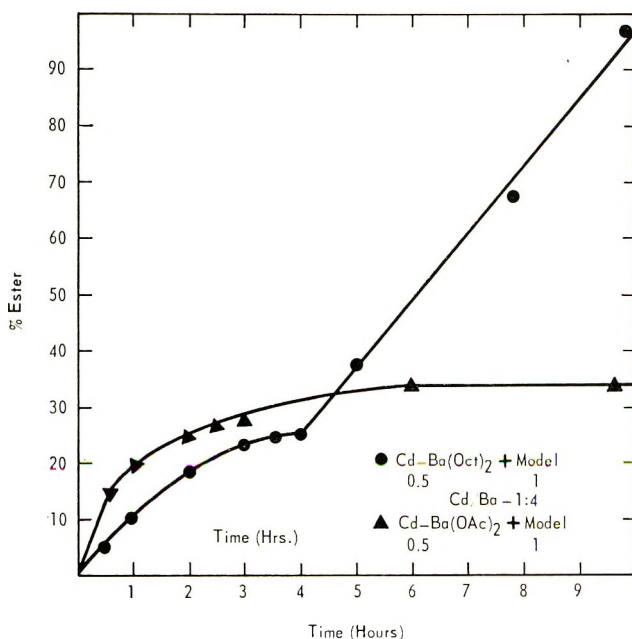


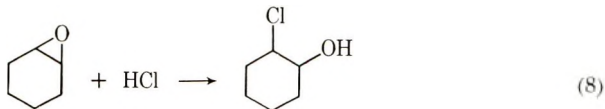
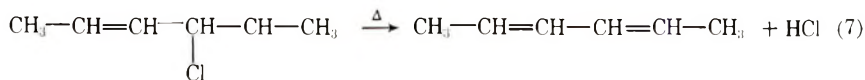
Fig. 2. Plot of ester formed vs. time for the reaction of Cd/Ba carboxylate mixtures with PVC model.

total conversion of the allylic hexenyl chloride mixture to the 2-ethylhexanoate ester (Fig. 2, Table II). The ligand transfer mechanism was further verified by the reaction of the model with a mixture 0.1 *M* in cadmium chloride and 0.4 *M* in barium acetate. With the PVC model at a concentration of 1 *M*, a 30% conversion to ester based on the quantity of cadmium chloride present was obtained. It is interesting to note that no dehydrohalogenation was observed in these experiments (Table II).

The data presented in this paper appear to parallel the results obtained by Onozuka,<sup>13</sup> in which the zinc/calcium acetate combinations as the covalent/ionic soap models were used. Work in this laboratory on the zinc model system was abandoned due to the deleterious effect of the accumulation of zinc chloride which, as a secondary reaction, functions to rapidly catalyze the degradation of the PVC model. In a recent paper by Onozuka,<sup>13</sup> specific reference is made to the necessity of the presence of a base in forming stable esters from metal carboxylates; the work reported herein fails to confirm this hypothesis. Klemchuk<sup>10</sup> performed similar esterifications with metallic soap stabilizers and 4-chloropentene-2 in the presence of chlorobenzene as solvent and revealed that esterification proceeds smoothly.

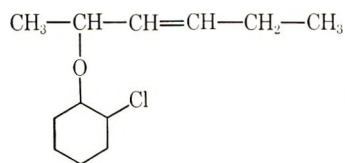
### Reaction of PVC Model with Cyclohexene Oxide

In the melt processing of PVC, epoxy plasticizers are known to impart good initial color stability to the polymer. This was originally believed to be due to the acid-accepting property of the oxirane function to form the corresponding chlorohydrin. In the initial reactions of cyclohexene oxide (epoxy plasticizer model) with the PVC model, the rate dehydrochlorination was expected to be retarded according to reactions (7) and (8).

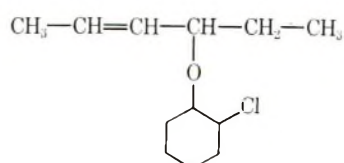


This reaction sequence would rid the system of hydrogen chloride which, it was expected, might catalyze further degradation of the PVC model. When an equimolar ratio of cyclohexene oxide and the allylic chloride mixture was allowed to react at 100°C, for 5 hr, vapor-phase chromatographic analysis of the product revealed total consumption of the reactants. The major component of the product mixture (65%) was believed to be cyclohexene chlorohydrin, according to eqs. (7) and (8); however, infrared spectrographic analysis of the product showed the absence of any hydroxyl absorption. Another significant feature of the infrared spectrum was a prominent band at 1100  $\text{cm}^{-1}$ , indicative of an ether linkage. Unsaturation was detected by an unsymmetrical carbon-hydrogen stretching band

at  $1710\text{ cm}^{-1}$  and a trans double bond absorption at  $975\text{ cm}^{-1}$ . This band was also present in the infrared spectrum of the allylic model. A mass spectral analysis of the product assigned the molecular weight at 217 ( $\text{C}_{12}\text{H}_{21}\text{OCl}$ ) and also indicated that the unsaturation occurs in an alkyl chain.<sup>17</sup> NMR analysis further verified unsaturation with a complex multiplet centered at 5.4 ppm. A complex pattern between 3.0 and 4.0 ppm was assigned to hydrogens adjacent to carbons containing ether oxygen, chlorine, and the double bond. Absorption between 1.2 and 2.0 ppm is characteristic of hydrogens in a cyclohexyl ring. A chemical investigation of the product by treatment with hydrogen chloride produced a rapid and exothermic degradation to cyclohexene chlorohydrin and 2,4-hexadiene. From these data, the structures IX and X have been assigned.



IX



X

A thermal study showed that the ether is completely stable at  $150^\circ\text{C}$  for 48 hr.

### Kinetics and Mechanism of Ether Formation

A brief investigation of the effect of solvents on the rate of the ether-forming reaction was made. Four solvents were selected to cover a wide range of dielectric constant, namely *n*-hexane ( $\epsilon = 1.89$ ), ethyl acetate ( $\epsilon = 6.02$ ), methyl ethyl ketone ( $\epsilon = 18.5$ ), and acetonitrile ( $\epsilon = 26.3$ ). The solutions were prepared  $0.172\text{ M}$  in PVC model with a slight excess of cyclohexene oxide ( $0.236\text{ M}$ ) and a trace of pyridine to minimize chlorohydrin. Table III gives data for the results of experiments run at  $150^\circ\text{C}$ . Solvents of low dielectric constant failed to enhance ether formation, whereas MEK and acetonitrile, markedly accelerated the reactions. In

TABLE III  
Reaction of Poly(vinyl Chloride) Model with Cyclohexene  
Oxide in Various Solvents;  $[\text{PVC Model}]_0 = 0.172\text{ M}$ ,  
 $[\text{Cyclohexene Oxide}]_0 = 0.236\text{ M}^a$

Solvent	Reaction time, hr	Reaction, % <sup>b</sup>	Dielectric constant ( $\epsilon$ )
<i>n</i> -Hexane	5.0	None	1.89
Ethyl acetate	5.0	10	6.02
Methyl ethyl ketone	5.0	50	18.50
Acetonitrile	3.0	50	26.30

<sup>a</sup> Reactions were run at  $150^\circ\text{C}$ .

<sup>b</sup> Disappearance of PVC model.

MEK, ether formation was the sole reaction, while in acetonitrile, chlorohydrin formation was observed to a small extent.

Tables IV and V contain rate data which fit a first-order plot for the disappearance of PVC model (Fig. 3). The reaction rates were run with 1:1 and 2:1 molar ratios of cyclohexene oxide: PVC model in methyl ethyl ketone. The rates were found to be the same within experimental error, thus, confirming the lack of effect of oxirane concentration on the etherification rate.

TABLE IV  
Reaction of Poly(vinyl Chloride) Model with Cyclohexene  
Oxide (1:1 Molar Ratio) in Methyl Ethyl Ketone;  
[PVC Model]<sub>0</sub> = 0.172 *M*, [Cyclohexene Oxide]<sub>0</sub> = 0.185 *M*<sup>a</sup>

Reaction time, hr	Concentration of model, <i>M</i>
0	0.172
1.0	0.132
2.0	0.113
3.0	0.096
5.0	0.059
6.0	0.042
11.0	0.020

<sup>a</sup>  $k = -3.92 \times 10^{-3} \text{ min}^{-1}$ .

TABLE V  
Reaction of Poly(vinyl Chloride) Model with Cyclohexene Oxide  
(1:2 Molar Ratio) in Methyl Ethyl Ketone;  
[PVC Model]<sub>0</sub> = 0.157 *M*, [Cyclohexene Oxide]<sub>0</sub> = 0.354 *M*<sup>a</sup>

Reaction time, hr	Concentration of 4-chlorohexene-2, <i>M</i>
0	0.157
1.0	0.133
2.0	0.112
3.0	0.098
4.0	0.086
5.0	0.071
6.0	0.053
7.0	0.045

<sup>a</sup>  $k = -2.99 \times 10^{-3} \text{ min}^{-1}$ .

The information presented here appears to be in agreement with an S<sub>N</sub>1 mechanism.<sup>18</sup> The following factors individually and collectively tend to support this assignment. (1) Nonpolar solvents fail to promote ether formation, whereas polar solvents carry the reaction to completion in a relatively short period of time. It is known that reactions, in which a charge development occurs, proceed most rapidly in polar solvents.<sup>18</sup> (2) The rate of ether formation in methyl ethyl ketone was found to follow first-order kinetics. An increase in concentration of oxide failed to alter the order or rate of reaction.



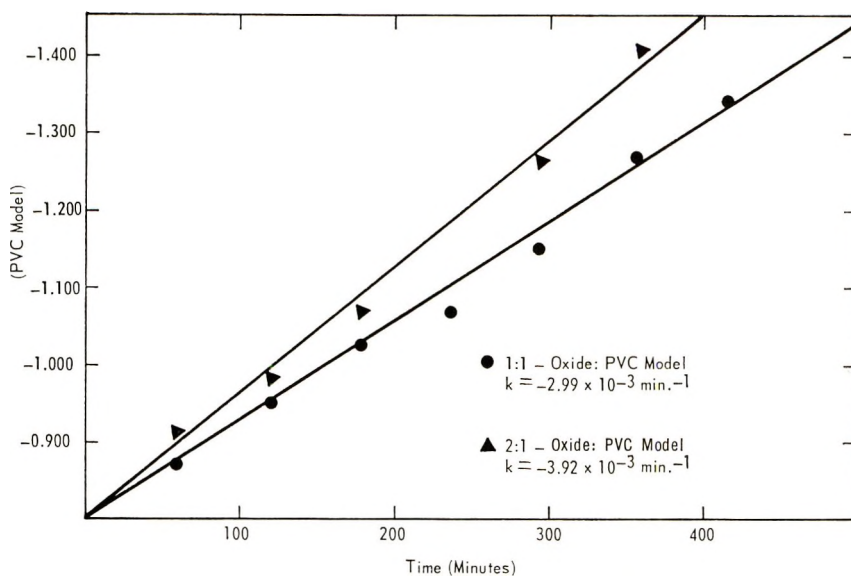
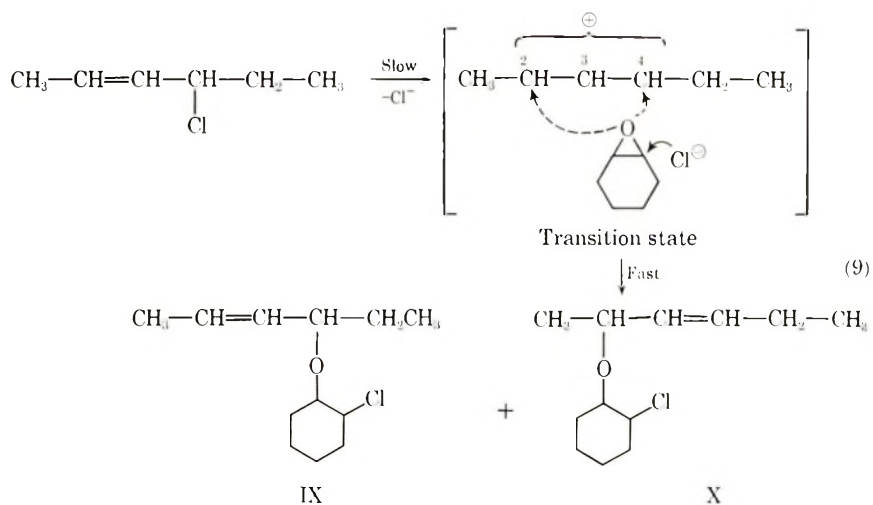


Fig. 3. Reactions of poly(vinyl chloride) model with cyclohexene oxide at 150°C in methyl ethyl ketone.

From these observations, one could suggest a possible mechanism for ether formation [eq. (9)].



In the transition state, the positive charge could be distributed over carbons 2, 3, and 4, particularly in polar solvents which are capable of supporting charge dispersal by solvation. It appears possible that the nucleophile (oxirane) may attack at either carbon 2 or 4.

### Reactions of the PVC Model with Selected Carboxylate Salts and Cyclohexene Oxide

**Role of Cadmium Carboxylate and Cadmium Chloride.** As pointed out in a preceding section, with cadmium acetate or 2-ethylhexanoate allylic chloride model reacts rapidly to give the corresponding esters (V and VI). With cyclohexene oxide present in addition to the metal soap model, the isomeric hexenyl ethers (IX and X) and some cyclohexene chlorohydrin are also formed. Table VI gives the results of this study. The experi-

TABLE VI  
Reaction of PVC Model with Cadmium Carboxylates  
and Cyclohexene Oxide in Tetrahydrofuran; [PVC Model]<sub>0</sub> = 0.26 M

Carboxylate ligand	PVC model/ oxide/salt	Reaction time, hr	Ester, %	Ether, %	Cl—OH, %
Acetate	1/2/2	3	55	20	0
2-Ethylhexanoate	1/2/1	3	53	5	32
2-Ethylhexanoate	8/8/1	6	17	11	15
2-Ethylhexanoate	1/1/trace	10	2.4	15	16
2-Ethylhexanoate	1/1/trace	10	—	10	11

mental data show that when a 1 M excess of cyclohexene oxide and salt is used, there is no competition from chlorohydrin formation, however, when the salt concentration is decreased, there is considerable degradation resulting in the formation of cyclohexene chlorohydrin.

In a separate group of experiments, the effect of cadmium chloride on the reaction of PVC model and cyclohexene oxide was investigated. It was previously shown that cadmium chloride functions as a catalyst for the degradation of the allylic chloride mixture (Table VII).

When a PVC model:oxide: CdCl<sub>2</sub> molar ratio of 4:4:1 was allowed to react, a considerable quantity of chlorohydrin was detected. Similar reactions with trace amounts of the cadmium salt and excess cyclohexene oxide produced ether as the major reaction product. A kinetic study in which the disappearance of PVC model was followed is shown as a first-order plot in Figure 4, in which the initial charge of PVC model was held

TABLE VII  
Reactions of the PVC Model with Cyclohexene Oxide  
in the Presence of Cadmium Chloride in Tetrahydrofuran;  
[PVC model]<sub>0</sub> = 0.26 M

Molar ratio, PVC model/oxide/CdCl <sub>2</sub>	Reaction time, hr	Ether, %	Cl—OH, %
4/4/1	6	18	21
1/1/trace <sup>a</sup>	6	15	10
1/2/trace <sup>a</sup>	6	26	9
1/4/trace <sup>a</sup>	6	40	7

<sup>a</sup> 2.7 × 10<sup>-4</sup> mole CdCl<sub>2</sub>.

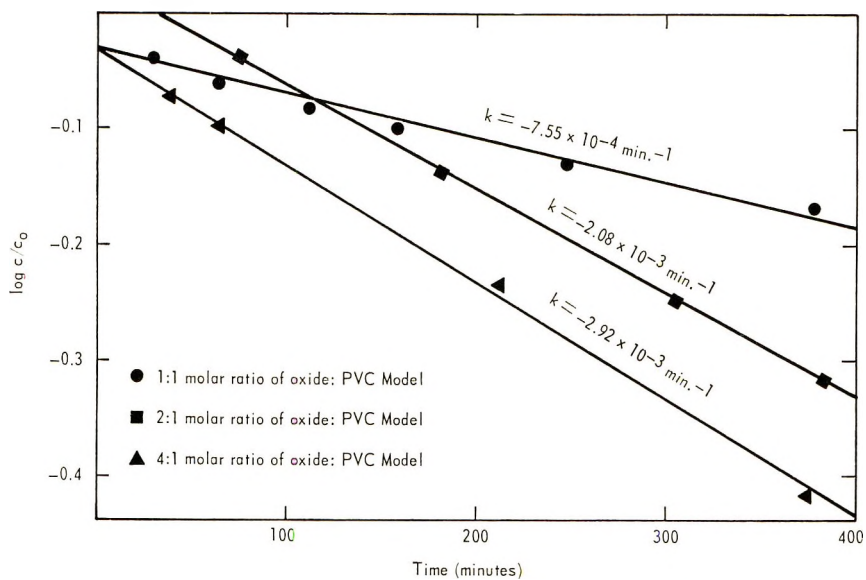


Fig. 4. Reaction of cyclohexene oxide with PVC model in THF at 60°C with a trace of  $\text{CdCl}_2$ .

constant while the oxide concentration was varied. These plots tend to deviate considerably from an ideal first-order reaction primarily because of competition from chlorhydrin formation. A first-order plot of ether formation is depicted in Figure 5 and appears to be independent of oxide

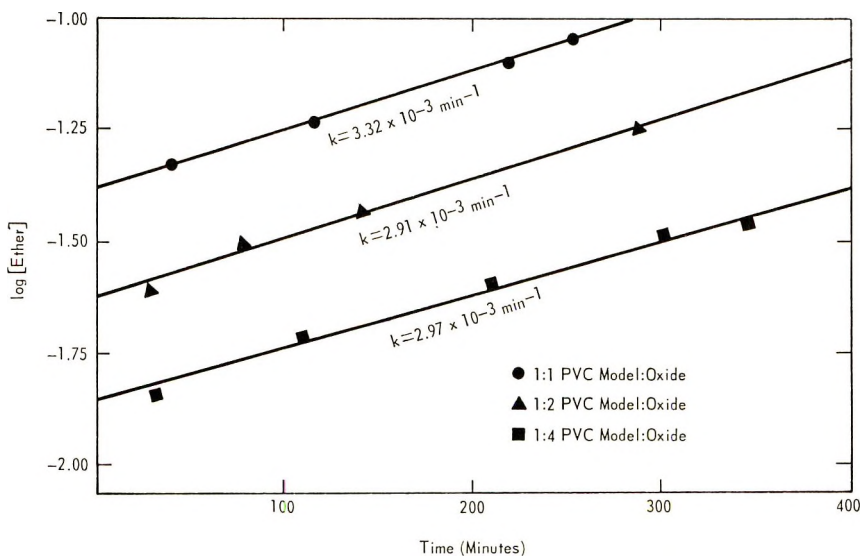
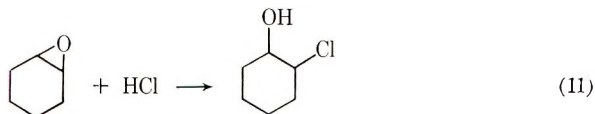
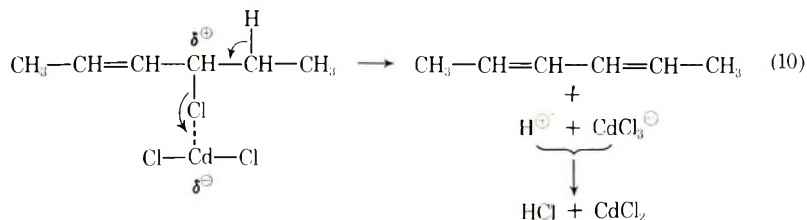


Fig. 5. Plot of  $\log [\text{Ether}]$  vs. time.

concentration. From these reactions, a suggested mechanism is presented in eq. (10) and (11).



This mechanism shows the possible reaction pathway when a deficiency of oxide is present and cadmium chloride functions to catalyze the collapse of the incipient carbonium ion to the diene. In the presence of excess nucleophile (cyclohexene oxide), the nucleophilic attack becomes more likely and this reaction becomes minimal while ether formation predominates [eq. (9)]. Thus, it appears that the rate-determining step is the formation of an allylic cation (VII).

**Reaction of the PVC Model and Cyclohexene Oxide with Barium/Cadmium Carboxylate Mixtures.** As a general trend in this series of reactions, esterification was observed to proceed slower than with cadmium carboxylates alone. Table VIII summarizes the significant results obtained from these reactions. A 1:1 molar ratio of oxide:PVC model in the presence of 0.5 mole Ba/Cd(OAc)<sub>2</sub>(4:1/Ba:Cd) reacted to give equimolar quantities of ester and ether; no chlorohydrin was observed.

TABLE VIII  
Reaction of PVC Model with Ba-Cd Carboxylates  
and Cyclohexene Oxide in Tetrahydrofuran; [PVC Model]<sub>0</sub> = 0.26 M

Ligand	Ba/Cd ratio	PVC model/oxide/salt	Reaction time, hr	Ester, %	Ether, %	Cl-OH, %
Acetate	4/1	2/2/1	4	16	14	0
Acetate	4/1	2/4/1	4	14	18	3
2-Ethylhexanoate	4/1	1/2/trace	3	3	0	0
2-Ethylhexanoate	4/1	1/4/trace	3	2.5	0	0
			20	7	21	6
2-Ethylhexanoate	4/1	2/2/1	6	27	4	0
			22	38	5	0

An identical reaction with the use of the soluble octanoate salt mixture similarly gave no chlorohydrin; however, ether formation was extremely slow, ether not appearing as a product until after 5 hr reaction time. At

the completion of the reaction, the ester:ether ratio was 8:1. Other experiments, summarized in Table VIII, in which the salt concentration was present in only trace quantities, again showed ether formation to be slow. However, even after an extended reaction time, only negligible quantities of chlorohydrin were detected. The retardation of chlorohydrin formation can be attributed to the prevention of any harmful accumulation of cadmium chloride which is perpetrated by ligand exchange of carboxylate from the barium salt. The barium carboxylate must always be present in excess. The slower esterification reaction with barium-cadmium mixture allows the etherifications process to begin and to compete effectively due to the relatively slow ligand exchange process. From these experiments it appears that cadmium chloride has a transitory existence as long as there is sufficient barium carboxylate present to engage in the ligand transfer mechanism. The major importance of the catalytic amounts of cadmium chloride is its ability to catalyze the formation of the thermally stable  $\alpha$ -chloroether which contributes to the explanation of the observed synergism incurred in the polymer stabilization.

**Effect of Metal Soaps on Cyclohexene Chlorohydrin.** A group of experiments was designed in order to investigate an earlier speculation that cyclohexene oxide is generated from cyclohexene chlorohydrin in the presence of metal soaps.<sup>14</sup> At 60°C in tetrahydrofuran, cyclohexene chlorohydrin was treated with the acetates and 2-ethylhexanoates of zinc and cadmium. Under these conditions, where esterification and etherification of the allylic model proceeded with little difficulty, no oxirane was found. Other reactions occurred at higher temperatures ( $\sim 125^\circ\text{C}$  in chlorobenzene); however, consistent with the low-temperature reactions, no oxirane formation was noted.

**Correlation of Model Experimental Data with Observed Data in the Polymer System.** Figure 6 displays a plot of color versus time for heat-treated samples of poly(vinyl chloride). These samples were exposed in an air oven at 170°C. Sample A contained no stabilizer and appeared to darken (dark amber after 10 min); this sample blackened after 90 min. Sample B contained the barium-cadmium soap stabilizer and was essentially colorless until after 30 min, at which time it immediately blackened. The study of the model system composed of the allylic hexenyl chloride mixture and barium-cadmium 2-ethylhexanoate showed that when an insufficient quantity of the octanoate salt was used, complete esterification (and resultant stabilization) occurred rapidly; then, even more rapidly, degradation began. Thus, it appears that the metal soap stabilizer in the polymer sample was exhausted after esterification; consequently, the accumulation of cadmium chloride functioned to catalyze degradation of the polymer. Sample C contains both the metal soap stabilizer and epoxy plasticizer. The heat-treated sample appears almost colorless with only slight yellowing after 1 hr. This may be interpreted by the performance of the PVC model in the presence of the barium-cadmium 2-ethylhexanoate mixture in conjunction with cyclohexene oxide. Esterification with con-

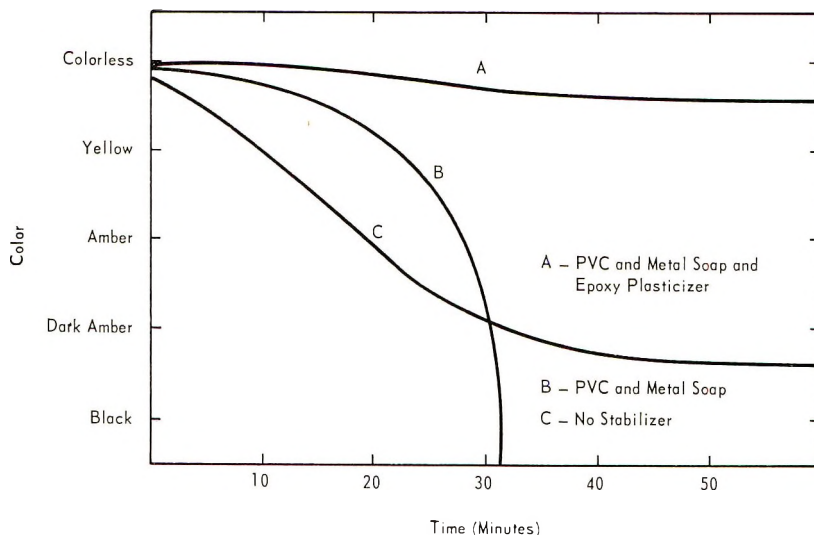


Fig. 6. Heat treatment of PVC at 170°C.

comitant ligand exchange and subsequent ether formation tend to contribute toward the synergistic stabilization effect observed in the polymer system.

## EXPERIMENTAL

### Materials

**Poly(vinyl Chloride) Model.** The mixture of 4-chlorohexene-2 and 2-chlorohexene-3 was obtained by the synthetic procedure reported by Shonle and Waldo.<sup>16</sup> The product was distilled under reduced pressure through a Nester-Faust spinning band column (bp 60°C/80 mm Hg). The allylic chloride mixture was used in all experiments without separation.

**Epoxy Plasticizer Model.** Cyclohexene oxide was obtained from Aldrich Chemical Co., distilled, and used without further purification.

**Metal Soap Stabilizer Models.** The 2-ethylhexanoates, cadmium (20% Cd), barium (15% Ba), calcium (5% Ca), and zinc (18% Zn), were secured as experimental samples from Shepherd Chemical Co. Anhydrous acetates were prepared from Fisher Certified reagents by pulverizing and heating at 110°C for 24 hr in a vacuum oven at 1 mm Hg and finally stored in a vacuum desiccator.

**Solvents.** Tetrahydrofuran (Fisher) was purified by treatment with solid potassium hydroxide and subsequently distilled over lithium aluminum hydride.

Methyl ethyl ketone was obtained from Fisher and used without further purification.

### Analysis

All reactions contained in this paper were monitored via vapor-phase chromatographic analysis. An F and M Model 5750 Research Chromatograph was employed with programmed temperature operation under the following conditions: injection temperature, 40°C; post-injection time, 5.0 min; program rate, 10°C/min; upper limit, 200°C for 4 min; column, 6-ft,  $\frac{3}{16}$ -in, stainless steel; 15% Apiezon-L on Chromosorb-W; order of elution, Solvent, 2-4-hexadiene, PVC model, epoxide, ester, chlorohydrin, decalin, and finally ether.

Decalin (*cis-trans* mixture) was used as an internal standard in each chromatographic analysis.

### Reactions of the Metal Carboxylates

All reactions were run in 100-ml three-necked round-bottom flasks fitted with a nitrogen inlet tube, condenser, and a rubber septum for analytical sampling. Stock solutions containing the allylic hexenyl chloride mixtures (0.26 *M*) cyclohexene oxide (where applicable), and decalin (internal standard; 0.5 g/50 ml solution) in tetrahydrofuran solvent were prepared. Aliquots (50 ml,  $1.27 \times 10^{-2}$  *M* PVC model) were removed and transferred to the 100-ml reaction flasks. While stirring with a Teflon-covered bar magnet, appropriate quantities of the salts were added, and the reaction mixture was immediately immersed in a constant-temperature bath at 60°C  $\pm$  2°C. Samples were withdrawn periodically and analyzed via vapor-phase chromatography.

Kinetic runs with cadmium chloride were run as described above (0.05 g CdCl<sub>2</sub>/50 ml was used).

### Kinetics of Uncatalyzed Ether Formation

Stock solutions were prepared as described above, 0.172 *M* and 0.157 *M* in PVC model and with methyl ethyl ketone as the solvent. The concentrations in cyclohexene oxide were 0.185 and 0.354 *M*, respectively, to give 1:1 and 2:1 oxide:PVC model mixtures. Aliquots (1 ml) were withdrawn with a hypodermic syringe and transferred into 11-mm, thick-walled Pyrex tubes. These tubes were evacuated (6 mm Hg) and sealed under a nitrogen atmosphere. The reaction tubes were finally immersed in a constant-temperature oil bath at 150  $\pm$  2°C. The tubes were removed at various intervals, immersed in liquid nitrogen, and opened. The contents were analyzed via vapor-phase chromatography.

### CONCLUSION

The degrading poly(vinyl chloride) model (mixture of 4-chlorohexene-2 and 2-chlorohexene-3) undergoes rapid esterification as the predominant reaction in the presence of a mixture of cadmium and barium 2-ethylhexanoates in conjunction with cyclohexene oxide (epoxy plasticizer model). The formation of catalytic amounts of cadmium chloride as a by-product

of the esterification was found to catalyze ether formation, 2-hexenyl-4-(2-chlorocyclohexyl) ether. The combination of these two reactions together with ligand transfer between cadmium chloride and barium carboxylate contribute much to the explanation of the synergism observed in the thermal stabilization of the polymer by combinations of epoxy plasticizers with barium-cadmium or zinc-calcium soap systems. The esters and the chloroethers were found to be thermally stable at 150°C; at this temperature, the PVC model is rapidly degraded to hydrogen chloride and 2,4-hexadiene.

The authors wish to express our sincere appreciation to Mr. L. H. Wartman for his invaluable assistance in the preparation of this manuscript.

### References

1. H. Mark and A. V. Tobolsky, *Physical Chemistry of High Polymers*, 2nd Ed. Interscience, New York, 1950, Vol. 2, p. 403.
2. W. I. Bengough, and R. G. W. Norrish, *Proc. Roy. Soc. (London)*, **A200**, 301 (1950).
3. J. D. Cotman, Jr., *Ann. N. Y. Acad. Sci.*, **57**, 417 (1953).
4. A. L. Scarborough, *Nat. Bur. Stand. Circ.*, **525**, 95 (1953).
5. D. Druesedow and C. F. Gibbs, *Nat. Bur. Stand. Circ.* **525**, 69 (1953).
6. E. J. Arlmann, *J. Polym. Sci.*, **12**, 543 (1954).
7. A. H. Frye and R. W. Horst, *J. Polym. Sci.*, **40**, 417 (1959).
8. W. I. Bengough and M. Onozuka, *Polymer*, **6**, 625 (1965).
9. T. Shimura and A. Saki, *Kogyo Kagaku Zasshi*, **70**, 995 (1967).
10. P. Klemchuk, paper presented at the 153rd National Meeting, American Chemical Society, Miami Beach, Florida, April 1967.
11. R. D. Deanin, H. H. Reynolds, and Y. Ozcayir, *J. Appl. Polym. Sci.*, **13**, 1247 (1969).
12. M. Onozuka, *J. Polym. Sci. A-1*, **5**, 2229 (1967).
13. M. Onozuka and M. Asahina, *J. Macromol. Sci. Revs. Macromol. Chem. C*, **3**, 235 (1969).
14. N. L. Perry, *Ind. Eng. Chem.*, **50**, 6, 862 (1958).
15. P. P. Hopf, paper presented at International Symposium on Macromolecular Chemistry, Moscow, 1960.
16. H. A. Shonle and J. H. Waldo, *J. Amer. Chem. Soc.*, **55**, 4649 (1933).
17. J. W. Lewis and W. F. Beach, "Mass Spectrometry—The Reaction Product of Cyclohexene Oxide and 4-Chlorohexene-2," File No. 1140, UCC Memorandum, Bound Brook, N. J., November 29, 1967.
18. E. S. Gould, *Mechanism and Structure in Organic Chemistry*, Holt, Rinehart and Winston, New York, 1959, p. 183.

Received February 16, 1970

Revised March 31, 1970



## Mechanism of the Polymerization of Trifluoroacetaldehyde Initiated by Azobisisobutyronitrile\*

W. K. BUSFIELD and R. W. HUMPHREY, *Department of Chemistry,  
The University, Dundee, Scotland*

### Synopsis

The polymerization of fluoral initiated by the photolyzed decomposition of azobisisobutyronitrile at low temperature has been studied. Up to 2% conversion, the effect of radical scavengers and the order with respect to initiator and light intensity indicate that the reaction occurs by a conventional radical polymerization mechanism. At about 2% conversion autoacceleration sets in and the rates become irreproducible. This is explained by typical occlusion phenomena. Tracer studies show that polymer prepared at high conversion contains initiator fragments indicating that primary propagation is by monomer addition to radicals. The reaction mechanism is discussed.

### INTRODUCTION

It has been known for some time that fluoral (trifluoroacetaldehyde) polymerizes in the presence of conventional free-radical initiators such as benzoyl peroxide<sup>1</sup> or azobisisobutyronitrile<sup>2</sup> (AIBN) but the free radical nature of the mechanism has not been established. No other aldehyde is known to polymerize across the carbonyl bond by a proven free-radical mechanism.

Recently Cairns et al.<sup>3</sup> have prepared copolymers of fluoral with a variety of olefinic monomers using conventional free-radical initiation procedures. If the copolymers were random copolymers or if the yields had been low, these experiments would have indicated conclusively that fluoral molecules can add to a free radical and polymerize by a conventional free-radical mechanism. However, neither condition was satisfied.

The polymerization of fluoral initiated by the photolyzed decomposition of AIBN in the absence of solvent appears homogeneous and was made the subject of a kinetic investigation. Because polymerization from the gas phase at monomer pressures greater than about 100 kNm<sup>-2</sup> occurs spontaneously and the monomer boils at 254°K, the experiments were carried out in the range 233–253°K. Polymer produced by this method when carried to high conversions is a transparent elastomer with low thermal

\* The work described in this paper was presented to the International Symposium on Macromolecular Chemistry, Budapest, 1969.

stability.<sup>2</sup> It is insoluble in all solvents except those in which it decomposes.

## DILATOMETRIC INVESTIGATION

### Experimental

**Materials.** Fluoral was prepared by the dehydration of fluoral hydrate as described in earlier publications.<sup>2</sup>

*Methyl methacrylate*, (MMA) and acrylonitrile, (AN) were commercial monomers freed from inhibitors, dried, and distilled under nitrogen.

*Azobisisobutyronitrile*, (AIBN) was recrystallized from petroleum ether. Its infrared and ultraviolet spectra were identical with those published.<sup>4,5</sup>

*p*-Benzoquinone, (BQ) was recrystallized from petroleum ether to a constant melting point.

Diphenyl picryl hydrazyl, (DDPH) was twice recrystallized from an anhydrous mixture of chloroform and diethyl ether. The purple-black product had an infrared spectrum identical with that published.<sup>6</sup>

**Procedure.** The dilatometers were cylindrically shaped vessels of volume about 1.5 ml and were filled by conventional high-vacuum techniques with AIBN, monomer, and inhibitor when required. No solvents were used. The polymerizations were carried out in a Townson Mercer Minus Seventy thermostat bath, the temperature of which was steady to within  $\pm 0.1^\circ\text{K}$  during experiments. Initiation was by the photolyzed decomposition of AIBN by use of an ultraviolet light from a medium- to high-pressure 250 Watt mercury lamp. The pyrex walls of the thermostat bath and reaction vessel effectively absorbed light of wavelength below 300  $m\mu$ . Conditions were such that only a small fraction of the incident light,  $I_0$  was absorbed by the system so that at constant  $I_0$  and cell depth  $d$  the absorbed light intensity  $I_a$  is directly proportional to the concentration of initiator molecules in the system.

$$I_a \propto [\text{AIBN}]$$

Similarly, at constant  $[\text{AIBN}]$  and  $d$ ,  $I_a \propto I_0$ : In general the rate of radical production in the system,  $R(\text{rad})$ , is given by:

$$R(\text{rad}) = 2I_a = 2kI_0[\text{AIBN}] \quad (1)$$

where  $k$  is a constant of proportionality.  $kI_0$  is a constant for each dilatometer and was determined by polymerizing MMA at  $273.2^\circ\text{K}$  in the dilatometer with both lamp and dilatometer in rigidly fixed and reproducible positions and at a known concentration of AIBN. From the experimentally determined rate of polymerization  $R_p$ ,  $[\text{AIBN}]$ , and the literature values of  $k_p/k_t^{1/2}$  ( $25.6 \times 10^{-3} \text{ mole}^{-1/2}\text{-sec}^{-1/2}$ )<sup>7</sup> and the initiator efficiency  $f$  in MMA (0.6),<sup>8</sup>  $kI_0$  was obtained from eqs. (2) and (3):

$$R_p = (k_p/k_t^{1/2})R_i^{1/2}[\text{MMA}] \quad (2)$$

$$R_i = 2f(kI_0)[\text{AIBN}] \quad (3)$$

where  $R_i$  is the rate of initiation. Five dilatometers were used in the series of experiments for which  $kI_0$  varied from  $1.2 \times 10^{-5}$  to  $3.0 \times 10^{-5} \text{ sec}^{-1}$ .

In the polymerization of fluoral, rates of polymerization in different dilatometers were all related to results in one dilatometer ( $kI_0 = 2.8 \times 10^{-5} \text{ sec}^{-1}$ ) for the purposes of comparison by use of eq. (4):

$$R_p \propto (kI_0)^{1/2} \quad (4)$$

The experiments designed to investigate the effect of varying  $I_0$  on  $R_p$  at constant [AIBN] were all carried out in the same dilatometer. Calibration corrections were thus not required.  $I_0$  was varied by placing a series of optical gauzes, previously calibrated on an ultraviolet spectrophotometer, in the light path.

**Yield Contraction Ratios.** These were measured for MMA and AN by the conventional method of precipitating, purifying, and weighing the polymer after a known volume contraction measured in the dilatometers.

This method was found to be unreproducible for fluoral, probably because of the difficulty of isolating the polymer without some decomposition occurring in the precipitation and purification stages. Reproducibility was obtained by using the following technique. After a known volume contraction, the dilatometer was opened, unreacted monomer pumped off on the vacuum line at  $273^\circ\text{K}$  and the polymer yield measured by weighing the dilatometer, before and after removing the polymer by pumping the vessel at  $400^\circ\text{K}$  to a constant weight. Over the range of 4–20% conversion the volume contraction  $\Delta V$  at  $243.2^\circ\text{K}$  was constant within experimental error at  $7.6 \pm 0.1 \text{ ml/mole}$ .  $\Delta V$ , calculated from the difference in density of polymer at  $293^\circ\text{K}$  (1.57 g/ml) and monomer at  $243^\circ\text{K}$  (1.41 g/ml), is 7.2 ml/mole.

## Results and Discussion

**Absence of Initiator.** Since the lowest energy electronic absorption band in fluoral has a maximum at  $297 \text{ m}\mu$ , no polymerization would be expected upon irradiation in the absence of initiator in Pyrex apparatus. This was confirmed experimentally at  $243^\circ\text{K}$ . No polymerization occurred even after several hours of irradiation.

It is interesting to note that even in all-quartz apparatus, irradiation at about  $250^\circ\text{K}$  failed to promote polymerization of fluoral alone. Thus the first excited state of fluoral, be it diradical or otherwise, is incapable of initiating polymerization.

**Overall Rate of Polymerization.** On irradiation, the rate of polymerization of fluoral in the presence of initiator varies with time according to the typical graph shown in Figure 1. The reaction may be divided into two distinct parts. Initially, polymerization occurs at a steady rate comparable to that which MMA polymerizes under identical condition. At about 2% conversion the reaction rate accelerates until it becomes comparable to that of AN polymerized under identical conditions.

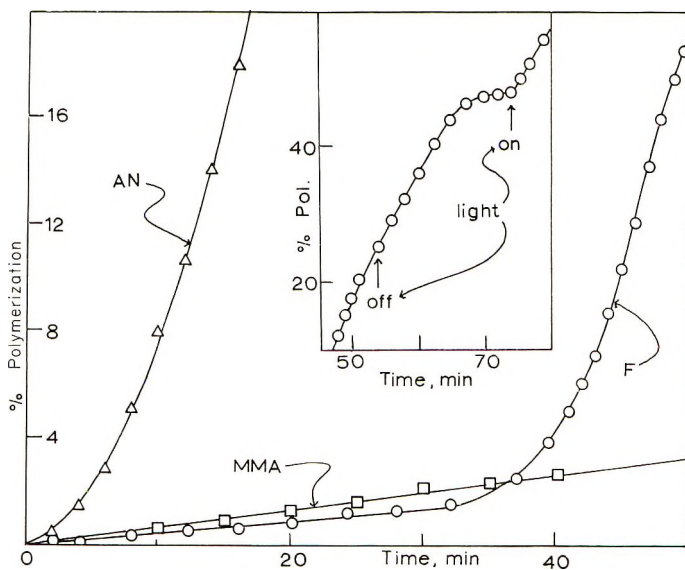


Fig. 1. Conversion-time graphs for the polymerization of (○) fluoral, (□) MMA and (△) AN at 243°K and constant [AIBN] and  $I_0$ . Inset: The effect of removing the incident light on the polymerization of fluoral.

**Initial Rate of Polymerization.** No induction periods were observed. The initial rate of polymerization was constant and reproducible at constant temperature, initiator concentration, and light intensity. The fact that the rate of conversion is similar to that of MMA indicates a high quantum yield and the occurrence of a chain mechanism. Experimentally it was observed that when the incident light was cut off, the rate dropped

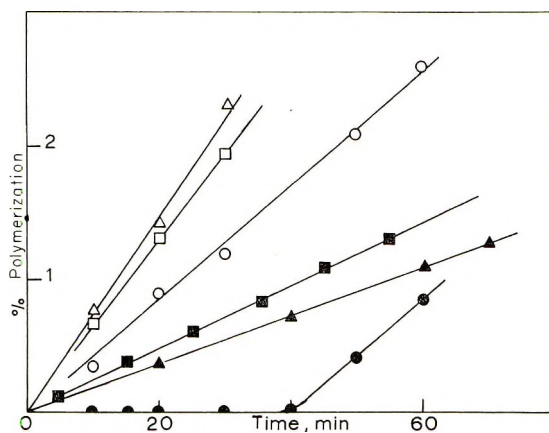


Fig. 2. Effect of varying (△, ▲) [AIBN] by a factor of 12, and (□, ■)  $I_0$  by a factor of 5 on the initial rate of polymerization of fluoral and the effect of added BQ: (●) BQ added and (○) an identical experimental in the absence of BQ on the initial rate of polymerization of fluoral.

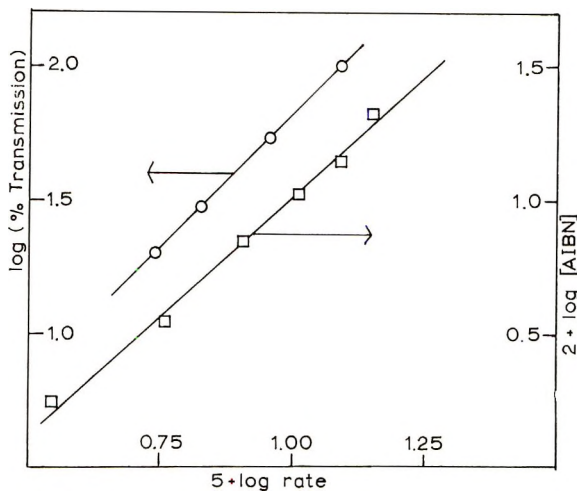


Fig. 3. Plots of log (initial rate) against log [AIBN], and log (percent  $I_0$  transmitted through gauze) for the polymerization of fluoral.

rapidly to zero showing that the chain termination step is rapid. On re-illumination the rate returned to its normal value.

The effects of varying the initiator concentration (0.02M to 0.2M) and the light intensity by a factor of 5 are shown in Figure 2. The initial rate is proportional to both  $[AIBN]^{1/2}$  and  $I_0^{1/2}$ , as shown by the graphs in Figure 3, indicating that the termination reaction is bimolecular and presenting strong evidence for the free radical nature of the polymerization.

The effect of adding BQ, a typical efficient radical scavenger, to the system is also shown in Figure 2. Addition of DPPH produced similar results. Complete inhibition was observed, thus providing conclusive evidence that, at least in the early stage of reaction, the polymerization occurs via a free-radical mechanism.

Assuming that one inhibitor molecule removes one radical, the rate of radical formation from initiator  $R(\text{rad})$  can be calculated from the inhibition time  $t$  and inhibitor concentration  $x$  by using eq. (5).

$$R(\text{rad}) = \frac{2[AIBN]}{t} \ln (1 - x/2[AIBN]) \quad (5)$$

Values of  $R(\text{rad})$  from separate experiments are compared in Table I with the value calculated from the light intensity derived from the MMA calibration experiments. The slight discrepancy in the results may be due to either solvent effects in the inhibition experiments or to taking too high a value for the efficiency of the radicals starting polymer chains in the calibration experiments. The value of 0.6, assumed for MMA, was measured at 323°K,<sup>8</sup> whereas these experiments were run at 273°K.

Assuming that the polymerization in the initial stages occurs by a conventional free-radical addition mechanism, values of  $k_p/k_t^{1/2}$  were calcu-

TABLE I  
Rates of Radical Formation Determined by Inhibitor  
Experiments Compared with those Calculated from MMA  
Calibration Experiments

Method	[AIBN] $\times$ 10 <sup>2</sup> , mole/l.	$R(\text{rad})/[\text{AIBN}] \times$ 10 <sup>4</sup> , sec <sup>-1</sup>
Inhibitor (BQ)	7.7	1.55
Inhibitor (BQ)	16.6	1.49
Inhibitor (DPPH)	10.7	1.11
MMA calibration		0.56

lated from the experimentally determined initial rates of polymerization measured at 233.2, 243.2, and 253.2°K by using the equations corresponding to eqs. (2) and (3). The corresponding activation energy difference,  $E_p - E_t/2$ , is 14.5 kJ/mole. These results are compared with data for typical olefinic monomers in Table II.

**The Second Stage of Polymerization.** After about 2% conversion the rate of polymerization accelerated to rates, which were not reproducible,

TABLE II  
Rate Constant Ratios and Activation Energies for  
Fluoral and Typical Olefinic Monomers Polymerized in  
a Similar Temperature Range

Monomer	Temp, °K	$k_p/k_t^{1/2} \times$ 10 <sup>3</sup> l <sup>1/2</sup> mole <sup>-1/2</sup> sec <sup>-1/2</sup>	$(E_p - E_t)/2$ , kJ/mole	Reference
Fluoral	253.2	6.7		This work
	243.2	5.2	14.5	
	233.2	3.7		
MMA	273.2	25.6		7
	243.2	9.1	19.0	This work
Styrene	273.2	5.1	21.3	9
		2.3	27.6	10
Vinyl acetate	273.2	63	19.6	11
	273.2	189	13.4	12
	258.2	135		

TABLE III  
Conversion and Time at Which Autoacceleration Was Observed at Various  
Initiator Concentrations

[AIBN] $\times$ 10 <sup>2</sup> , mole/l.	Start of autoacceleration	
	Conversion, %	Time, min
3.57	1.7	60
7.14	2.0	60
10.7	1.9	46
14.3	1.7	32
21.4	1.9	30

but were similar to those observed for the polymerization of AN polymerized under identical conditions (see Fig. 1). The onset of this second stage occurred at a percentage conversion approximately independent of the initiator concentration (Table III).

When the incident light was switched off during the second stage, the polymerization continued in the dark period at a slowly decreasing rate for at least 20 min (see insert, Fig. 1). On re-illumination, polymerization continued at its former rate. This contrasts with the behavior observed in the initial stages, see previous section. These observations indicate that during the second stage the system is behaving like a typical heterogeneous polymerization system where polymer precipitates during the reaction. A typical example is the polymerization of AN in the absence of solvent which as shown in Figure 1, occurs at a similar rate. The currently accepted explanation of the autoacceleration phenomenon<sup>13</sup> is that the active species become trapped in the precipitating polymer matrix, so that bimolecular termination reactions involving two polymer radicals become diffusion-controlled and slow, while propagation reactions between monomer and polymer radicals occur at the normal rate, since monomer has no diffusion problems.

In the case of fluoral, one objection to this theory is that no precipitation is observed even after the autoacceleration period had been passed. However it is likely that gelation occurs at the acceleration point, since in addition to the kinetic effects already described, we have observed, in our attempts to find solvents for polyfluoral, that visually clear "solutions" are formed in solvents such as acetone or trifluoroacetic anhydride. These "solutions" will not pass through fine porosity filter disks. Polymer in the form of a gel becomes trapped in the disk, while only solvent passes through. Thus it is probable that during polymerization the polymer forms a highly solvated and transparent gel as a separate phase when in contact with monomer. Below 2% conversion the polymer is soluble and the system homogeneous. It is worth noting that the increase in macro viscosity at 2% conversion is thought to be insufficient for the phenomenon to be explained by a Trommsdorff effect, although the distinction is, of course, slight.

### TRACER EXPERIMENTS

If initiation of polymerization is by radical addition to the carbonyl bond, then initiator fragments should be present in the resultant polymer. The most successful method of detecting such fragments is that of isotopic labeling of the initiator used in the polymerization, followed by measurements of the specific activity of the resultant polymer.

AIBN may be conveniently labeled with <sup>14</sup>C, the weak  $\beta$  particles from which are most efficiently counted using liquid scintillation methods. Since no satisfactory solvent is known for polyfluoral, a modification of the suspension method developed by Davies and Cocking<sup>14</sup> was used. In order

to use this method the polymer samples had first to be stabilized by refluxing with acetic anhydride in chloroform solution,<sup>2</sup> a process in which it was assumed that acetylation only occurs at hydroxyl endgroups and does not affect endgroups involving initiator fragments. Thus only positive results are meaningful.

### Experimental Aspects

The <sup>14</sup>C-labeled AIBN was prepared from <sup>14</sup>C-labeled acetone by methods described in the literature<sup>5,15</sup> and was recrystallized from petroleum ether.

A sample of fluoral containing 1 mole-% of labeled initiator was polymerized to high conversion by irradiation at 243°K. The polymer was stabilized by refluxing with an excess of acetic anhydride in chloroform for 24 hr and rinsed thoroughly by successive periods of stirring in fresh chloroform. It was dried *in vacuo*. During stabilization 27% of the polymer decomposed.

A suspension made by stirring stabilized polymer in acetone was added dropwise to weighed Whatman GF/A 2.1 cm glass fiber paper disks. After drying *in vacuo* and reweighing, the disks were placed on the bottom of a 10-ml sample vial containing 2.0 ml of scintillant mixture (1.500 g PPO and 0.150 g of POPOP in 500 ml toluene). Each was counted in an Ekco M5402 liquid scintillation counter connected to a M506A digital scalar timer. The disk was then removed from the vial and a count of the remaining scintillant liquid taken (background 2) in order to provide a measure of the rate of transfer of activity from the sample to the solution caused by dissolution of the polymer. The disk was refluxed in fresh chloroform, dried, and recounted. This latter process was repeated until constant results were obtained.

The specific activity of the initiator was measured in a similar manner.

### Results and Conclusions

The results are given in Table IV. The background readings for the polymer sample show that the polymer is almost completely insoluble in the scintillant mixture. The constancy of the counts per gram per second over the range of polymer weights used shows that self absorption is negligible.

TABLE IV  
Count Rates for Initiator and Polymer Samples

Sample	Weight, mg	Average counts $\times 10^3$ , sec <sup>-1</sup>			Counts/- g-sec
		Back. 1	Sample	Back. 2	
Initiator	9.7	337	20,895	20,670	2131
Initiator	10.5	351	23,101	22,983	2200
Polymer	39.1	660	4,335	802	46.9
Polymer	22.6	658	2,628	756	43.8
Polymer	31.9	664	3,800	789	49.2
Polymer	35.0	672	4,044	808	48.2



In the case of initiator however, the second background count is the same as the sample count showing that during the time of counting, the initiator dissolves completely in the scintillant mixture. This means that the counting efficiency for the initiator samples will be less than that for the polymer samples because of the quenching effect of initiator in solution. It is unlikely that this difference will amount to more than 10%.<sup>16</sup> Thus the average degree of polymerization calculated by assuming equal counting efficiency is a minimum value.

The main conclusion, however, is that the polyfluoral prepared by this method carried to high conversion contains chemically bound initiator fragments, even after stabilization by acetylation. It is therefore likely that the polymer molecules have different endgroups, one an initiator fragment,

(CH<sub>3</sub>)<sub>2</sub>CCN and one a group amenable to acetylation such as hydroxyl. Assuming one initiator fragment per polymer molecule, the average degree of polymerization of the stabilized polymer is at least 39.

### THE REACTION MECHANISM

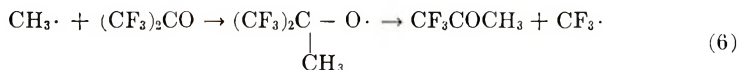
The results of the dilatometric experiments, especially those with free-radical scavengers, show conclusively that free radicals are essential active intermediates in the early stages of the polymerization. The kinetic analysis suggests that the mechanism in the early stages is similar to that observed for conventional vinyl monomers which form soluble polymers and are polymerized by the same technique, in particular, that the termination reaction is second-order if initiation is first-order.

The case for the mechanism of polymerization after the autoacceleration period is not so clear-cut. If acceleration is due to an "occlusion" phenomenon similar to that found for precipitating polymer systems, then free radicals are involved in this region also. Since the polymer prepared in the high-conversion experiment designed for tracer analysis contained a high proportion of initiator fragments, polymer formed after the autoacceleration period apparently contains chemically bound initiator fragments, indicating that it was formed by monomer addition to (CH<sub>3</sub>)<sub>2</sub>CCN radicals.

The results of copolymerization studies in the Dupont laboratories<sup>3</sup> show that fluoral forms copolymers with ethylene, acrylates, styrene, acrylonitrile and other vinyl compounds when polymerized to high conversion with peroxides or azonitriles under a wide range of temperatures and pressures. However, the authors do not say whether the polymers are random or block copolymers of just a mixture of homopolymers. In some preliminary experiments we have shown that fluoral does not copolymerize with either styrene or MMA when initiated by the photolyzed decomposition of AIBN at 243°K and polymerized to low conversion. At high conversion only a mixture of homopolymers is produced. However, fluoral does form copolymers with AN both at high and low conversion under the same conditions. These copolymers have not been completely characterized at this stage. These findings show that fluoral can add to certain free radicals but

may be more selective than most vinyl monomers. Further copolymerization work is required to clarify this situation.

Radical addition reactions to a carbonyl bond adjacent to perfluoroalkyl groups have been detected in the gas phase, but only to ketones. For example, Pritchard and Steacie<sup>17</sup> and subsequently Whittle<sup>18</sup> have postulated the step (6)



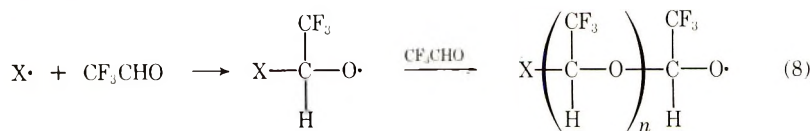
in a study of the reaction of methyl radicals with hexafluoroacetone. Similar reactions have been suggested in the corresponding study of  $\text{CCl}_3\cdot$  reactions with hexafluoroacetone.<sup>19</sup> However no radical addition reactions to aldehydes are known, and indeed one might expect hydrogen abstraction to occur, leaving behind a ketyl radical:



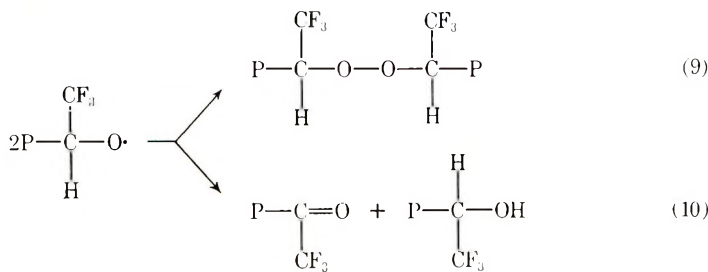
Such abstraction reactions could only end in regeneration of monomer and ultimately in the formation of radical combination products of the type

CN  
|  
CF<sub>3</sub>COCOCF<sub>3</sub> and CF<sub>3</sub>COC(CH<sub>3</sub>)<sub>2</sub>.

No polymer would be formed. Abstraction reactions cannot be ruled out entirely but, because polymer yields of over 95% are attainable, they are only of minor importance in this system. In addition the low temperature of reaction and the fact that the initiator radicals,  $(\text{CH}_3)_2\dot{\text{C}}\text{CN}$ , show little tendency to abstract<sup>20</sup> will favor addition to fluoral. On the basis of the work on radical addition to hexafluoroacetone in the gas phase<sup>17-19</sup> described above, it is postulated that propagation occurs by addition of radicals to the carbon atom of the carbonyl group in fluoral, as shown by the reaction sequence (8), where  $\text{X}\cdot$  is  $(\text{CH}_3)_2\dot{\text{C}}\text{CN}$ .



Although the termination reaction must be bimolecular, there is no conclusive evidence to indicate whether combination [reaction (9)], disproportionation [reaction (10)] or both occurs.



Either mechanism is compatible with the fact that polymer prepared by this method is known to have low thermal stability.<sup>2</sup>

We wish to acknowledge an equipment grant and a maintenance grant (R. W. H.) from the Science Research Council, an equipment grant from Esso (Chemicals) Ltd., and the helpful discussions with Dr. I. S. McLintock regarding the tracer work.

### References

1. D. R. Husted and A. H. Ahlbrecht, Brit. Pat. 719,877 (1954).
2. W. K. Busfield, *Polymer*, **9**, 479, (1968).
3. T. Le S. Cairns, E. T. Cline, and P. J. Graham, U.S. Pat. 2,828,287 (1958).
4. P. Holliday, Collection of Courtaulds Ltd., Coventry.
5. C. G. Overberger, M. T. O'Shaughnessy, and H. Shalit, *J. Amer. Chem. Soc.*, **71**, 2661, (1949).
6. W. Otting and H. Kaimer, *Ber.*, **87**, 1205 (1954).
7. C. H. Bamford and M. J. S. Dewar, *Proc. Roy. Soc. (London)*, **A197**, 356 (1949).
8. L. M. Arnett and J. H. Peterson, *J. Amer. Chem. Soc.*, **74**, 2031 (1952).
9. C. H. Bamford and M. J. S. Dewar, *Proc. Roy. Soc. (London)*, **A195**, 308 (1948).
10. M. S. Matheson, E. E. Auer, E. B. Bevilaqua, and E. J. Hart, *J. Amer. Chem. Soc.*, **73**, 1700 (1951).
11. M. S. Matheson, E. E. Auer, E. B. Bevilaqua, and E. J. Hart, *J. Amer. Chem. Soc.*, **71**, 2610 (1949).
12. G. Dixon-Lewis, *Proc. Roy. Soc. (London)*, **A198**, 510 (1949).
13. C. H. Bamford and A. D. Jenkins, *Proc. Roy. Soc. (London)*, **A228**, 220 (1955).
14. J. W. Davies and E. C. Cocking, *Biochim. Biophys. Acta*, **115**, 511 (1966).
15. Y. Nomura, Japan. Pat. 2467 (1964); *Chem. Abstr.*, **60**, 14405h (1964).
16. I. S. McLintock, private communication.
17. G. O. Pritchard and E. W. R. Steacie, *Can. J. Chem.*, **35**, 1216 (1957).
18. E. Whittle and R. D. Giles, *Trans. Faraday Soc.*, **61**, 1425 (1965).
19. W. G. Alcock and E. Whittle, *Trans. Faraday Soc.*, **62**, 134 (1966).
20. J. C. Bevington, *J. Chem. Soc.*, **1954**, 3707.

Received March 31, 1970

Revised April 28, 1970

## Prehump in the Gel-Permeation Chromatography Fractionation of Pulp Cellulose Acetate

L. J. TANGHE, W. J. REBEL, and R. J. BREWER,\* *Polymer Technology Division, Eastman Kodak Company, Rochester, New York 14650*

### Synopsis

GPC chromatograms of cellulose acetate made from wood pulp customarily show a shoulder or small separate peak at the high end of the DP distribution. Material isolated from this "prehump" area is considerably enriched in mannose and xylose, and the size of the prehump in acetates from different pulps correlates with the amount of hemicellulose in the pulp. Prehump is not ordinarily found in cellulose acetate made from linters but was induced by adding mannan at the start of the acetylation, or by prolonging the acetylation beyond the time when the cellulose acetate sulfate triester is first formed. Products of poor solubility, as indicated by increased haze and false viscosity, resulted in both cases. Prehump was reduced in pulp cellulose acetate by many of the steps which give products of improved solubility: mercerization of cellulose prior to acetylation, use of more sulfuric acid catalyst, replacement of part of the acetic acid with methylene chloride during acetylation, and by removal of a small amount of high viscosity or poorly soluble material by fractional precipitation.

### INTRODUCTION

Gel-permeation chromatography (GPC) has been used to examine cellulose nitrate<sup>1-5</sup> cellulose acetate,<sup>5</sup> and cellulose carbanilate.<sup>6</sup> Segal observed<sup>4</sup> that cellulose nitrate from wood pulp has a broader DP distribution than that from cotton; in the former there was "also some unexplainably very high DP material."

We also have observed elution of abnormally large amounts of material at the high end of the DP distribution of cellulose acetate made from wood pulp. Since this is observed characteristically as a small separate peak prior to the main peak, we propose to designate it by the term, "prehump." In some instances merely a shoulder instead of a separately resolved peak is observed. Cellulose acetate from linters ordinarily does not show this behavior.

The present paper is an attempt to explain the prehump obtained in the GPC fractionation of certain cellulose esters. We have correlated the size of the prehump with other properties of the ester; we have found methods to reduce the size of the prehump in wood pulp acetate and to generate it in cotton linters acetate.

\* Present address: Research Laboratories, Tennessee Eastman Company Division, Kingsport, Tennessee 37662.

## EXPERIMENTAL

### Starting Materials

Most of the celluloses were commercial sulfite wood pulps and were used without modification. Acetylation grade cotton linters also were used without further purification. Two cellulose samples were prepared by cooking cotton linters in a Kraft liquor in the presence of spruce or birch chips. Mannan<sup>7</sup> was obtained by extraction of ivory nuts with aqueous sodium hydroxide containing borax buffer. Acetylation grade wood pulp was mercerized by treatment with 12% sodium hydroxide for 2 hr at 20°C.

### Acetylation of Cellulose

Cellulose was acetylated by two methods, both of which are solution processes employing acetic acid, acetic anhydride, and sulfuric acid catalyst. On a laboratory scale, the acetates were prepared in glass bottles according to the method of Tanghe et al.<sup>8</sup> On a larger scale, cellulose was acetylated in stainless steel mixers according to methods previously described.<sup>9</sup> Mercerized cellulose was rewet with water and dehydrated with acetic acid prior to acetylation.

After esterification was complete, the ester was hydrolyzed to acetone solubility (39–40% acetyl). The hydrolyzed ester was precipitated into distilled water, thoroughly washed, and any combined sulfate was stabilized as the sodium salt.

Cellulose acetate viscosity series were obtained as described elsewhere.<sup>10</sup>

### Analysis of Cellulose Esters

Hydroxyl was determined by carbanilation.<sup>11</sup> Cellulose acetate was hydrolyzed to its component sugars which were converted to trimethylsilyl ethers; these were analyzed by vapor-phase chromatography for glucose, mannose, and xylose.<sup>12,13</sup>

GPC chromatographs of the cellulose esters were obtained as previously described<sup>14</sup> on Waters Model 100 and 200 instruments with the use of 1 ml of 0.5% solutions of the esters in tetrahydrofuran. The instruments were operated at ambient temperatures with columns of upper permeability ranges 100,000, 8000, and 3000 Å. The columns were calibrated with polystyrene standards.

The areas of main peak and prehumpp were calculated as the products of their heights and their widths at half-height.

### Fractional Precipitation of Pulp Cellulose Acetate

To a stirred solution (2.5%) of pulp cellulose acetate in acetone, water was added slowly until turbidity resulted. The precipitated fraction (5–10%) was isolated by centrifugation and decanting.

The large fraction in solution was obtained by evaporation of the solution to dryness.

### Fractional Extraction of Pulp Cellulose Acetate

Pulp cellulose acetate (25 g) was extracted by tumbling overnight at room temperature in 1000 g of an acetone-water (54:46 by weight) mixture. The soluble fraction (5–10%) was isolated by filtration and evaporation of the filtrate to dryness.

## RESULTS AND DISCUSSION

### Effect of Hemicellulose on GPC Prehump

Eleven cellulose acetates prepared in bottles were examined by GPC with the use of tetrahydrofuran as solvent. Nine of the eleven samples showed prehump of varying degree. The acetate from cotton linters did not have a prehump.

When these acetates are listed in order of increasing mannose and xylose concentration, there is a corresponding increase in the area of the GPC prehump (Table I). The progressive increase in the size of the prehump can be seen graphically for selected samples shown in Figure 1.

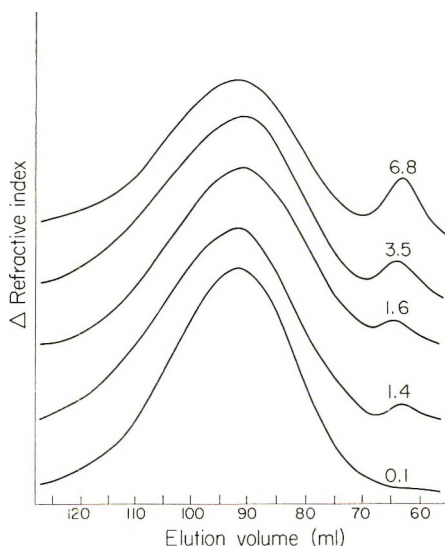


Fig. 1. Effect of hemicellulose (mannose + xylose) on GPC prehump of cellulose acetates. The numbers on the curves indicate the per cent mannose plus xylose.

It should be noted that linters cooked in Kraft liquor in the presence of wood (especially birch) pulp chips absorbed hemicellulose and the corresponding acetates showed a prehump (Table I).

### Isolation of Prehump Material

A pulp cellulose acetate prepared in an acetylation mixer was fractionated by GPC and the eluates representing the prehump and the main peak were

TABLE I  
Analysis of Cellulose Acetates

Sample	Cellulose source	Mannose, % <sup>a</sup>	Xylose, % <sup>a</sup>	Prehump, % of total area <sup>b</sup>
1	Cotton linters	0.0	0.1	0.0
2	Cotton linters <sup>c</sup>	0.0	0.3	1.2
3	Eastern spruce	0.7	0.1	0.0
4	Hardwood sulfite	0.7	0.3	2.0
5	Southern pine	1.3	0.1	2.3
6	Western hemlock	1.4	0.2	3.2
7	Southern pine	1.3	0.8	4.0
8	Eastern spruce	1.5	1.1	6.0
9	Southern pine	2.7	0.8	5.4
10	Cotton linters <sup>d</sup>	0.2	5.6	4.9
11	Alder	3.0	3.8	8.8

<sup>a</sup> By vapor-phase chromatography, per cent sugar based on cellulose.

<sup>b</sup> Calculated from GPC chromatograms.

<sup>c</sup> Cooked in Kraft liquor in the presence of spruce chips.

<sup>d</sup> Cooked in Kraft liquor in the presence of birch chips.

collected separately. Twenty repetitions of the fractionation of a relatively concentrated ester solution (2.0% instead of 0.5%) were required to obtain sufficient material for analysis which required micro-analytical techniques.

The data in Table II show that the combined prehump fractions from

TABLE II  
Sugar Analysis of Pulp Cellulose Acetate Fractions Obtained by GPC

Fraction	Mannose, % <sup>a</sup>	Xylose, % <sup>a</sup>
Unfractionated ester	1.2	0.4
From prehump of GPC elution curve	9.4	4.3
From main peak of GPC elution curve	0.8	0.3

<sup>a</sup> By vapor-phase chromatography.

GPC were highly enriched in mannose (9.4%) and xylose (4.3%) when compared to the unfractionated ester which contained 1.2% mannose and 0.4% xylose. The fraction isolated from the main peak showed a decrease in both mannose and xylose.

The evidence presented strongly supports the concept that prehump in cellulose acetate is caused by hemicellulose. However, the method of acetylation also seems to affect prehump. Acetates prepared in acetylation mixers had larger prehump areas than acetates of the same hemicellulose content prepared in bottles, possibly since the former were prepared with smaller amounts of sulfuric acid catalyst and at lower liquid:cellulose ratios during esterification.<sup>8,9</sup> The method of bottle acetylation was designed for optimum solubility on a laboratory scale.

### Generation of GPC Prehump in Lint Cellulose Acetates

It was observed repeatedly that solutions (in acetic acid, acetone, and tetrahydrofuran) having excessive haze and color were obtained from cellulose acetates rich in hemicellulose. Therefore, it was felt that poor solubility could be the general cause of prehump in cellulose acetates. Since hemicellulose is responsible for poorer solubility of some cellulose acetates in tetrahydrofuran, it is regarded as a specific cause of prehump. If poor solubility is the cause of prehump, it should be possible to introduce prehump to lint acetates by preparing them to be poorly soluble. Conversely, it should be possible to eliminate or reduce prehump from pulp acetates by improving their solubility.

It has been previously mentioned that acetates prepared from cotton linters cooked in Kraft liquors in the presence of wood chips showed a prehump (Table I). Solutions of these acetates were hazy indicating poor solubility.

When cotton linters containing 5% ivory nut mannan were acetylated, the resulting acetate showed a prehump (Fig. 2) whose area (6%) compared favorably with the amount of mannan. Solutions of this acetate were also hazy, showing poor solubility.

Lint cellulose acetates prepared to have high false viscosity are less soluble than normal lint acetates. Concentrated solutions of cellulose acetates from linters are hazy and may have false viscosity<sup>15</sup> when the acetylation is extended considerably beyond the point where cellulose acetate sulfate triester is first formed. A series of acetates showing this behavior was prepared in the manner described.<sup>15</sup> The samples, removed at various times after formation of the triester, and hydrolyzed separately to acetone solubility (approximately 4.0% hydroxyl), showed progressively decreasing intrinsic viscosity (Table III). The decreased solubility

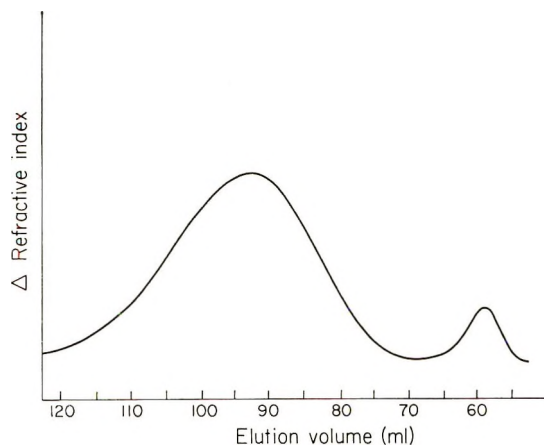


Fig. 2. GPC fractionation of cellulose acetate prepared from linters-mannan (95:5 by weight).



TABLE III  
Lint Cellulose Acetates Prepared to Have Severe False Viscosity

Sample	Total esterification time, min	Intrinsic viscosity <sup>a</sup>	Viscosity in concentrated solution, Poise <sup>b</sup>	Absorbance <sup>c</sup>	
				425 m $\mu$ <sup>d</sup>	625 m $\mu$ <sup>e</sup>
A	97 <sup>f</sup>	2.28	1370	0.034	0.023
B	120	2.16	950	0.025	0.011
C	150	2.01	555	0.027	0.012
D	180	1.87	430	0.046	0.017
E	210	1.73	280	0.157	0.105
F	225	1.64	334	0.262	0.137
G	240	1.57	436	0.361	0.187
H	255	1.51	Insoluble	0.519	0.234
I	270	1.46	"	0.668	0.287

<sup>a</sup> In acetone.

<sup>b</sup> In 97.5% aqueous acetone at 4:1 solvent:ester (by weight).

<sup>c</sup> Determined on hydrolysis solutions in 1-cm cells.

<sup>d</sup> A measure of color and haze.

<sup>e</sup> A measure of haze.

<sup>f</sup> At which time a clear, fiber-free esterification solution resulted.

of the samples taken between 97 and 270 min esterification is shown by the drastic increase in color and haze. The viscosity in concentrated solution passed through a minimum with time and finally was not measurable due to the insolubility of the acetates.

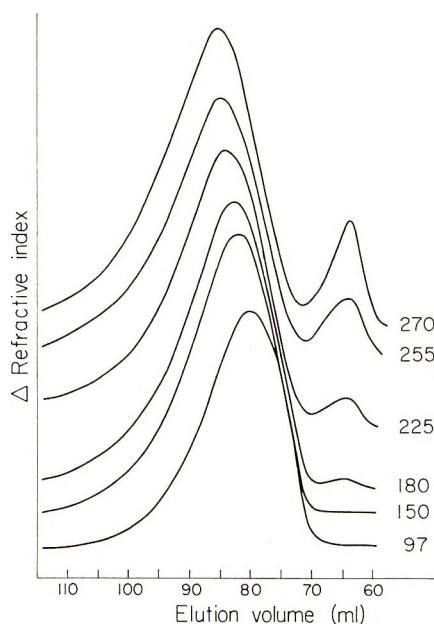


Fig. 3. Effect of increased esterification time on GPC prehumplike of lint cellulose acetates. The esterification time is increased from 97 to 270 min.

The GPC chromatograms in Figure 3 show the increase in prehump with increased esterification time. Samples esterified 97–150 min showed normal distribution curves, whereas the 180-min sample showed the first indication of prehump. Those samples esterified 225–270 min showed still larger prehump areas (Fig. 3) and false viscosity (Table III), as indicated by an increase in viscosity in concentrated solution with decreasing intrinsic viscosity.

While the size of prehump correlated with the amount of mannose and xylose in a series of pulp esters (Table I and Fig. 1), these sugar components are not essential for prehump, since they were absent in this series from linters.

### Elimination or Reduction of Prehump in Pulp Cellulose Esters

Esters of improved solubility were prepared by using more reactive pulps, modifying the esterification procedure, and purifying the resulting ester.

**Water Activation of Cellulose.** Swelling of cellulose with water followed by dehydration with acetic acid increases its reactivity toward esterification and gives an ester of improved solution clarity, but when this technique is employed there is no effect on either the size or position of the GPC prehump of the resulting acetate.

**Mercerization of Cellulose.** Mercerization removes some of the impurities from cellulose and increases its reactivity substantially provided the cellulose is acetylated without drying, or if dried, is rewet with water and dehydrated with acetic acid. Mercerization also reduces false viscosity,<sup>16</sup> and the resulting acetates contain smaller amounts of mannose and xylose (Table IV).

TABLE IV

Acetates from pulp cellulose	Mannose, %	Xylose, %
Mercerized	0.7	0.6
	0.7	0.4
Unmercerized	1.1	0.8
	1.4	0.6

For these reasons, the effect of mercerization on GPC prehump was investigated. The samples from unmercerized pulp cellulose (samples 1–6, Table V and Fig. 4) consistently showed a relatively large prehump. In the mercerized samples (samples 10–12, Table V and Fig. 5) the prehump was reduced and located at a slightly higher elution volume (68.5 ml) than in the unmercerized samples (65.5 ml).

**Increase in Catalyst Concentration.** Sulfuric acid catalyst, 7% based on dry weight of cellulose, was used in the mixer acetylations described above. The use of more catalyst gives an acetate of higher combined sulfate<sup>9</sup> and improved solubility (lower false viscosity).<sup>15</sup>

Table VI gives the results of GPC fractionation of cellulose acetates prepared with 7, 14, and 21% sulfuric acid catalyst. There was no change in the size of the prehum in going from 7 to 14% catalyst, but the use of 21% catalyst slightly reduced the area of the prehum.

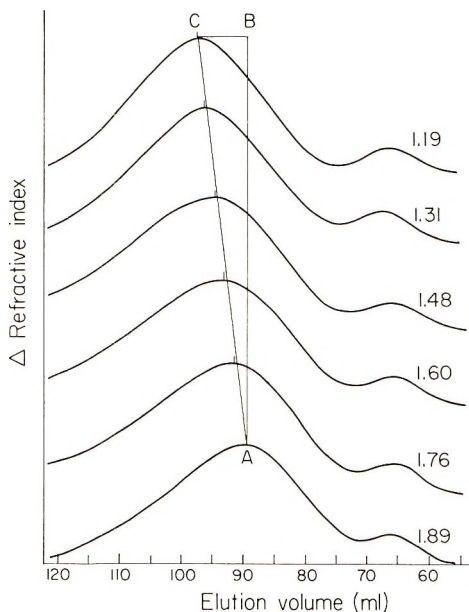


Fig. 4. GPC elution curves of unmercerized pulp cellulose acetates of decreasing intrinsic viscosity. Numbers on the curves correspond to the samples in Table V.

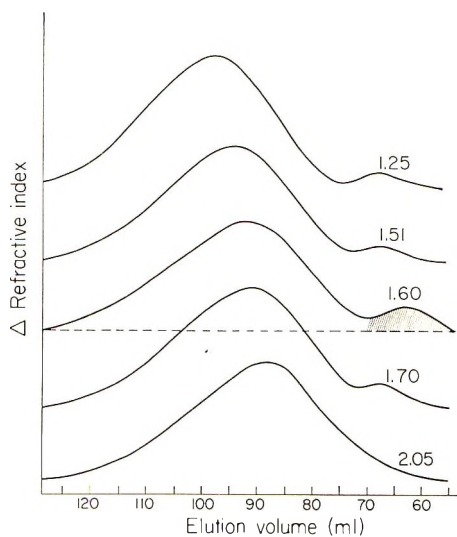


Fig. 5. GPC elution curves of mercerized pulp cellulose acetates of decreasing intrinsic viscosity. Numbers on the curves correspond to the samples in Table V. The curve with the shaded area is an unmercerized control.

TABLE V  
 GPC Fractionation of Acetates From Mercerized and Unmercerized  
 Pulp Cellulose

Sample	Intrinsic viscosity <sup>a</sup>	Prehump, % of total area <sup>b</sup>	Maxima (elution volume, ml)	
			Prehump	Main peak
Unmercerized				
1	1.89	10.8 <sup>c</sup>	65.0	89.0
2	1.76	8.6	65.0	91.0
3	1.60	9.1	65.0	92.0
4	1.48	8.3	65.5	93.5
5	1.31	7.9	66.5	96.5
6	1.19	7.1	66.5	98.0
Mercerized				
7	2.05	d	—	88.5
8	1.89	d	—	89.0
9	1.70	d	—	91.5
10	1.51	4.3	68.5	93.5
11	1.37	5.0	68.5	95.0
12	1.25	4.5	68.5	97.5

<sup>a</sup> In acetone.

<sup>b</sup> Calculated from GPC chromatograms.

<sup>c</sup> Value high due to poor resolution.

<sup>d</sup> Values too small for accurate measurement due to poor resolution.

TABLE VI  
 GPC Fractionation of Pulp Cellulose Acetates Prepared  
 With Increased Catalyst

Sample	Catalyst, % <sup>a</sup>	Intrinsic viscosity <sup>b</sup>	Prehump, % of total area <sup>c</sup>
1	7	1.58	8.5
2	7	1.60	8.3
3	14	1.65	7.9
4	14	1.74	9.4
5	21	1.61	7.7
6	21	1.55	7.1

<sup>a</sup> Weight-% of sulfuric acid based on dry weight of cellulose.

<sup>b</sup> In acetone.

<sup>c</sup> Calculated from GPC chromatograms.

**Increase in Anhydride Concentration.** Extra acetic anhydride (4 parts instead of the usual 2.8 parts per part of dry cellulose) was used during acetylation to improve the solubility of the resulting cellulose acetate, but this had no effect on either the size or the position of the GPC prehump.

**Methylene Chloride Diluent During Acetylation.** The replacement of half of the acetic acid with an equal volume of methylene chloride during acetylation reduces the false viscosity of the resulting cellulose acetate.<sup>15</sup> Cellulose acetates prepared in this manner and fractionated by GPC showed a reduction in prehump (4.5% of total area) when compared to a control

without methylene chloride in the esterification solution (prehump 8.3% of total area).

**Decrease in Intrinsic Viscosity of Cellulose Acetate.** A decrease in viscosity normally gives a cellulose acetate of better solubility, but accentuates the GPC prehump through better resolution from the main peak. Table V presents data on the GPC fractionation of cellulose acetates over wide ranges of intrinsic viscosity. There is a large shift (line BC, Fig. 4) in the main peak to higher elution volumes (Table V, samples 1-6; 89 to 98 ml), while the position of the prehump remains fairly constant (65 to 66.5 ml). This gives a better separation of the prehump from the main peak as the viscosity of the ester is reduced. However, the decrease in viscosity does not appreciably reduce the size of the prehump.

**Increase in Acetyl Content.** The degree of substitution (DS) of cellulose acetates strongly affects their solubility in most solvents, including tetrahydrofuran. When cellulose acetates of the same intrinsic viscosity (1.5), but with varying DS (38-42% acetyl), were prepared and fractionated by GPC there was no difference in the size of the prehump observed. Acetates containing over 42% acetyl were insoluble in tetrahydrofuran.

**Preparation of Higher Acyl Esters.** Mixed esters of cellulose containing acetyl and higher acyl groups have improved solubility over the simple acetates. When fractionated by GPC, cellulose acetate butyrate had no prehump, and acetate propionate had a smaller prehump than an acetate prepared from the same pulp source.

### Fractionation of Pulp Cellulose Acetate

Small fractions were removed from the high end of the DP distribution of cellulose acetate by fractional precipitation, and from the low end by

TABLE VII  
Fractionation of Pulp Cellulose Acetate

Fraction	Weight, %	In- trinsic vis- cosity <sup>a</sup>	Man- nose, % <sup>b</sup>	Xylose, % <sup>b</sup>	Prehump, % of total area <sup>c</sup>
Original ester	100	1.55	0.8	0.5	7.3
Precipitated <sup>d</sup>	12.7	2.48	3.8	0.5	22
Remainder	87.3	1.42	0.8	0.2	None
Extracted <sup>e</sup>	10.0	0.55	Trace	1.4	None
Remainder <sup>f</sup>	90.0	1.72	0.7	0.3	7.5

<sup>a</sup> In acetone.

<sup>b</sup> By vapor-phase chromatography.

<sup>c</sup> Calculated from GPC chromatograms.

<sup>d</sup> From 2.5% acetone solution with water.

<sup>e</sup> With acetone-water (54:46 by weight).

<sup>f</sup> Curve almost identical to that of original ester in Fig. 6.

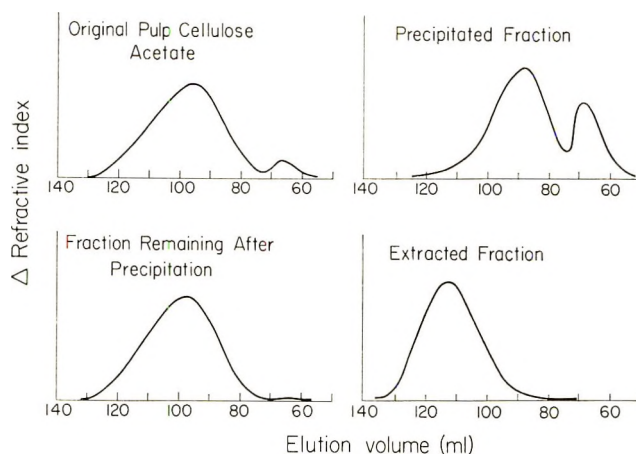


Fig. 6. Effect of fractional precipitation and extraction on the GPC prehum of pulp cellulose acetate.

fractional extraction. The high-viscosity fraction (Table VII, 2.48 intrinsic viscosity) precipitated from acetone solution with water, contained a large amount of mannose (3.8%) and showed a massive prehum (Fig.

TABLE VIII  
Factors Affecting Prehum in Pulp Cellulose Acetate

Modification of	Effect on prehum
Starting cellulose	
Swell with water and dehydrate with acetic acid	None
Mercerize	Reduction
Esterification procedure	
Increase in catalyst	Slight reduction
Increase in anhydride	None
Replace part of the acetic acid with methylene chloride	Reduction
Reduce viscosity of ester	None
Reduce acetyl of ester	None
Esterify with acetic anhydride and propionic anhydride <sup>a</sup>	Reduction
<i>n</i> -butyric anhydride <sup>a</sup>	Elimination
Completed ester	
Filter solution	None
Centrifuge solution	None
Remove low-viscosity fraction by extraction	None
Remove high-viscosity fraction by precipitation	Elimination

<sup>a</sup> Sufficient to give mixed ester containing 0.75 higher acyl per anhydroglucose unit.

6, prehump 22% of total area). The unfractionated ester showed a prehump of 7.3% of the total area. The material remaining after precipitation of the high viscosity fraction had little or no GPC prehump.

The low intrinsic viscosity fraction extracted from pulp acetate with acetone-water (Table VII, 0.55 intrinsic viscosity) showed no prehump and only trace amounts of mannose; the xylose (1.4%) concentrated in the extracted fraction did not cause a prehump. The material remaining after extraction gave analyses (Table VII) and a GPC elution curve almost identical with those of the unfractionated ester.

Concentrated solutions of cellulose esters show improved clarity when filtered; small amounts of insoluble material are removed. However, such filtration had no effect on the size or position of the GPC prehump of pulp cellulose acetate indicating that the material causing prehump passed through the filter media.

High-speed centrifugation (31,000*g*) removes small amounts (0.2 to 0.4%) of insoluble material from a solution of pulp cellulose acetate. The material removed by centrifugation is highly enriched in hemicellulose (mannose and xylose) and the centrifuged solution exhibits improved clarity. However, high-speed centrifugation of various pulp cellulose acetates had no effect on the amount or position of their GPC prehump. This is probably due to the small amount of material removed by such a process when compared to the prehump area of approximately 8%.

The effects of the above modifications of starting cellulose, esterification procedure, and completed ester on GPC prehump are summarized in Table VIII.

The authors are indebted to Mr. E. W. Holroyd, Jr., of the Polymer Technology Division for the sugar analyses and to Mrs. Sharon Bailey and Mrs. Geraldine Rittersbach of the Industrial Laboratory for the gel-permeation chromatography fractionations.

## References

1. L. Segal, *J. Polym. Sci., B*, **4**, 1011 (1966).
2. G. Meyerhoff and S. Jaovanovic, *J. Polym. Sci. B*, **5**, 495 (1967).
3. L. Segal, paper presented to Division of Carbohydrate Chemistry, 153rd Meeting, American Chemical Society, Miami, Fla., April 1967; paper 34.
4. L. Segal, in *Analytical Gel Permeation Chromatography (J. Polym. Sci. C, 21)* J. F. Johnson and R. S. Porter, Eds., Interscience, New York, 1968, p. 267.
5. T. E. Muller and W. J. Alexander, in *Analytical Gel Permeation Chromatography (J. Polym. Sci. C, 21)*, J. F. Johnson and R. S. Porter, Eds., Interscience, New York, 1968, p. 283.
6. R. J. Brewer, L. J. Tanghe, S. Bailey, and J. T. Burr, *J. Polym. Sci. A-1*, **6**, 1697 (1968).
7. J. K. Watson and D. R. Henderson, *Tappi*, **40**, 686 (1957).
8. L. J. Tanghe, L. B. Genung, and J. W. Mench, in *Methods in Carbohydrate Chemistry*, R. L. Whistler, Ed., Vol. III, Academic Press, New York-London, 1963, p 194.
9. C. J. Malm, L. J. Tanghe, and B. C. Laird, *Ind. Eng. Chem.*, **38**, 77 (1946).
10. R. J. Brewer, L. J. Tanghe and S. Bailey, *J. Polym. Sci. A-1*, **7**, 1635 (1969).
11. C. J. Malm, L. J. Tanghe, B. C. Laird, and G. D. Smith, *Anal. Chem.*, **26**, 188 (1954).

12. C. C. Sweeley, R. Bentley, M. Makita, and W. W. Wells, *J. Amer. Chem. Soc.*, **85**, 2497 (1963).
13. C. C. Sweeley and B. Walker, *Anal. Chem.*, **36**, 1461 (1964).
14. J. Cazes, *J. Chem. Ed.*, **43**, A567 (1966).
15. C. J. Malm and L. J. Tanghe, *Tappi*, **46**, 629 (1963).
16. G. A. Richter and L. E. Herdle, *Ind. Eng. Chem.*, **49**, 1451 (1957).

Received January 21, 1970



## Relationship Between Membrane Potential and Electrolyte Uptake by Ion-Exchange Membranes

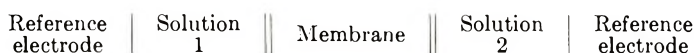
N. LAKSHMINARAYANAI AH and FASIH A. SIDDIQI,\*  
*Department of Pharmacology, University of Pennsylvania School of  
 Medicine, Philadelphia, Pennsylvania 19104*

### Synopsis

Electrical potentials arising across three cation-selective membranes of low water content when they separate solutions of different concentration of the same NaCl electrolyte have been measured at 25°C. Also, electrolyte uptake by these membranes when they are in equilibrium with different solutions of NaCl has been estimated. These data together with the apparent membrane transport number derived from membrane potential have been used to check a simple relation given by Lakshminarayanaiah.

### INTRODUCTION

The electrical potentials arising across membranes separating different salt solutions are usually measured by using cells of the type:



The reference electrode may be a reversible electrode of the type Ag-AgCl in chloride solutions or calomel connected to the solutions through KCl-agar bridges. In the former case, the total potential is equal to the sum of electrode potential and membrane potential. In the latter case, the cell potential directly gives the membrane potential. These measurements are not unambiguous as they involve all the extra nonthermodynamic assumptions about single-ion activity coefficients, diffusion potentials at KCl bridges, etc. These measurements are taken as routine to characterize the selectivity of membranes.<sup>1</sup>

The membrane potential measured at different concentrations,  $C_1$  and  $C_2$  ( $C_2 > C_1$ ), of the same electrolyte is related to the transport number of the cation in the case of cation-exchange membrane by the relation:

$$\bar{i}_{+(\text{app})} = (E/2E_{\text{max}}) + 0.5 \quad (1)$$

\* On study leave from the Department of Chemistry, Aligarh Muslim University Aligarh, India.

where  $E$  is the membrane potential measured by using calomel electrodes and KCl-agar salt bridges,  $E_{\max}$  is the theoretically possible maximum value of the membrane potential given by the equation:

$$E_{\max} = \left( \frac{RT}{F} \right) \ln (a_1/a_2) \quad (2)$$

where  $a_1$  and  $a_2$  are the activities of the two solutions of concentrations  $C_1$  and  $C_2$  and  $R$ ,  $T$ , and  $F$  have their usual significance. The cation transport number given by eq. (1) is not a true value as it does not take into account the transfer of water and so is called the apparent transport number  $\bar{l}_{+(\text{app})}$ . This has been related to the true transport number ( $\bar{l}_+$ ) by two treatments which are reviewed elsewhere by Lakshminarayanaiah.<sup>2</sup> Treatment one gives the relation,<sup>2-4</sup>

$$\bar{l}_+ = \bar{l}_{+(\text{app})} + 0.018m_{\pm} \bar{l}_w \quad (3)$$

where  $\bar{l}_w$  is the transport number of water and  $m_{\pm}$  is the mean molality of the solution used in the measurements. Treatment two, originally given by Oda and Yawataya<sup>5</sup> is expressed by Arnold and Swift<sup>6</sup> in the form

$$\bar{l}_+ = \left( \frac{\bar{l}_w}{\bar{W}_e} \right) (1 + \bar{S}) + \bar{l}_{+(\text{app})} [1 - (\bar{l}_w/\bar{W}_e)] \quad (4)$$

where  $\bar{W}_e$  is the number of moles of water per equivalent of fixed ion-exchange site in the membrane and  $\bar{S}$  is the equivalent of coions per equivalent of fixed site sorbed by the membrane.

Lakshminarayanaiah,<sup>2</sup> working with crosslinked phenol sulfonate membranes of high water content (>50%) showed that eqs. (3) and (4) generated identical values for  $\bar{l}_+$  and consequently the two equations were considered equivalent, leading to a simple relationship between electrolyte uptake and  $\bar{l}_{+(\text{app})}$ , viz.,

$$m_{\pm} = \bar{X}_m [\bar{S} + \bar{l}_{-(\text{app})}] \quad (5)$$

where  $\bar{X}_m$  is the number of equivalents of fixed groups associated with 1000 g of membrane interstitial water and  $\bar{l}_{+(\text{app})} + \bar{l}_{-(\text{app})} = 1$ . In this paper, electrolyte uptake, membrane potential and other relevant measurements are presented to check the validity of eq. (5) in the case of three cation-exchange membranes of low water content (<22%).

## EXPERIMENTAL

### Membranes

Three cation-exchange membranes of different water content and exchange capacity were used in this study. Polyethylene-styrene graft copolymer type AMF C-104 membrane containing sulfonic acid groups was supplied by the American Machine and Foundry Company. The other two membranes were prepared from Parlodion [purified pyroxylin (nitrocellulose), Mallinckrodt] and sulfonated polystyrene (SPS) following

the method reviewed by Neihof.<sup>7</sup> A 2% solution of Parlodion (P) in alcohol-ether (3:1) containing 0.25 g of SPS was used to prepare a P-SPS membrane of high charge density. Again, 2% P solution containing 0.025 g of SPS was used to prepare a P-SPS membrane of low charge density. About 10 ml of the P-SPS solution was spread on a clean, dry glass plate by using a Boston-Bradley doctor blade (Gardner Laboratory, Bethesda, Md). The solution was allowed to dry in air for about 3 hr and then dried in an oven at 80°C for another hour, after which the membrane was removed from the glass plate under water. The doctor blade was adjusted to give a membrane, about 0.02 mm thick, after drying. The AMF membrane was about 0.12 mm thick. All the membranes were conditioned in deionized water and converted to the Na form by equilibrating them with 1N NaCl solution. These membranes were washed thoroughly with deionized water and equilibrated with the required NaCl solution with frequent solution changes.

### Water Content

Pieces of membrane equilibrated with the appropriate NaCl solution were blotted with filter paper, placed in a weighing bottle and weighed. They were then dried to constant weight in a vacuum desiccator at 70°C. The accuracy of this measurement was  $\pm 5\%$ .

### Exchange Capacity and Coion Uptake

A known weight of surface dried membrane already equilibrated in the required NaCl solution was treated with exactly 10 ml of 0.1N HNO<sub>3</sub> solution and kept stirred for about 24 hr. The liquid was decanted carefully and the membrane was washed a number of times with deionized water. The decanted liquid with the washings was analyzed for its acid content in the usual way. The chloride was estimated by using Aminco-Cotlove automatic chloride titrator (American Instrument Company, Silver Spring, Md.). The overall accuracy of these estimations was determined by the homogeneity of the membranes used, and we therefore estimate the accuracy of these measurements to be  $\pm 5\%$ .

### Membrane Potential

These measurements were made following the procedures described elsewhere.<sup>8</sup> Calomel and KCl-agar bridges were used in the measurements. Here again, for any given membrane, although the potentials could be measured accurate to  $\pm 0.5$  mV on the 30-mV scale of a 151 Keithley micro-voltmeter, the overall accuracy (about 5%) was determined by the different membranes used in the measurements.

## RESULTS AND DISCUSSION

The different equilibrium parameters determined for the membranes as a function of external electrolyte concentration are given in Table I

and the membrane potentials are given in Table II. The  $\bar{l}_{+(\text{app})}$  values calculated from eq. (1) are related to the molality of the external solution by the interpolation procedure described by Oda and Yawataya<sup>5</sup> and illustrated by Lakshminarayanaiah.<sup>2</sup> The values of  $\bar{l}_{+(\text{app})}$  so derived and re-

TABLE I  
Parameters for the Membrane in Equilibrium with NaCl Solution at 25°C

Parameter	Electrolyte solution,		High-charge P-SPS	Low-charge P-SPS
	N	AMF C-104		
Water content, g/100 g wet membrane	0.001	13.0	21.0	8.5
	0.01	13.0	20.8	8.0
	0.1	12.5	20.5	7.5
	0.5	12.0	19.0	7.0
Exchange capacity, meq/g wet membrane	0.001	0.560	0.410	0.037
	0.01	0.500	0.420	0.038
	0.1	0.504	0.437	0.039
	0.5	0.558	0.445	0.040
Chloride (coion) uptake, meq/g wet membrane	0.001	$0.4 \times 10^{-3}$	$1.5 \times 10^{-3}$	$1.5 \times 10^{-3}$
	0.01	$1.1 \times 10^{-3}$	$2.1 \times 10^{-3}$	$2.3 \times 10^{-3}$
	0.1	$1.6 \times 10^{-3}$	$4.6 \times 10^{-3}$	$6.4 \times 10^{-3}$
	0.5	$9.1 \times 10^{-3}$	$12.8 \times 10^{-3}$	$6.8 \times 10^{-3}$

TABLE II  
Emf's across Membrane Cell at 25°C

Hg, Hg <sub>2</sub> Cl <sub>2</sub>   Saturated KCl-agar		NaCl (m <sub>1</sub> )	Membrane	NaCl (m <sub>2</sub> )	Saturated KCl-agar	Hg <sub>2</sub> Cl <sub>2</sub> , Hg
Emf, mV						
m <sub>1</sub>	m <sub>2</sub>	a <sub>1</sub>	a <sub>2</sub>	AMF C-104	High-charge P-SPS	Low-charge P-SPS
0.001004	0.002004	0.00098	0.00193	17.4	16.8	12.5
0.002004	0.005005	0.00193	0.00473	22.3	21.8	14.8
0.005005	0.1005	0.00473	0.00932	16.7	16.2	11.8
0.01005	0.02005	0.00932	0.0180	16.0	15.5	11.5
0.02005	0.05006	0.0180	0.0428	21.0	19.6	12.5
0.05006	0.1006	0.0428	0.0783	14.5	12.5	9.8
0.1006	0.2026	0.0783	0.148	14.0	11.3	8.5
0.2026	0.5066	0.148	0.344	18.2	13.0	10.5
0.5066	1.024	0.344	0.666	12.8	8.0	7.3

lated to the concentration of the external solution are given in Figure 1 for the three membranes. The values of  $m_{\pm}$ ,  $\bar{X}_m$ , and  $\bar{S}$  derived from the results of Table I are given in Table III. From these values  $\bar{l}_{-(\text{app})}$  is calculated using eq. (5). These calculated values of  $\bar{l}_{+(\text{app})}$  along with

TABLE III  
Parameters for the Membrane in Contact with NaCl Solution

Membrane	External solution molality $m_{\pm}$	$\bar{X}_m$ , eq/1000 g water	$m_{Cl^-}$ , eq/1000 g water $\times 10^{-3}$	$\bar{S}_m$ , eq (Cl $^-$ ) per eq. of $\bar{X}_m \times 10^{-3}$	$I_{(app)}$ [eq. (5)] $\times 10^{-3}$	$\bar{I}_{(app)}$	
						Calcd	Found
AMF C-104	0.001004	4.31	3.1	0.7	-0.5	1.001	0.999
	0.01005	3.84	8.2	2.1	+0.5	1.000	0.976
	0.1006	4.02	12.8	3.2	+1.8	0.998	0.954
	0.5066	4.65	75.8	16.3	+92.7	0.907	0.905
High-charge P-SPS	0.001004	1.95	7.2	3.6	-3.0	1.003	0.985
	0.01005	2.02	10.1	5.2	-0.03	1.000	0.962
	0.1006	2.13	22.4	10.5	+36.7	0.963	0.884
	0.5066	2.39	67.4	28.2	+184	0.816	0.776
Low-charge P-SPS	0.001004	0.44	17.6	40.6	-38.0	1.038	0.963
	0.01005	0.48	28.5	60.1	-39.0	1.039	0.840
	0.1006	0.52	84.7	163	+30.0	0.970	0.796
	0.5066	0.57	97.0	170	+715	0.285	0.733

those values derived from membrane potential measurements are also given in Table III.

Comparison of the results given in the last two columns of Table III indicate that the calculated values of  $\bar{l}_{+(app)}$  [eq. (5)] are close (within 5%) to the corresponding observed values in the case of AMF C-104 membrane; whereas in the case of the other P-SPS membrane of high charge density, the agreement lies between 2 and 10%. In the case of the P-SPS membrane of low charge density, the agreement is poor, although in the very dilute region the divergence is about 7%. This study restricted to one

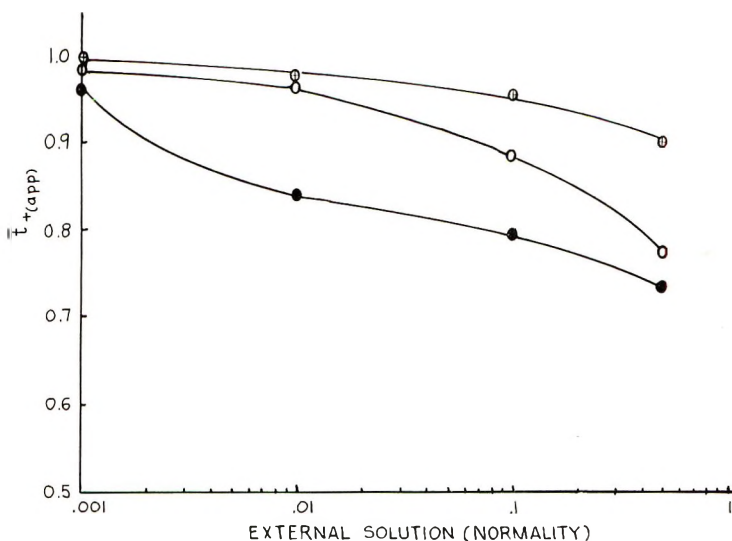


Fig. 1. Apparent transport number  $[\bar{l}_{+(app)}]$  derived from membrane potential data related to the external solution concentration: (⊕) AMF C-104 membrane; (○) P-SPS membrane of high charge density; (●) P-SPS membrane of low charge density.

electrolyte and three membranes of low water content (<22%) leads to the conclusion that eq. (5) could be used, in the case of high charge density membrane, to predict values for  $\bar{l}_{+(app)}$  (within 10%) from the electrolyte content of the membrane phase. It seems to be inapplicable to membranes of low charge and low water content. Whether it can predict values for membranes of low charge and high water content requires further investigation.

The work was supported by Public Health Service Grant NB-08163-01.

### References

1. N. Lakshminarayanaiah, *Transport Phenomena in Membranes*, Academic Press, New York, 1969, p. 196.
2. N. Lakshminarayanaiah, *J. Phys. Chem.*, **73**, 97 (1969).
3. D. K. Hale and D. J. McCauley, *Trans. Faraday Soc.*, **57**, 135 (1961).

4. V. Subrahmanyam and N. Lakshminarayanaiah, *J. Sci. Ind. Res. (India)*, **21B**, 229 (1962).
5. Y. Oda and T. Yawataya, *Bull. Chem. Soc. Japan*, **29**, 673 (1956).
6. R. Arnold and D. A. Swift, *Austral. J. Chem.*, **20**, 2575 (1967).
7. R. Neihof, *J. Phys. Chem.*, **58**, 916 (1954).
8. N. Lakshminarayanaiah and V. Subrahmanyam, *J. Polym. Sci. A*, **2**, 4491 (1964).

Received February 17, 1970

## Catalytic Action of Metallic Salts in Autoxidation and Polymerization. IV. Polymerization of Methyl Methacrylate by Cobalt(II) or (III) Acetylacetonate-*tert*-Butyl Hydroperoxide or Dioxane Hydroperoxide

ZENJIRO OSAWA, TETSUAKI SHIBAMIYA, and TOSHIO KAWAMATA, *Department of Polymer Chemistry, Faculty of Engineering, Gunma University, Kiryu City, Gunma, Japan*

### Synopsis

Polymerization of methyl methacrylate was carried out by four initiating systems, namely, cobalt(II) or (III) acetylacetonate-*tert*-butyl hydroperoxide (*t*-Bu HPO) or dioxane hydroperoxide (DOX HPO). Dioxane hydroperoxide systems were much more effective for the polymerization of methyl methacrylate than *tert*-butyl hydroperoxide systems, and cobaltous acetylacetonate was more effective than cobaltic acetylacetonate in both hydroperoxides. The initiating activity order and activation energy for the polymerization were as follows: Co(acac)<sub>2</sub>-DOX HPO ( $E_a$ -9.3 kcal/mole) > Co(acac)<sub>3</sub>-DOX HPO ( $E_a$  = 12.4 kcal/mole) > Co(acac)<sub>2</sub>-*t*-Bu HPO ( $E_a$  = 15.1 kcal/mole) > Co(acac)<sub>3</sub>-*t*-Bu HPO ( $E_a$ -18.5 kcal/mole). The effects of conversion and hydroperoxide concentration on the degree of polymerization were also examined. The kinetic data on the decomposition of hydroperoxides catalyzed by cobalt salts gave a little information for the interpretation of polymerization process.

### INTRODUCTION

In the course of studies on the metal salt-catalyzed thermal oxidative degradation of isotactic polypropylene, we found<sup>1</sup> that the catalytic action of metal salts for the degradation of the polymer was in the following order: Co > Mn > Cu > V ≫ Ni > Ti ≈ Ca ≈ Ag ≈ Zn > Al > Mg ≈ Cd > control ≈ Ba ≈ Sr, and for the decomposition of *tert*-butyl hydroperoxide as a model compound of the polymeric hydroperoxide the order was: Co ≫ Mn > Cr > Ti > Ni > Fe ≈ Cu > Zn > Ag > Mg > Ba > Ca > Al > Cd > control.

From this background we have become interested in the initiating action of vinyl polymerization with the metallic salt-hydroperoxide system and the mechanism of decomposition of hydroperoxide by metallic salts.<sup>2-4</sup>

In a previous paper<sup>2</sup> we showed that cobalt(II) or (III) acetylacetonate-dioxane hydroperoxide initiating systems were extremely effective for the polymerization of methyl methacrylate. We reported, furthermore, that



the initiating systems could give polymeric ultraviolet stabilizers from 2-hydroxy-4-acryloyloxy-benzophenone and 2-hydroxy-4-methacryloyloxy-benzophenone which could polymerize neither by anionic initiators, such as Grignard reagents, and *n*-butyllithium nor by conventional radical initiators such as benzoyl peroxide and azobisisoacrylonitrile.<sup>5</sup>

In the present paper we describe investigations on polymerization of methyl methacrylate by four initiating systems, namely, cobalt(II) or (III) acetylacetonate-*tert*-butyl hydroperoxide or dioxane hydroperoxide.

## EXPERIMENTAL

### Reagents

Commercial cobaltous acetylacetonate (Tokyo Kasei Co. Ltd.) was recrystallized from benzene-petroleum ether. Commercial cobaltic acetylacetonate was used without further purification.

Reagent-grade benzene was washed four times with 5% sulfuric acid of its volume, then with dilute sodium hydroxide solution and finally with distilled water. After drying with calcium chloride, it was distilled at 79–81°C.

A 2-l. portion of reagent-grade dioxane containing 27 ml of concentrated hydrochloric acid and 200 ml of distilled water was refluxed for 12 hr under a nitrogen atmosphere. After cooling, potassium hydroxide pellets were added, and the upper layer solution was transferred to another flask, then fresh potassium hydroxide was freshly added and allowed to stand overnight. The upper layer solution was refluxed for 12 hr with sodium wire and was distilled at 100–101°C.

Methyl methacrylate was washed with saturated aqueous sodium hydrogen sulfite solution, then with an aqueous solution of 20% sodium chloride containing 5% sodium hydroxide, and finally with an aqueous solution of 20% sodium chloride. It was distilled under vacuum after removal of water by sodium sulfate.

*tert*-Butyl hydroperoxide, which was kindly donated by Nihon Yushi Co. Ltd., was used as received. Dioxane hydroperoxide was prepared by bubbling through oxygen under ultraviolet irradiation.

### Polymerization

Polymerization was carried out in a glass tube under nitrogen. The polymerization conditions were as follows: monomer, 4 ml (3.74 mole/l.); solvent, 6 ml; cobaltous acetylacetonate,  $2.58 \times 10^{-3}$  mole/l.; cobaltic acetylacetonate,  $2.94 \times 10^{-3}$  mole/l.; *tert*-butyl hydroperoxide,  $1.14 \times 10^{-2}$  mole/l.; dioxane hydroperoxide,  $1.04 \times 10^{-2}$  mole/l. After polymerization, the contents of the tube were poured into a large amount of methanol to precipitate the polymer. The polymer obtained was purified by precipitation with the chloroform-methanol solvent system as usual.

The degree of polymerization of the polymers was measured viscometrically in benzene solution at 25°C with the aid of the intrinsic viscosity-molecular weight relationship of Fox et al.<sup>6</sup>

### Decomposition of Hydroperoxide

Solvent (benzene and dioxane) and catalyst were added to a 100-ml three-necked round-bottomed flask equipped with a reflux condenser and a stirrer, and kept at 40, 50, or 60°C for 30 min, at which time hydroperoxide was added. Decomposition of hydroperoxide was measured by iodometry on 5-ml aliquots during the reaction. In dioxane hydroperoxide, decomposition was carried out under nitrogen.

### RESULTS AND DISCUSSION

Figures 1 and 2 give typical conversion-time curves of the polymerization kinetics for  $\text{Co}(\text{acac})_2$ -*t*-Bu HPO and  $\text{Co}(\text{acac})_3$ -*t*-Bu HPO, respectively.

Figures 3 and 4 give conversion-time curves for  $\text{Co}(\text{acac})_2$ -DOX HPO and  $\text{Co}(\text{acac})_3$ -DOX HPO, respectively. As shown in Figures 1-4, for the initial stage of the polymerization a linear conversion-time correlation was found in all series of the experiments. It was, therefore, possible to calculate the overall polymerization rate ( $R_p$ ) from the data obtained for the initial stage of the polymerization. The results calculated are listed in

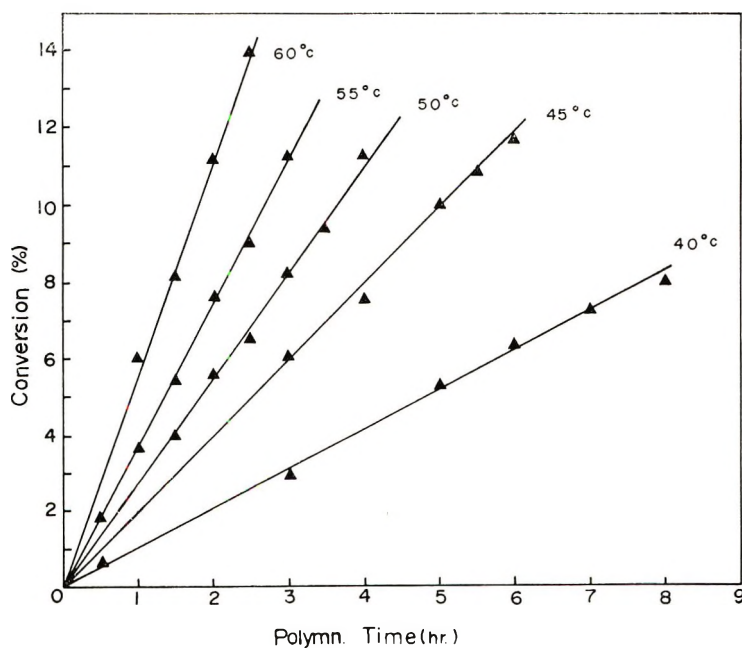


Fig. 1. Polymerization kinetics of MMA in benzene initiated by  $\text{Co}(\text{acac})_2$ -*t*-Bu HPO.

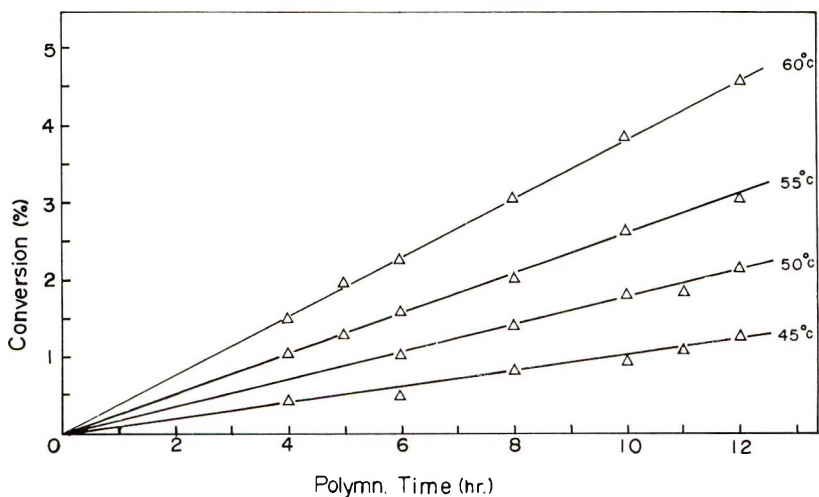


Fig. 2. Polymerization kinetics of MMA in benzene initiated by  $\text{Co}(\text{acac})_3$ -*t*-Bu HPO.

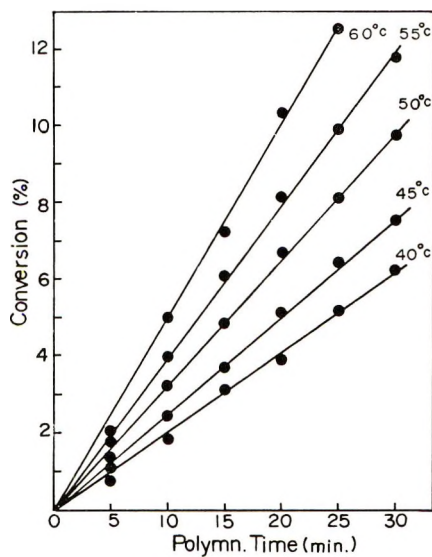


Fig. 3. Polymerization kinetics of MMA in dioxane initiated by  $\text{Co}(\text{acac})_2$ -DOXHPO.

Table I. Remarkable differences in polymerization of the four initiating systems were observed, and results briefly reported in a previous paper were confirmed.<sup>2</sup> Namely, in cobalt(II), or (III) acetylacetonate-hydroperoxide initiated systems, dioxane hydroperoxide is much more effective than *tert*-butyl hydroperoxide, and cobaltous acetylacetonate is more effective than cobaltic acetylacetonate in both hydroperoxides. Thus, the effective initiating order for the polymerization of methyl methacrylate is

TABLE I  
 Polymerization Rate ( $R_p$ ), Activation Energy ( $E_a$ ), and Frequency  
 Factor ( $A$ )

	Temp, °C	<i>tert</i> -Butyl Co(acac) <sub>2</sub>	hydroperoxide Co(acac) <sub>3</sub>	Dioxane hydroperoxide Co(acac) <sub>2</sub>	Dioxane hydroperoxide Co(acac) <sub>3</sub>
$R_p \times 10^5$ , mole/l.-sec	40	1.08	—	12.8	7.0
	45	2.04	0.111	15.8	9.0
	50	2.88	0.188	20.3	12.5
	55	3.83	0.278	24.8	16.8
	60	5.81	0.403	31.5	23.3
$E_a$ , kcal/mole		15.1	18.5	9.3	12.4
$A$ , mole/l.-sec		$4.53 \times 10^5$	$6.45 \times 10^6$	$3.88 \times 10^2$	$2.86 \times 10^4$

as follows:  $\text{Co}(\text{acac})_2\text{-DOX HPO} > \text{Co}(\text{acac})_3\text{-DOX HPO} > \text{Co}(\text{acac})_2\text{-}t\text{-Bu HPO} > \text{Co}(\text{acac})_3\text{-}t\text{-Bu HPO}$ . Arrhenius plots of the kinetic data are shown in Figure 5; a straight-line correlation is observed for each series. The apparent activation energies and frequency factors for the polymerization are also listed in Table I. From Table I it is obvious that the more effective the initiating system, the lower activation energy.

The relation between the degree of polymerization and conversion was examined in each series and the results are shown in Figures 6 and 7. As shown in Figures 6 and 7 the degree of polymerization-conversion curves are quite different in each series at the initial stage of polymerization. The  $\text{Co}(\text{acac})_2\text{-}t\text{-Bu HPO}$  initiating system gives a higher degree of polymerization than  $\text{Co}(\text{acac})_3\text{-}t\text{-Bu HPO}$  and gives the highest degree of polymerization of the four series. The degree of polymerization with the  $\text{Co}(\text{acac})_3\text{-}$

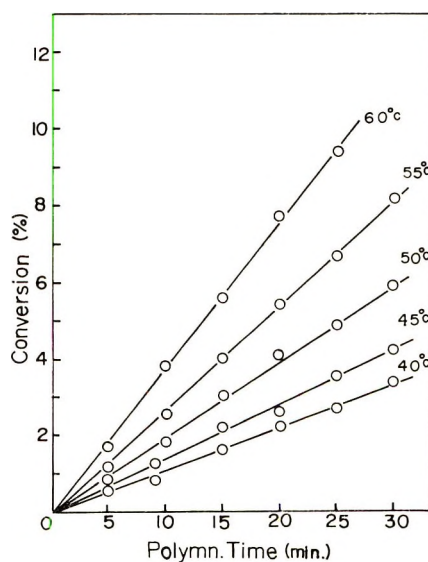


Fig. 4. Polymerization kinetics of MMA in dioxane initiated by  $\text{Co}(\text{acac})_3\text{-DOX HPO}$ .

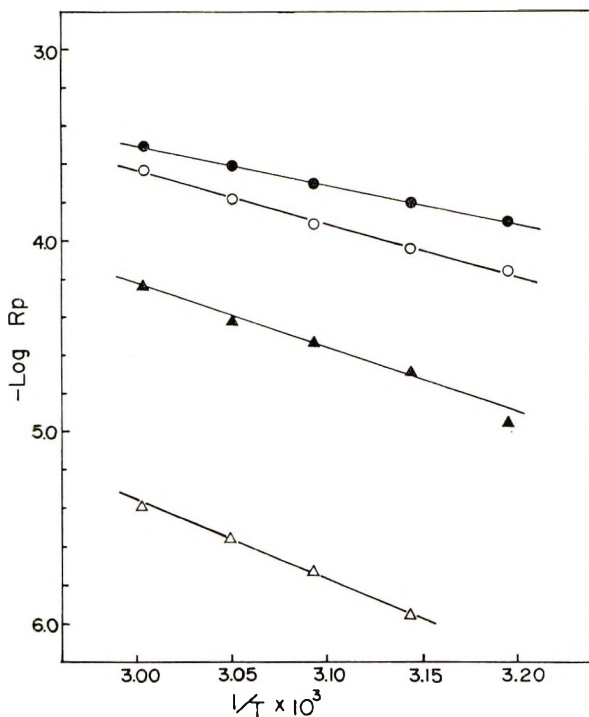


Fig. 5. Arrhenius plots for the polymerization of MMA: (▲)  $\text{Co}(\text{acac})_2$ -*t*-Bu HPO; (●)  $\text{Co}(\text{acac})_2$ -DOX HPO; (△)  $\text{Co}(\text{acac})_3$ -*t*-Bu HPO; (○)  $\text{Co}(\text{acac})_3$ -DOX HPO.

DOX HPO initiating system is higher than that with  $\text{Co}(\text{acac})_2$ -DOX HPO. In addition, the degree of polymerization does not increase appreciably with increasing conversion in general. An example is shown in Figure 6, where the  $\text{Co}(\text{acac})_3$ -*t*-Bu HPO initiating system gives only a polymer with a degree of polymerization of 840 after 54 hr polymerization at 50°C.

Both the  $\text{Co}(\text{acac})_2$ -*t*-Bu HPO and  $\text{Co}(\text{acac})_3$ -DOX HPO series show relatively good temperature dependence on the degree of polymerization, namely, the lower the polymerization temperature, the higher the degree of polymerization. However,  $\text{Co}(\text{acac})_3$ -*t*-Bu HPO and  $\text{Co}(\text{acac})_2$ -DOX HPO series give polymers with lower degree of polymerization, and it is difficult to observe a clear temperature dependence.

The effect of hydroperoxide concentration on the degree of polymerization was examined in divalent cobalt salt series. Figures 8 and 9 show conversion-time curves for  $\text{Co}(\text{acac})_2$ -*t*-Bu HPO and  $\text{Co}(\text{acac})_2$ -DOX HPO initiating series.

The relation between the degree of polymerization and conversion is shown in Figure 10. With the  $\text{Co}(\text{acac})_2$ -DOX HPO initiating system, a remarkable dependence of hydroperoxide concentration on degree of polymerization is observed. The degree of polymerization increases

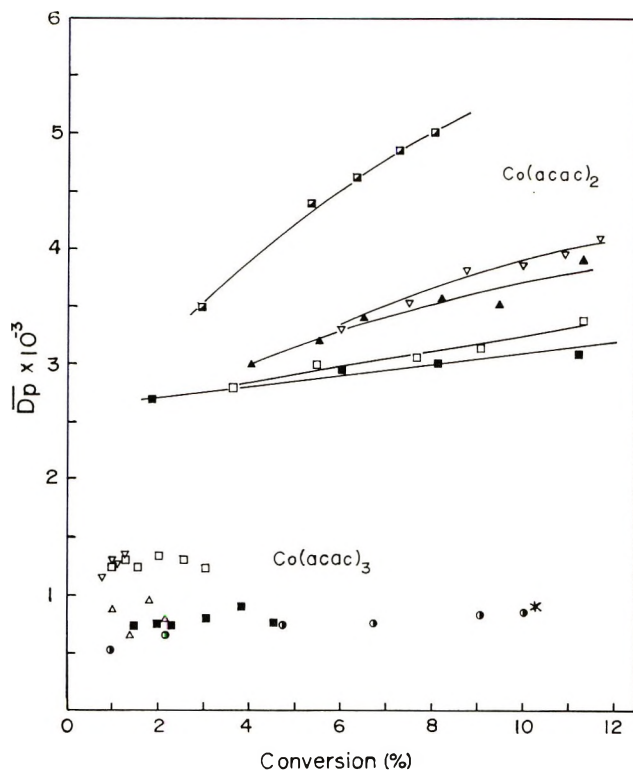


Fig. 6. Dependence of degree of polymerization on conversion for polymerization of MMA in benzene initiated by Co salt-*t*-Bu HPO: (■) 40°C; (▼) 45°C; (▲) 50°C; (□) 55°C; (■) 60°C; (●\*)  $\text{Co}(\text{acac})_3$  50°C, 54 hr, DP 840.

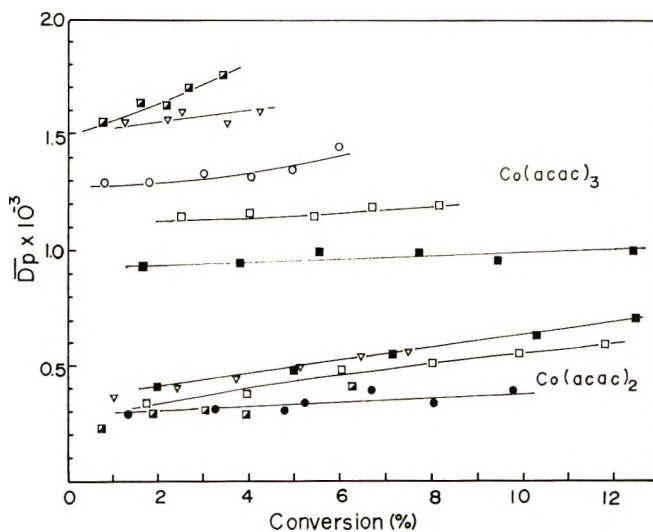


Fig. 7. Dependence of degree of polymerization on conversion for the polymerization of MMA in dioxane initiated by Co salt-DOX IPO: (□) 40°C; (▼) 45°C; (●) and (○) 50°C; (□) 55°C; (■) 60°C.

markedly with decrease in hydroperoxide concentration, and at concentrations lower than  $1.23 \times 10^{-3}$  mole/l. it increases with increasing conversion, although at  $1.04 \times 10^{-2}$  mole/l. it scarcely increases with increasing conversion.

On the other hand, with the  $\text{Co}(\text{acac})_2$ -*t*-Bu HPO initiating system, the degree of polymerization is not affected markedly by either hydroperoxide concentration and conversion.

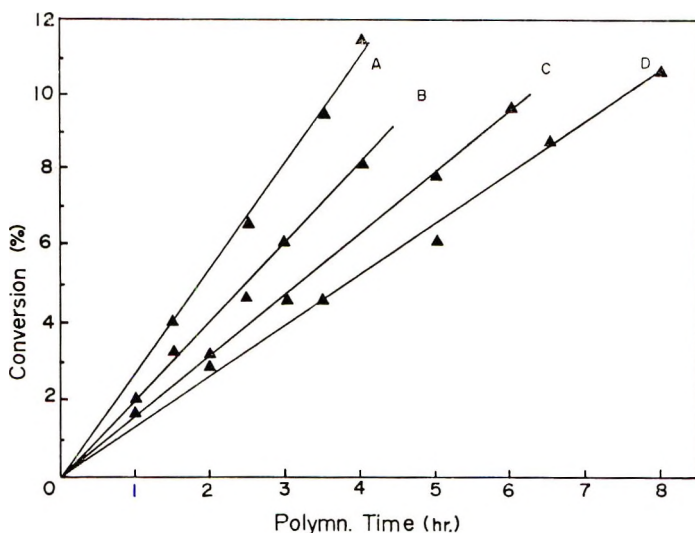


Fig. 8. Effect of hydroperoxide concentration on conversion in the system  $\text{Co}(\text{acac})_2$ -*t*-Bu HPO with MMA: (A)  $1.14 \times 10^{-2}$  mole/l.; (B)  $5.12 \times 10^{-3}$  mole/l.; (C)  $1.10 \times 10^{-3}$  mole/l.; (D)  $5.56 \times 10^{-4}$  mole/l.

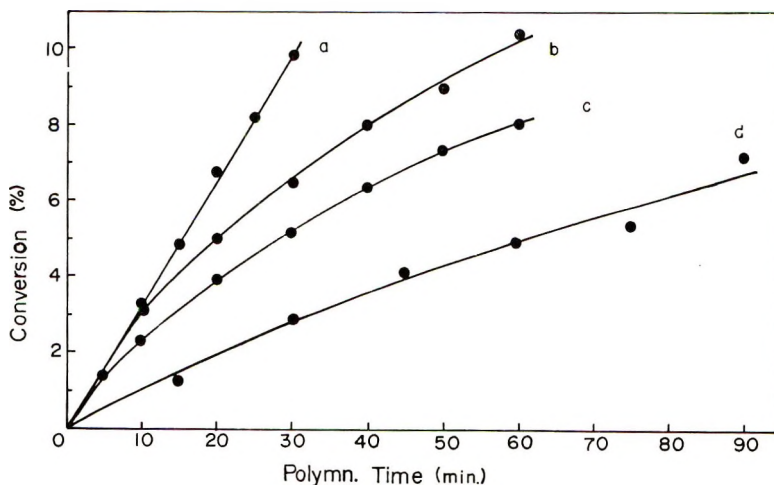


Fig. 9. Effect of hydroperoxide concentration on conversion in the system  $\text{Co}(\text{acac})_2$ -DOX HPO with MMA: (a)  $1.04 \times 10^{-2}$  mole/l.; (b)  $7.03 \times 10^{-3}$  mole/l.; (c)  $1.23 \times 10^{-3}$  mole/l.; (d)  $4.31 \times 10^{-4}$  mole/l.

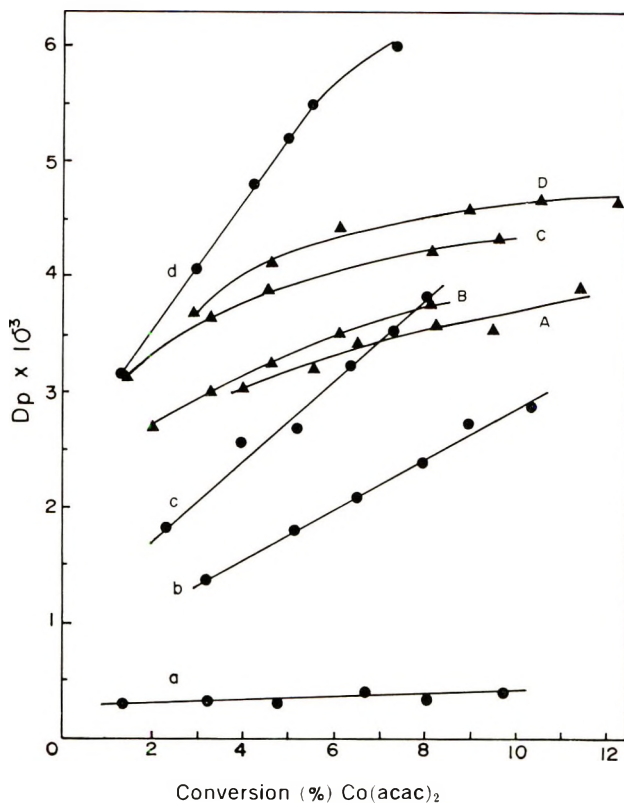


Fig. 10. Relation between degree of polymerization and conversion of MMA: (A) *t*-Bu HPO,  $1.14 \times 10^{-2}$  mole/l.; (B) *t*-Bu HPO,  $5.12 \times 10^{-3}$  mole/l.; (C) *t*-Bu HPO,  $1.10 \times 10^{-3}$  mole/l.; (D) *t*-Bu HPO,  $5.56 \times 10^{-4}$  mole/l.; (a) DOX HPO,  $1.04 \times 10^{-2}$  mole/l.; (b) DOX HPO,  $7.03 \times 10^{-3}$  mole/l.; (c) DOX HPO,  $1.23 \times 10^{-3}$  mole/l.; (d) DOX HPO,  $4.31 \times 10^{-4}$  mole/l.

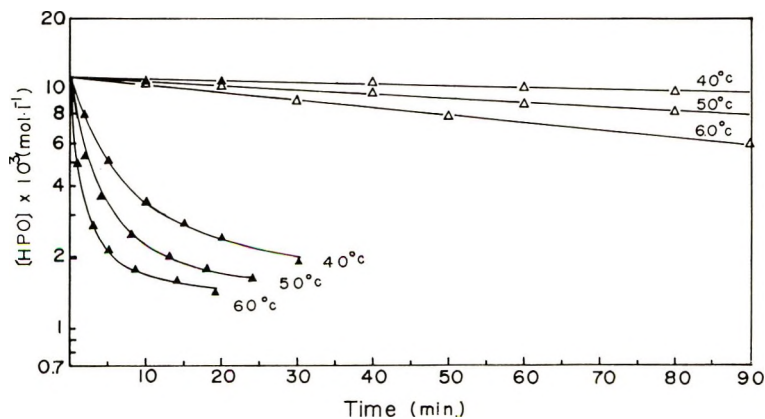


Fig. 11. Decomposition of *tert*-butyl hydroperoxide by  $\text{Co}(\text{acac})_2$  and  $\text{Co}(\text{acac})_3$ : (▲)  $\text{Co}(\text{acac})_2$ ; (△)  $\text{Co}(\text{acac})_3$ .



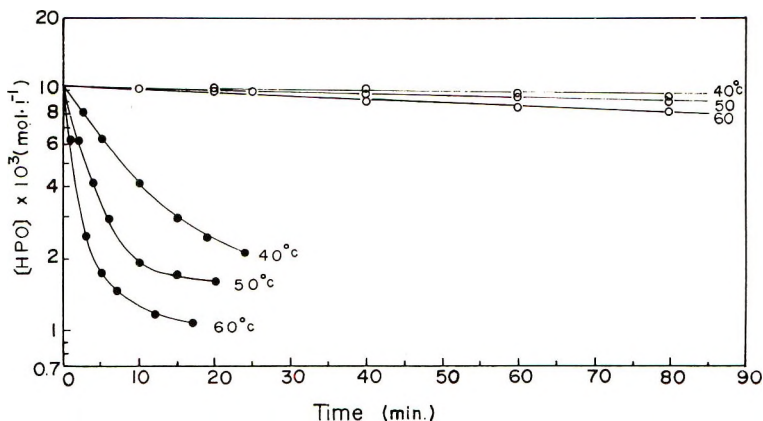


Fig. 12. Decomposition of dioxane hydroperoxide by  $\text{Co}(\text{acac})_2$  and  $\text{Co}(\text{acac})_3$ : (●)  $\text{Co}(\text{acac})_2$ ; (○)  $\text{Co}(\text{acac})_3$ .

To elucidate the results mentioned above, the  $\text{Co}(\text{II})$  or  $(\text{III})$  acetylacetonate-catalyzed decomposition of hydroperoxide was carried out under the same conditions as used for polymerization. The decomposition curves for *tert*-butyl hydroperoxide and dioxane hydroperoxide are shown in Figures 11 and 12, respectively. The marked difference in the polymerization rate among four initiating systems may be caused by various factors such as the decomposition rate of hydroperoxide, activity of primary radical, and so on.

As demonstrated in Figures 11 and 12, the divalent cobalt salt is much more effective for the decomposition of both *tert*-butyl hydroperoxide and dioxane hydroperoxide than trivalent cobalt salt. In cobaltous acetylacetonate almost more than 80% of hydroperoxide is decomposed within 30 min, while in cobaltic acetylacetonate only 10–20% of hydroperoxide is decomposed. This probably means that a large number of primary radicals are produced at the initial stage of polymerization in divalent systems. On the other hand, in trivalent systems primary radicals are produced slowly and continuously through the polymerization reaction. The explanations mentioned above are clearly demonstrated in the rate of polymerization (see Figs. 1–4 and Table I).

One should also notice that cobalt salt–dioxane hydroperoxide initiating systems are much more effective for the polymerization of methyl methacrylate than cobalt salt–*tert*-butyl hydroperoxide systems. A difference in reactivity of primary radicals between the ones produced from *tert*-butyl hydroperoxide and from dioxane hydroperoxide seems to play an important role in this. Primary radicals produced from *tert*-butyl hydroperoxide in benzene seem to be more reactive than those from dioxane hydroperoxide in dioxane. The degree of polymerization seems to suggest these facts. For example, in the  $\text{Co}(\text{acac})_2$ –*t*-Bu HPO system, a large number of primary radicals produced at the beginning of polymerization in benzene (Fig. 11) seem to be consumed relatively easily by interaction of primary radicals

themselves or polymer radicals of fairly low molecular weight. In other words, termination reactions may occur easily at the very beginning of polymerization, and a limited number of polymer radicals can continue growing and give polymers with higher degree of polymerization (see Fig. 6). In  $\text{Co}(\text{acac})_3$ -*t*-Bu HPO the supply of primary radicals persists through the polymerization, and they terminate growing polymer radicals to give polymers with lower degree of polymerization (Fig. 6).

On the other hand, in cobalt salt-dioxane hydroperoxide systems, primary radicals produced from dioxane hydroperoxide in dioxane seem to be rather less reactive than that from *tert*-butyl hydroperoxide. In other words, the consumption of primary radicals by interaction of primary radicals themselves or primary radicals and growing polymer radicals seems to be less probable, and the propagating reaction occurs relatively favorably in dioxane hydroperoxide systems. Therefore, in  $\text{Co}(\text{acac})_2$ -DOX HPO a large number of growing polymers is present in the system, which in turn causes higher possibility of termination reaction between growing polymer radicals to give polymers with lower degree of polymerization (Fig. 7), while in the  $\text{Co}(\text{acac})_3$ -DOX HPO system, the concentration of growing polymer radicals is lower than that of the  $\text{Co}(\text{acac})_2$ -DOX HPO system because of a slower rate of decomposition of hydroperoxide. Therefore the termination reaction between polymer radicals seems to be probable. As shown in Figure 7, the degree of polymerization in the  $\text{Co}(\text{acac})_3$ -DOX HPO system is higher than that in the  $\text{Co}(\text{acac})_2$ -DOX HPO system. Furthermore the propriety of the above explanation is confirmed by Figure 10, where the supply of primary radicals is extremely affected by the initial concentration of dioxane hydroperoxide. Namely, a remarkable increase in the degree of polymerization is clearly observed at lower concentration of dioxane hydroperoxide, i.e., at concentrations of hydroperoxide lower than  $1.23 \times 10^{-3}$  mole/l., the degree of polymerization increases with increasing both hydroperoxide concentration and conversion, while at higher hydroperoxide concentration,  $1.04 \times 10^{-2}$  mole/l., no appreciable change in the degree of polymerization is observed.

The decomposition rate of hydroperoxide and activity of primary radicals seem to be not enough to explain a remarkable difference in the rate of polymerization and the degree of polymerization among four initiating systems. However, the chain-transfer constant seems not to be a definitive factor, since it is 0.075 for benzene and 0.22 for dioxane at 80°C.<sup>7</sup>

In general, the activation energy for overall radical polymerization is shown in eq. (1):<sup>8</sup>

$$E_a = E_p + \frac{1}{2}(E_d - E_t) \quad (1)$$

where  $E_a$ ,  $E_p$ ,  $E_d$ , and  $E_t$  are activation energy for overall polymerization, for propagation, for the decomposition of initiator, and for termination, respectively. As shown in Table I, remarkable differences in overall activation energy among four initiating systems are also observed, and the higher the rate of polymerization, the lower the activation energy.  $E_a$

could be obtained by the decomposition of hydroperoxide. Therefore cobalt salt-catalyzed decomposition of hydroperoxide was carried out parallelly and the activation energies estimated for the decomposition of hydroperoxides. The results obtained are shown in Table II. The results, how-

TABLE II  
Decomposition Rate  $k$  and Activation Energy  $E_a$

	Temp, °C	<i>tert</i> -Butyl hydroperoxide		Dioxane hydroperoxide	
		Co(acac) <sub>2</sub>	Co(acac) <sub>3</sub>	Co(acac) <sub>2</sub>	Co(acac) <sub>3</sub>
$k \times 10^2$ , l./mole-min; [Co(acac) <sub>2</sub> ] or min <sup>-1</sup> : [Co(acac) <sub>3</sub> ] <sup>a</sup>	40	1.52	0.073	2.20	0.169
	50	3.90	0.161	5.00	0.407
	60	9.70	0.286	9.20	0.725
$E_a$ , kcal/mole		14.8	15.1	19.2	13.8

<sup>a</sup> In cobaltous acetylacetonate, second order reaction with respect to hydroperoxide; in cobaltic acetylacetonate, first-order reaction with respect to hydroperoxide.

ever, are inconsistent with the activation energies for the polymerization of methyl methacrylate unless  $E_p$  and  $E_t$  are changed by the initiating systems. Little information is available for the interpretation of polymerization mechanism.

Bamford,<sup>9,10</sup> Otsu<sup>11</sup> and others<sup>12,13</sup> reported that metallic acetylacetonates themselves could initiate vinyl polymerization; therefore one should consider the interactions between primary radicals, monomer, metallic ions, and polymer radicals which may affect the polymerization process. On these points further experiments are necessary to elucidate the detail reaction mechanism.

One should, however, notice that cobalt salt-dioxane hydroperoxide initiating systems are quite effective and unique for the vinyl polymerization. Further experiments on the various metallic salts and dioxane hydroperoxide and tetrahydrofuran hydroperoxide initiating systems will be published in future.

The authors wish to thank Professor Y. Ogiwara for his kind advice on these experiments.

## References

1. Z. Osawa, T. Shibamiya, and K. Matsuzaki, *Kogyo Kagaku Zasshi*, **71**, 552 (1968).
2. Z. Osawa, and T. Shibamiya, *J. Polym. Sci. B*, **6**, 721 (1968).
3. Z. Osawa, M. Suzuki, Y. Ogiwara and K. Matsuzaki, *Kogyo Kagaku Zasshi*, **73**, 110 (1970).
4. Z. Osawa, T. Shibamiya, Y. Ogiwara, and K. Matsuzaki, *Kogyo Kagaku Zasshi*, **73**, 115 (1970).
5. Z. Osawa, paper presented at the 17th Polymer Chemistry Meeting, Kyoto, Japan, 1969.
6. P. J. Flory, *Principles of Polymer Chemistry*, Cornell Univ. Press, Ithaca, N. Y., 1953 p. 312.
7. G. E. Ham, *Vinyl Polymerization*, Dekker, New York, 1967, p. 54.

8. F. W. Billmeyer, *Textbook of Polymer Science*, Interscience, New York, 1962, p. 287.
9. C. H. Bamford, G. C. Eastmond, and J. A. Rippon, *Trans. Faraday Soc.*, **59**, 2548 (1963).
10. C. H. Bamford and D. J. Lind, *Chem. Ind. (London)*, **1965**, 1627.
11. T. Otsu, N. Minami, and Y. Nishikawa, *J. Macromol. Sci. Chem.*, **2**, 902 (1968).
12. E. G. Kastning, H. Naarmann, H. Reis, and C. H. Berdning, *Angew. Chem.*, **77**, 313 (1965).
13. Y. Itakura, H. Tanaka, and H. Ito, *Kogyo Kagaku Zasshi*, **70**, 1227 (1967).

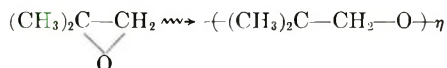
Received December 4, 1969.

## Radiation-Induced Polymerization of Isobutylene Oxide\*

R. S. BAUER and W. W. SPOONCER,  
*Shell Development Company, Emeryville, California 94608*

### Synopsis

In the absence of oxygen, liquid isobutylene oxide is polymerized by high energy radiation. The resultant polyethers may possess the same gross structures as those prepared by Lewis acid catalysis:



The reaction is characterized by (1) a small, apparent activation energy (2.7 kcal/mole), (2) a polymerization rate proportional to the first power of the dose rate, (3) inhibition by Lewis bases, and (4) moderate inhibition by free-radical scavengers. The molecular weights of the polymers increase with decreasing temperatures of polymerizations. These results will be discussed in terms of a cationic propagation mechanism.

### INTRODUCTION

The radiation-induced polymerization of certain epoxides has already been well documented.  $\gamma$ -Rays from  $^{60}\text{Co}$  have been used to initiate the polymerization of *o*-diepoxyethylbenzene,<sup>1</sup> 1,2,3,4-diepoxybutane,<sup>2</sup> and cyclohexene oxide.<sup>3</sup> Both styrene oxide and propylene oxide<sup>4</sup> have been polymerized with  $\gamma$ -rays and electrons from a linear accelerator. We now wish to describe the facile radiation-induced polymerization of isobutylene oxide and present evidence to support a proposed ionic propagation mechanism.

### EXPERIMENTAL

#### Isobutylene Oxide

Isobutylene oxide was prepared by slowly adding 1-chloro-2-methyl-2-propanol (obtained from the hydration of methallyl chloride with sulfuric acid<sup>5</sup> to potassium hydroxide pellets at such a rate that the temperature of the resulting distillate did not exceed 55°C. The resulting material was dried with calcium sulfate, heated under reflux overnight with potassium

\* Presented in part at the Pacific Conference on Chemistry and Spectroscopy, Anaheim, California, October 1969.

hydroxide, and fractionally distilled onto calcium hydride. Finally the product was heated under reflux for 24 hr over calcium hydride and then fractionally distilled again; bp 50.5°C (uncorrected).

### Sample Preparation

Irradiation ampoules were charged by transferring 8 ml of isobutylene oxide to a receiver on a vacuum line containing barium oxide. After the monomer had been in contact with the barium oxide for approximately 15 min it was transferred under reduced pressure to a weighed irradiation ampoule. The sample was degassed at low pressure using three freeze-thaw cycles, the tubes sealed, and the weight of sample determined.

Since the polymerization was sensitive to differences in the condition of the surface of the glass-irradiation ampoules, the ampoules were filled with chromic acid cleaning solution, cleaned by heating them on a steam bath for about 4 hr, washed several times in sequence with distilled water, once with dilute ammonium hydroxide, and finally with distilled water. The ampoules were stored at 110°C at least 24 hr before filling.

### Irradiation Procedure

The sealed ampoules and their contents were irradiated, while rotating in a vertical beam of x-rays and bremsstrahlung generated from a 3-Mev Van de Graff generator, beneath a slanted target. Temperature control was effected by immersing the ampoules in Dewar flasks containing Dry Ice-isopropanol ( $-80^{\circ}\text{C}$ ) or liquid nitrogen ( $-196^{\circ}$ ); the temperature between 20 and  $-80^{\circ}\text{C}$  was controlled by Dry Ice-cooled isopropanol. The doses were determined by previous ceric ion dosimetry. Dose-rate studies were conducted by attenuation to two different dose rates and irradiating to the same total dose. The  $G$  value refers to the number of molecules of monomer polymerized per 100 eV of energy absorbed.

The following is a typical example. The oxide (6.23 g, 0.087 mole) was irradiated at  $-4^{\circ}\text{C}$  to a total dose of  $1.71 \times 10^6$  rad at a dose rate of  $1.71 \times 10^7$  rad/hr. Volatile materials were removed under reduced pressure and the polymer (2.65 g, 41.7% conversion,  $G$  3031) dried under high vacuum at room temperature overnight. Its reduced specific viscosity in diphenyl ether ( $150^{\circ}\text{C}$ ) was 0.049 dl/g.

### Viscosity and Molecular Weight Determinations

Viscosity measurements were carried out in diphenyl ether at  $150^{\circ}\text{C}$ . These are reported as the reduced specific viscosity ( $\eta_{sp}/c$ ) and were run at a polymer concentration of 0.30 g/100 ml of solvent. The molecular weights of three samples were determined by light-scattering measurements in diphenyl ether at  $150^{\circ}\text{C}$ . A plot (Fig. 1) of the reduced specific viscosity versus the weight-average molecular weight is linear over the range investigated.

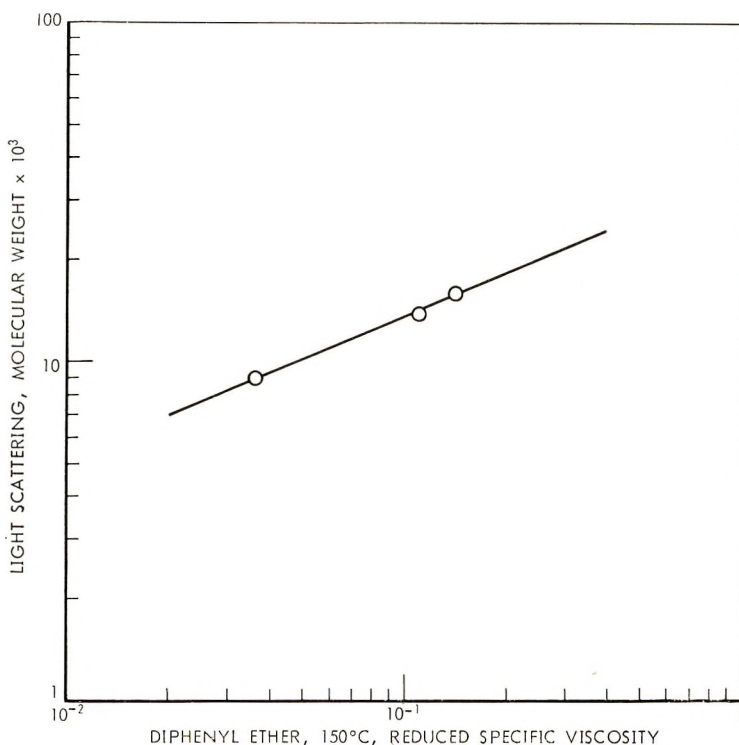


Fig. 1. Reduced specific viscosity of poly(isobutylene oxide) vs. molecular weight.

## RESULTS

As can be seen from Table I, the  $G$  for polymerization of isobutylene oxide, over the temperature range studied, increases with increasing temperature of polymerization. An Arrhenius plot (Fig. 2) of these data ob-

TABLE I  
Effect of Dose Rate on the Polymerization of Isobutylene Oxide<sup>a</sup>

Temp, °C	Dose rate, rad/hr	Yield, %	$G$ value	$\eta_{sp}/c$
3-6	$1.71 \times 10^7$	42.4	3300	0.032
3-6	$4.27 \times 10^6$	56.8	4420	0.035
-4	$1.71 \times 10^7$	42.4	3031	0.049
-4	$4.27 \times 10^6$	40.3	3240	0.067
-20	$1.71 \times 10^7$	33.7	2620	0.039
-20	$4.27 \times 10^6$	33.5	2610	0.062
-40	$1.71 \times 10^7$	20.4	1470	0.057
-40	$4.27 \times 10^6$	18.2	1410	0.084
-50	$1.71 \times 10^7$	19.0	1470	0.062
-50	$4.27 \times 10^6$	20.2	1540	0.112
-78	$1.71 \times 10^7$	2.87	223	0.138
-78	$4.27 \times 10^6$	3.79	295	0.138

<sup>a</sup> Total dose,  $1.17 \times 10^6$  r.e.d.

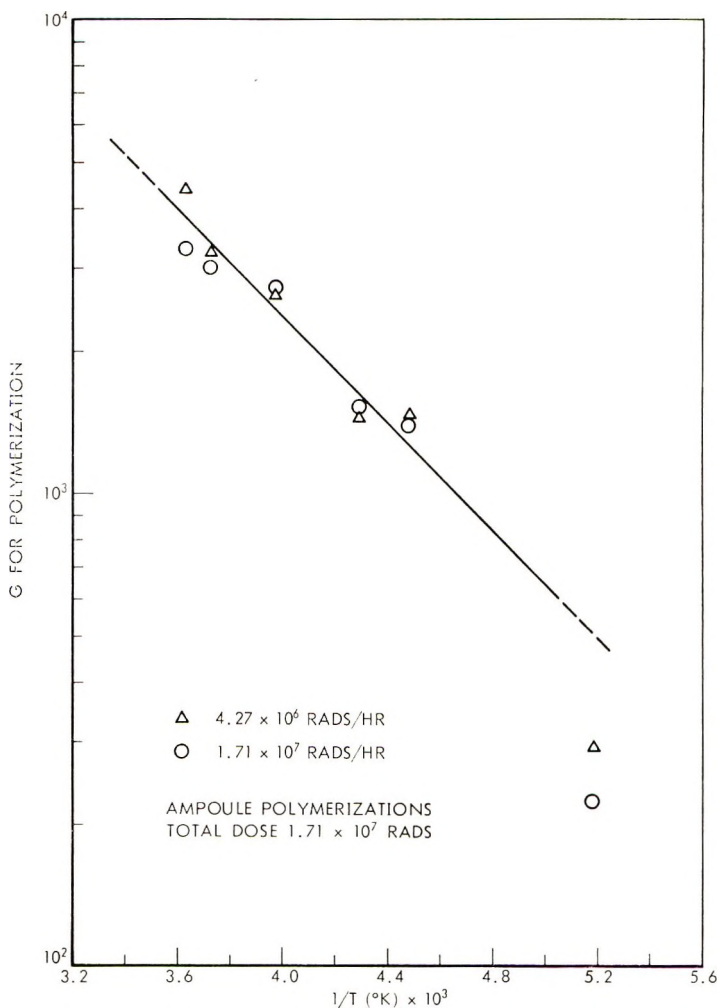
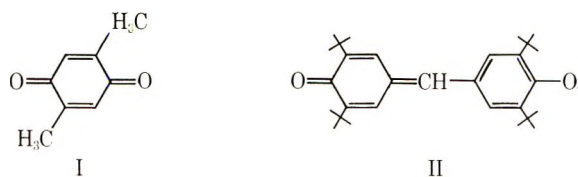


Fig. 2. Rate of isobutylene oxide polymerization by bremsstrahlung vs. temperature of reaction between 60 and  $-80^{\circ}\text{C}$ .

tained at two different dose rates to the same total dose, shows good linearity with an apparent overall activation energy of 2.7 kcal/mole in the temperature range  $-40^{\circ}\text{C}$  to  $6^{\circ}\text{C}$ . Since isobutylene oxide solidifies below  $-60^{\circ}\text{C}$ , the observed discontinuity between  $-50^{\circ}\text{C}$  and  $-78^{\circ}\text{C}$  may be due to the difference in the physical state of the monomer. In addition, it was observed, over the temperature range examined, that the  $G$  value for polymerization appears to be essentially constant over a tenfold difference in total dose delivered—that is, the conversion is linear with dose (Table II).

From the data in Table III it is noted that, although the free-radical scavengers 2,5-dimethylquinone (I) and galvinoxyl (II) slightly inhibit the radiation-induced polymerization of isobutylene oxide, inhibition is not





significant when compared with the effect of Lewis bases (Table IV). The major effect of the free-radical inhibitors is to cause an increase in molecular weight in their presence, suggesting an inhibition of radiation-induced free radical chain degradation.

TABLE II  
Effect of Total Dose on the Radiation-Induced Polymerization of Isobutylene Oxide

Temp, °C	Dose, rad	Dose rate, rad/hr	Conversion, %	G value
-40	$1.71 \times 10^6$	$1.71 \times 10^7$	20.4	1470
-40	$1.71 \times 10^6$	$4.27 \times 10^6$	18.2	1410
-40	$3.33 \times 10^5$	$2.18 \times 10^6$	3.3	1301
-40	$1.67 \times 10^5$	$2.18 \times 10^6$	2.1	1695

TABLE III  
Effect of Free-Radical Inhibitors on the Radiation-Induced Polymerization of Isobutylene Oxide<sup>a</sup>

Inhibitor, wt-%	Temp, °C	Yield, %	G value	$\eta_{sp}/c$
1.0 <sup>b</sup>	0 to -5	40.0	2035	0.16
1.0	-20	4.6	358	0.067
1.0	-20	10.0	796	0.067
1.0	-50	6.5	503	0.10
1.0	-50	4.9	384	0.10
1.0	-78	2.2	174	0.13
0.1	0	20.1	1570	0.086
0.1	-20	5.4	423	0.065
0.1	-40	9.7	755	0.13
0.1	-78	5.2	400	0.14
1.0 <sup>c</sup>	0 to -5	6.6	512	0.083

<sup>a</sup> Radiation: x-rays  $1.71 \times 10^6$  rads at  $1.71 \times 10^7$  rads/hr.

<sup>b</sup> 2,5-Dimethylbenzoquinone unless otherwise indicated.

<sup>c</sup> Galvinoxyl.

To gain some insight into the mechanism of inhibition by methanol isotopic alcohol (as  $^{14}\text{CH}_3\text{O}^3\text{H}$ ) was irradiated with isobutylene oxide. It was found that ca. 4 equivalents of carbon (as methoxyl) entered the polymer chain, based on a weight-average molecular weight of 10,000 (probably on the order of one methoxyl per number-average molecular weight, i.e., one per molecule). The fate of the hydrogen is unknown.

TABLE IV  
Effect of Lewis Bases on the Radiation-Induced Polymerization of Isobutylene Oxide

Lewis base	Temp, °C	Yield, %	G value
Blank	-4	42.4	3031 <sup>a</sup>
Dimethylformamide, ca. 1.0%	-4	0.26	29 <sup>a</sup>
Triethylamine, ca. 1.0%	-4	0.037	20 <sup>a</sup>
Blank	-30	45.0	755 <sup>b</sup>
Methanol, ca. 5 mole-%	-30	0.51	8.6 <sup>b</sup>

<sup>a</sup>  $1.71 \times 10^6$  rad at  $1.71 \times 10^7$  rad/hr.

<sup>b</sup>  $8 \times 10^6$  rad at  $5.48 \times 10^6$  rad/hr.

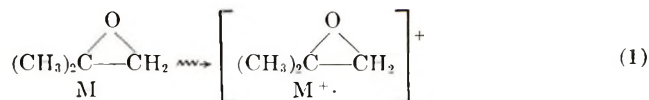
## DISCUSSION

The data clearly delineate a cationic mechanism for the radiation-induced polymerization of liquid isobutylene oxide. A low activation energy indicates: a low energy for initiation and termination relative to that for propagation; a *G* value independent of dose rate at any given temperature, a rate dependent on the first power of the dose rate; a *G* value independent of total dose, therefore a conversion which is linear with dose; very marked inhibition by Lewis bases and only moderate inhibition by free radical scavengers.

The radiation-induced polymerizations of several solid epoxides have been diagnosed as proceeding via cationic propagations. In general, the rates of these polymerizations are much faster in the solid than in the liquid state and apparent activation energies in the solid state are negative. Propylene oxide<sup>4</sup> polymerizes cationically only in the presence of an added substrate in the glassy state. 1,2,3,4-Diepoxybutane<sup>2</sup> polymerizes cationically with an activation energy of 0.4 kcal/mole. Cyclohexene oxide<sup>3</sup> is polymerized in the liquid state ionically with an activation energy of -2 kcal/mole.

A plausible mechanism in the polymerization of isobutylene oxide is as shown in eqs. (1)-(5).

Initiation:



Propagation:



Chain Transfer:



Termination:



Inhibition and Termination:



Initiation could occur by ion-radical formation;\* stabilization of the growing polymer chain would be enhanced by the formation of a tertiary carbonium ion, solvation of which, in the liquid phase, could be by monomer. Termination could occur by electron recombination (first-order process) followed by proton elimination and hydroxyl-endgroup formation. Inhibition by Lewis bases, triethylamine and dimethylformamide, may be the result of electron donation to growing polymer chain or protonation of these bases by the polymer cation. The incorporation of  $^{14}\text{CH}_3\text{O}^-$  into the polymer suggests methoxyl endgroups have resulted with proton liberation from the methanol.

The authors gratefully thank Mr. E. R. Bell and Dr. C. D. Wagner for their helpful suggestions and Mr. A. D. Jeong and Mr. C. T. Alwine for their assistance in the experimental part of this work.

### References

1. C. Aso and Y. Sita, *Makromol. Chem.*, **73**, 141 (1964).
2. C. F. Parrish and D. E. Harmer, *J. Polym. Sci. A-1*, **5**, 1015 (1967).
3. D. Cardischi, A. Mele and R. Rufa, *Trans. Faraday Soc.*, **64**, 2794 (1968).
4. Y. Tabota, Y. Fujita, and K. Oshima, *J. Polym. Sci. B*, **6**, 715 (1968).
5. J. Burgin and G. Hearne, *Ind. Eng. Chem.*, **53**, 385 (1941).

Received February 20, 1970

\* A referee has called to the authors attention that a chain transfer to monomer is in part probably responsible for initiation. He points out this is indicated by the data in Table I. In the absence of chain transfer, since  $G_{\text{initiation}} = G(-\text{monomer})/\text{DP}$ , the data at  $-20^{\circ}\text{C}$  would yield an estimate of  $G_{\text{initiation}}$  of approximately 15. This must imply that not all chains are not directly initiated by radiation.

## Polymerization of *cis*- and *trans*-Cinnamitriles by Anionic Catalysts

YOSHIAKI KOBUE, TAKAYUKI FUENO,\* and  
JUNJI FURUKAWA, *Department of Synthetic Chemistry, Kyoto  
University, Yoshida Kyoto, Japan*

### Synopsis

*cis*- and *trans*-cinnamitriles were polymerized in the presence of various anionic catalysts such as Grignard reagent, alkali metal naphthalenes, and calcium zinc tetraethyl. It was found that both monomers undergo concurrent geometrical isomerization as well as polymerization. Investigation on the calcium zinc tetraethyl catalyst showed that the *trans*-nitrile had polymerizability noticeably greater than that of the *cis* isomer. Polymers resulting from these isomeric monomers had different microstructures. These results seem to be interpretable in terms of the four-centered coordination model of the transition state.

### INTRODUCTION

In a previous communication,<sup>1</sup> we reported on anionic polymerizations of crotonic ester and crotonitrile with particular attention to the relative reactivities of each pair of geometrical isomers. The main feature revealed was that the *trans* isomer was far more amenable to polymerization in the presence of stereospecific anionic catalysts. In view of the lack of information concerning the structure-reactivity relationships in anionic polymerizations, investigations of this sort may be of some value to understanding the mechanism of anionic chain propagation, especially with regard to the stereo-controlling action of the catalysts involved.

In this paper we will deal with the relative reactivities of *cis*- and *trans*-cinnamitriles under anionic polymerization conditions. It has been found that both the *cis*- and *trans*-nitriles more or less easily undergo geometrical isomerization in the presence of various anionic polymerization catalysts and that the *trans* isomer is more polymerizable than the *cis* isomer. Calcium zinc tetraethyl allowed the *cis* and *trans* monomers to enter into different types of stereoregular polymers.

\* Present address: Faculty of Engineering Science, Osaka University, Toyonaka, Osaka, Japan.

## EXPERIMENTAL

### Materials

The *cis* and *trans* isomers of cinnamionitrile were prepared by the condensation of benzaldehyde with an equimolar amount of cyanoacetic acid, followed by decarboxylation in the presence of pyridine.<sup>2</sup> By fractional distillation through an 80-cm column under reduced pressure, these were separated into the *cis* isomer, bp 115°C/12 mm, and the *trans* isomer, bp 128°C/12 mm. These were redistilled under nitrogen immediately before use. Vapor-phase chromatography (VPC) showed that the isomeric purities of these monomers were no less than 99%.

Toluene, diethyl ether, 1,4-dioxane, and tetrahydrofuran (THF) were purified by ordinary methods and dried over sodium dispersion in the presence of benzophenone ketyl under nitrogen.

Calcium zinc tetraethyl complex (CaZnEt<sub>4</sub>) was prepared from granulated calcium metal and diethylzinc in toluene according to Gilman.<sup>3</sup> Since the complex was sparingly soluble in toluene, the catalyst was used as a suspension in toluene. *n*-Butylmagnesium bromide was prepared by the standard method in diethyl ether. Di(*n*-butyl)magnesium was obtained from the above Grignard solution by adding dioxane followed by filtration through a sintered glass filter.<sup>4</sup> Alkali metal naphthalenes (lithium, sodium, and potassium) were prepared from equimolar amounts of metal and naphthalene in THF.

### Polymerization Procedure

A 12-ml portion of monomer solution in toluene was placed in a glass-stoppered flask of ca. 50 ml content with a side arm for nitrogen inlet. After the mixture was thermostatted at 25.0°C, a 0.3-ml portion of CaZnEt<sub>4</sub> suspension in toluene was introduced by use of a syringe under magnetic stirring, and the reaction started. The catalysts used in this study included the alkali metal naphthalenes, di(*n*-butyl)magnesium, and *n*-butylmagnesium bromide. Diethyl ether and tetrahydrofuran were also used as solvents. In all experiments, the initial concentrations of monomer and catalyst were 0.5 and  $2.5 \times 10^{-2}$  mole/l, respectively. The polymerization temperature was 25°C, unless otherwise noted. After a specified time of reaction, the reaction mixture was poured into a methanolic hydrochloric acid solution. The resulting polymer was filtered, washed several times with methanol containing a small amount of hydrochloric acid, and then dried *in vacuo* at room temperature.

### Kinetic Measurements

The reaction was conducted as described above. At specified intervals of time, a small portion of the reaction mixture was sampled with a syringe, and a small amount of methanolic hydrochloric acid was added to the aliquot in order to stop the reaction. The residual monomers, both *cis* and *trans*, were determined by VPC. Tetralin (12 vol-%) was used as internal

standard. A Yanagimoto gas chromatograph, Model GCG 550 T, was used. A 2.25 m  $\times$  3 mm column packed with 30% poly(ethylene glycol) 20 M on Celite 545 (80–100 mesh) was operated at 180°C with hydrogen as carrier gas. Peak integration was carried out by use of a Kimura Denshi electronic integrator, Model E-2A. It was found by calibration that the internal standard method was sufficient for linear correlation of the obtained peak areas to the isomer concentrations.

## RESULTS

### Polymerization and Isomerization

The courses of reaction of each of the *cis* and *trans* nitriles were followed by gas-chromatographic analysis for several catalyst–solvent systems. It

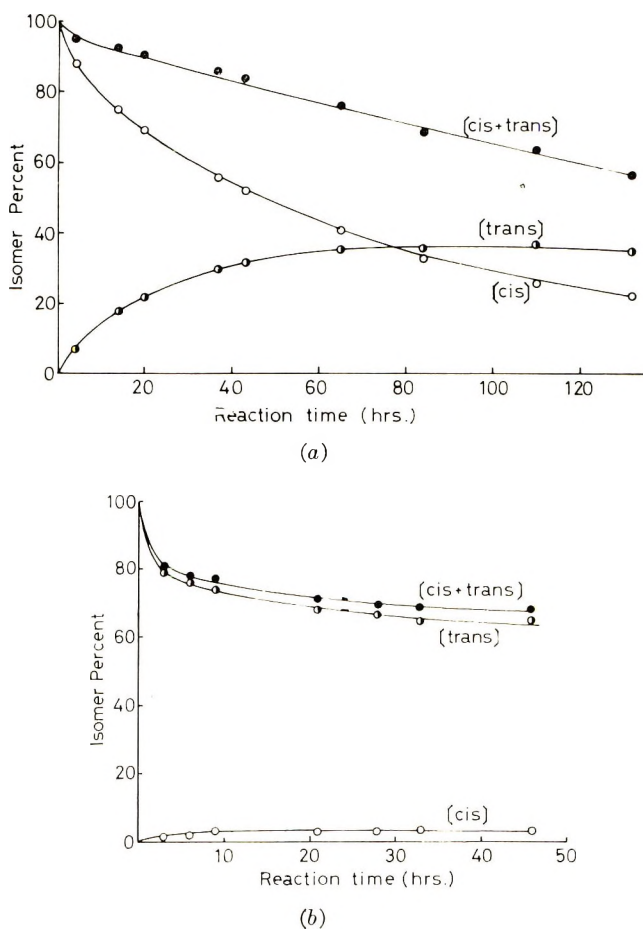
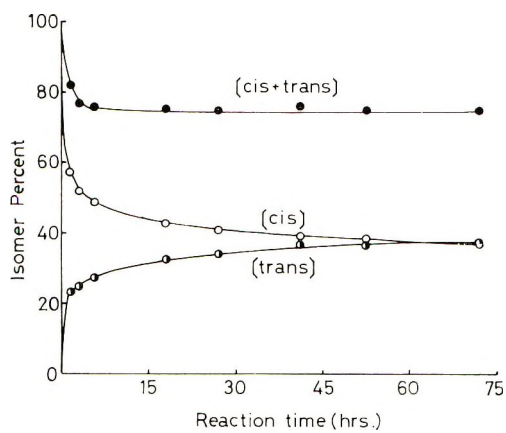
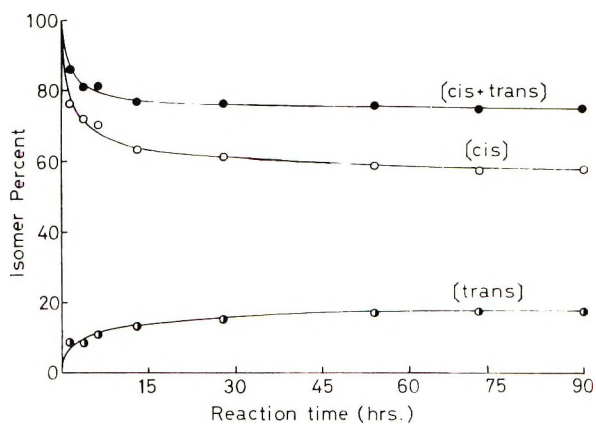


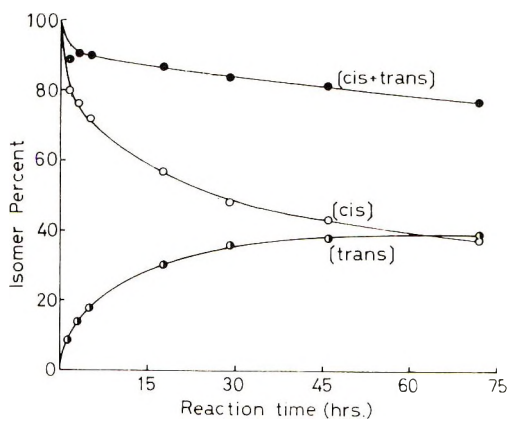
Fig. 1. Reaction mode of cinnamonitriles: (a) reaction of *cis*-cinnamonitrile with  $\text{CaZnEt}_4$  in toluene at 25.0°C; (b) reaction of *trans*-cinnamonitrile with  $\text{CaZnEt}_4$  in toluene at 25.0°C.



(a)



(b)



(c)

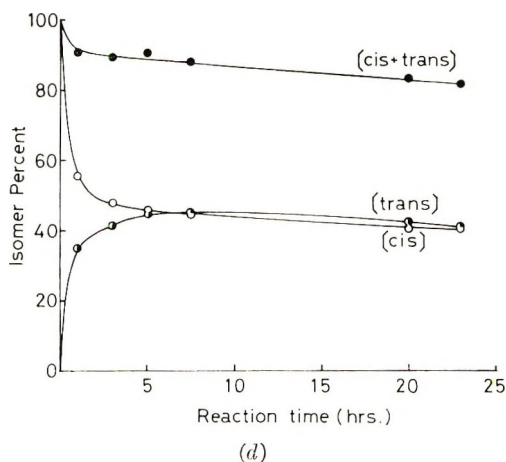


Fig. 2. Reaction mode of cinnamitriles: (a) *cis*-cinnamitrile with  $n\text{-Bu}_2\text{Mg}$  in toluene at  $25.0^\circ\text{C}$ ; (b) *cis*-cinnamitrile with Li naphthalene in THF at  $25.0^\circ\text{C}$ ; (c) *cis*-cinnamitrile with Na naphthalene in THF at  $25.0^\circ\text{C}$ ; (d) *cis*-cinnamitrile with K naphthalene in THF at  $25.0^\circ\text{C}$ .

was found that the concurrent polymerization and isomerization reactions occurred in all the cases investigated.

The results for the case of the calcium zinc tetrachethyl-toluene system are graphically shown in Figure 1. At the final stage of reaction, the residual monomer contained predominantly the *trans* isomer, regardless of whether the reaction had been started with pure *cis* or *trans* monomer. It is apparent from Figure 1 that the *cis* monomer is far more subject to isomerization than its *trans* isomer.

The reaction in other catalyst-solvent systems was investigated only for the *cis*-nitrile. The results are shown graphically in Figure 2. The catalyst systems investigated included di(*n*-butyl)magnesium (Fig. 2a),

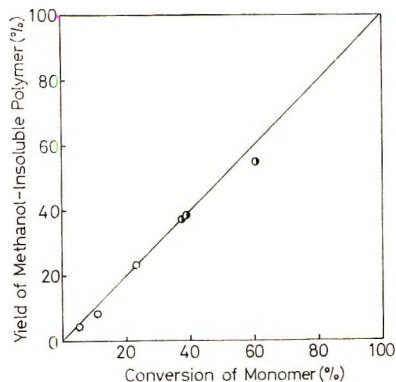


Fig. 3. Plots of the conversions of monomer vs. the percentage yields of methanol-insoluble polymers formed: (O) starting monomer *cis*; (●) starting monomer *trans*. Catalyst,  $\text{CaZnEt}_4$ ; solvent, toluene; polymerization temperature, room temperature.



lithium naphthalene (Fig. 2*b*), sodium naphthalene (Fig. 2*c*), and potassium naphthalene (Fig. 2*d*). These classes of catalyst have been found to induce isomerization of the *cis* monomer to its *trans* isomer at quite an early stage of the reaction, thus invalidating any comparison of the relative reactivity of geometrical isomers.

### Relative Polymerizability

In order to compare relative reactivities of *cis* and *trans* isomers, calcium zinc tetraethyl was chosen as catalyst, because of its relatively large ability of inducing polymerization compared with isomerization reaction and of its high stereocontrolling ability in polymerizations of polar olefins.<sup>5-8</sup>

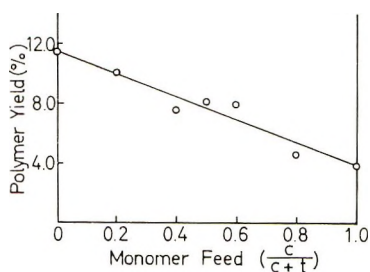


Fig. 4. Effect of isomer composition on polymer yield in toluene at 25.0°C. Polymerization time, 1 hr.

In Figure 3 the monomer conversions obtained by VPC analysis are plotted against the percentage yields of methanol-insoluble polymers which resulted from polymerizations of initially pure *cis* and *trans* monomers by the action of  $\text{CaZnEt}_4$  as catalyst. It may be seen in Figure 3 that the polymer yields are in essential agreement with the consumption of monomer. This observation indicates that no side reaction other than polymerization and isomerization is appreciable under the experimental conditions used here.

Comparison of the data in Figures 1*a* and 1*b* indicates that the *trans* monomer is more amenable to polymerization than is the *cis* isomer. In order to make this point more convincing, several monomer mixtures, in which the starting isomer composition was varied, were subjected to polymerization for 1 hr under identical conditions. The polymer yields observed in these comparative experiments are plotted against the isomer composition in Figure 4. It is evident from Figure 4 that the *trans* isomer has a higher polymerizability than the *cis* isomer; the polymer yield decreases almost linearly with increasing *cis* content in the monomer feed.

### Polymer Structure

Figure 5 shows the infrared absorption spectra of the low-conversion *cis-trans* copolymers which resulted from the monomer mixtures of various compositions. The increase in the content of *cis* isomer causes continuous

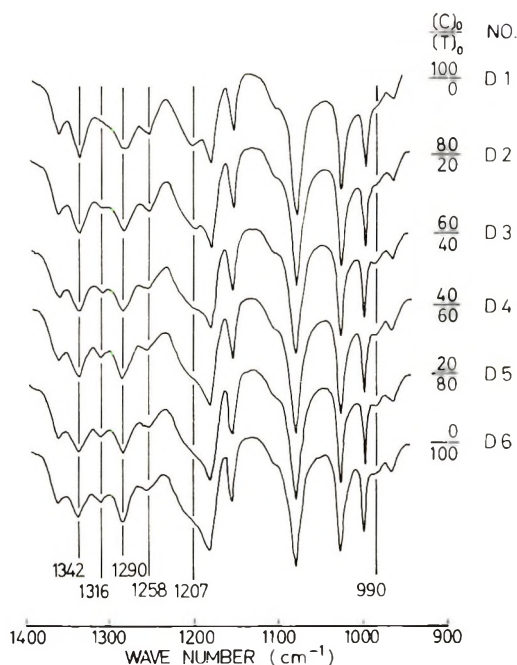


Fig. 5. Infrared spectra of polycinnamitriles prepared from various isomer compositions. Polymerization time, 1 hr.

increases of the absorptions at 1342, 1258, and 1207  $\text{cm}^{-1}$  and decreases of those at 1316, 1290, and 990  $\text{cm}^{-1}$ . This fact suggests that the copolymer resulting from *cis* and *trans* isomers have different structures. The reasons for this difference will be discussed later.

The effect of isomerization on polymer structure is shown in Figure 6. The polymers obtained from the *trans* isomer show the identical spectral features at different conversions. In contrast, the spectra of the polymers obtained from the *cis* isomer exhibit apparent dependence on conversion; that is, the polymer obtained at low conversion (3.8%) has a spectrum definitely different from that of the polymers obtained from the *trans* isomer, whereas at high conversions, such differences become relatively immaterial.

The above observations may be interpreted as follows. When polymerization of the *cis* monomer occurs, the polymer produced at earlier stages of polymerization consists exclusively of the *cis* monomer units. As polymerization proceeds, however, the monomer composition gradually changes on account of the concurrent isomerization reaction, which permits the formation of polymers of increasing content of the *trans* monomer units. Thus, the *cis-trans* copolymer should contain a large fraction of *trans* monomer units at later stages of the polymerization. In the case of the polymerization of the *trans* isomer, such a variation in polymer structure should be very small because of its resistance to isomerization as well as its high polymerizability compared to the *cis* isomer.



Under the present polymerization conditions, the *trans* isomer is more reactive than the *cis*, as has already been described. This finding is compatible with our previous proposal that *trans* monomers should generally be more reactive than *cis* isomers in stereospecific anionic polymerization.<sup>1</sup> This requires greater stabilization of the *trans* isomers at the transition state, because their ground-state stabilities are not greatly different from those of the corresponding *cis* isomers.<sup>9,10</sup>

Various mechanisms have so far been proposed by many authors<sup>11</sup> for the stereospecific anionic polymerizations of acrylic esters and nitriles. In general, the interaction of catalyst with polymer end and with monomer is assumed to be the primary factor controlling the stereoregulation.

Figure 7 gives possible models of the transition states for the polymerizations of the *cis* and *trans* isomers, respectively. The alkyl group in the *cis* monomer (Fig. 7a) would make the transition state of the four-centered complex type energetically less favorable than in the case where the alkyl group is situated *trans* to the polar functional group X (Fig. 7b), especially when the catalysts are strongly coordinated to X. Thus, the observed relative reactivities seem to be explained satisfactorily in terms of the four-centered coordination model of the transition state, as was suggested previously for anionic polymerizations of crotonic ester and crotononitriles.<sup>1</sup>

### References

1. Y. Kobuke, J. Furukawa, and T. Fueno, *J. Polym. Sci. A-1*, **5**, 2701 (1967).
2. J. Ghosez, *Bull. Soc. Chim. Belg.*, **41**, 477 (1932).
3. H. Gilman, R. N. Meals, G. O'Donnell, and L. A. Woods, *J. Amer. Chem. Soc.*, **65**, 268 (1943).
4. C. R. Noller, *J. Amer. Chem. Soc.*, **53**, 635 (1931).
5. S. Inoue, T. Tsuruta, and J. Furukawa, *Makromol. Chem.*, **32**, 97 (1959).
6. Y. Nakayama, T. Tsuruta, J. Furukawa, A. Kawasaki, and G. Wasai, *Makromol. Chem.*, **43**, 76 (1961).
7. T. Makimoto, T. Tsuruta, and J. Furukawa, *Makromol. Chem.*, **50**, 116 (1961).
8. R. Fujio, T. Tsuruta, and J. Furukawa, *Makromol. Chem.*, **52**, 233 (1961).
9. P. Bruylants and A. Christiaen, *Bull. Soc. Chim. Belg.*, **34**, 144 (1925).
10. G. B. Kistiakowsky and W. R. Smith, *J. Amer. Chem. Soc.*, **58**, 2428 (1936).
11. T. Fujimoto, N. Kawabata, and J. Furukawa, *J. Polym. Sci. A-1*, **6**, 1209 (1968) and 22 references therein.

Received June 2, 1969

## Number of Crosslinked Monomer Units per Weight-Average Primary Chain at the Gel Point in the Emulsion Polymerization of 1,3-Dienes

L. E. DANNALS, *Uniroyal, Inc., Chemical Division,  
Naugatuck, Connecticut 06770*

### Synopsis

Without new assumptions, it is demonstrated that at the gel point in mercaptan-regulated, 1,3-diene emulsion polymerizations, the number of crosslinked monomer units per weight-average primary chain is larger than one. The divergence of this number from one increases as the nonrandomness of the crosslinked monomer units distribution and the heterogeneity of primary chain size increase. According to the available experimental data, this number ranges from 1.11 to 1.29. Crosslink density values and rate constants of crosslinking to propagation, which were calculated assuming this number to be one, are consequently increased. It is also demonstrated, for postulated systems, that this number may be larger or smaller than one, depending on the type of nonrandomness of the crosslinked monomer units distribution. In either case, the divergence of this number from one also increases as the nonrandomness of the crosslinked monomer units distribution and the heterogeneity of primary chain size increase.

### Introduction

The crosslinking reaction occurring during the mercaptan-regulated, emulsion polymerization of 1,3-dienes has been studied by Morton et al.,<sup>1-3</sup> who used the gelpoint method. Their creative work, both theoretical and experimental, included relative rate equations and constants of crosslinking to chain propagation for emulsion systems that were developed from a base by Flory<sup>4</sup> for homogeneous systems. The equations for emulsion systems indicate that the crosslink density, which is the fraction of polymerized monomer units involved in crosslinks, is almost independent of the extent of conversion of monomer to polymer. In Uniroyal, Inc., laboratories, however, the crosslink density of emulsion polybutadiene, determined by the use of radioactive mercaptan,<sup>5</sup> was found to be larger than that obtained using the gel point method.

In their determination of the crosslink density at the gel point, from which rate constants were calculated, Morton et al.<sup>1-3</sup> used the assumption that there is exactly one crosslinked monomer unit per weight-average primary chain at the gel point as indicated by Stockmayer.<sup>6</sup> This assumption requires that the crosslinked monomer units be randomly distributed. For homogeneous polymerization of 1,3-dienes, Flory,<sup>4</sup> using his relative

rate equation of crosslinking to propagation, showed that the polymer formed at higher conversions has a larger crosslink density than that formed at lower conversions. It was also indicated<sup>4</sup> that this nonrandomness in the crosslinked monomer units distribution would result in less than one crosslinked monomer unit per weight-average primary chain at the gel point, but that for ordinary purposes, this nonrandomness probably could be ignored up to 60–70% conversion. However, since this nonrandomness, according to the accepted mechanism of 1,3-diene crosslinking, depends only on the relative rate equation of crosslinking to propagation, it appeared that a study of the nonrandom distribution of crosslinked monomer units consequent to the rate equations for emulsion systems might give better agreement between radioactive mercaptan and gel point crosslink density results and make the latter method more nearly valid.

### Summary

There is always more than one crosslinked monomer unit per weight-average primary chain at the gel point in mercaptan-regulated, 1,3-diene emulsion systems. The number of such crosslinked units increases with increasing heterogeneity of primary chain size and, for butadiene only, with decreasing gel point conversion. These conclusions require no new assumptions.

At a given gel point conversion or final conversion, emulsion 1,3-diene polymer formed at lower conversions has a larger crosslink density than that formed at higher conversions. In a mercaptan-regulated, 1,3-diene emulsion system, the shorter primary chains have a larger crosslink density than the longer ones.

For the experimental data at hand, there are 1.11 to 1.29 crosslinked monomer units per weight-average primary chain at the gel point in mercaptan-regulated, 1,3-diene emulsion systems. This observation increases the relative rate constants of crosslinking to chain propagation and reduces the difference between radioactive mercaptan and gel point crosslink density results for polybutadiene by 22 and 32%.

If it is considered that mercaptan reacts in a homogeneous 1,3-diene system as it does in an emulsion system, there will be less than one crosslinked monomer unit per weight-average primary chain at the gel point. This number decreases with increasing heterogeneity of primary chain size or with increasing gel point conversion: at 60% conversion it can be less than 0.9.

It is shown, by means of a postulated, mercaptan-regulated system, that if the lower conversion polymer has the larger crosslink density, there will be more than one crosslinked monomer unit per weight-average primary chain at the gel point, but if the higher conversion polymer has the larger crosslink density, the number of such crosslinked units per weight-average primary chain at the gel point will be less than one. In either case, the divergence from one will increase with increasing heterogeneity of primary

chain size and with increasing deviation from random of the distribution of crosslinked monomer units.

### Assumptions

The assumptions and postulates previously advanced<sup>1-4,6,7</sup> are accepted here with a single exception: that there is exactly one crosslinked monomer unit per weight-average primary chain at the gel point in the mercaptan-regulated, emulsion polymerization of 1,3-dienes. Stockmayer's<sup>6</sup> expression for the appearance of gel, on which mathematical operations are performed to make it respond to nonrandom distribution of crosslinked monomer units, is necessary here. Flory's<sup>4</sup> mechanism for crosslinking in 1,3-diene polymerization, that indicates a crosslink is formed by the reaction of a growing chain with a residual double bond in previously formed polymer so that the crosslinked monomer units are distributed equally between the polymer being formed and that which has been formed, is used here. It is also assumed<sup>4</sup> that at the instant of formation of a crosslink, all polymerized monomer units have equal probability of being involved in the crosslink and that the fraction of polymerized monomer units that is involved in crosslinks is very small. Bardwell and Winkler's<sup>7</sup> contention that transfer with mercaptan is the main termination mechanism and that the mercaptan reaction is first-order with respect to chain propagation, as well as the relative rate equations of crosslinking to propagation for 1,3-diene emulsion systems, proposed and used by Morton et al.,<sup>1-3</sup> are considered valid. Two postulated systems are presented, without argument for their acceptance, to show how the number of crosslinked monomer units per weight-average primary chain at the gel point may vary, but no new assumptions are required for this paper as it applies to mercaptan-regulated, 1,3-diene emulsion systems.

### Conventions, Terms, Symbols, and Definitions

The following conventions, terms, symbols, and definitions are used in subsequent sections. Some of the symbols used here for a particular quantity differ from those used previously for that quantity.

When "moles" is used, the words, "per mole of monomer initially present in the system," should be appended.

Rate constant or rate equation, as applied to either the crosslinking or mercaptan reaction, mean a rate relative to chain propagation.

Chain(s) means primary chain(s) which are the polymeric structures that would exist if no crosslinking had taken place.

Units- $x$  means polymerized monomer molecules that are involved in crosslinks.

$V$  denotes the number of moles of polymerized monomer that is involved in crosslinks. For this quantity,  $\nu$  has been used elsewhere.

$P$  denotes the crosslink density, which is the ratio of moles of polymerized monomer involved in crosslinks to the total moles of polymerized monomer.

This ratio may apply to the whole system, certain size primary chains, or polymer formed at a particular conversion.  $\rho$  has been used for this quantity in previous work.

The gel point is that point in the course of a polymerization immediately before there is a finite probability of gel being present in the system. It is thus considered here that there is no gel in the system at the gel point. The course of a polymerization is usually followed by the fractional conversion of monomer to polymer. At the gel point the fractional conversion is called the gel point conversion.

$\alpha$  denotes the number of moles of polymerized monomer in the whole system and is thus the fractional conversion of monomer to polymer. Initially the conversion is zero,  $\alpha_0$ . The final or gel point conversion,  $\alpha_2$ , is constant for a particular polymerization. In consideration of previously accepted assumptions,  $\alpha_2$  should not exceed 0.6 for emulsion polymerizations or mercaptan-regulated systems. Furthermore, the necessary assumptions have not been established as applicable or not for polymerization in which the final conversion exceeds the gel point conversion. The use of  $\alpha_2 = 0.9$  in some of the figures is for expository reasons only. Conversion is sometimes expressed here as  $\alpha/\alpha_2$ , which is the fraction of the final or gel point conversion attained.

Random distribution of units- $x$  requires that the probability of a polymerized monomer molecule being involved in a crosslink be equal for all such molecules no matter in which category of all considered divisions of the system they are. This probability is  $P$ , the crosslink density. It is assumed here that at the instant of formation of a crosslink by a growing chain, all previously polymerized monomer molecules have equal probability of being involved in this crosslink. If the system at  $\alpha_2$  conversion is considered to be divided into categories according to the conversion at which the polymer was formed or according to the size of primary chains, it is found that the probability  $P$  differs among the categories, and this situation is called nonrandom distribution of units- $x$ . Deviation from random distribution of units- $x$  is larger or smaller as the difference between extreme values of  $P$ , for a family of categories, increases or decreases.

The purpose here, or present purpose, is to determine the calculated results without introducing an error of more than 0.004 of the value through the use of error terms or imperfections that are accepted here to simplify the mathematical expressions and allow a more general treatment of the various systems.

### Nonrandom Distribution of Units- $x$ with Respect to Conversion

The nonrandom distribution of units- $x$  with respect to the conversion at which the polymer is formed, will be demonstrated for emulsion polybutadiene. This procedure is essentially the same as that given<sup>4</sup> for the homogeneous, 1,3-diene systems. The proposed crosslinking rate equation for emulsion polybutadiene is<sup>1</sup>

$$dV/d\alpha = 2K(1 + 0.44\alpha) \quad (1)$$



in which  $K$  is the rate constant. Since half of the units- $x$  occur in the polymer being formed, these units- $x$ ,  $V_i$ , are formed at a rate given by half of eq. (1),

$$dV_i/d\alpha = K(1 + 0.44\alpha) \quad (2)$$

The other half of the units- $x$  appear in polymer previously formed, so that the rate at which these units- $x$ ,  $V_q$ , are formed is also given by half of eq. (1),

$$dV_q = K(1 + 0.44\alpha)d\alpha \quad (3)$$

Now consider the polymer formed during a brief interval at  $\alpha'$  conversion during which  $m$  moles of monomer polymerize. The units- $x$  which are acquired by the  $\alpha'$  polymer at the instant of its formation,  $V_i'$ , is given from eq. (2) as,

$$V_i' = m[dV_i/d\alpha]_{\alpha'} = mK(1 + 0.44\alpha') \quad (4)$$

Since it is assumed that units- $x$  that appear in the previously formed polymer are distributed at random at the instant of their formation, the units- $x$  acquired by any part of this polymer will be proportional to its weight fraction. Thus at any subsequent conversion,  $\alpha$ , the  $\alpha'$  polymer will acquire  $m/\alpha$  of the units- $x$  appearing in the previously formed polymer. It should be noted that the  $m/\alpha$ -based distribution introduces an imperfection since some of the polymerized units in both the  $\alpha'$  polymer and the whole system have been involved in crosslinks and thus have zero probability of participating in additional crosslinking reactions. A more nearly valid distribution would be based on the ratio of polymerized monomer units that are not units- $x$  in the  $\alpha'$  polymer to such polymerized monomer units in the whole system. This aspect of the random distribution assumption will be discussed later and here the  $m/\alpha$ -based distribution will be used, so that the rate at which the  $\alpha'$  polymer acquires units- $x$  after its formation is, from eq. (3),

$$dV_q' = mdV_q/\alpha = (mK/\alpha)(1 + 0.44\alpha)d\alpha \quad (5)$$

The total units- $x$ ,  $V_q'$ , acquired by the  $\alpha'$  polymer as the polymerization proceeds from  $\alpha'$  to the final conversion  $\alpha_2$ , is given by

$$V_q' = mK \int_{\alpha'}^{\alpha_2} (1/\alpha)d\alpha + 0.44mK \int_{\alpha'}^{\alpha_2} d\alpha \quad (6)$$

which becomes,

$$V_q' = mK(\ln \alpha_2 - \ln \alpha' + 0.44\alpha_2 - 0.44\alpha') \quad (7)$$

The total units- $x$  in the  $\alpha'$  polymer,  $V'$ , is equal to the sum of  $V_i'$  and  $V_q'$  and thus is found by adding eqs. (4) and (7):

$$V' = mK(1 + \ln \alpha_2 + 0.44\alpha_2 - \ln \alpha') \quad (8)$$

Then  $P_\alpha$ , the crosslink density of polymer formed at any conversion  $\alpha$  is found by dividing eq. (8) by  $m$  and changing  $\alpha'$  to  $\alpha$ ,

$$P_\alpha = V'/m = K(1 + \ln \alpha_2 + 0.44\alpha_2 - \ln \alpha) \quad (9)$$

The total units- $x$  in the system  $V_s$  at  $\alpha_2$  conversion is given by the definite integral of eq. (1) between  $\alpha_0$  and  $\alpha_2$ ,

$$V_s = 2K \int_{\alpha_0}^{\alpha_2} d\alpha + 2K(0.44) \int_{\alpha_0}^{\alpha_2} \alpha d\alpha \quad (10)$$

which becomes

$$V_s = 2K(\alpha_2 + 0.22\alpha_2^2) \quad (11)$$

The crosslink density of the system  $P_s$  at  $\alpha_2$ , is given by dividing eq. (11) by  $\alpha_2$ ,

$$P_s = V_s/\alpha_2 = K(2 + 0.44\alpha_2) \quad (12)$$

A term much used in subsequent argument  $P_{\alpha'}$  is defined as

$$P_{\alpha'} = P_{\alpha}/P_s \quad (13)$$

and is called the relative crosslink density. It is the crosslink density of polymer formed at  $\alpha$  conversion relative to the crosslink density of the whole system at the final conversion. For an emulsion polybutadiene system,  $P_{\alpha'}$  is found by dividing eq. (9) by eq. (12),

$$P_{\alpha'} = (1 + \ln \alpha_2 + 0.44\alpha_2 - \ln \alpha)/(2 + 0.44\alpha_2) \quad (14)$$

and, for later convenience, the constants of eq. (14) are combined,

$$P_{\alpha'} = (D - \ln \alpha)/E \quad (15)$$

From calculations of the crosslinking rate constants for emulsion systems of isoprene<sup>2</sup> and 2,3-dimethylbutadiene,<sup>3</sup> it can be deduced that the crosslinking rate equation for these systems is considered to be

$$dV/d\alpha = 2K/C \quad (16)$$

where  $C$  denotes the ratio [monomer]/[polymer] and is constant for a single polymerization. By argument similar to that above, it can be shown that, for these systems,

$$P_{\alpha'} = (1 + \ln \alpha_2 - \ln \alpha)/2 \quad (17)$$

For 1,3-diene homogeneous systems, the expression for  $P_s$  has been given.<sup>4</sup> For later convenience, the constants of this expression, other than the rate constant, will be combined and called  $J$ , which is defined by

$$P_s = K(-2/\alpha_2)[\alpha_2 + \ln(1 - \alpha_2)] = KJ \quad (18)$$

and since an expression for  $P_{\alpha}$  for 1,3-diene homogeneous systems is also available,<sup>4</sup>  $P_{\alpha'}$  for this system is,

$$P_{\alpha'} = [\alpha/(1 - \alpha) + \ln(1 - \alpha) - \ln(1 - \alpha_2)]/J \quad (19)$$

In Figure 1,  $P_{\alpha'}$  for emulsion polybutadiene obtained by using eq. (14) at  $\alpha_2$  values of 0.1 and 0.9 and  $P_{\alpha'}$  for 1,3-diene homogeneous systems obtained by using eq. (19) at  $\alpha_2$  values of 0.2 and 0.6 have been plotted

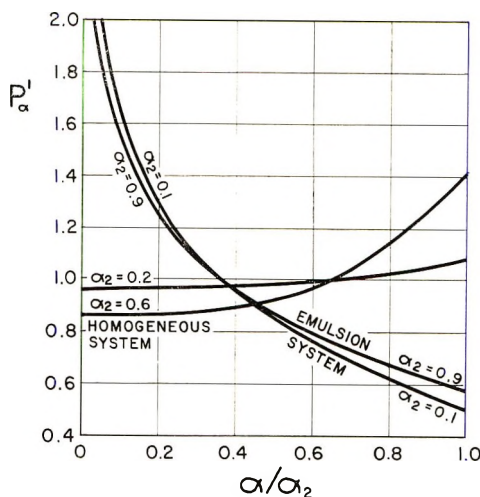


Fig. 1. Relative crosslink density of 1,3-diene polymer  $P'_\alpha$ , vs. the conversion at which the polymer is formed,  $\alpha/\alpha_2$ , the fraction of the final conversion attained, for the indicated  $\alpha_2$  values, according to eq. (14) for the emulsion system and to eq. (19) for the homogeneous system.

versus  $\alpha/\alpha_2$ , the fraction of the final conversion attained. It is thus a plot, for the two systems, of the relative crosslink density of polymer as a function of the conversion at which the polymer is formed. It also shows how the distribution of units- $x$  with respect to conversion deviates from random: if  $P'_\alpha$  were 1 for all values of  $\alpha/\alpha_2$ , the units- $x$  distribution would be random with respect to conversion. It should be noted that the two systems differ qualitatively in two respects: (a) the polymer that has the larger crosslink density is formed at the lower conversions in the emulsion system but at the higher conversions in the homogeneous system; and (b) as the final conversion  $\alpha_2$  increases, the distribution of units- $x$  becomes more nearly random for the emulsion system, but less nearly random for the homogeneous system. The emulsion system shows greater deviation from random for the units- $x$  distribution, at the indicated  $\alpha_2$  values, than does the homogeneous system. If eq. (17) for isoprene or 2,3-dimethylbutadiene emulsion polymerization were plotted in this figure, it would be very near the butadiene emulsion system plot for  $\alpha_2 = 0.1$ , but would show greater deviation from random for the units- $x$  distribution. The isoprene and 2,3-dimethylbutadiene emulsion systems would show no variation in the units- $x$  distribution with changes in  $\alpha_2$ .

For emulsion systems, eqs. (14) and (17) indicate that  $P'_\alpha$  becomes very large as  $\alpha$  approaches zero. There is a limit imposed by eq. (13), that  $P'_\alpha$  cannot exceed, since  $P_\alpha$  cannot exceed 1, at which value every polymerized monomer unit has been involved in a crosslink. These very large values of  $P'_\alpha$  in emulsion systems are ascribed to that aspect of the random distribution of units- $x$  assumption used in eq. (5), where this distribution is made

TABLE I  
Effect of the Number of Crosslinked Monomer Units per Weight-Average Primary Chain at the Gel Point on Experimentally Determined Crosslink Densities and Crosslinking to Propagation Rate Constants of Mercaptan-Regulated, 1,3-Diene Emulsion Systems

	2,3-Dimethylbutadiene																					
	Butadiene							Isoprene														
	60°C, 70°C, $r = r =$							60°C, 70°C, $r = r =$														
	40°C, $r = 4.32$	50°C, $r = 3.83$	60°C, $r = 3.26$	70°C, $r = 2.86$	80°C, $r = 2.49$	70°C, $r = 3.10$	80°C, $r = 2.70$	1	2	3	4	5	6	7	8	9	10	11	12	13	14	
Expt. No.	3.30	5.60	3.70	5.80	5.80	7.22	0.87	1.45	2.03	2.90	0.428	0.428	0.428	0.428	0.428	0.428	0.428	0.428	0.428	0.428	0.428	0.428
$R_0 \times 10^4$ , mercaptan charge <sup>a</sup>	0.46	0.60	0.38	0.57	0.40	0.50	0.40	0.50	0.50	0.64	0.45	0.49	0.32	0.47								
$\alpha$ , gel point conversion <sup>a</sup>	1.987	2.592	1.455	2.183	1.304	1.630	1.328	1.430	1.245	1.504	1.395	1.519	0.864	1.269								
$r\alpha_0$ , indicator of chain size heterogeneity	1.237	1.294	1.177	1.252	1.157	1.193	1.177	1.191	1.166	1.213	1.186	1.203	1.113	1.169								
$P_s \bar{Y}_s$ , number of crosslinked monomer units per weight-average chain <sup>b</sup>	2.25	2.54	3.30	3.10	4.60	4.69	0.694	0.935	1.27	1.47	0.305	0.284	0.368	0.370								
Crosslink density	2.78	3.29	3.88	3.88	5.32	5.60	0.817	1.114	1.48	1.78	0.362	0.342	0.410	0.433								
$P_s \times 10^4$ , assuming one cross-linked monomer unit per weight-average chain <sup>a</sup>	5.90	5.53																				
$P_s \times 10^4$ , by use of radioactive mercaptan <sup>c</sup>																						
Crosslinking to propagation rate constant	1.02	1.12	1.52	1.38	2.11	2.11	0.34	0.43	0.52	0.60	0.122	0.114	0.147	0.148								
$K \times 10^4$ , assuming one cross-linked monomer unit per weight-average chain <sup>a</sup>	1.26	1.45	1.79	1.73	2.44	2.52	0.40	0.51	0.61	0.73	0.145	0.137	0.164	0.173								
$K \times 10^4 = K^u P_s \bar{Y}_s$																						

<sup>a</sup> Literature data for butadiene,<sup>1</sup> isoprene,<sup>2</sup> and 2,3-dimethylbutadiene,<sup>3</sup> except that  $P_s^u$  for the latter two monomers has been calculated by taking the reciprocal of the given weight-average weight of primary chains.

<sup>b</sup> Calculated from the data given here by using eq. (41) for butadiene and eq. (43) for the other monomers.

<sup>c</sup> Interpolated results from Howland et al.<sup>5</sup> at equivalent number-average weight of primary chains.

according to the fraction of polymerized monomer units rather than the fraction of such units that are not units- $x$ . Although it is not apparent, the homogeneous system also suffers some distortion from this source.

For the present purpose, this imperfection does not appear to be important. From the experimental data of Table I, the lowest maximum value of  $P_{\alpha}'$  in an emulsion system is 1695. If  $\alpha_2$  is taken as 0.6 in eq. (14), the fraction of the total polymer that has high  $P_{\alpha}'$  values may be calculated and by integration of this equation, the fraction of the total units- $x$  in this polymer fraction may be determined. These results are given in Table II.

TABLE II

$P_{\alpha}'$	Fraction of total polymer having this or higher $P_{\alpha}'$ values	Fraction of total units- $x$ in this polymer fraction
5	$4.3 \times 10^{-5}$	$2.3 \times 10^{-4}$
10	$5.2 \times 10^{-10}$	$5.4 \times 10^{-9}$
100	$1.7 \times 10^{-98}$	$1.7 \times 10^{-96}$
1000	$2.0 \times 10^{-983}$	$2.0 \times 10^{-980}$

Thus if the units- $x$  from any of the above polymer fractions were distributed among the other polymer fractions in the system, there would be no detectable effect on the distribution according to the present purpose.

A more nearly valid expression for  $P_{\alpha}'$  for polyisoprene or poly-2,3-dimethylbutadiene can be derived by argument analogous to that of eqs. (1)–(14) by starting with eq. (16) and at the eq. (5) step, distributing units- $x$  according to the fraction of polymerized monomer units that are not units- $x$ . This is,

$$P_{\alpha}' = \left[ 1 + \frac{C - K}{K} (1 - e^{-[K/(C-2K)][-\ln(\alpha/\alpha_2)]}) \right] / 2 \quad (20)$$

At  $\alpha_0$ , eq. (20) shows a finite value of  $P_{\alpha}'$ , corresponding to  $P_{\alpha} = 1$ , and thus satisfies the accepted crosslinking mechanism. Since eq. (16) was originally applied to butadiene,<sup>1</sup> eq. (20) may be compared to eq. (17), for all the experiments described in Table I, to estimate the error introduced by the use of the latter expression. It can be demonstrated that for the available experimental data, eq. (17) misplaces 0.00024 or less of the total units- $x$ . Since the ultimate use of  $P_{\alpha}'$  here is to obtain an averaged integrated value of the function  $P_{\alpha}'e^{r\alpha}$  from  $\alpha_0$  to  $\alpha_2$ , it can be estimated for experiment 2 of Table I, which has the largest  $r\alpha_2$  value, that the use of eq. (17) rather than eq. (20) will introduce a fractional error of only 0.000015 in the integrated  $P_{\alpha}'e^{r\alpha}$  function. Thus the use of eqs. (14) or (17), which allow less involved and more general expressions than the more nearly valid eq. (20), is considered satisfactory for the present purpose.

### Nonrandom Distribution of Units- $x$ with Respect to Chain Size

Although the solution of the principal problem here does not require a determination of the relation between the crosslink density of chains and their size, some discussion of this nonrandomness is given to introduce terms that are essential to subsequent argument. Chains- $y$  means chains containing  $y$  molecules of polymerized monomer. Thus,  $y$  may be any positive integer, but in the expressions of this section, it is constant at some unspecified value. The weight fraction of chains- $y$  in the whole system at  $\alpha_2$  conversion  $\bar{W}_y$  is the ratio of moles of polymerized monomer in chains- $y$  to the total moles of polymerized monomer in the whole system. The instantaneous weight fraction of chains- $y$ ,  $W_{y\alpha}$ , is this same ratio for polymer formed during a brief interval at  $\alpha$  conversion.

To determine the crosslink density of chains- $y$  for the whole system at  $\alpha_2$  conversion, consider that the system is made up of a very large number of portions, each one of which contains  $\Delta\alpha$  moles of polymerized monomer and may be represented by a unique value of  $\alpha$ . It is important here and in subsequent argument to understand that the crosslink density of all polymer, including chains- $y$ , in any portion is  $P_\alpha$ . The units- $x$  acquired by chains- $y$  in each portion is given by  $W_{y\alpha}P_\alpha\Delta\alpha$ , and if the number of portions is made infinite, the expression for  $V_y$ , the total units- $x$  in chains- $y$  at  $\alpha_2$ , is,

$$V_y = \sum_{\alpha_0}^{\alpha_2} W_{y\alpha}P_\alpha\Delta\alpha = \int_{\alpha_0}^{\alpha_2} W_{y\alpha}P_\alpha d\alpha \quad (21)$$

If eq. (21) is divided by  $\alpha_2\bar{W}_y$ , the total moles of polymerized monomer in chains- $y$  for the whole system at  $\alpha_2$  conversion, an expression for the crosslink density of chains- $y$ ,  $P_y$ , results,

$$P_y = \frac{V_y}{\alpha_2\bar{W}_y} = \frac{1}{\alpha_2\bar{W}_y} \int_{\alpha_0}^{\alpha_2} W_{y\alpha}P_\alpha d\alpha \quad (22)$$

The relative crosslink density of chains- $y$ ,  $P_y'$ , is defined by dividing equation (22) by  $P_s$  and this operation changes  $P_\alpha$  to  $P_\alpha'$ ,

$$P_y' = \frac{P_y}{P_s} = \frac{1}{\alpha_2\bar{W}_y} \int_{\alpha_0}^{\alpha_2} W_{y\alpha}P_\alpha' d\alpha \quad (23)$$

Bardwell and Winkler,<sup>7</sup> on the basis of assumptions for mercaptan regulation of polymerizations mentioned above, have expressed  $\bar{W}_y$  and  $W_{y\alpha}$  in terms of  $R_0$ , the initial moles of mercaptan,  $r$ , the mercaptan rate constant, and  $\alpha_2$ . If their expression for  $W_{y\alpha}$  is entered in eq. (23) and the equivalent of  $P_\alpha'$  from eq. (15) is also substituted, there results, for a mercaptan-regulated, butadiene emulsion system,

$$P_y' = \frac{1}{\alpha_2\bar{W}_y} \int_{\alpha_0}^{\alpha_2} y(rR_0e^{-r\alpha})^2(1 - rR_0e^{-r\alpha})^{y-1}[(D - \ln \alpha)/E]d\alpha \quad (24)$$

The calculation of eq. (24) was done by R. L. Trost, Uniroyal, Inc., Chemical Division, Naugatuck, Conn., who obtained solutions for over fifty

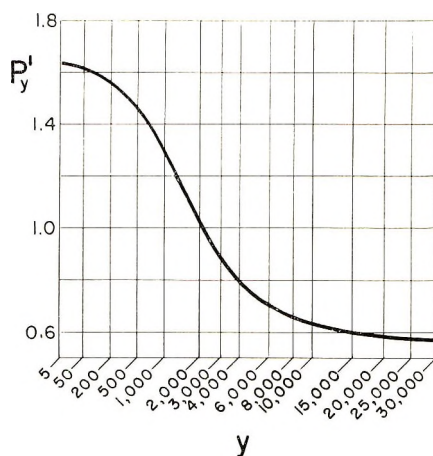


Fig. 2. Relative crosslink density of mercaptan-regulated, emulsion polybutadiene primary chains  $P'_y$  vs. the number of polymerized monomer molecules in the primary chain  $y$ , according to several solutions of eq. (24), at different values of  $y$ , but with  $\alpha_2 = 0.57$ ,  $r = 3.83$ , and  $R_0 = 5.8 \times 10^{-4}$ .

values of  $y$  by a Simpson's rule computer program in which  $\alpha_2 = 0.57$ ,  $r = 3.83$  and  $R_0 = 5.8 \times 10^{-4}$  which thus represents experiment 4 of Table I. Several of these solutions have been used to plot  $P'_y$  versus  $y$  in Figure 2, in which  $y$  is on a cube-root scale so that various chain sizes can be distinguished. This plot shows that the shorter primary chains have a larger crosslink density than the longer ones in a mercaptan-regulated, emulsion polymerization of butadiene.

#### Number of Units- $x$ per Weight-Average Chain at the Gel Point

At the gel point in a polymerization, which is the conversion immediately before the first appearance of insoluble polymer, Stockmayer<sup>6</sup> proposed the expression,

$$1 = \sum_{y=1}^{y=\infty} (y-1) \bar{W}_y P_s^u \quad (25)$$

where  $P_s^u$  is the crosslink density of a system in which there is random distribution of units- $x$  and is constant for all values of  $y$  and  $\bar{W}_y$ . The explanation of eq. (25) starts with the random choice of chain I which has a units- $x$  and through this is attached to chain II. The probability that chain II contains  $y$  monomer units is  $\bar{W}_y$ . The probability that chain II has additional crosslinked units, that is, other than the one that links it to chain I, is given by the number of polymerized monomer units available for becoming additional crosslinked units,  $(y-1)$ , times the probability that any polymerized monomer molecule may have been involved in the formation of a crosslink,  $P_s^u$ . If this probability of chain II being attached to a third chain, when averaged over all possible chain sizes, exceeds one, there

is a finite probability that a chain chosen at random will be part of a gel configuration.

Equation (25) may be divided by  $P_s^u$  and the summation expanded to

$$\frac{1}{P_s^u} = \sum_{y=1}^{y=\infty} y \bar{W}_y - \sum_{y=1}^{y=\infty} \bar{W}_y \quad (26)$$

The second sigma term is 1, while the first is equivalent to the weight-average weight of the primary chains  $\bar{Y}_g$ , which is usually quite large, so that the 1 can be ignored and the expression written as,

$$P_s^u \bar{Y}_g = 1 \quad (27)$$

The term  $P_s^u \bar{Y}_g$  is the number of crosslinked monomer units per weight-average primary chain at the gel point if the crosslinked monomer units are randomly distributed and this number is 1. The principal term of this paper is  $P_s \bar{Y}_g$  which is the number of crosslinked monomer units per weight-average chain at the gel point if the crosslinked monomer units are not randomly distributed and this number is not 1.

Equation (27) has been used<sup>1</sup> to calculate  $P_s^u$ , and with eq. (12) or a similar one derived from eq. (16)  $K^u$ , the crosslinking rate constant for mercaptan-regulated, 1,3-diene emulsion systems in which units- $x$  are randomly distributed.<sup>1-3</sup> This use required mercaptan information, the gel point conversion, and an expression for  $\bar{Y}_g$  evolved by Bardwell and Winkler.<sup>7</sup> Their assumptions lead to an expression for the instantaneous weight-average weight of chains,  $Y_\alpha$ ,

$$Y_\alpha = (2e^{r\alpha}/rR_0) - 1 \quad (28)$$

The averaged, integrated value of  $Y_\alpha$ , over the conversion range is  $\bar{Y}_g$ ,

$$\bar{Y}_g = \frac{1}{\alpha_2} \int_{\alpha_0}^{\alpha_2} Y_\alpha d\alpha = \frac{2}{rR_0\alpha_2} \int_{\alpha_0}^{\alpha_2} e^{r\alpha} d\alpha - \frac{1}{\alpha_2} \int_{\alpha_0}^{\alpha_2} d\alpha \quad (29)$$

which becomes,

$$\bar{Y}_g = [2(e^{r\alpha_2} - 1)/r^2 R_0 \alpha_2] - 1 \quad (30)$$

Bardwell and Winkler's expression for  $\bar{Y}_g$ , which was derived using the chain continuation probability variable does not, because of a secondary assumption, have the  $-1$  term of eq. (30). The  $-1$  term is retained here because of its effect on an error term appearing in subsequent argument.

For nonrandom distribution of units- $x$ , the only member of the sigma terms of eq. (25) which must be changed to describe the conditions immediately before the appearance of gel is the probability that any of the remaining polymerized monomers units,  $y - 1$ , in chain II, have been involved in crosslinks. This probability is  $P_y$  which replaces  $P_s^u$  to give,

$$1 = \sum_{y=1}^{y=\infty} (y - 1) \bar{W}_y P_y \quad (31)$$



Now this system, at the gel point, can be divided into a very large number of portions, each one of which was formed at a unique value of  $\alpha$  and contains  $\Delta\alpha$  moles of polymerized monomer. The crosslink density of all the polymer in any portion is  $P_\alpha$  which thus applies to every chain size and its weight fraction  $W_{y\alpha}$  in that portion. The compound probability of additional units- $x$  in chain II for any particular portion  $\beta_\alpha$  is then

$$\beta_\alpha = P_\alpha \sum_{y=1}^{y=\infty} (y-1)W_{y\alpha} \quad (32)$$

The summation in eq. (32) may be expanded and converted in a manner analogous to that used on eq. (25) to give,

$$\beta_\alpha = P_\alpha(Y_\alpha - 1) \quad (33)$$

Since each  $\beta_\alpha$  is  $\Delta\alpha/\alpha_2$  of the total probability of the system, which at the gel point is equal to 1, the conditions for the first appearance of gel in a system which has nonrandom distribution of units- $x$  with respect to conversion, if the number of portions is made infinite, is

$$1 = \sum_{\alpha_0}^{\alpha_2} \frac{P_\alpha(Y_\alpha - 1)\Delta\alpha}{\alpha_2} = \frac{1}{\alpha_2} \int_{\alpha_0}^{\alpha_2} P_\alpha(Y_\alpha - 1)d\alpha \quad (34)$$

If eq. (34) is divided by  $P_s$ , thus converting  $P_\alpha$  to  $P_\alpha'$ , and if  $Y_\alpha$  is replaced by its equivalent from eq. (28), there results,

$$\frac{1}{P_s} = \frac{2}{rR_0\alpha_2} \int_{\alpha_0}^{\alpha_2} e^{r\alpha} P_\alpha' d\alpha - \frac{2}{\alpha_2} \int_{\alpha_0}^{\alpha_2} P_\alpha' d\alpha \quad (35)$$

Since the averaged integrated value of  $P_\alpha'$ , over the conversion range must be 1, eq. (35) becomes

$$\frac{1}{P_s} = \frac{2}{rR_0\alpha_2} \int_{\alpha_0}^{\alpha_2} e^{r\alpha} P_\alpha' d\alpha - 2 \quad (36)$$

which is an expression for the crosslink density at the gel point of a mercaptan-regulated system in which the nonrandom distribution of cross-linked monomer units with respect to conversion is described by  $P_\alpha'$ .

The crosslink density at the gel point of a mercaptan-regulated, butadiene emulsion system is given by the expression resulting from the substitution for  $P_\alpha'$  in eq. (36), its equivalent from eq. (15). This is

$$\frac{1}{P_s} = \frac{2}{rR_0\alpha_2 E} \left[ D \int_{\alpha_0}^{\alpha_2} e^{r\alpha} d\alpha - \int_{\alpha_0}^{\alpha_2} e^{r\alpha} \ln \alpha d\alpha \right] - 2 \quad (37)$$

which becomes

$$\frac{1}{P_s} = \frac{2}{rR_0\alpha_2 E} \left\{ \frac{De^{r\alpha}}{r} - \left[ \frac{e^{r\alpha} \ln \alpha}{r} - \frac{\ln \alpha}{r} - \frac{1}{r} \sum_{n=1}^{n=t} \frac{(r\alpha)^n}{n(n!)} \right] \right\}_{\alpha_0}^{\alpha_2} - 2 \quad (38)$$

and

$$\frac{1}{P_s} = \frac{2}{r^2 R_0 \alpha_2 E} \left[ De^{r\alpha} - (e^{r\alpha} - 1) \ln \alpha + \sum_{n=1}^{n=t} \frac{(r\alpha)^n}{n(n!)} \right]_{\alpha_0}^{\alpha_2} - 2 \quad (39)$$

For  $\alpha_0$ , all terms in eq. (39) except the first are zero. Then if  $F$  is allowed to stand for the sigma term at  $\alpha_2$ , which is an infinite series that becomes accurate for the present purpose, at  $t = 20$  or less, and if  $D$  and  $E$  are given their constant values from the eq. (14)–(15) transformation, eq. (39) becomes

$$\frac{1}{P_s} = \frac{2[(1 + 0.44\alpha_2)(e^{r\alpha_2} - 1) + F]}{r^2 R_0 \alpha_2 (2 + 0.44\alpha_2)} - 2 \quad (40)$$

Dividing eq. (40) into eq. (30) and dropping the  $-1$  term from the numerator and the  $-2$  term from the denominator in favor of an error term  $G$  yields

$$P_s \bar{Y}_g = \frac{2 + 0.44\alpha_2}{1 + 0.44\alpha_2 + F/(e^{r\alpha_2} - 1)} + G \quad (41)$$

The symbol,  $P_s \bar{Y}_g$ , is read as the number of crosslinked monomer units per weight-average chain at the gel point. Equation (41) applies to mercaptan-regulated, polybutadiene emulsion systems. The error term  $G$  is evaluated with

$$G = [(x - 1)/(z - 2)] - (x/z) \quad (42)$$

after  $P_s \bar{Y}_g$  has been calculated without  $G$ , by allowing  $\bar{Y}_g + 1$  to stand for  $x$  and  $x/P_s \bar{Y}_g$  for  $z$ . For the experimental data of Table I for polybutadiene,  $G$  is not larger than 0.0008.

Equation (41), without  $G$ , has been plotted in Figure 3, at  $\alpha_2$  values of 0.1 and 0.9. Marked on the figure, by experiment number from Table I,

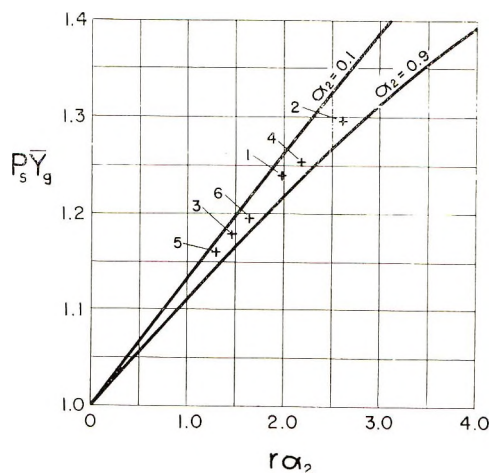


Fig. 3. Number of crosslinked monomer units per weight-average primary chain at the gel point  $P_s \bar{Y}_g$  in a mercaptan-regulated emulsion polybutadiene system vs.  $r\alpha_2$ , an indicator of the heterogeneity of primary chain size, at the indicated values of  $\alpha_2$ , according to eq. (41) without the error term  $G$ . The location of experimental data points is indicated by experiment number from Table I.

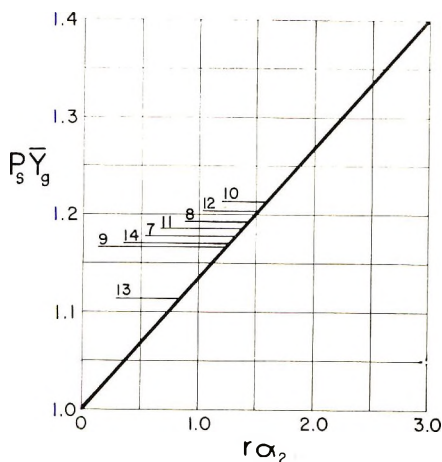


Fig. 4. Number of crosslinked monomer units per weight-average primary chain at the gel point  $P_s \bar{Y}_g$  in mercaptan-regulated emulsion polyisoprene or poly-2,3-dimethylbutadiene systems vs.  $r\alpha_2$ , an indicator of heterogeneity of primary chain size, according to eq. (43) without the error term,  $G$ . The location of experimental data points is indicated by experiment number from Table I.

is the location of experimental data points and within the range of these, the necessary assumptions are considered valid. It can be observed that  $P_s \bar{Y}_g$  is always greater than 1 and increases with increasing  $r\alpha_2$ . Bardwell and Winkler<sup>7</sup> have shown that, for a mercaptan-regulated polymerization at  $\alpha_2$  conversion, the heterogeneity index, i.e., the ratio for primary chains of the weight-average weight to the number-average weight, is a function only of and increases with  $r\alpha_2$ .  $P_s \bar{Y}_g$ , then, increases with increasing heterogeneity of primary chain size, as measured by  $r\alpha_2$ . It can be shown, starting with eq. (34), that if  $Y_\alpha$  is constant, over the conversion range (which means that the heterogeneity index has its initial or instantaneous value of nearly 2 during the entire polymerization),  $P_s \bar{Y}_g$  would be 1, regardless of the extent of deviation from random of the units- $x$  distribution. In order for  $P_s \bar{Y}_g$  to diverge from 1, there must be both a heterogeneity index greater than the instantaneous value and a nonrandom distribution of units- $x$ .

It may also be observed in Figure 3 that  $P_s \bar{Y}_g$  increases with decreasing  $\alpha_2$  at constant  $r\alpha_2$ . This is caused by larger deviation from random of the units- $x$  distribution with decreasing  $\alpha_2$  as was shown in Figure 1 for this system.

If eq. (17) is used to replace  $P_{\alpha'}$  with its equivalent in eq. (36), an expression for  $P_s \bar{Y}_g$  in a mercaptan-regulated, emulsion system of polyisoprene or poly-2,3-dimethylbutadiene is acquired by argument analogous to that of eqs. (37)–(41). This is

$$P_s \bar{Y}_g = \frac{2}{1 + F/(e^{r\alpha_2} - 1)} + G \quad (43)$$

For the appropriate experimental data of Table I,  $G$  here is not larger than 0.0003. Equation (43), without  $G$ , has been plotted in Figure 4. Marked on the figure, by experiment number of Table I, is the location of experimental data points and within range of these, the necessary assumptions may be considered valid. The observations made for polybutadiene in Figure 3, hold for Figure 4, except that there is no variation in  $P_s \bar{Y}_g$  with  $\alpha_2$  at constant  $r\alpha_2$ , since the deviation from random of the units- $x$  distribution for polyisoprene or poly-2,3-dimethylbutadiene emulsion systems does not change with variations in  $\alpha_2$ .

### Postulated Systems

If it is assumed that the mercaptan regulation of 1,3-diene homogeneous systems meets Bardwell and Winkler's conditions,<sup>7</sup> then an expression for  $P_s \bar{Y}_g$  for these systems is obtained by replacing  $P_{\alpha'}$  in eq. (36) with its equivalent from eq. (19) and conducting operations analogous to those of eqs. (37)–(41). This is

$$P_s \bar{Y}_g = \frac{J(e^{r\alpha_2} - 1)}{1 + \ln(1 - \alpha_2) - e^{r\alpha_2}[(r + 1) \ln(1 - \alpha_2) + 1] - rH} + G \quad (44)$$

where  $J$  is defined by eq. (18) and  $H$  is

$$H = (r + 1) \sum_{n=1}^{\infty} \frac{1}{n} \int_{\alpha_0}^{\alpha_2} \alpha^n e^{r\alpha} d\alpha \quad (45)$$

In this argument, use is made of the expression,

$$\ln(1 - \alpha) = -[\alpha + (\alpha^2/2) + (\alpha^3/3) + (\alpha^4/4) \dots]$$

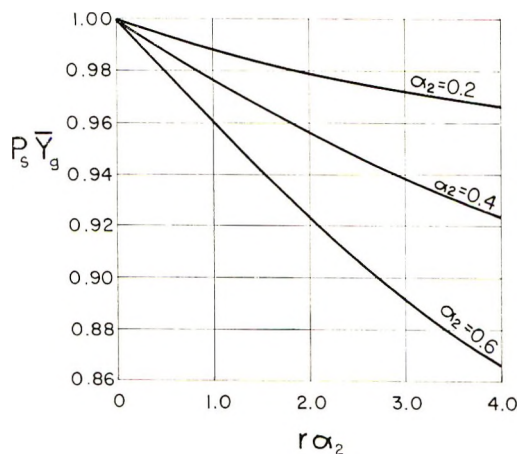


Fig. 5. Number of crosslinked monomer units per weight-average primary chain at the gel point  $P_s \bar{Y}_g$  for a postulated, mercaptan-regulated 1,3-diene homogeneous system vs.  $r\alpha_2$ , an indicator of the heterogeneity of primary chain size, at the indicated values of  $\alpha_2$ , according to eq. (44) without the error term  $G$ .

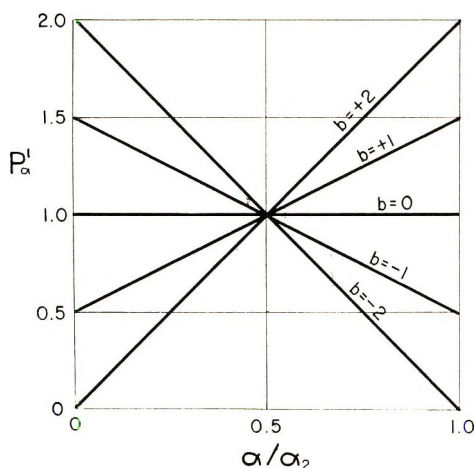


Fig. 6. Relative crosslink density of polymer  $P'_\alpha$  vs. the conversion at which the polymer is formed  $\alpha/\alpha_2$ , the fraction of the final conversion attained, for a postulated system complying with eq. (46) and the effect of the sign and value of the term  $b$  on the distribution of crosslinked monomer units.

The best computation of  $H$ , found here, consists of use of the formula,

$$\int \alpha^n e^{r\alpha} d\alpha = \frac{\alpha^n e^{r\alpha}}{r} - \frac{n}{r} \int \alpha^{n-1} e^{r\alpha} d\alpha$$

and for the present purpose,  $H$  is accurate at  $v = 10$  or less. Without experimental data, the value of  $G$  can only be estimated: if  $\bar{V}_g$  is 2000 or more,  $G$  will be less than 0.0005.

Equation (44) has been plotted, without  $G$ , in Figure 5 for  $\alpha_2$  values of 0.2, 0.4, and 0.6. It can be observed that  $P_s \bar{V}_g$  for a mercaptan-regulated, 1,3-diene homogeneous system is less than 1 and decreases with increasing heterogeneity of chain size, as measured by  $r\alpha_2$ , and with increasing gel point conversion  $\alpha_2$ . The latter effect is ascribed to the greater deviation from random of the units- $x$  distribution as the final or gel point conversion  $\alpha_2$  increases. This was demonstrated in Figure 1.

For both emulsion and homogeneous systems of mercaptan-regulated, 1,3-diene polymerization,  $P_s \bar{V}_g$  diverges from 1 as the heterogeneity of chain size increases and as the deviation from random of the units- $x$  distribution increases. Whether  $P_s \bar{V}_g$  is larger or smaller than 1 depends on the location of the polymer, with respect to conversion, that has the higher crosslink density. These observations can be confirmed by postulating a system in which the units- $x$  distribution is described by

$$P'_\alpha = (b\alpha/\alpha_2) - (b/2) + 1 \quad (46)$$

in which  $b$  is a term to effect various distributions of units- $x$  with respect to conversion. Equation (46) has been plotted in Figure 6 as  $P'_\alpha$  versus  $\alpha/\alpha_2$ , the fraction of the final conversion attained, at values of  $b$  that cause

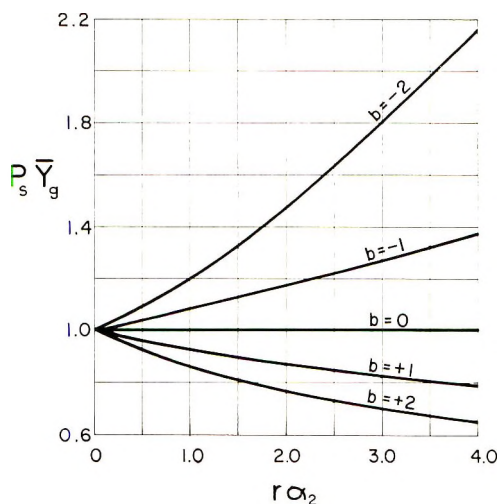


Fig. 7. Number of crosslinked monomer units per weight-average primary chain at the gel point  $P_s \bar{Y}_g$  vs.  $r\alpha_2$ , an indicator of the heterogeneity of primary chain size, for a postulated system complying with eq. (47), at various crosslinked monomer units distributions, as indicated by the sign and value of the term  $b$  and shown in Fig. 6.

the higher crosslink density polymer to be formed at the higher conversions, +2 and +1; cause the higher crosslink density polymer to be formed at lower conversions, -2 and -1; and cause random distribution of units- $x$ , 0. It should be observed that as the absolute value of  $b$  increases, the deviation from random of the units- $x$  distribution increases.

If it is also considered that the system having the units- $x$  distribution described by eq. (46) meets Bardwell and Winkler's conditions<sup>7</sup> of mercaptan regulation, then an expression for  $P_s \bar{Y}_g$  may be obtained by substituting eq. (46) in eq. (36) and conducting operations after the eqs. (37)–(41) pattern. This gives

$$P_s \bar{Y}_g = \frac{1}{b[e^{r\alpha_2}(r\alpha_2 - 1) + 1]/[r\alpha_2(e^{r\alpha_2} - 1)] - b/2 + 1} + G \quad (47)$$

Equation (47) has been plotted, without  $G$ , in Figure 7 for the same values of  $b$  as used in Figure 6. The comparison of these two figures shows that as the absolute value of  $b$  increases, the deviation from random of the units- $x$  distribution increases and the divergence from 1 of  $P_s \bar{Y}_g$  increases for a given value of  $r\alpha_2$ . It can also be observed that  $P_s \bar{Y}_g$  is larger than 1 if the lower conversion polymer has the larger crosslink density and is smaller than 1 if the higher conversion polymer has the larger crosslink density. In either case, the divergence from 1 of  $P_s \bar{Y}_g$  increases as the heterogeneity of chain size, as measured by  $r\alpha_2$ , increases. Only with random distribution of units- $x$ ,  $b = 0$ , or at the instantaneous heterogeneity index,  $r\alpha_2 = 0$ , is there exactly 1 units- $x$  per weight-average chain at the gel point.

### Experimental Data

In Table I, eqs. (41) and (43) have been used to calculate  $P_s \bar{V}_g$  from experimental data on mercaptan-regulated emulsion systems for butadiene, isoprene, and 2,3-dimethylbutadiene, which have previously been reported.<sup>1-3</sup> It is shown that  $P_s \bar{V}_g$  ranges from 1.11 to 1.29 for these data. The crosslink densities and crosslinking rate constants, which had been calculated on the assumption that there is 1 units- $x$  per weight-average chain at the gel point, have been multiplied by  $P_s \bar{V}_g$  and are thus increased by 11 to 29%. The difference between radioactive mercaptan<sup>5</sup> and gel point crosslink density results for polybutadiene has been reduced by 22 and 32%. These changes in the calculated results do not alter the qualitative crosslinking relations among the monomers or among the polymerization temperatures.

The evaluation and suggestions to improve the presentation of this work by Emanuel G. Kontos and Wendell V. Smith, Uniroyal, Inc., Research Center, Wayne, New Jersey, are acknowledged with thanks.

### References

1. M. Morton and P. P. Salatiello, *J. Polym. Sci.*, **6**, 225 (1951).
2. M. Morton, J. A. Cala, and I. Piirma, *J. Polym. Sci.*, **15**, 167 (1955).
3. M. Morton and W. E. Gibbs, *J. Polym. Sci., A*, **1**, 2679 (1963).
4. P. J. Flory, *J. Amer. Chem. Soc.*, **69**, 2893 (1947).
5. L. H. Howland, A. Nisonoff, L. E. Dannals, and V. S. Chambers, *J. Polym. Sci.*, **17**, 115 (1958).
6. W. H. Stockmayer, *J. Chem. Phys.*, **12**, 125 (1944).
7. J. Bardwell and C. A. Winkler, *Can. J. Res.*, **B27**, 119 (1949).

Received February 10, 1970

**Mobility of the Ring Structure and the Characteristics of Crosslinked Polymers: The Structural Effect of the Eleven-Membered Ring and Its Homologs upon the Dynamic Mechanical Properties and Glass Transition Temperature of Crosslinked Diallyl Succinate Polymers**

SHINICHI ISAOKA, MAKIHIKO MORI, AKIO MORI, and JU KUMANOTANI, *The Engineering Research Institute, Faculty of Engineering, The University of Tokyo, Tokyo, Japan*

**Synopsis**

Dynamic mechanical properties and glass transition temperatures were measured for crosslinked polymers derived from diallyl succinate monomers. The mobility of the diester having an eleven-membered ring and of homologous structures which are introduced in the crosslinked polymer system, is discussed on the basis of the parameter for cyclization polymerization of a monomer, dynamic mechanical properties, and glass transition temperature. Control of the mobility of the ring structure and its homologous structures involved in the crosslinked polymers was attempted by modification of the substituent at the 1- or 1,2-position of diallyl succinate, and the diallyl succinate monomers were derived from the succinic acid and its derivatives: succinic acid, methyl succinic, ethyl succinic, and chlorosuccinic acids; *cis*-1,2-dicarboxylic acids of cyclopropane, cyclobutane, cyclopentane, and cyclohexane; *cis*-1,3- and 1,4-dicarboxylic acids of cyclohexane, and phthalic acid. The results obtained are explained well on the basis of the mobility of the ring and homologous structures.

**INTRODUCTION**

It is well known that mechanical and thermal properties of polymers are closely related to both the polymer structure and segmental motions of polymers.

Representative three-dimensional polymers such as rubberlike materials, paint films, and thermosetting resins, which have different network structures, show characteristic behaviors in their mechanical and thermal properties. Therefore the effect of the ring structures upon the properties of polymers should be studied more extensively in connection with the mobility of the rings involved in the polymer matrix or with the environment affecting their mobility.



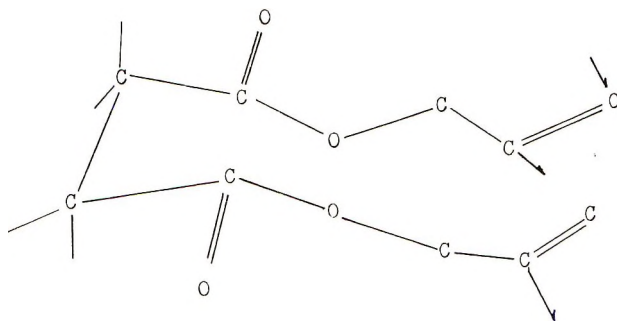
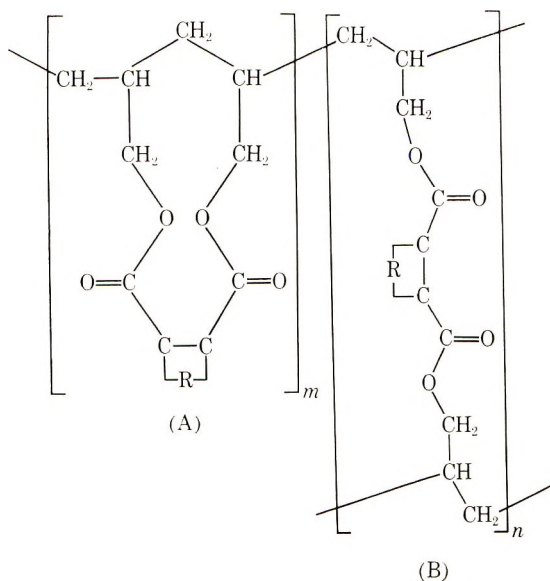


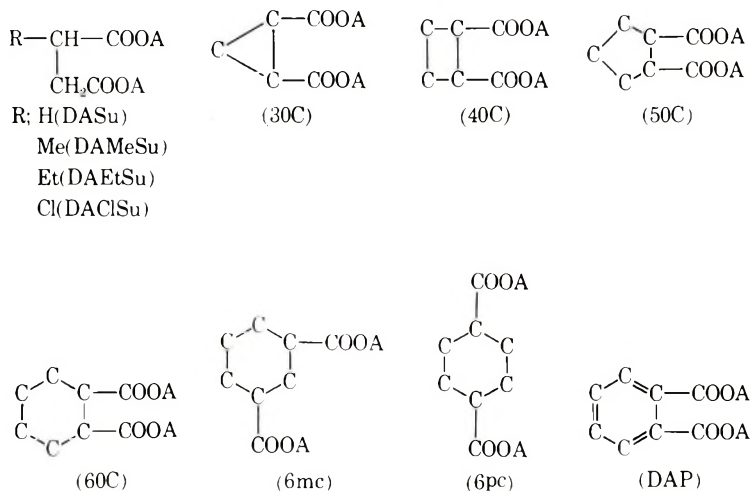
Fig. 1. Conformation of diallyl succinate monomers in cyclization polymerization. Arrows indicate possible links in cyclization.

According to Simpson and Holt,<sup>1</sup> it has already been demonstrated that  $\alpha,\omega$ -diallyl ester monomers undergo radical cyclization polymerization to give polymeric materials involving cyclic diester rings, and diallyl succinate shows an exceptionally high tendency to cyclize, because it has, as shown in Figure 1, two carbonyl groups situated antiparallel, and the two terminal vinyl groups have favorable conformations for cyclization polymerization. The conformations were elucidated by its abnormally low dipole moment<sup>2</sup> and viscosity.<sup>3</sup>

It was already established by Simpson that diallyl succinate-type monomers such as diallyl succinate and diallyl phthalate undergo cyclization polymerization to give polymeric materials (prepolymers) involving eleven-membered diester rings having the structure I.



Accordingly, in considering the influence of mobility of the ring units involved in the crosslinked polymers upon the viscoelastic properties and glass transition temperatures, we have investigated the crosslinked polymers derived from diallyl succinate-type monomers having various substituents, where A denotes an allyl group. In the present system, the



## II

prepolymers were prepared by radical polymerization of a diallyl ester monomer and then the crosslinked polymers (see II) were obtained therefrom by a peroxide-curing method.

The mobility of the diester having an eleven-membered ring (A) and its analogous B unit that is, involved in the prepolymer can readily be changed by modification of substituents situated at 1- or 1,2-position of diallyl succinate. The diallyl ester monomers of the following succinic and its derivatives were used; succinic acid, methyl-, ethyl-, and chlorosuccinic acid; *cis*-1,2-dicarboxylic acids of cyclopropane, -butane, -pentane, and -hexane; *cis*-1,3- and 1,4-dicarboxylic acids of cyclohexane and phthalic acid.

It is also demonstrated by Haward<sup>4</sup> that the reactivity of  $\alpha,\omega$ -diallyl ester monomers for cyclization polymerization is closely related to the probability of an ester to take cyclic conformations in the final cyclization polymerization step. Therefore, it is reasonable that a monomer with a larger reactivity for the cyclization polymerization would give a more rigid A and B structure.

Consequently, on the basis of this interpretation of the mobility of the A and B structure introduced in the crosslinked polymers, the reactivity of a monomer for cyclization polymerization was taken as a parameter.

Finally, viscoelastic behavior and glass transition temperature were measured for the crosslinked polymers; the results are discussed on the basis of the mobility of the A and B structures.

## EXPERIMENTAL

## Materials

The diallyl esters were prepared according to the methods described in literature. The absence of *trans* isomers in the *cis*-diallyl esters was confirmed by means of gas chromatographic analysis. Constants were diallyl succinate (DASu), bp 119–121°C/7 mm Hg,  $n_D^{25}$  1.4490; diallyl methylsuccinate(DAMeSu), bp 80–82°C/1 mm Hg,  $n_D^{25}$  1.4460; diallyl ethylsuccinate(DAEtSu), bp 85–90°C/1 mm Hg, diallyl *cis*-1,2-cyclopropane dicarboxylate(30C),<sup>5</sup> bp 128–133°C/5 mm Hg,  $n_D^{25}$  1.4672; diallyl *cis*-1,2-cyclobutane dicarboxylate(40C),<sup>6</sup> bp 128–131°C/6 mm Hg,  $n_D^{25}$  1.4682; diallyl *cis*-1,2-cyclopentane dicarboxylate(50C),<sup>7</sup> bp 125.5–128.0°C/4.5 mm Hg; diallyl *cis*-1,2-cyclohexane dicarboxylate(60C),<sup>8</sup> bp 134.5–135.5°C/4 mm Hg,  $n_D^{25}$  1.4728; diallyl *cis*-1,3-cyclohexane dicarboxylate (6mc),<sup>9</sup> bp 149.5–150.0°C/4 mm Hg,  $n_D^{25}$  1.4720; diallyl *cis*-1,4-cyclohexane dicarboxylate(6pc)<sup>10</sup>, bp 158.0–160.5°C/9 mm Hg,  $n_D^{25}$  1.4720; diallyl phthalate(DAP), bp 153.0–155.5°C/4 mm Hg.

## Polymerization of Diallyl Esters

A mixture of given amounts of monomer, azobisisobutyronitrile(AIBN) as initiator, and dioxane was placed in a 50-ml glass tube which was evacuated, flushed with nitrogen, and sealed. After the reaction, the prepolymer obtained by pouring the resulting solution into a 10-fold volume of *n*-hexane was purified by reprecipitation from its acetone solution with *n*-hexane and dried *in vacuo*. The prepolymers thus obtained were solid or viscous liquids, the molecular weight of which was measured to be between 3000 and 7000 by means of vapor pressure osmometry (VPO). The reaction conditions and the result obtained are summarized in Table I.

TABLE I  
Synthesis of Prepolymers

Monomer	[M] <sub>0</sub> , mole/l. <sup>a</sup>	[I] <sub>0</sub> , mole/l. <sup>b</sup>	Reaction temp, °C	Time, hr	Yield, %	Degree of cyclization,
DAP	1	bulk	70	10	25	47
	2	3.5	"	24	28	54
	3	2.3	"	40	28	64
	4	1.2	"	40	30	74
60C	1	1.2	80	20	13	70
	2	2.2	"	"	21	60
	3	bulk	"	"	8	43
DASu	1	0.7	"	"	20	51
	2	2.5	"	"	24	58
DAMeSu	0.6	"	70	"	17	60
	30C	2.6	"	80	"	36

<sup>a</sup> Initial monomer concentration.

<sup>b</sup> Initial concentration of radical initiator (AIBN).

### Preparation of Test Specimens

The test specimen ( $0.2\text{--}1.0 \times 1.5\text{--}3.0 \times 20\text{--}30$  mm) was prepared by cutting the crosslinked polymers made by either of two methods. (The second of the following methods was used when the film could not be made by the first method due to brittleness of films.)

In the first method, (method a) the acetone was removed from a solution of prepolymer (100 parts) and dicumyl peroxide (3 parts) in acetone (100 parts), was at  $40^\circ\text{C}$  *in vacuo*. The powder thus obtained was dried further at room temperature *in vacuo* for 2 days, and then molded at  $160^\circ\text{C}$  and a pressure of  $150\text{ kg/cm}^2$  for 15 min.

In the second method (method b) a solution of a prepolymer (100 parts) and dicumyl peroxide (2 parts) in acetone (100 parts) was coated on tin plates. After evaporation of the acetone at room temperature, the plates were kept at  $160^\circ\text{C}$  for 30 min and cooled to room temperature in an atmosphere of nitrogen. The film was stripped off by an amalgam method.

The specimens thus obtained were found on the basis of infrared spectral absorptions at  $910$  and  $990\text{ cm}^{-1}$  to have no allyl groups.

### Measurements of Dynamic Mechanical Properties and Glass Transition Temperatures

Dynamic mechanical measurements were carried out at 3.5, 11, 35, and 110 Hz over a temperature range from 30 to  $250^\circ\text{C}$  with a direct-recording type of viscoelastomer (Vibron DDV-II, Toyo Sokki Co. Ltd.). Thus, the relationship between loss tangent and the temperature  $T_m$  of maximum loss tangent were observed. The activation energy of the movement of segments was also obtained from the measured dependence of frequency upon  $\tan \delta_{\text{max}}$ .

The glass transition temperature ( $T_g$ ) was measured by dilatometry.

## RESULTS AND DISCUSSION

### Reactivity of Diallyl Ester Monomers in Cyclization Polymerization

Simpson and Holt<sup>1</sup> divided the intramolecular reactions into two types, chain cyclization and multiple crosslinking, and demonstrated that the actual intramolecular reaction is dependent mainly on the number of chain atoms in each consecutive addition ring. It is statistically accepted that the intramolecular cyclization with tetrafunctional monomers leads to the formation of the possible smallest ring.

Thus, the tendency of diallyl succinate monomers to cyclize is reasonably discussed on the basis of the ease of formation of an eleven-membered ring, although the tendency might be enhanced somewhat by the multiple crosslinking reaction, which is responsible for the rigidity of the prepolymer, and an increased ease of assuming a favorable conformation for cyclization

The tendency of cyclization in diallyl succinate monomers is interpreted in terms of  $R_c$  proposed by Smets,<sup>11</sup> which is the ratio of velocity constant for cyclization  $k_c$  to that for propagation  $k_p$ . The  $R_c$  values measured by the method of Smets and Minoura<sup>11,12</sup> are presented in Table II. The data indicate that (1) the ease of cyclization polymerization decreases in the following sequence: DAP, 50C, 30C, 60C, 40C, DAETsU, DAMeSu, DASu, and DAClSu, and (2) that the diallyl *cis*-1,2-cyclohexane dicarboxylate has higher  $R_c$  values than corresponding 1,3- and 1,4-isomers.

TABLE II  
Reactivity for Cyclization Polymerization of Diallyl Succinate and  
Its Derivatives (80°C)

Monomer	$R_c^a$
DAP	3.21
60C	1.88
50C	2.71
40C	1.42
30C	1.90
DAMeSu	1.00
DAETsU	1.07
DASu	0.74
DAClSu	0.00
6mc	0.14
6pc	0.27

<sup>a</sup> $R_c$  is obtained experimentally from the Smets equation:  $1/F_d = 1 + R_c/[M]_0$ , where  $R_c = k_c/k_p$ , and  $F_d$  is the degree of unsaturation,  $[M]_0$  is initial concentration of monomer.

The reactivity for cyclization polymerization of a monomer is discussed below on the basis of the ease of assuming the cyclic conformation as described by Figure 1.

DAClSu, which did not show the cyclization polymerization, would not assume the cyclic conformation owing to the repulsive action between chloro and allyloxycarboxylic groups.

The DASu which is expected to form mostly mobile A and B structures among the esters employed, exhibited the lowest  $R_c$  value, whereas DAMeSu and DAETsU, which may have more favorable conformations for cyclization polymerization due to the *gem*-effect<sup>13</sup> of a methyl or ethyl group, showed a larger  $R_c$  value than DASu.

30C, in which carbonyl groups are conjugated with a cyclopropane ring consisting of a carbon-carbon bond with 1.5 pi-bond order is assumed to give a larger  $R_c$  value than DAMeSu, because the *cis*-1,2-cyclopropane dicarboxy group becomes planar due to the above conjugation effect; the  $R_c$  value was found to be markedly larger than that for the DAMeSu. On account of the effect of the rigid character of four membered ring, the observable  $R_c$  value (1.42) for 40C was found to be larger than that (1.26) for diallyl 1,2-dimethylsuccinate, which was calculated approximately by

adding a compensation factor ( $\Delta R_c = 0.28$ ) for a methyl group to the  $R_c$  value of DAMeSu.

50C, in comparison with 40C, exhibited an increased  $R_c$  value which is next to that of DAP. It became evident that this is attributable to the smaller strain inherent in the cyclopentane ring compared to the cyclobutane for the formation of the cyclic conformation illustrated in Figure 1.

The smaller  $R_c$  value for 60C compared to 50C can be ascribed to the more mobile flipping character of the cyclohexane ring between equatorial and axial types of chair forms.

DAP, among the diallyl ester monomers used, has mostly favorable conformations for cyclization polymerization, since the probability of cyclic conformations is markedly increased relative to 30C due to the larger conjugation effect between carbonyl groups of ester and benzene ring; the largest  $R_c$  value is given for the DAP.

The order of the  $R_c$  value for 60C, 6mc, and 6pc can be explained on the basis of their relative ease of affording eleven, twelve, and thirteen-membered rings in the cyclization polymerization, as shown by Holt for the cyclization polymerization of  $\alpha,\omega$ -diallyl esters.

### Effect of Ring Mobility in Polymers upon Dynamic Mechanical Properties and Glass Transition Temperatures

Viscoelastic properties and glass transition temperature of crosslinked polymers are usually affected by the degree of the crosslinking. Accordingly, in characterization of crosslinked polymers, much attention has been devoted to preparing and employing test specimens having the same degree of crosslinking. Since the prepolymers employed, when cured under the present conditions, show no discernible absorption peak at  $910\text{ cm}^{-1}$  in the infrared region which is attributable to the allyl group, it is reasonably assumed that the prepolymers with the same degree of cyclization result in crosslinked polymers with the same degree of crosslinking. Therefore, the character of prepolymer with approximately 50% degree of cyclization degree was compared.

TABLE III  
Characteristic Temperatures  $T_g$  and  $T_m$  of Crosslinked  
Polymers Derived from Diallyl Succinate Monomers

Monomer (and degree of cyclization of prepolymer)	$T_g$ , °C <sup>a</sup>	$T_m$ , °C <sup>b</sup>
DAP (54)	118	219
60C (43)	54	190, 145
40C (50)	75	—
30C (50)	110	202
DASu (50)	50	149, 90

<sup>a</sup> By dilatometry.

<sup>b</sup>  $T_m$  is the temperature of  $\tan \delta_{\max}$  measured at 3.5 Hz by dynamic mechanical measurement.

Upon the characterization of the polymers, the measured dynamic mechanical properties,  $T_m$  and  $T_g$  were discussed in connection with the ease of segmental motion of the A and B structures (see Fig. 2 and Table III) for crosslinked DAP, 30C, 60C, and DASu polymers.

Figure 2 shows the dependence of degree of crosslinking upon the loss tangent-temperature relation, which was measured for crosslinked diallyl phthalate and 60C polymers prepared from the corresponding prepolymers with different degrees of cyclization. The  $T_m$  of the crosslinked polymers prepared from the prepolymers with a 50% degree of cyclization which is designated  $T_{m,50}$  was found to be 222°C and 191°C for the DAP and 60C, respectively. The  $T_{m,50}$  as well as the loss tangent-temperature relation can be obviously discussed with the mobility of the A and B structures in the present crosslinked polymer system, even if there would be accompanied with a minor effect upon the  $T_{m,50}$  due to the difference in the degree of crosslinking.

It should be noted that the ease of segmental motions reflecting the mobility of the A and B structure of the crosslinked polymers can be correlated with that in cyclization polymerization of the monomers. On the basis of these considerations, the ease of segmental motion of the present crosslinked polymers is expected to decrease in the following order of groups: DAP, 50C, and 30C > 60C and DAMeSu > DASu.

As may be seen in Figure 2 and Table III, the order of the measured  $T_m$  or  $T_g$  is clearly in good agreement with these considerations, excepting for

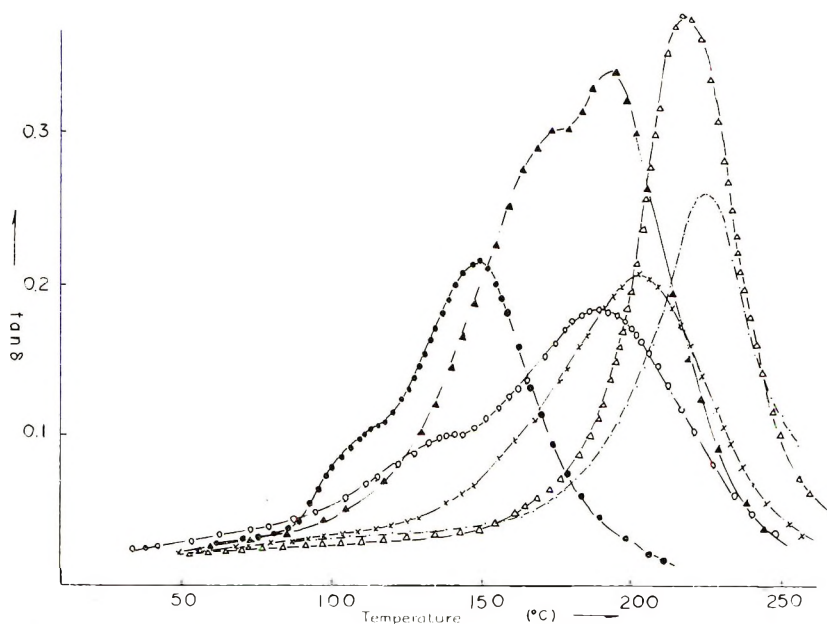


Fig. 2. Plot of  $\tan \delta$  vs. temperature for diallyl succinate polymers: (·) DAP (47%); ( $\Delta$ ) DAP (54%); ( $\times$ ) 30C (50%); ( $\circ$ ) 60C (43%); ( $\blacktriangle$ ) 60C (60%); ( $\bullet$ ) DASu (51%). The number in blanket is the degree of cyclization of a prepolymer.

60C. Furthermore, in the case of the polymers with a mostly rigid A and B structure, such as the DAP and 30C, only the sharp  $\alpha$ -transition could be observed, while in the case of the polymers with a more mobile A and B structure such as the crosslinked DASu and 60C polymers, a  $\beta$ -transition could also be observed, meaning that the crosslinked polymers which have mobile A and B structures capable of undergoing various modes of segmental motions show a more broad curve of the loss tangent-temperature relation than those with the less modes of the segmental motions. The influence of the chemical structure upon the character of some polymers is detailed below.

**30C.** In comparison with DAP, the  $T_{m,50}$  was found a little lower, presumably due to (1) a smaller conjugation effect of the carbonyl group with cyclopropane and (2) a smaller bulky effect of the cyclopropane ring compared to that of the benzene ring of diallyl phthalate, leading to the greater mobility of the eleven-membered ring (A), and the less restriction of structure B towards segmental motions than in DAP.

**60C.** The  $T_m$  of crosslinked 60C was found to be 195°C, a little lower than that of 30C. The mobility of structures A and B is assumed to be approximately same for the crosslinked 60C and 30C polymers, judging from the measured  $R_c$  values and  $T_m$ . Nevertheless, the order of their  $T_g$  is reversed (see Table III). The lower  $T_g$  for crosslinked 60C may reflect the segmental motions in smaller scale due to the flipping character of the cyclohexane ring, whereas, the higher  $T_m$  of the 60C refers to the temperature at which larger-scale segmental motions begin. These results clearly suggest the contribution of the flipping motions of the cyclohexane ring involved in the crosslinked 60C polymers to the small-scale motions. The observation of both  $\alpha$ - and  $\beta$ -transitions at lower temperatures is indicative of the mobile character of the A and B structures involved in the polymer matrix.

### Apparent Activation Energy

In order to get further information on the mobility of the A and B structure, activation energies were measured for the movement of segments involving the A and B structure by measuring dependence of fre-

TABLE IV  
Apparent Activation Energy of Movement of Segments of  
Crosslinked Polymers Derived from Diallyl Succinate Type Monomers

Monomer (and degree of cyclization of prepolymer)	$\Delta H$ , kcal/mole	$-\Delta S$ , cal/mole
DAP (54)	120 $\pm$ 5	50 $\pm$ 5
30C (50)	110	50
60C (43)	90	34
	95	45
DASu (51)	65	35
	75	45



quency upon  $T_m$ . Table IV indicates that the DAP polymers have the largest activation energy and the DASu polymer the smallest. Obviously the other measured values are also reasonable for explaining the ease of movement of the A and B structures.

### References

1. W. Simpson and T. Holt, *Proc. Roy. Soc. (London)*, **A238**, 154 (1956).
2. C. P. Smith and W. S. Walls, *J. Amer. Chem. Soc.*, **53**, 527 (1931).
3. A. E. Dunston, *J. Chem. Soc.*, **1913**, 133.
4. R. N. Haward, *J. Polym. Sci.*, **14**, 535 (1954).
5. L. L. McCoy, *J. Amer. Chem. Soc.*, **80**, 6468 (1958).
6. E. R. Buchman, *J. Amer. Chem. Soc.*, **64**, 2696 (1942).
7. A. H. Blatt, Ed., *Organic Syntheses*, Coll. Vol. 2, Wiley, New York, 1943, p. 531.
8. N. Rabjohn, Ed., *Organic Syntheses*, Coll. Vol. 4, Wiley, New York, 1963, pp. 304, 890.
9. F. Ramirez, *J. Amer. Chem. Soc.*, **74**, 5785 (1952).
10. H. G. Dehm, U.S. Pat. 2,888,484 (1959).
11. G. Smets, *J. Polym. Sci. A*, **2**, 1491 (1963).
12. Y. Minoura, *J. Polym. Sci. A*, **3**, 2149 (1965).
13. K. E. Ziegler, *Ann.*, **528**, 143 (1937).

Received January 8, 1970

Revised April 2, 1970

## Studies on the Polymerization of Methyl Methacrylate Activated by Azobisisobutyramidine

SATYENDRA NATH GUPTA and UMA SHANKAR NANDI,  
*Department of Macromolecules, Indian Association of the Cultivation of  
Science, Calcutta-32, India*

### Synopsis

Kinetic studies on methyl methacrylate polymerization were carried out with water-soluble 2,2'-azobisisobutyramidine (ABA). The rate of polymerization was proportional to the square root of the initiator concentration in the solvents chloroform, methanol, and dimethyl sulfoxide (DMSO), which confirms the bimolecular nature of the termination reaction. The monomer exponent was unity in chloroform but in methanol and DMSO the rate of polymerization passed through a maximum when plotted against the monomer concentration. This behavior in methanol has been attributed to be due to the enhanced rate of production of radical with increasing proportion of methanol. The rate of decomposition of the ABA has been observed to be faster in methanol than in chloroform. The situation becomes more complicated with DMSO, which was found to reduce the value of  $\delta = (2k_t)^{1/2}/k_p$  in methyl methacrylate polymerization. The rate of polymerization was observed to be highly dependent on the nature of the solvent, the rate increasing with increased electrophilicity of the solvent. The dependence of  $R_p$  on the solvent has been explained in the light of the stabilization of the transition state due to increased solvation of the basic amidine group of the initiator with the increased electrophilicity of the solvent.

Azoamidines, in view of their polar character, form a distinct class of azo initiators and their decomposition as well as their behavior in a polymerizing system are both complex and interesting.

Although the preparation of the dihydrochloride<sup>1</sup> of 2,2'-azobisisobutyramidine (ABA·2HCl) dates back to 1952, thorough polymerization studies with the free base have not yet been carried out. Dougherty<sup>2</sup> studied the decomposition rates and products of ABA·2HCl in water, and Hammond and Newman<sup>3</sup> isolated the free base (ABA) and studied the decomposition rates of the base and also its dinitrate. Dekking<sup>4-6</sup> used ABA·2HCl to prepare clay initiators and found an increased rate of decomposition and stability of the free radicals in a clay medium. He also used the clay initiator to polymerize certain monomers. Breitenbach and Kuchner<sup>7</sup> used ABA·2HCl as activator in the emulsion polymerization of styrene. Rate of radical formation, rate of polymerization, and the viscosity number of the polymers were measured, and it was observed that the polymerization proceeded according to theoretical consideration.

In this background it was thought worthwhile to study the role of the free base, 2,2'-azobisisobutyramidine (ABA) as a free-radical initiator in a polymerizing system. The present communication reports results of such a study on methyl methacrylate polymerization in solutions of different solvents.

## EXPERIMENTAL

### Methyl Methacrylate

The stabilized methyl methacrylate supplied by Koch-Light Laboratories Ltd. was first washed repeatedly with 5% caustic soda till free of stabilizer, followed by washing with distilled water, and finally dried over calcium chloride. The dried monomer was fractionally distilled under reduced pressure, and the middle fraction was collected for use in the polymerization studies.

### Solvent

Dimethyl sulfoxide (British Drug House) was dried over calcium hydride after removal of most of the water which might be present as benzene azeotrope. The final dried product was then fractionally distilled under reduced pressure and the middle fraction was collected and stored in a well-stoppered amber colored bottle.

All other solvents were of analytical reagent quality and purified by conventional methods.<sup>8</sup>

### Initiator

The azobisisobutyramidine (ABA) was prepared according to the method followed by Hammond and Newman<sup>3</sup> from its dihydrochloride (obtained from Du Pont De Nemour & Co.).

### Polymerization

The rates of polymerization were determined dilatometrically. After introducing the required amount of the solution the dilatometer was sealed under vacuum. Any dissolved air was removed by repeated flushing with nitrogen by using the freeze-thaw technique. The bulb of the dilatometer was covered with black paper and immersed in a thermostatic bath. The polymerization was allowed to continue up to a maximum of 5% conversion. The polymer was precipitated with methanol followed by reprecipitation from benzene solution. It was then dried under vacuum and finally weighed to constant weight.

### Decomposition of ABA

The rates of thermal decomposition of the initiator were determined by monitoring the gas evolved in a modified apparatus as described by Bolland.<sup>9</sup>

### Molecular Weight

The number-average molecular weight of the unfractionated samples was determined viscometrically in benzene at 30°C with the help of the following equation<sup>10</sup> relating the intrinsic viscosity  $[\eta]$  with the number-average molecular weight  $\bar{M}_n$

$$[\eta] = 8.69 \times 10^{-5} \bar{M}_n^{-0.78}$$

## RESULTS

### Dependence of the Rate of Polymerization $R_p$ on the Initiator Concentration

In the vast literature of free-radical-initiated polymerization of methyl methacrylate<sup>11,12</sup> and styrene<sup>13</sup> by azo compounds and peroxides it was generally observed that the rate of polymerization  $R_p$  was directly proportional to the square root of the initiator concentration  $[I]^{1/2}$  over a wide range of initiator concentration in accordance with the general kinetics derived from the assumption of bimolecular termination. ABA was also observed to follow the same relationship in the three solvents, chloroform,

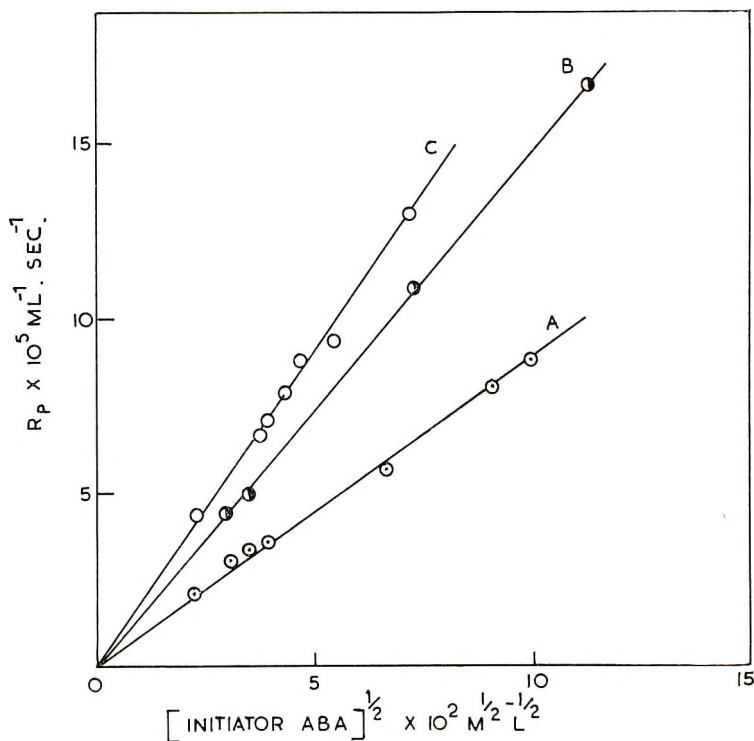


Fig. 1. Dependence of  $R_p$  on the concentration of ABA in various solvents: (A) chloroform; (B) DMSO; (C) methanol. Concentration of methyl methacrylate, 4.65 mole/l., temperature 60°C.

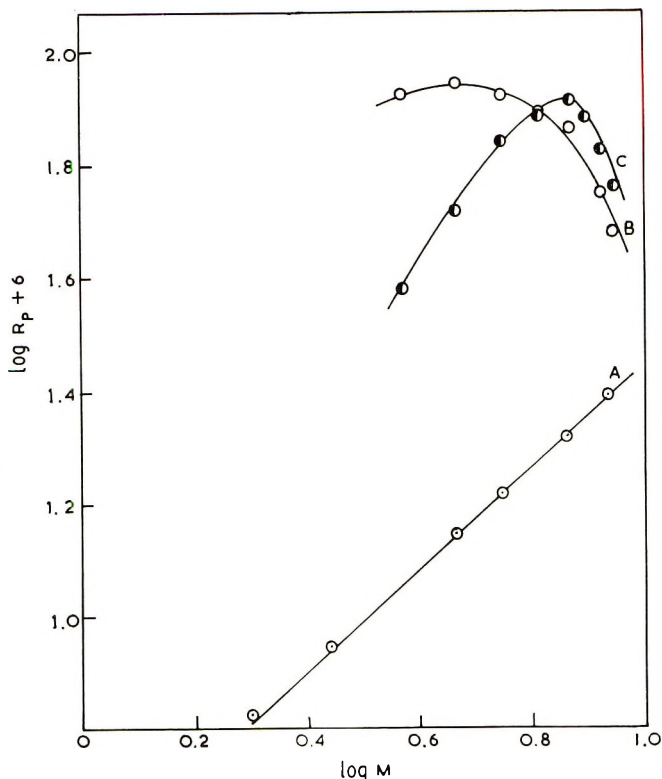


Fig. 2. Variation of  $R_p$  with the concentration of methyl methacrylate (60°C): (A)  $5.106 \times 10^{-4}$  mole/l. ABA in chloroform; (B)  $5.76 \times 10^{-4}$  mole/l. ABA in DMSO; (C)  $8.737 \times 10^{-4}$  mole/l. ABA in methanol.

methanol, and dimethyl sulfoxide (DMSO) in which the rates of polymerization of methyl methacrylate was studied with 50-fold or more variation of the initiator concentrations. In all the cases the curves (Fig. 1) obtained by plotting  $R_p$  against  $[I]^{1/2}$  was linear and passed through the origin but at different slopes, increasing in the order of the solvents chloroform < DMSO < methanol, though the monomer concentration remained the same in each case. As the initiator was not soluble in the monomer no bulk experiment could be carried out.

### Dependence of $R_p$ on Monomer Concentration

The rates of polymerization of methyl methacrylate was determined at various concentrations of the monomer in three different solvents. The plot of  $\log R_p$  against  $\log [M]$  is shown in the Figure 2. In chloroform the plot was linear with a slope of 0.9, which is very near to the unity demanded by the general kinetic relationship. In the cases of the solvents methanol and DMSO, the rates passed through a maximum and then decreased with increasing of monomer concentration.

### Activation Energy of the Polymerization Reaction

The rate of polymerization of methyl methacrylate at fixed monomer and initiator concentrations was determined at different temperatures varying from 50°C to 90°C in the solvents chloroform and methanol. From the Arrhenius plot of  $\log R_p$  versus  $1/T$  (Fig. 3), the activation energies of the overall polymerization reaction were computed. The values for  $E_{R_p}$  in chloroform and methanol are 15.7 kcal/mole and 14.1 kcal/mole, respectively. The rate equation can be written as

$$R_p = (k_p/k_t^{1/2})(k_d[I]f)^{1/2}[M] \quad (1)$$

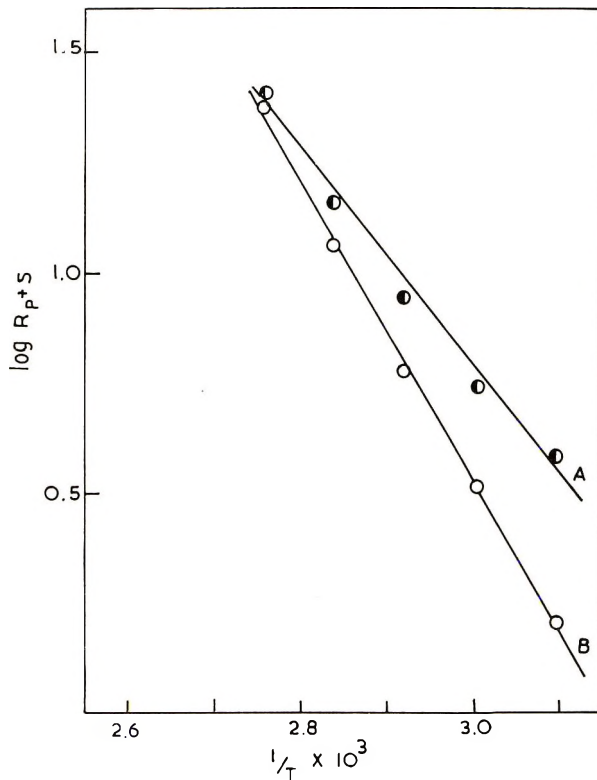


Fig. 3. Determination of the activation energy of the polymerization reaction: (A)  $0.437 \times 10^{-3}$  mole/l. ABA in methanol; (B)  $1.23 \times 10^{-3}$  mole/l. ABA in chloroform. Methyl methacrylate concentration, 4.65 mole/l.

where  $f$  is the initiator efficiency, and the corresponding relationship for the activation energies would be

$$E_{\text{overall}} = E_p - \frac{1}{2}E_t + E_d \quad (2)$$

On substituting the value of 4.9 kcal/mole reported by Matheson et al.<sup>17</sup> for  $E_p - \frac{1}{2}E_t$  in the polymerization of methyl methacrylate, the value of

$E_d$ , the energy of activation of the decomposition of the initiator in chloroform and methanol was found to be 21.6 and 18.4 kcal/mole, respectively.

**Evaluation of initiator transfer ( $C_I$ );  $(2k_t)^{1/2}/k_p(\delta)$ ;  
Rate of Initiation  $R_i$ , and Efficiency  $f$**

As ABA is insoluble in most of the monomers (e.g., methyl methacrylate, styrene, acrylonitrile), attempts were made to determine the coefficient of initiator transfer  $C_I$  from data obtained for solution polymerization. ABA is not highly soluble in chloroform which moreover has a relatively high transfer coefficient and hence posed some difficulty in determination of  $C_I$  at low concentrations of the initiator. The plot of  $1/\bar{P}_n$  versus  $R_p$  (Fig. 4) is linear in all the solvents studied, indicating negligible chain transfer with initiator as observed with 2,2'-azobisisobutyronitrile. Attempts were

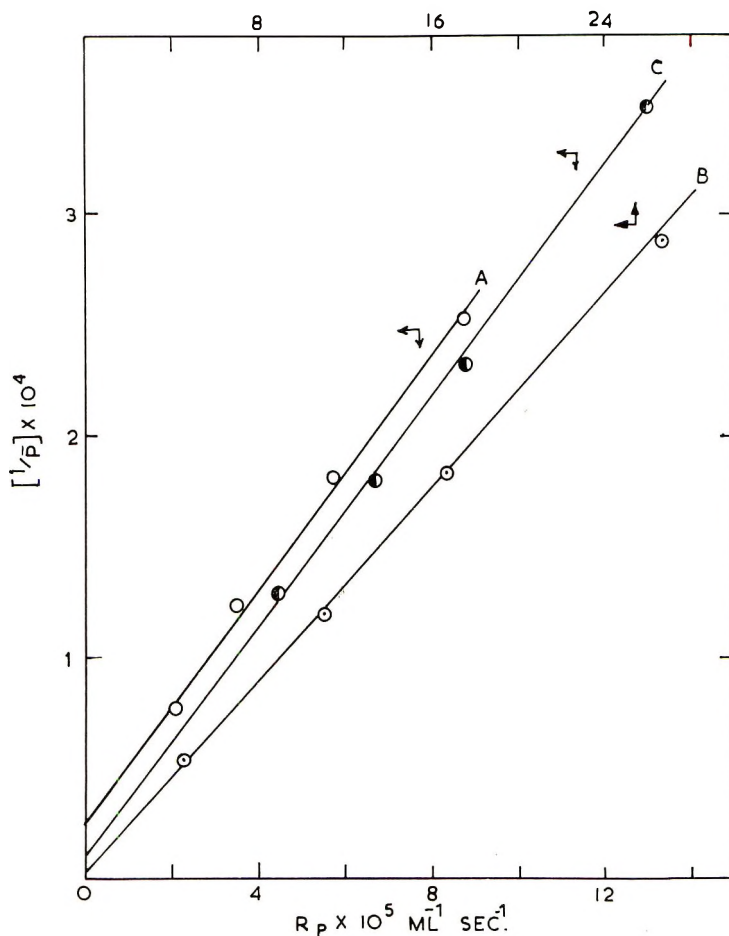


Fig. 4. Reciprocal degree of polymerization vs  $R_p$  (60°C): (A) in chloroform; (B) in DMSO; (C) in methanol. Methyl methacrylate concentration, 4.65 mole/l.

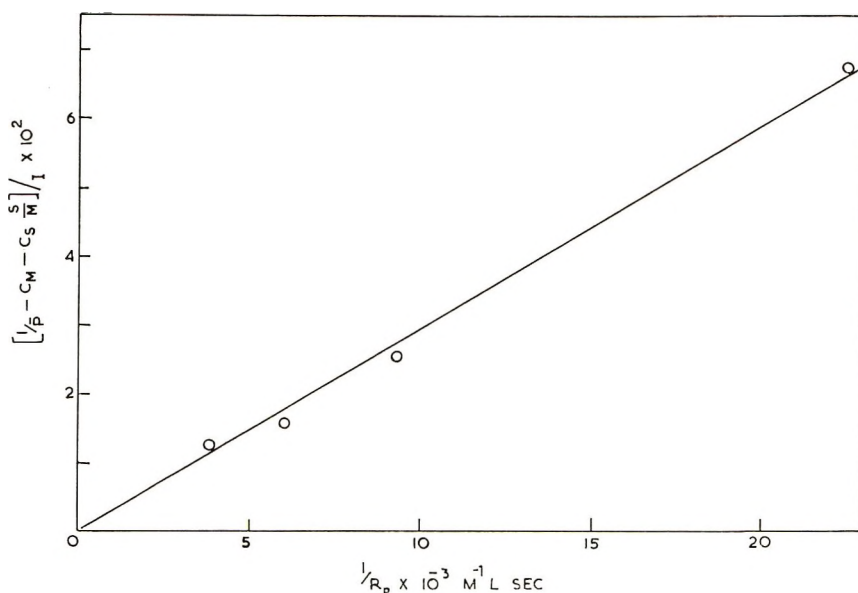


Fig. 5. Evaluation of initiator transfer constant of ABA (60°C; 4.65 mole/l. methyl methacrylate in DMSO).

made to evaluate  $C_I$  in DMSO which has a very low transfer and also is a good solvent for ABA. The general equation for the number-average degree of polymerization ( $\bar{P}_n$ ) can be written as

$$\frac{1}{\bar{P}_n} = C_M + C_S([S]/[M]) + C_I([I]/[M]) + R_p(\delta^2/[M^2]) \quad (3)$$

where  $C_M$ ,  $C_S$ ,  $C_I$  are chain transfer constants for monomer (M), solvent (S) and initiator (I), respectively. The equation can be written

$$\frac{1}{\bar{P}_n} = C_M + C_S([S]/[M]) + C_I([I]/[M]) + k_d f [I]/R_p \quad (4)$$

where  $k_d$  and  $f$  are the rate constant for decomposition and efficiency of the initiator, respectively.  $C_I$  was obtained<sup>14</sup> from the intercept of the plot of  $\{(1/\bar{P}_n) - C_M - C_S([S]/[M])\}/[I]$  versus  $1/R_p$ . The value of  $0.71 \times 10^{-5}$  for  $C_S$  for DMSO has been determined from work carried out in this laboratory and has been reported in an earlier publication.<sup>15</sup> The value of  $C_M (1 \times 10^{-5})$  has been taken from the work of Baysal and Tobolsky.<sup>18</sup> In the present case the straight line obtained passed through the origin indicating the value of  $C_I$  to be almost zero (Fig. 5).

The value of  $\delta$  could be obtained from the slope of the plot of  $1/\bar{P}_n$  against  $R_p$  at a fixed monomer concentration (Fig. 4). A value of 7.7 was obtained in experiment carried out at 4.65 mole/l. monomer concentration in chloroform and methanol. In DMSO under otherwise identical conditions and monomer concentration this value obtained was as low as 4.8, a value com-



parable to 4.65 obtained from AIBN-initiated polymerization in the same solvent-monomer mixture.<sup>15</sup>

By utilizing the value of  $\delta$  just obtained the rate of initiation  $R_i$  ( $R_p^2 = / [M^2]\delta^2$ ) has been calculated (Table I). Since  $R_i = 2k_d f[I]$  the product of

TABLE I  
Evaluation of  $\delta$ ,  $R_i$ , and  $fk_d$  at 60°C at  
MMA Concentration of 4.65 mole/l.

Solvent	[I] × 10 <sup>3</sup> , mole/l.	$R_p \times 10^6$ , mole/l.- sec.	$(1/\bar{P}_n) \times 10^4$	$\delta$ , (mole- sec/l.) <sup>1/2</sup>	$R_i \times 10^8$ , mole/l.- sec	$R_i/2[I]$ × 10 <sup>6</sup> , ( $fk_d$ ), sec <sup>-1</sup>
Chloroform	4.44	2.03	0.7649	7.7	0.1089	1.197
	15.43	3.43	1.235		0.3033	0.9824
	44.44	5.65	1.818		0.8422	0.9484
	98.49	8.77	2.519		2.031	1.030
Methanol	5.05	4.41	1.289	7.7	0.512	5.059
	11.60	6.73	1.799		1.224	5.273
	21.30	8.81	2.334		2.048	4.808
	51.80	12.97	3.484		4.442	4.287
DMSO	5.30	4.45	0.542	4.81	0.212	2.001
	52.98	10.84	1.182		1.257	1.188
	105.90	16.62	1.830		2.955	1.395
	211.90	26.65	2.867		7.600	1.794

the efficiency and the rate of decomposition of the initiator,  $fk_d$  could be obtained from  $R_i$ . Of course the value of  $R_i$  is an average value from beginning to end, considering the low reaction time required for dilatometry and very low decomposition rate of the initiator, the initiator concentration used in the present calculation was the initial value and not its arithmetic mean.

### Decomposition of ABA

Hammond et al. reported that during the thermal decomposition of ABA in DMSO ammonia was evolved along with nitrogen. On the other hand, spectrophotometric assay at the azo absorption peak was not possible due to the formation of certain interfering elements which increased the optical density at the wavelength concerned. However, to have a comparative study we have determined the decomposition rates of ABA in methanol and chloroform by monitoring the evolved gas from time to time (Fig. 6). The actual values which could be obtained by calculating the nitrogen alone might be a bit low due to the possibility of evolution of ammonia. We obtained values for  $k_d$  of  $1.45 \times 10^{-6}$  and  $0.71 \times 10^{-6}$  in methanol and chloroform, respectively, at 60°C. The values are quite comparable to the value ( $3.68 \times 10^{-6}$  sec<sup>-1</sup> in DMSO at 70°C) obtained by Hammond and Newman.<sup>3</sup>

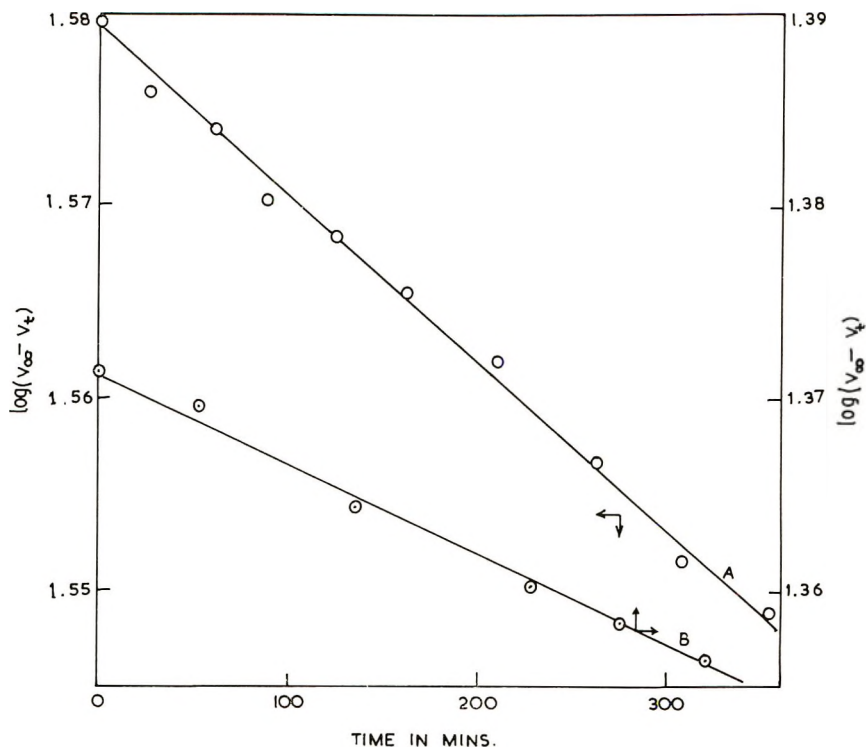


Fig. 6. Determination of the rate of decomposition of ABA: (A) in methanol; (B) in chloroform.

## DISCUSSION

Equation (1) for the rate of polymerization can be represented as  $R_p = \text{const.} (k_{df})^{1/2} [I^{1/2}]$  at constant monomer concentration. The comparatively wide difference in the slopes of the plot of  $R_p$  versus  $[I^{1/2}]$  at constant  $[M]$  in chloroform and methanol is possibly due to the difference in the value of  $(k_{df})$ ; if  $f$  is assumed to be constant this would mean a difference in the decomposition rates of the initiator ABA. As it has been shown that ABA decomposes more readily in methanol than in chloroform, the value of the slope in methanol will be greater than that in chloroform as long as  $\delta$  and  $f$  remain constant. The comparatively low slope in DMSO is probably due to the low value of  $\delta$  as was observed with AIBN<sup>15</sup> also but this does not rule out the possibility that the rate of decomposition of ABA might also be different in this solvent. The passing of the linear plot of  $R_p$  versus  $[I^{1/2}]$  through the origin is concordant with the observation that there is no appreciable induction period on the polymerization of methyl methacrylate with this initiator.

In solutions of chloroform, the order of reaction with respect to monomer concentration was very near to unity, but in DMSO and methanol

$R_p$  increased with increasing concentration of monomer, passed through a maximum, and then decreased. The latter observation probably indicates that the factors responsible for the variation of  $R_p$  with the concentration of the solvent in both methanol and DMSO are identical, although methanol is a precipitant for the polymer while DMSO is not so. The effect, therefore, might be for various reasons: (a) the production of radical from ABA is higher in these solvents than in the monomer itself; (b) the termination rate is decreased from coiling of the polymer or similar effect.

In the first case of higher rate of decomposition of ABA in methanol or DMSO, addition of solvent at high concentration of the monomer could substantially enhance the rate of radical production thereby enhancing the rate of polymerization. At the same time, as  $R_p$  is dependent on the monomer concentration, one should expect  $R_p$  to be decreasing due to dilution effect. If both these effects do operate one would observe a balance between the two effects. If the enhancement of  $R_p$  due to addition of solvent at high monomer concentration exceeds the dilution effect we would observe increase in the overall  $R_p$ . The subsequent fall above a critical concentration would be observed when the dilution effect would be much more effective than the increase in  $R_p$  due to higher decomposition rate. Of course the possibility of primary radical termination cannot be completely ruled out.

On the other hand the enhancement of  $R_p$  with the addition of solvent very near to bulk concentration of the monomer cannot be due to decreased termination rate owing to coiling of the polymer chain in the presence of a nonsolvent (methanol). This is because in these systems the monomer concentration is sufficiently high to prevent such coiling. At the same time no such effect can possibly be expected to occur in the case of DMSO which is a solvent for the polymer. Further, such reduced termination rate would result in higher molecular weight with higher  $R_p$ . On the contrary, the degree of polymerization decreased, as is usually observed with increasing solvent concentration. In fact with identical concentration of monomer and ABA,  $R_p$  in methanol is much higher than that in chloroform. This difference in  $R_p$  in the methanol and chloroform is virtually absent if the initiator is replaced by AIBN as shown later. From all these factors it seems that the increase in  $R_p$  with the addition of solvent at high monomer concentration is due to higher rate of radical production from ABA.

In DMSO the situation is more complicated in view of the decrease of the value of  $\delta$  with increasing concentration of DMSO as has been observed with AIBN-initiated polymerization of methyl methacrylate<sup>15</sup> in which after an initial linear plot a plateau was obtained in the range 70–95% of monomer (MMA) concentration. On the contrary, with ABA as initiator  $R_p$  steadily rose with DMSO concentration rather than remaining constant. This undoubtedly indicated the possibility of enhanced rate of radical production with increasing DMSO concentration.

The possibility of increased rate of decomposition of ABA in methanol is also supported by the activation parameter. The activation energies of the decomposition of ABA in chloroform and methanol are 21.6 and 18.4 kcal/mole, respectively, as obtained from the polymerization experiments, indicating that the decomposition of ABA is energetically more favored in methanol than in chloroform.

The knowledge of the rate of initiation of a polymer chain  $R_i$  has been utilized in evaluating the efficiency factor  $f$  and  $k_d$  the unimolecular rate constant for decomposition of ABA. If the  $k_d$  values as obtained from nitrogen monitoring method by Hammond et al.<sup>3</sup> or by us be inserted in this equation the efficiency factor  $f$  comes out to be higher than unity, which is rather absurd. Consequently the value of  $f$  obtained by Hammond et al. from oxidation studies has been used, and the value of  $k_d$  obtained therefrom is quite high in comparison with the experimental values of  $k_d$ . This points to two alternatives; either all the nitrogen is not evolved in the decomposition, i.e., there is retention of nitrogen of the azo group to at least a part of the radicals which are formed by stepwise breakage of the C—N bond (unlike the simultaneous breakage of both the C—N bonds reported in cases of most azonitriles), or ABA can produce free radicals in some other way without the decomposition of the azo group.

The plot of  $1/\bar{P}_n$  versus  $R_p$  used in the determination of  $\delta$  did not pass through the origin. The intercept is a measure of the transfer to monomer  $C_M$  and the transfer to solvent  $C_S$  and decreased in the order, chloroform > methyl alcohol > DMSO. If  $C_M$  is known to be a constant ( $1 \times 10^{-5}$  at 60°C), this order can be taken as a guide for the values of  $C_S$  for these solvents and is in the same order as reported in the literature,<sup>15,16,19</sup> i.e.,  $4.54 \times 10^{-5}$ ,  $2 \times 10^{-5}$ , and  $0.71 \times 10^{-5}$  for chloroform, methyl alcohol, and DMSO, respectively.

In accordance with other azo initiators, ABA does not seem to have any perceptible transfer reaction under the present experimental conditions.

#### **Action of Solvent on the Polymerization Rates of Methyl Methacrylate Initiated by ABA**

It was observed that solvents have a pronounced effect on the rate of polymerization of methyl methacrylate initiated by ABA. The values of  $R_p$  in different solvents at fixed concentrations of the monomer and ABA are given in Table II. AIBN is well known to be insensitive to solvent variation, and hence for comparison  $R_p$  observed under identical conditions in methanol and chloroform initiated by AIBN are also shown in Table II. As AIBN did not show any marked difference in the rate of polymerization in solvents of widely divergent character, variations observed with ABA can possibly be attributed to the variation of the rate of decomposition of ABA in the solvents concerned.

The variation of the rate of polymerization in different solvents can be explained in the light of the protonating power of a solvent. Hammond et al.<sup>3</sup> found that on protonation of the amidine by an acid the rate of de-

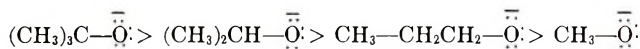
TABLE II  
 Dependence of  $R_p$  on the Nature of the Solvent<sup>a</sup>

Solvent	$R_p \times 10^5$ , mole/l.-sec	Intrinsic viscosity $[\eta]$ (benzene, 35°C), dl/g
Dimethyl sulfate	11.99	2.16
Dimethyl sulfoxide	5.00	3.75
Methanol	7.10	1.88
Ethanol	5.63	2.18
Butanol	5.14	2.78
Chloroform	3.30	3.03
Acetone	2.69	3.06
Dimethylformamide	4.24	—
Benzene (9.16%) + methanol (8.4%)	3.75	—
Chloroform (9.34%) + methanol (6.6%)	3.67	2.72
Methanol <sup>b</sup>	7.04	—
Chloroform <sup>b</sup>	6.97	—

<sup>a</sup> Concentration of ABA in all the cases except as noted was  $1.23 \times 10^{-3}$  mole/l.

<sup>b</sup> The initiator was AIBN,  $1.39 \times 10^{-3}$  mole/l.

composition of the azo compound was enhanced considerably. A similar type influence though to a much lower extent, may be produced by an electrophilic solvent which will solvate the basic amidine group, causing a decrease in the energy of the transition state. It is found that the rate of polymerization increased with the increase of the acidity of the solvents or with the increase of the solvation power of the solvent to the initiator. As the basic ABA is electron-donating it will be solvated more and more easily with increasing electrophilicity of the solvents. In case of the following solvents the electrophilic character decreases in the following order: water > methanol > ethanol > butanol > acetone. The base strength decreases as follows,



In accordance with the above explanation it is observed that the  $R_p$  in the solvents concerned increases in the same order as the increase of the acidity of the solvent. Hence, in all probability, the major cause for the variation in the rate of polymerization can be attributed to the variation in the decomposition rate of ABA as was actually measured with methanol and chloroform.

A more direct measurement of the relative protophilic properties can be obtained from the values of hydrogen ion conductances in different solvents under identical conditions. The conductance of an ion under the same electrical influence is a measure of its speed in the solvent. This in turn will depend on the viscosity of the solvent and the volume of the ion, i.e., the extent of solvation of the ion. The higher the protophilic nature or less

TABLE III  
Dependence of  $R_p$  on  $\lambda_0\mu$

Solvent	$\lambda_0\mu$ at 25°C, <sup>a</sup> poise-cm <sup>2</sup> /ohm	$R_p \times 10^4$ , mole/l.-sec.	$\lambda_0\mu/R_p \times 10^{-4}$
Water	3.14	—	—
Methanol	0.77	0.7095	1.085
Ethanol	0.64	0.5628	1.137
Acetone	0.28	0.2692	1.040

<sup>a</sup> Data of Glasstone.<sup>20</sup>  $\lambda_0$  is the equivalent conductance of hydrogen ion at infinite dilution (in cm<sup>2</sup>/ohm) and  $\mu$  is the viscosity of the solvent in poise.

the electrophilic character of the solvent, the higher the solvation of the hydrogen ion and the less the value of the product of hydrogen ion conductance and viscosity ( $\lambda_0\mu$ ). It can be seen from Table III that the rate of polymerization varied almost directly with the product of hydrogen ion conductance and viscosity in solvents whose  $\lambda_0\mu$  could be collected. This proves the role of electrophilic nature of the solvent on the variation of the  $R_p$  with the present initiator, probably on account of its increased rate of decomposition with the increasing solvating power of the solvent to the basic initiator.

### References

1. R. W. Upson (to Du Pont), U. S. Pat. 2,599,299 (1952).
2. J. J. Dougherty, *J. Amer. Chem. Soc.*, **83**, 4849 (1961).
3. G. S. Hammond, and J. Newman, *J. Amer. Chem. Soc.*, **85**, 1501 (1963).
4. G. Henri and G. Dekking, *J. Appl. Polymer Sci.*, **9**(5), 1641-51 (1965).
5. G. Henri and G. Dekking, U. S. Pat. 3,208,984 (1965); *Chem. Abstr.*, **63**, 18384f (1965).
6. G. Henri and G. Dekking, U. S. Pat. 3,285,907 (1967); *Chem. Abstr.*, **67**, 43439a (1967).
7. J. W. Breitenbach and K. Kuchner, *Monatsh Chem.*, **97**, 662 (1966).
8. A. Weissberger and E. S. Proskauer, Eds., *Organic Solvents Technique of Organic Chemistry*, Vol. VII, Interscience, New York, 2nd ed., 1955.
9. J. L. Bolland, *Proc. Roy. Soc. (London)*, **A186**, 218 (1946).
10. T. G. Fox, J. B. Kinsinger, H. F. Mason, and E. M. Schuele, *Polymer*, **3**, 71 (1962).
11. A. Conix and G. Smets, *J. Polym. Sci.*, **10**, 525 (1953).
12. L. M. Arnett, *J. Amer. Chem. Soc.*, **74**, 2027 (1952).
13. G. V. Schulz and E. Husemann, *Z. Physik. Chem.*, **B39**, 246 (1938).
14. U. S. Nandi and S. R. Palit, paper presented at International Symposium on Macromolecules, Milano, 1954; *Ric. Sci.* **25** (1955).
15. S. N. Gupta and U. S. Nandi, *J. Polym. Sci. A-1*, in press.
16. R. N. Chadha, J. S. Shukla, and G. S. Misra, *Trans. Faraday Soc.*, **53**, 240 (1957).
17. M. S. Matheson, E. E. Auer, E. B. Bevilacqua, and E. J. Hart, *J. Amer. Chem. Soc.*, **71**, 497 (1949).
18. B. Baysal and A. V. Tobolsky, *J. Polym. Sci.*, **8**, 529 (1952).
19. B. Bhattacharyya and U. S. Nandi, unpublished results from this Laboratory.
20. S. Glasstone, *Textbook of Physical Chemistry*, 2nd Ed., 1956, p. 897.

Received December 30, 1969

## NOTES

***Polymerization of Vinyl Chloride and Copolymerization with  
Ethylene Catalyzed by Triethylaluminum-Cuprous  
Chloride-Carbon Tetrachloride***

## INTRODUCTION

Polymerization of vinyl chloride catalyzed by organometallic compounds has been carried out by many authors.<sup>1,2</sup> Recently, polymerizations of vinyl chloride with  $\text{AlEt}_3\text{-THF-CCl}_4$  and phenyltitanium- $\text{CCl}_4$  were reported by Breslow et al.<sup>3</sup> and Razuvayev et al.<sup>4,5</sup> as polymerization catalysts. Yamazaki et al.<sup>6</sup> and Azuma et al.<sup>7</sup> carried out polymerization of vinyl chloride by using  $\text{Ti}(\text{OBu})_4\text{-AlEtCl}_2$  or  $\text{Ti}(\text{OBu})_4\text{-AlEtCl}_2\text{-CCl}_4$  and  $\text{AlEt}_2(\text{OCH}_2\text{-CH}_2\text{X})\text{-VOCl}_3$  (where X is a halogen,  $\text{NR}_2$ ) catalyst.

In the present investigation, polymerization of vinyl chloride was accomplished with  $\text{AlEt}_3\text{-CuCl}$  catalyst, which was reported in a previous paper<sup>8</sup> on the polymerization and copolymerization of the other monomers. However, this catalyst had been also used by Furukawa et al.<sup>9</sup> in vinyl chloride polymerization. The present authors found that  $\text{AlEt}_3\text{-CuCl-CCl}_4$  catalyst was extremely effective for vinyl chloride polymerization, and the catalyst was used for copolymerization of vinyl chloride with ethylene also.

Copolymerization by other methods has been extensively reported in the literature.<sup>10-17</sup>

## EXPERIMENTAL

In a 40-cc stainless steel autoclave, an ampoule containing an *n*-hexane solution of the reaction product (black-brown precipitate) of cuprous chloride with triethylaluminum was placed. Then at Dry Ice temperature the given quantity of vinyl chloride was charged into the autoclave and flushed with nitrogen stream. After the lid of autoclave closed the ampoule was broken by a steel ball in the ampoule and the polymerization was carried out. The polymerization product was poured into methanol containing a small quantity of hydrochloric acid and the precipitate was washed repeatedly with methanol.

In ethylene-vinylchloride copolymerization, after charging of vinyl chloride, ethylene charged into the autoclave. The quantity of ethylene charged was determined by weighing.

The chlorine content of the copolymer product was determined by the combustion flask method.

## RESULTS

The results of polymerization of vinyl chloride catalysed by the triethylaluminum-cuprous chloride-carbon tetrachloride system are tabulated in Table I. Results for copolymerization of ethylene with vinyl chloride are summarized in Tables II and III.

Figure 1 shows the composition curve of ethylene-vinyl chloride copolymerization. It was found that the copolymerization rate decreased as the quantity of ethylene in the monomer mixture increased, a fact already established in copolymerizations by the other methods.<sup>10-12</sup>

TABLE I  
 Polymerization of Vinyl Chloride by  $\text{AlEt}_3\text{-CuCl}$  Catalyst at  $20^\circ\text{C}$  (Solvent, *n*-Hexane, 5 cc)

No.	VCl <sub>2</sub> g	$\text{AlEt}_3$ , mole	CuCl, mole	$\text{CCl}_4$ , cc	Polymer yield, g	Polymeriz. time, hr	Inherent viscosity (THF, $30^\circ\text{C}$ )
1	16	0.0012	0.00099	0	2.03	17	
2	21	"	"	0	1.84	15	
3	22	"	"	0.5	Quantitative	19	
4	25	"	"	0.2	Quantitative	19	1.35
5	22	"	"	1.0	Quantitative	19	1.37
6	23	"	"	1.5	Quantitative	19	1.30
7	21	$\text{AlEt}_2\text{Cl-}$ $\text{AlEt}_3$					
		(0.00148: 0.00122)					
8	15	0.0012	0.00099	0	2.91	19	
			CuCl <sub>2</sub> : 0.00039	0	0.796	20	
9	15	"	"	0.2	7.17	20	



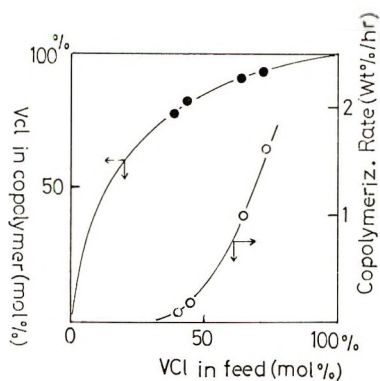


Fig. 1. Plots of (●) VCl in copolymer vs. VCl in feed and (○) copolymerization rate vs. VCl in feed in copolymerization with ethylene catalyzed by  $\text{AlEt}_3\text{-CuCl}$  in the presence of 0.2 cc  $\text{CCl}_4$ .

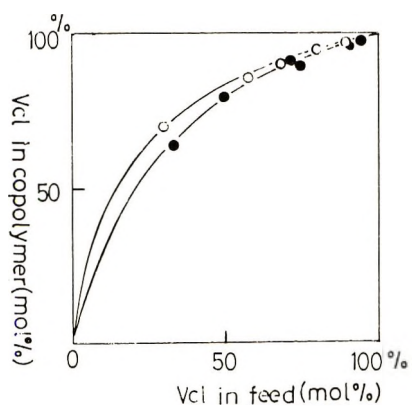


Fig. 2. Plots of VCl in copolymer vs. VCl in feed in copolymerization with ethylene catalyzed by  $\text{AlEt}_3\text{-CuCl}$  in the presence of 1.0 cc  $\text{CCl}_4$ : (○) this work; (●) data of Burkhardt and Zutty.<sup>16</sup>

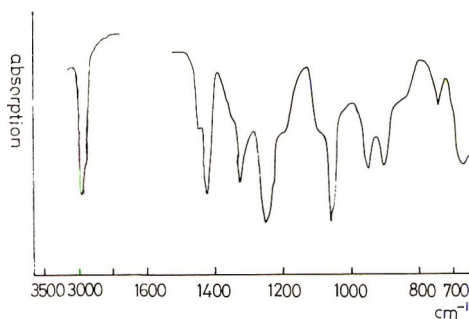


Fig. 3. Infrared spectrum of ethylene-vinyl chloride copolymer (sample 4 of Table III).

TABLE II  
Copolymerization of Ethylene with Vinyl Chloride by  
AlEt<sub>3</sub>-CuCl-CCl<sub>4</sub> Catalyst at 20°C for 20 hr<sup>a</sup>

No.	Monomers charged		Polymer, g	Conversion %	Copoly- merization rate, wt-% hr	Inherent viscosity (THF, 30°C)
	VCl, mole	Ethylene, mole				
1	0.304	0	Quantitative	100		1.30
2	0.336	0.143	7.90	31.6	1.58	0.58
3	0.256	0.143	3.72	18.6	0.93	0.51
4	0.176	0.250	0.89	4.9	0.25	0.32
5	0.160	0.250	0.13	0.76	0.038	0.27

TABLE III  
Copolymerization of Vinyl Chloride with Ethylene by AlEt<sub>3</sub>-CuCl-CCl<sub>4</sub>  
Catalyst at 20°C for 22 hr<sup>a</sup>

No.	Monomers charged		Polymer, g	Conversion, %
	VCl, mole	Ethylene, mole		
1	0.38	0.0357	5.1	19.6
2	0.304	0.0714	2.98	14.2
3	0.32	0.142	1.30	13.0
4	0.222	0.161	2.55	13.8
5	0.079	0.180	2.28	22.8
6	0.064	0.214	b	—

<sup>a</sup> Reaction conditions: AlEt<sub>3</sub>, 0.00122 mole; CuCl, 0.00099 mole; CCl<sub>4</sub>, 1.0 cc, solvent, *n*-hexane, 5 cc.

<sup>b</sup> Small quantity of sticky material.

An increase in quantity of carbon tetrachloride did not affect the composition of the copolymer, as shown in Figure 2. That is, the curves in Figures 1 and 2 were identical. It should be noted that these composition curves were similar to those obtained by Burkhardt and Zutty<sup>16</sup> for copolymerizations at high pressure.

The infrared spectrum of an ethylene-vinyl chloride copolymer is shown in Figure 3 and at 745 cm<sup>-1</sup>. The absorption due to the -CH<sub>2</sub>-CH<sub>2</sub>-CHCl- group<sup>10</sup> is evident. The results in the present experimental and the previous paper<sup>8</sup> indicate that AlEt<sub>3</sub>-CuCl or AlEt<sub>3</sub>-CuCl-CCl<sub>4</sub> catalysts may act as radical initiators. The initiation mechanism will be described in a future publication.

#### References

1. G. E. Ham, *Vinyl Polymerization*, Vol. 1, Part 1, Dekker, New York, 1967, p. 353.
2. L. Reich and A. Schindler, *Polymerization by Organometallic Compounds*, Wiley, New York, 1966, pp. 175, 438, 439, 661.
3. D. S. Breslow, D. L. Christman, H. H. Epsy, and C. A. Lukach, *J. Appl. Polym. Sci.*, **11**, 73 (1967).
4. G. A. Razuvaev, K. S. Minsker, V. N. Latiaeva, and Yu. A. Sangalov, *Dokl. Akad. Nauk SSSR*, **163**, 906 (1965).
5. K. S. Minsker, Yu. A. Sangalov, and G. A. Razuvayev, in *Macromolecular Chemistry, Prague (1965)* *J. Polym. Sci. C*, **16**, O. Wichterle and B. Sedláček, Eds., Interscience, New York, 1967, p. 1489.

6. N. Yamazaki, K. Sasaki, and S. Kambara, *Kogyo Kagaku Zasshi*, **68**, 881 (1965).
7. H. Azuma, K. Watabe, and S. Namikawa, *J. Polym. Sci. B*, **5**, 1125 (1967); *Kogyo Kagaku Zasshi*, **71**, 560 (1968).
8. W. Kawai, M. Ogawa, and T. Ichihashi, paper presented at 23th Meeting of Japanese Chemical Society, April 1970.
9. J. Furukawa, T. Tsuruta, and S. Shiotani, *J. Polym. Sci.*, **40**, 237 (1959).
10. A. Misono and Y. Uchida, *Bull. Chem. Soc. Japan*, **40**, 2366 (1967).
11. A. Misono and Y. Uchida, *Bull. Chem. Soc. Japan*, **39**, 2458 (1966).
12. B. Erussalimsky, N. Tumarkin, F. Duntoff, S. Lyubetzky, and A. Goldenberg, *Makromol. Chem.*, **104**, 288 (1967).
13. T. Otsu, T. Lai, Y. Kinoshita, A. Nakamachi, and M. Imoto, *Kogyo Kagaku Zasshi*, **71**, 904 (1968).
14. Ethyl Corporation, Japanese Pat. 44-2474 (1969).
15. T. Otsu, Y. Kinoshita, and A. Nakamachi, *Makromol. Chem.*, **115**, 275 (1968).
16. R. D. Burkhart and N. L. Zutty, *J. Polym. Sci. A*, **1**, 1137 (1963).
17. M. Hagiwara, T. Miura, and T. Kagiya, *J. Polym. Sci. A-1*, **7**, 513 (1969).

WASABURO KAWAI  
MASAJI OGAWA  
TAICHI ICHIHASHI

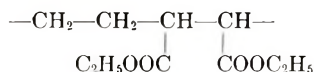
Government Industrial Research Institute  
Osaka, Japan

Received March 11, 1970

Revised May 1, 1970

**Solubility Parameter of Ethylene-Diethyl  
Fumarate Copolymer**

We have prepared a copolymer of ethylene and diethyl fumarate believed to have an alternating structure and determined its solubility parameter  $\delta$  to be 9.5 by the method of maximum intrinsic viscosity.<sup>1</sup> This agrees very well with a value of 9.35 reported<sup>2</sup> for poly(ethyl acrylate). The closeness of the  $\delta$  values of these two systems is interesting if one compares the structural features. The repeating unit of an alternating copolymer of ethylene and diethyl fumarate is the following:



It is identical to a homopolymer of ethyl acrylate in which the monomers are linked in a head-to-head fashion. The close agreement of the  $\delta$  values of these two systems suggests that: (1) the polymer-solvent interaction of poly(ethyl acrylate) is the same whether the monomers are linked in a head-to-head or head-to-tail fashion; (2) the solution properties and solvent resistance of an alternating copolymer of ethylene-diethyl fumarate and of poly(ethyl acrylate) are very similar.

**EXPERIMENTAL**

**Preparation of the Copolymer**

A mixture of 330 g (11.8 g mole) of ethylene, 86.1 g (0.5 mole) of diethyl fumarate, 1 g of benzoyl peroxide, 50 ml of benzene, and 200 ml of water in a one-liter autoclave was heated at 60°C, with agitation, for 5 hr. The maximum pressure was 4500 psig. The product, weighing 104.8 g, was a tough elastomer. The copolymer was purified by dissolving in toluene followed by precipitation in petroleum ether.

ANAL. Calcd for 1:1 copolymer: C, 59.98%; H, 8.05%. Found: C, 60.29%; H, 7.96%.

Since under the reaction conditions it was considered unlikely that fumarate units would link together, we assumed that the product was an alternating copolymer. Although some published reactivity ratios show that fumarate radical does add to diethyl fumarate under some conditions, those data were obtained at much higher temperature (150°C).<sup>3</sup>

TABLE I  
Intrinsic Viscosity in Various Solvents

Solvent	Solubility parameter $\delta$ , (cal/cc) <sup>1/2</sup>	Intrinsic viscosity $[\eta]$ at 30°C, dl/g	
		Ethylene-diethyl fumarate	Poly(ethyl acrylate)
Butyl acetate	8.55	0.215	0.211
Toluene	8.90	0.236	—
Ethyl acetate	9.05	0.238	—
Ethyl formate	9.40	0.340	0.316
Chloroform	9.54	0.349	—
Methyl acetate	9.60	0.231	0.217
Ethyl benzoate	9.70	0.231	0.239
Acetone	9.84	0.218	—
Chlorobenzene	10.07	0.238	—
Diethyl malonate	10.3	0.215	0.214

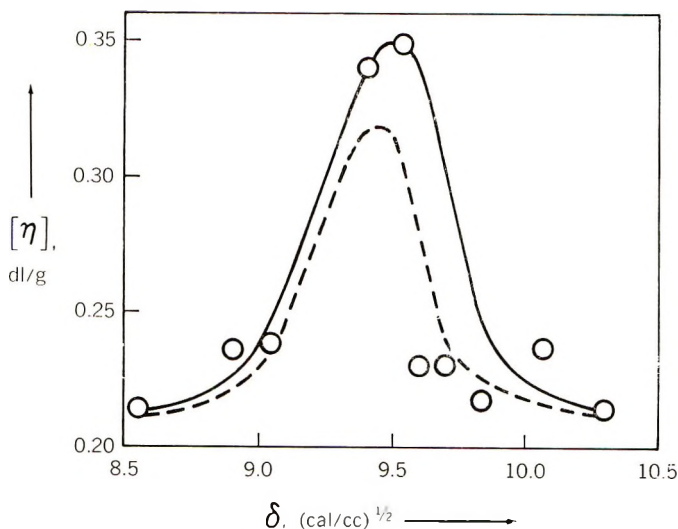


Fig. 1. Intrinsic viscosity  $[\eta]$  of a 1:1 copolymer of ethylene and diethyl fumarate as a function of the solubility parameter  $\delta$  of the solvent; (---) curve for a low molecular weight polymer of ethyl acrylate.

#### Determination of Solubility Parameter

The method of Mangaraj<sup>1</sup> was followed. The solvents in which the intrinsic viscosities were determined, their  $\delta$  values, and the measured intrinsic viscosities are listed in Table I. Some data obtained for an ethyl acrylate polymer of low molecular weight prepared in our laboratory are also shown for comparison.

The plot of intrinsic viscosity versus solubility parameter is shown in Figure 1. From the graph, the  $\delta$  value of the copolymer was estimated to be 9.5. This agrees very well with a value of about 9.4 for poly(ethyl acrylate) determined by the same method (broken line).

Mangaraj et al.<sup>4</sup> have also determined the solubility parameter of poly(vinyl propionate), which is isomeric with the polymers described above. Their  $\delta$  values from maximum intrinsic viscosity range from 8.8 to 8.9. They are lower than those of poly(ethyl acrylate), 9.35–9.40, but about the same as for propyl acetate (8.75) or ethyl propionate (8.90–8.95).

#### References

1. D. Mangaraj, S. K. Bhatnagar, and S. B. Rath, *Makromol. Chem.*, **67**, 75 (1963).
2. D. Mangaraj, S. Patra, and S. B. Rath, *Makromol. Chem.*, **67**, 84 (1963).
3. F. E. Brown and G. E. Ham, *J. Polym. Sci. A*, **2**, 3623 (1964).
4. D. Mangaraj, S. Patra, P. C. Roy, and S. K. Bhatnagar, *Makromol. Chem.*, **84**, 225 (1965).

A. J. YU\*  
R. H. GOBRAN  
R. F. FOERSTER

Thiokol Chemical Corporation  
Trenton, New Jersey 08607

Received April 2, 1970

\* Present address: Stauffer Chemical Co., Dobbs Ferry, N. Y.

## ERRATUM

### **Polymerization of Epoxides with Dialkylaluminum Acetylacetonate Catalyst Systems**

IRVING KUNTZ and W. R. KROLL

[article in *J. Polym. Sci. A-1*, **8**, 1601 (1970)]

Page 1602, last line: the correct index of refraction for allyl glycidyl ether is  $n_D^{20}$  1.4348.

# Selected Titles in Polymer Technology from Wiley-Interscience

## POLYMER CHEMISTRY OF SYNTHETIC ELASTOMERS

Edited by JOSEPH P. KENNEDY and ERIK G. M. TÖRNQVIST, both at the Esso Research and Engineering Company

Parts 1 and 2 of Volume 23 of the High Polymer series, edited by H. Mark, S. Marvel, H. W. Melville, and P. J. Flory

"The contributing authors, all well-known and experts in their fields, have handled their topics well...the excellent organization of the material makes it a valuable treatise on elastomers..."

—Record of Chemical Progress

"The two volumes taken together represent an excellent review of the rapidly advancing field of synthetic elastomers."

—SPE Journal

"This publication is a must for anyone who is involved with polymer formation."

—Rubber Chemistry & Technology

### PART I

Contents: Structure-Property Relationships for Elastomeric Materials—W. R. Krigbaum and J. V. Dawkins. The Historical Background of Synthetic Elastomers with Particular Emphasis on the Early Period—Erik G. M. Törnqvist. The Status and Future of Elastomer Technology, 1966—G. Alliger and F. C. Weissert. Elastomers by Radical and Redox Mechanisms: Butadiene-Styrene Rubbers (SBR) and Rubbers from Substituted Butadienes and Styrenes—C. A. Uraneck. Nitrile Rubber and Other Nitrogen-Containing Rubbers Except Polyurethanes—W. Hofmann. Neoprene—C. Hargreaves. Acrylic Elastomers—H. A. Tucker and A. H. Jorgensen. Fluorine-Containing Elastomers—J. R. Cooper. Elastomers by Cationic Mechanisms: Polyisobutene and Butyl Rubber—J. P. Kennedy. Poly (vinyl Ethers)—J. Lal. Elastomers from Cyclic Ethers—A. Ledwith and C. Fitzsimmonds. Elastomeric Polyacetals—O. Vogl. Author Index. Subject Index.

### PART II

Contents: Elastomers from Catalysts of the Alkali Metals—L. E. Forman. Elastomers by Coordinated Anionic Mechanism: Diene Elastomers—G. Natta and L. Porri. Ethylene-Propylene Rubbers—G. Natta, A. Valvassori, and G. Sartori. Elastomers from Cyclic Olefins—G. Natta and G. Dall'Asta. Elastomers by Condensation Polymerization: Polyurethane Elastomers—J. H. Saunders. The Chemistry of Silicone Elastomers—F. M. Lewis. Polysulfide and Monosulfide Elastomers—R. H. Gobran and M. B. Berenbaum. Elastomers by Miscellaneous or Unknown Mechanisms: Liquid Rubbers—J. Furukawa, S. Yamashita, and S. Ido. Catalysis by Transition Metals Salts in Water and Other Polar Solvents—R. E. Rinehart. Poly(thiocarbonyl Fluoride) and Related Elastomers—W. H. Sharkey. Elastomers by Postpolymerization Techniques: Halogenation—H. S. Makowski. Cyclized and Isomerized Rubber—M. A. Golub. Author Index for Part II. Cumulative Subject Index for Parts I and II.

Part I 1968 490 pages \$25.00  
Part II 1969 554 pages \$27.50

## ENVIRONMENTAL EFFECTS ON POLYMERIC MATERIALS

Edited by DOMINICK V. ROSATO, Technical Editor, Plastics World and Engineering Consultant, and ROBERT T. SCHWARTZ, Chief, Nonmetallic Materials Division, Air Force Materials Laboratory, Dayton

Two Volumes in the Polymer Engineering and Technology series: Executive editor, D. V. Rosato

This two-volume set fulfills an important, growing need for more information on the degradation of materials. Industrial and academic experts have contributed reviews and data concerning major developments in protective polymers. The reviews cover different environments, materials, processing, testing, service life, fundamentals of degradation, rheology, design criteria, material selection, and technical business decision related to the overall subject. The volumes provide an ideal reference set for those in research, engineering, marketing, buying, and management who use plastics. They are invaluable for those developing new equipment and finding new uses for plastics.

### VOLUME I: ENVIRONMENTS

Contents: An Introduction to the Plastics Industry—W. Skinner and J. D. Goldhar. Cavitation Erosion—D. H. Kallas and J. Z. Lichtman. Rain Erosion—N. E. Wahl. Weathering—G. R. Rugger. Chemical Propulsion Exhaust—D. L. Schmidt. Hypersonic Atmospheric Flight—D. L. Schmidt. Radiation—J. H. Bowen, Jr. and D. V. Rosato. Other Properties and Characteristics (Corrosive, Thermal, Space, Biological, Ocean Fire)—D. V. Rosato. Service Life versus Environment—D. V. Rosato. Author Index. Subject Index.

Volume I 1968 1,228 pages \$42.00

### VOLUME II: MATERIALS

Contents: Fibers—J. H. Ross. Protective Flight Clothing and Sea Survival Equipment—M. B. Hays and C. A. Cassola. Solid Lubricants—M. J. Devine. Coatings—P. A. DiMattia. Elastomers—J. K. Sieron and R. G. Spain. Reinforced Plastics—A. G. H. Dietz, H. S. Schwartz and D. V. Rosato. Other Materials (Building and Construction, Packaging, Transportation, Shoes, Electronics, Foams, Films, Adhesives)—D. V. Rosato and F. J. Riel. Summary Review (Consumption, Armor, Aircraft, Selection Chronology, Plastics Age)—D. V. Rosato. Author Index. Subject Index for Volumes I and II.

Volume II 1968 1,002 pages \$42.00

Two Volume Set: \$67.20

## WILEY-INTERSCIENCE

a division of JOHN WILEY & SONS, Inc.  
605 Third Avenue, New York, N. Y. 10016

In Canada:

22 Worcester Road, Rexdale, Ontario, Canada

# MAN-MADE FIBERS:

## Science and Technology

Edited by H. F. Mark, *Polytechnic Institute of Brooklyn*,  
S. M. Atlas, *Bronx Community College*,  
and E. Cernia *ABCD, Rome, Italy*

“Experts from many countries contributed to these volumes, which present the latest knowledge about spinning of synthetic fibers and their structure, properties, and application. Volume 1 covers structural principles of fiber-forming polymers; physical fundamentals of fiber-spinning processes; fundamental aspects of wet-spinning and dry-spinning solutions; principles of melt-spinning and spinning in emulsions and suspension; transition phenomena; role of chain folding in fibers; morphology of synthetic fibers and conjugate fibers. Volumes 2 and 3 discuss specific types of fibers in detail, including electrical applications of glass fibers.”

—*Mechanical Engineering*

“... the series is highly recommended to the student and the practitioner of fiber science and technology.”

—*American Scientist*

“With the publication of the third volume of ‘Man-made fibers,’ it is now clear that we have a notable addition to textile literature, valuable both as reference source and as a text-book.”

—*The Textile Institute and Industry*

Volume 1:	1967	432 pages	\$19.95
Volume 2:	1968	493 pages	\$21.00
Volume 3:	1968	706 pages	\$29.95

**wiley** 

**WILEY-INTERSCIENCE** a division of  
JOHN WILEY & SONS, Inc., 605 Third Avenue, New York, N.Y.

In Canada: 22 Worcester Road, Rexdale, Ontario



## Contents (continued)

L. E. DANNALS: Number of Crosslinked Monomer Units per Weight-Average Primary Chain at the Gel Point in the Emulsion Polymerization 1,3-Dienes . . . . .	2989
SHINICHI ISAOKA, MAKIHIKO MORI, AKIO MORI, and JU KUMANOTANI: Mobility of the Ring Structure and the Characteristic of Crosslinked Polymers: The Structural Effect of the Eleven-Membered Ring and Its Homologs upon the Dynamic Mechanical Properties and Glass Transition Temperature of Crosslinked Diallyl Succinate Polymers . . . . .	3009
SATYENDRA NATH GUPTA and UMA SHANKAR NANDI: Studies on the Polymerization of Methyl Methacrylate Activated by Azobisisobutyramidine . . . . .	3019
NOTES	
WASABURO KAWAI, MASAJI OGAWA, and TAICHI ICHIHASHI: Polymerization of Vinyl Chloride and Copolymerization with Ethylene Catalyzed by Triethylaluminum-Cuprous Chloride-Carbon Tetrachloride . . . . .	3033
A. J. YU, R. H. GOBRAN, and R. F. FOERSTER: Solubility Parameter of Ethylene-Diethyl Fumarate Copolymer . . . . .	3039
ERRATUM . . . . .	3041

The *Journal of Polymer Science* publishes results of fundamental research in all areas of high polymer chemistry and physics. The *Journal* is selective in accepting contributions on the basis of merit and originality. It is not intended as a repository for unevaluated data. Preference is given to contributions that offer new or more comprehensive concepts, interpretations, experimental approaches, and results. Part A-1 *Polymer Chemistry* is devoted to studies in general polymer chemistry and physical organic chemistry. Contributions in physics and physical chemistry appear in Part A-2 *Polymer Physics*. Contributions may be submitted as full-length papers or as "Notes." Notes are ordinarily to be considered as complete publications of limited scope.

Three copies of every manuscript are required. They may be submitted directly to the editor: For Part A-1, to C. G. Overberger, Department of Chemistry, University of Michigan, Ann Arbor, Michigan 48104; and for Part A-2, to T. G. Fox, Mellon Institute, Pittsburgh, Pennsylvania 15213. Three copies of a short but comprehensive synopsis are required with every paper; no synopsis is needed for notes. Books for review may also be sent to the appropriate editor. Alternatively, manuscripts may be submitted through the Editorial Office, c/o H. Mark, Polytechnic Institute of Brooklyn, 333 Jay Street, Brooklyn, New York 11201. All other correspondence is to be addressed to Periodicals Division, Interscience Publishers, a Division of John Wiley & Sons, Inc., 605 Third Avenue, New York, New York 10016.

Detailed instructions in preparation of manuscripts are given frequently in Parts A-1 and A-2 and may also be obtained from the publisher.

# Wiley-Interscience Books for the Polymer Scientist...

## X-RAY DIFFRACTION METHODS IN POLYMER SCIENCE

By LEROY E. ALEXANDER, *Carnegie-Mellon University*.

*A volume in the Wiley Series on the Science and Technology of Materials*, edited by J. E. Burke, B. Chalmers, and J. A. Krumhanzl

"...an excellent book that deserves to be read by everyone working in X-Ray diffraction or attempting to use the results of such a study."

—*SPE Journal*

Here is a comprehensive treatment of the X-ray diffraction methods used in the stereochemical and physical characterization of polymers. The book presents information on X-ray diffraction by polymers that has previously been available only in scattered literature. It emphasizes experimental and interpretative procedures which yield quantitative parameters rather than qualitative or descriptive information.

The material specifically meets the needs of scientists engaged in the study of "linear" synthetic macromolecules. But research scientists who wish to understand the applications of X-ray diffraction to the study of polymers, as well as other semi-crystalline materials, will also find this book extremely rewarding.

**Contents:** Introduction to X-Ray Diffraction by Polymers. Instrumentation. Degree of Crystallinity in Polymers. Preferred Orientation in Polymers. Macrostructure from Small-Angle Scattering. Microstructure from Wide-Angle Diffraction. Lattice Distortions and Crystallite Size. Appendix. Name Index. Subject Index.

1969 582 pages \$27.95

## PLASTIC FOAMS

**The Physics and Chemistry of Product Performance and Process Technology**

By CALVIN J. BENNING, *International Paper Company*.

*Two volumes in the Polymer Engineering and Technology series:* Executive editor, D. V. Rosato

"These two volumes...comprise a comprehensive treatise on all types of plastic foams. Every conceivable type of plastic from urethane and styrene to polysulphone is discussed...this is a very well written set. The concepts are clearly described and easy to follow.

"All workers in the field of expanded plastics should find this set interesting and valuable. Its completeness and thoroughness are commendable."

—*SPE Journal*

## VOLUME I: Chemistry and Physics of Foam Formation

Contents: Polystyrene Foam. Polyurethane Foam. Polyolefin Foams. Polyvinyl-Chloride Foams. Phenolic Foam. Urea-Formaldehyde Foams. Polyvinyl Alcohol-Formaldehyde Foam. Epoxy Foams. Acrylonitrile and Acrylate Copolymer Foams. Pyranil Foam. Synthetic Rubber and Silicone Foams. Miscellaneous Cellular Plastics. Expandable Beads and Spheres. Inorganic Foams. Index.

## VOLUME II: Structure, Properties, and Application

Contents: Physics and Chemistry of Foam Formation and Stability. Relationship between Foam Morphology and the Physical Properties of Cellular Plastics. Relationship between Polymer Structure and Properties in Plastic Foams. Modification of Foam Structures. Laboratory Procedures for Predicting Foam Process and Performance. Engineering Properties of Cellular Plastics. Applications for Cellular Materials. Appendices. Index.

1969 1028 pages \$75.00

## STATISTICAL MECHANICS OF CHAIN MOLECULES

By PAUL J. FLORY, *Stanford University*

"This is a beautiful book which excels by the depth of its approach, by the clarity of its presentation, and by the abundance of stimulating ideas which will pave the way for further developments."

—*Journal of Applied Polymer Science*

"This volume should be on the bookshelf of anyone who needs to understand the properties of chain molecules..."

—*Laboratory Equipment Digest*

"On almost every page can be found evidence of the author's vast reading and of the freshness of outlook found only when an active author is contributing to the field himself...The book is thoroughly recommended to all serious workers in this field."—*Nature*

New methods for discerning the equilibrium properties of chain molecules are presented in this volume and are explained with the utmost mathematical simplicity. Artificial models so much in use for this purpose can now be abandoned in favor of a more realistic approach. This book should mark the beginning of a new era in the interpretation of the properties of macromolecules.

**Contents:** Analysis of the Spatial Configurations of Chain Molecules and Treatment of Simplified Model Chains. Random-Coil Configurations and Their Experimental Characterization. Configurational Statistics of Chain Molecules with Interdependent Rotational Potentials. Moments of Chain Molecules. Symmetric Chains. Asymmetric Vinyl Chains. Polypeptides, Proteins, and Analogs. The Statistical Distribution of Configurations. Optical Properties and Radiation Scattering. Appendices. Author Index. Subject Index.

1969 432 pages \$17.50

**wiley**

## WILEY-INTERSCIENCE

A division of JOHN WILEY & SONS, Inc.

605 Third Avenue, New York, N. Y. 10016

In Canada: 22 Worcester Road, Rexdale, Ontario